

REMEDICATION OF VOLTAGE REGULATION ISSUES IN MICROGRID WITH INTERMITTENT RENEWABLE ENERGY SOURCES

THESIS

SUBMITTED IN PARTIAL FULFILLMENT OF THE REQUIREMENTS
FOR THE AWARD OF THE DEGREE
OF

DOCTORATE OF PHILOSOPHY

Submitted by:

RITIKA GOUR
(2K14/PhD/EE/07)

Under the supervision of

PROF. VISHAL VERMA
EED, DTU



DEPARTMENT OF ELECTRICAL ENGINEERING
DELHI TECHNOLOGICAL UNIVERSITY
(Formerly Delhi College of Engineering)
Bawana Road, Delhi-110042

DECLARATION

I, RITIKA GOUR (2K14/PhD/EE/07) hereby declare that the work, which is being presented in the thesis entitled, “**REMEDIATION OF VOLTAGE REGULATION ISSUES IN MICROGRID WITH INTERMITTENT RENEWABLE ENERGY SOURCES**” submitted for partial fulfillment of the requirements for the award of the degree of Doctor of Philosophy is an authentic record of my own work carried out under the guidance of Prof. VISHAL VERMA, EED, DTU. The matter embodied in the dissertation work has not been plagiarized from anywhere and the same has not been submitted for the award of any other degree or diploma in full or in part.

Submitted by:-

RITIKA GOUR

(2K14/PhD/EE/07)

Electrical Engineering Department

DEPARTMENT OF ELECTRICAL ENGINEERING
DELHI TECHNOLOGICAL UNIVERSITY
(Formerly Delhi College of Engineering)



CERTIFICATE

This is to certify that the thesis entitled, "REMEDIATION OF VOLTAGE REGULATION ISSUES IN MICROGRID WITH INTERMITTENT RENEWABLE ENERGY SOURCES," submitted by Ms. Ritika Gour, Roll No. 2K14/PhD/EE/07, a research scholar in the Electrical Engineering Department at Delhi Technological University (formerly Delhi College of Engineering), is a dissertation work carried out by her under my guidance during the session 2014-2023 towards the partial fulfillment of the requirements for the award of the degree of Doctor of Philosophy.

Throughout the duration of her research, she has shown dedication and commitment towards her work, and her findings have contributed to the field of voltage regulation and devising solutions for maintaining voltage profiles in microgrids under high penetration of RES to suit the conventional protection scheme for undisturbed operation of radial feeder in the distribution system. The use of hybrid distributed Voltage regulators for voltage regulation in a microgrid with high penetration of RES, their non-intersecting control, detailed analysis for estimating voltage at different nodes in the micro-grid, is the uniqueness of her thesis, which is a valuable addition to the literature.

I am confident that she will continue to excel in her future endeavors and wish her all the best in her academic and professional pursuits.

Prof. Vishal Verma
Professor EED, DTU
Supervisor

ACKNOWLEDGMENT

I am humbled and grateful for the opportunity to express my gratitude to all those who have contributed to the successful completion of my work. It is with great pleasure that I extend my deepest appreciation to my supervisor, Prof. Vishal Verma, whose guidance, supervision, and unwavering support have been invaluable throughout my research journey. I am truly fortunate to have had the privilege of working with him, and his mentorship has been a lifelong experience that will stay with me forever.

I would also like to extend my thanks to Prof. Pragati Kumar, Head of the Department of Electrical Engineering at DTU Delhi, and all the faculty, staff members, and research scholars of the Electrical Engineering Department, for their timely help and support. Special thanks go to Prof. Uma Nangia, Head DRC, Department of Electrical Engineering DTU Delhi, for her constant encouragement throughout my PhD period. I am grateful to Mr. Anil Butola, Dr. Amritesh Kumar, Vandana Arora, Aditya Narula, Pankhuri Asthana, Tarun Jangid and Shirish Rayjada for their help and support during my work in the laboratory.

I would also like to acknowledge and express my deepest appreciation to my parents, Mrs. Neelan Gour and Mr. Mohan Lal Gour, for their unwavering love, support, patience, and encouragement. My sisters Kritika Gour, Shrutika Gour, Sudha Singh, and Suman Singh, brother Nagesh Singh, and all my family members have been a constant source of support throughout. Their unconditional support and love have been instrumental in enabling me to achieve my goals. I would also like to give thanks to my father-in-law Late Dharm Raj Singh and mother-in-law Late Kamala Singh for their blessings from heaven.

Lastly, I owe a debt of gratitude to my husband, Dr. Ramesh Singh, and my son, Darsh Singh, whose unwavering support has been my driving force throughout my research journey. Their love, understanding, and encouragement have been a constant source of inspiration and have made this achievement possible.

REMEDICATION OF VOLTAGE REGULATION ISSUES IN MICROGRID WITH INTERMITTENT RENEWABLE ENERGY SOURCES

ABSTRACT

This thesis focuses on investigating voltage regulation issues in radial distribution feeder under high penetration of intermittent renewable energy sources (RES). While integrating RES into the radial distribution systems and/or microgrids offers numerous benefits, including reducing greenhouse gas emissions and enhancing energy security, however, it presents several challenges that must be addressed to ensure a smooth transition of power system from conventional sources to RES. The intermittent nature of RES systems and their high penetration level causes voltage variation and power flow reversal, leading to system instability and suboptimal performance.

To address the challenges related to voltage regulation, the thesis presents a comprehensive literature review of the RES connectivity issues into the microgrids, and the technical difficulties that microgrids face due to RES intermittency. The study investigates different voltage regulator options, including OLTC transformers, DVRs, STATCOMs, and BESS, for radial feeders having high penetration of RES. New method for analysis, new control scheme for application of hybrid voltage regulators, simulation under MATLAB Simulink environment is investigated. The performance of the comprehensive system is investigated under different operating conditions, such as RES intermittency, load perturbation, and source voltage perturbations.

The study explores the viability of non-intersecting control scheme for a hybrid voltage regulation technique that combines preventive and remedial methods to optimize system performance and stability. The study also investigates different hybrid combinations of two or more voltage regulation devices for maintaining the voltage profile of the feeder for the microgrid and distribution system. The investigation has been largely focused for the duo of OLTC transformer and DVR for their autonomous yet coordinated operation, through new control scheme. The control is extended to inclusion of smart grid connected

inverters (GCI), making it third type of distributed voltage regulator, for maintaining a better voltage profile throughout the radial feeder/microgrid. Simulation results are presented, under extreme conditions such as overvoltage and light loading occurring together, and similarly undervoltage and heavy loading conditions occurring together, to verify the efficacy of the new control scheme for voltage regulator, to maintain the voltage profile of the radial feeder/microgrid.

Furthermore, the thesis explores two-port ABCD based analytical approach, for determining the node voltage and branch current by dividing the whole grid into smaller sections, to handle a larger microgrid with multiple RES connected to estimate the impact on voltage levels brought on by the high penetration of RES. The method is validated on an 11-node radial microgrid with multiple RES connected to it, under uniform and non-uniform sectional parameters and different operating conditions.

The research focuses on the integration and control of various voltage regulators in the microgrid/distribution system in a distributed way to ensure smooth operation and minimizing the disturbances.

Further the newly developed concept of analysis based on ABCD parameter is successfully applied for determining the requirement of the number of distributed voltage regulators and their correct location with capacity for an N-node radial microgrid. The theoretical results obtained are also dully validated by placing the distributed voltage regulators in the considered microgrid at estimated locations as per the developed analytical tool, to draw out smooth voltage profile of the microgrid under uniform and non-uniform feeder distribution cases.

Overall, this thesis presents a comprehensive analysis of various voltage regulation techniques and their applications in microgrids with high RES penetration. The findings of this research will be useful in designing and implementing optimal voltage regulation solutions for microgrids with high RES penetration to ensure their smooth operation and optimal performance.

TABLE OF CONTENTS

	Declaration	<i>i</i>
	Certificate	<i>iii</i>
	Acknowledgment	<i>v</i>
	Abstract	<i>vii</i>
	List of Figures	<i>xiii</i>
	List of Tables	<i>xxiii</i>
	Abbreviation	<i>xxv</i>
1	INTRODUCTION	1
1.1	Motivation for the thesis	1
1.2	Glances of the power sector in India	2
1.3	Changing trend of power generation	3
1.4	Renewable energy sources and their advantages	5
1.5	Operating modes of RES	7
1.6	Intermittent nature of RES	9
1.7	Challenges faced due to intermittent nature and high penetration of RES.	10
1.8	Scope of Work	13
1.9	Organization of Thesis	14
2	LITERATURE SURVEY	17
2.1	General	17
2.2	Need for the voltage regulators.	17
2.3	Preventive Measures for voltage regulation	18
2.3.1	Smart Grid Connecting Inverter (GCI)	18
2.3.2	Battery Energy Storage System (BESS)	20

2.4	Curative Measures for voltage regulation	21
2.4.1	On-Load Tap Changing Transformer (OLTC-T)	22
2.4.2	Static Synchronous Compensator (STATCOM)	25
2.4.3	Dynamic Voltage Restorer (DVR)	28
2.4.4	Hybrid Voltage Regulators	32
2.5	Concept of Microgrid	33
2.5.1	Control of Voltage Regulators	34
2.5.2	Location of Voltage regulators	36
2.6	Research Opportunities/ Identified Research Gap	37
2.7	Objectives of Thesis	38
3	ANALYSIS, SIMULATION AND PERFORMANCE EVALUATION OF VOLTAGE REGULATORS	41
3.1	General Overview	41
3.2	OLTC Transformer	42
3.2.1	Analysis of OLTC transformer	42
3.2.2	Control of OLTC transformer	48
3.2.3	Simulation Diagram of OLTC transformer	49
3.2.4	Performance Evaluation of OLTC transformer	49
3.3	Static Synchronous Compensator (STATCOM)	57
3.3.1	Analysis of STATCOM	58
3.3.2	Control of STATCOM	61
3.3.3	Simulation Diagram of STATCOM	63
3.3.4	Performance Evaluation of STATCOM	63
3.4	Battery Energy Storage System (BESS)	70
3.4.1	Analysis of BESS	72
3.4.2	Control of BESS	74

3.4.3	Simulation Diagram of BESS	75
3.4.4	Performance Evaluation of BESS	76
3.5	Dynamic Voltage Restorer (DVR)	82
3.5.1	Analysis of DVR	85
3.5.2	Control of DVR	88
3.5.3	Simulation Diagram of DVR	89
3.5.4	Performance Evaluation of DVR	90
3.6	Comparison of different voltage regulators for radial microgrid/distribution fed with RES	98
3.7	Conclusion	103
4	HYBRID CONFIGURATIONS FOR VOLTAGE REGULATION	105
4.1	General Overview	105
4.2	OLTC Transformer and DVR Hybrid for Voltage Regulation	106
4.2.1	System Considerations for OLTC-T and DVR Hybrid	106
4.2.2	Analysis for OLTC-T and DVR Hybrid	107
4.2.3	Control of OLTC-T and DVR Hybrid	110
4.2.4	Simulation Diagram for OLTC-T and DVR Hybrid	114
4.2.5	Performance Evaluation of OLTC-T and DVR Hybrid	115
4.3	OLTC Transformer and DVR Hybrid duo supported by smart GCI for Voltage Regulation	127
4.3.1	Control of trio for voltage regulation	128
4.3.2	Analysis of Smart GCI	129
4.3.3	Control of Smart GCI	130
4.3.4	Performance Evaluation of OLTC-T and DVR Hybrid	132
4.4	Conclusion	137

5	ANALYSIS OF RADIAL MICROGRID WITH HIGH PENETRATION OF RES	139
5.1	General Overview	139
5.2	Radial Microgrid Configuration and Analysis	139
5.3	Validation of Analysis with MATLAB Simulation	147
5.4	Conclusion	160
6	ANALYSIS AND EVALUATION OF VOLTAGE REGULATOR QUANTITY AND PLACEMENT IN RADIAL MICROGRID	161
6.1	General	161
6.2	Location and Number of the voltage regulator(s)	161
6.2.1	Algorithm to find the location of the voltage regulator(s)	162
6.3	Capacity of voltage regulator	164
6.4	Application of algorithm in an 11-node radial microgrid: case study	169
6.5	Conclusion	179
7	MAIN CONCLUSION AND FUTURE SCOPE OF WORK	181
7.1	Main Conclusion	181
7.2	Future Scope of Work	183
	References	185
	List of Publications	199

LIST OF FIGURES

Figure No.	Figure Title	Pg. No.
Fig. 1.1	Pie chart showing power share percentage from various sources	3
Fig. 1.2	Bar chart showing the trend of various sources of energy	5
Fig. 1.3	Off-grid mode operation of RES with its local loads	7
Fig. 1.4	Grid-Connected RES system with loads	8
Fig. 2.1 (a)	Block diagram of a normal transformer	22
Fig. 2.1 (b)	Block diagram of an OLTC transformer	22
Fig. 2.2	Block diagram of STATCOM	26
Fig. 2.3	Block diagram of DVR	29
Fig. 2.4	Distribution feeder without RES	34
Fig. 2.5	Radial Microgrid/Distribution feeder with RES	34
Fig. 3.1	Single line diagram of OLTC transformer for voltage regulation in radial microgrid with RES penetration	42
Fig. 3.2(a)	Equivalent circuit of OLTC transformer referred on secondary side of transformer	43
Fig. 3.2(b)	Simplified equivalent circuit of OLTC transformer referred on the secondary side of transformer.	43
Fig. 3.3	Tap position controller of OLTC Transformer	48
Fig. 3.4	MATLAB simulation diagram of radial microgrid with OLTC transformer as voltage regulator	48
Fig. 3.5	Voltage and current waveforms in radial microgrid with OLTC transformer as voltage regulator during RES intermittency.	50

Fig.	3.6	Voltage profile of radial microgrid with OLTC transformer as voltage regulator during RES intermittency at $I_{RES} = 5 \text{ A}$	51
Fig.	3.7	Voltage profile of radial microgrid with OLTC transformer as voltage regulator during RES intermittency at $I_{RES} = 50 \text{ A}$	51
Fig.	3.8	Voltage profile of radial microgrid with OLTC transformer as voltage regulator during RES intermittency at $I_{RES} = 180 \text{ A}$	52
Fig.	3.9	Voltage and current waveforms in radial microgrid with OLTC transformer as voltage regulator during load perturbation condition	53
Fig.	3.10	Voltage Profile of radial microgrid with OLTC transformer as voltage regulator during load perturbation at light loading condition.	54
Fig.	3.11	Voltage Profile of radial microgrid with OLTC transformer as voltage regulator during load perturbation at rated loading condition	54
Fig.	3.12	Voltage Profile of radial microgrid with OLTC transformer as voltage regulator during load perturbation at heavy loading condition	55
Fig.	3.13	Voltage and current waveforms in radial microgrid with OLTC transformer as voltage regulator during source perturbation condition	56
Fig.	3.14	Voltage Profile of radial microgrid with OLTC transformer as voltage regulator during source perturbation at rated voltage from source side	57
Fig.	3.15	Voltage Profile of radial microgrid with OLTC transformer as voltage regulator during source perturbation at undervoltage from source side	57
Fig.	3.16	Voltage Profile of radial microgrid with OLTC transformer as voltage regulator during source perturbation at overvoltage from source side	58

Fig.	3.17	Single line diagram of STATCOM for voltage regulation in radial microgrid with RES penetration	58
Fig.	3.18	Phasor diagram of STATCOM for voltage regulation at its PCC	60
Fig.	3.19	Block diagram for gating pulse control for STATCOM	61
Fig.	3.20	MATLAB simulation diagram of radial microgrid with STATCOM as voltage regulator	62
Fig.	3.21	Expanded simulation diagram for STATCOM	62
Fig.	3.22	Voltage and current waveforms in radial microgrid with STATCOM as voltage regulator during RES intermittency.	64
Fig.	3.23	Voltage profile of radial microgrid with STATCOM as voltage regulator during RES intermittency at $I_{RES} = 5 \text{ A}$	65
Fig.	3.24	Voltage profile of radial microgrid with STATCOM as voltage regulator during RES intermittency at $I_{RES} = 50 \text{ A}$	65
Fig.	3.25	Voltage profile of radial microgrid with STATCOM as voltage regulator during RES intermittency at $I_{RES} = 180 \text{ A}$	66
Fig.	3.26	Voltage and current waveforms for voltage regulation in considered radial microgrid with STATCOM as voltage regulator during load perturbation condition	67
Fig.	3.27	Voltage Profile of radial microgrid with STATCOM as voltage regulator during load perturbation at light loading condition.	68
Fig.	3.28	Voltage Profile of radial microgrid with STATCOM as voltage regulator during load perturbation at rated loading condition	68
Fig.	3.29	Voltage Profile of radial microgrid with STATCOM as voltage regulator during load perturbation at heavy	69

		loading condition	
Fig.	3.30	Voltage and current waveforms for voltage regulation in considered radial microgrid with STATCOM as voltage regulator during source perturbation.	70
Fig.	3.31	Voltage Profile of radial microgrid with STATCOM as voltage regulator during source perturbation at rated voltage from source side	71
Fig.	3.32	Voltage Profile of radial microgrid with STATCOM as voltage regulator during source perturbation at undervoltage from source side	71
Fig.	3.33	Voltage Profile of radial microgrid with STATCOM as voltage regulator during source perturbation at overvoltage from source side	72
Fig.	3.34	Single line diagram of BESS for voltage regulation in radial microgrid with RES penetration	72
Fig.	3.35	Block diagram for gating pulse control for BESS	74
Fig.	3.36	MATLAB simulation diagram of radial microgrid with BESS as voltage regulator	75
Fig.	3.37	Voltage and current waveforms for voltage regulation in considered radial microgrid with BESS as voltage regulator during RES intermittency condition	77
Fig.	3.38	Voltage profile of radial microgrid with BESS as voltage regulator during RES intermittency at $I_{RES} = 5$ A	78
Fig.	3.39	Voltage profile of radial microgrid with BESS as voltage regulator during RES intermittency at $I_{RES} = 50$ A	78
Fig.	3.40	Voltage profile of radial microgrid with BESS as voltage regulator during RES intermittency at $I_{RES} = 180$ A	79
Fig.	3.41	Voltage and current waveforms for voltage regulation in considered radial microgrid with BESS as voltage	80

		regulator during load perturbation condition	
Fig.	3.42	Voltage Profile of radial microgrid with BESS as voltage regulator during load perturbation at light loading condition.	81
Fig.	3.43	Voltage Profile of radial microgrid with BESS as voltage regulator during load perturbation at rated loading condition	81
Fig.	3.44	Voltage Profile of radial microgrid with BESS as voltage regulator during load perturbation at heavy loading condition	82
Fig.	3.45	Voltage and current waveforms for voltage regulation in considered radial microgrid with BESS as voltage regulator during source perturbation condition	83
Fig.	3.46	Voltage Profile of radial microgrid with BESS as voltage regulator during source perturbation at rated voltage from source side	84
Fig.	3.47	Voltage Profile of radial microgrid with BESS as voltage regulator during source perturbation at undervoltage from source side	84
Fig.	3.48	Voltage Profile of radial microgrid with BESS as voltage regulator during source perturbation at overvoltage from source side	85
Fig.	3.49	Single line diagram of DVR for voltage regulation in radial microgrid with RES penetration	85
Fig.	3.50	Phasor diagram of DVR for voltage regulation at its PCC	87
Fig.	3.51	Block diagram for gating pulse control for DVR	88
Fig.	3.52(a)	MATLAB simulation diagram of radial microgrid with DVR as voltage regulator	89
Fig.	3.52(b)	Expanded simulation diagram for DVR	89
Fig.	3.53	Voltage and current waveforms for voltage regulation in considered radial microgrid with DVR as voltage	91

		regulator during RES intermittency condition	
Fig.	3.54	Voltage profile of radial microgrid with DVR as voltage regulator during RES intermittency at $I_{RES} = 5$ A	92
Fig.	3.55	Voltage profile of radial microgrid with DVR as voltage regulator during RES intermittency at $I_{RES} = 50$ A	92
Fig.	3.56	Voltage profile of radial microgrid with DVR as voltage regulator during RES intermittency at $I_{RES} = 180$ A	93
Fig.	3.57	Voltage and current waveforms for voltage regulation in considered radial microgrid with DVR as voltage regulator during load perturbation condition	94
Fig.	3.58	Voltage Profile of radial microgrid with DVR as voltage regulator during load perturbation at light loading condition.	95
Fig.	3.59	Voltage Profile of radial microgrid with DVR as voltage regulator during load perturbation at rated loading condition	95
Fig.	3.60	Voltage Profile of radial microgrid with DVR as voltage regulator during load perturbation at heavy loading condition	96
Fig.	3.61	Voltage and current waveforms for voltage regulation in considered radial microgrid with DVR as voltage regulator during source perturbation condition	97
Fig.	3.62	Voltage Profile of radial microgrid with DVR as voltage regulator during source perturbation at rated voltage from source side	98
Fig.	3.63	Voltage Profile of radial microgrid with DVR as voltage regulator during source perturbation at undervoltage from source side	98
Fig.	3.64	Voltage Profile of radial microgrid with DVR as voltage regulator during source perturbation at	99

overvoltage from source side

Fig.	4.1	Pictorial representation of voltage regulation range of OLTC transformer and DVR in radial microgrid	106
Fig.	4.2	Single line diagram of OLTC transformer and DVR hybrid for voltage regulation in radial microgrid with RES penetration	107
Fig.	4.3	Equivalent circuit system having both OLTC transformer and DVR	109
Fig.	4.4(a)	Block diagram for mode select line for hybrid voltage regulator in radial microgrid	111
Fig.	4.4(b)	Inter-turn regulation: Tap position controller for OLTC transformer	111
Fig.	4.4(c)	Block diagram for controlling VSC of DVR	112
Fig.	4.5	MATLAB Simulink diagram for testing of OLTC transformer and DVR hybrid for voltage regulation in radial microgrid	113
Fig.	4.6	Voltage and current waveforms in radial microgrid with OLTC transformer and DVR as voltage regulator during RES intermittency.	116
Fig.	4.7	Voltage profile of radial microgrid with OLTC transformer and DVR as voltage regulator during RES inrtermittency at $I_{RES} = 50$ A	117
Fig.	4.8	Voltage profile of radial microgrid with OLTC transformer and DVR as voltage regulator during RES intermittency at $I_{RES} = 70$ A	118
Fig.	4.9	Voltage profile of radial microgrid with OLTC transformer and DVR as voltage regulator during RES intermittency at $I_{RES} = 220$ A	118
Fig.	4.10	Voltage and current waveforms in radial microgrid with OLTC transformer and DVR as voltage regulator during Load Perturbation (Load between	120

OLTC transformer and DVR).

Fig.	4.11	Voltage profile of radial microgrid with OLTC transformer and DVR as voltage regulator during Load Perturbation (Load between OLTC transformer and DVR) at light loading condition	121
Fig.	4.12	Voltage profile of radial microgrid with OLTC transformer and DVR as voltage regulator during Load Perturbation (Load between OLTC transformer and DVR) at rated loading condition	121
Fig.	4.13	Voltage profile of radial microgrid with OLTC transformer and DVR as voltage regulator during Load Perturbation (Load between OLTC transformer and DVR) at heavy loading condition	122
Fig.	4.14	Voltage and current waveforms in radial microgrid with OLTC transformer and DVR as voltage regulator during Load Perturbation (Load between DVR and RES).	123
Fig.	4.15	Voltage profile of radial microgrid with OLTC transformer and DVR as voltage regulator during Load Perturbation (Load between DVR and RES) at light loading condition	124
Fig.	4.16	Voltage profile of radial microgrid with OLTC transformer and DVR as voltage regulator during Load Perturbation (Load between DVR and RES) at rated loading condition	124
Fig.	4.17	Voltage profile of radial microgrid with OLTC transformer and DVR as voltage regulator during Load Perturbation (Load between DVR and RES) at heavy loading condition	125
Fig.	4.18	Voltage and current waveforms in radial microgrid with OLTC transformer and DVR as voltage regulator during source perturbation.	126

Fig.	4.19	Voltage profile of radial microgrid with OLTC transformer and DVR as voltage regulator during source perturbation at rated voltage from source side	127
Fig.	4.20	Voltage profile of radial microgrid with OLTC transformer and DVR as voltage regulator during source perturbation at undervoltage from source side	127
Fig.	4.21	Voltage profile of radial microgrid with OLTC transformer and DVR as voltage regulator during source perturbation at overvoltage from source side	128
Fig.	4.22	Power shifting curve for RES	130
Fig.	4.23	Block diagram for mode control of smart GCI	131
Fig.	4.24	Voltage and current waveforms in radial microgrid with OLTC transformer, DVR and smart GCI as voltage regulator during overvoltage and light loading condition	133
Fig.	4.25	Voltage profile of radial microgrid with OLTC transformer, DVR and smart GCI as voltage regulator during overvoltage and light loading condition	134
Fig.	4.26	Voltage and current waveforms in radial microgrid with OLTC transformer, DVR and smart GCI as voltage regulator during undervoltage and heavy loading condition	135
Fig.	4.27	Voltage profile of radial microgrid with OLTC transformer, DVR and smart GCI as voltage regulator during undervoltage and heavy loading condition	136
Fig.	5.1	Single line diagram of 'N' node radial microgrid	140
Fig.	5.2(a)	Single Line Diagram of Section between nodes '0' and '2'	143
Fig.	5.2(b)	ABCD parameter equivalent of Section between nodes '0' and '2'	143
Fig.	5.3	ABCD Equivalent circuit of considered 'N' node radial microgrid	144

Fig.	5.4(a)	Single line diagram of 11 node radial microgrid	148
Fig.	5.4(b)	ABCD Equivalent circuit of considered 11 node radial microgrid	148
Fig.	5.5	Simulation diagram of 11 node radial microgrid	149
Fig.	6.1	Flowchart to show the location and number of voltage regulator to be installed.	163
Fig.	6.2	Simulation diagram for 11 node radial microgrid with intermittent renewable energy sources with 2 DVR connected	173
Fig.	6.3	Voltage profile of uniform feeder 11 node radial microgrid with RES connected under normal operating conditions	174
Fig.	6.4	Voltage profile of uniform feeder 11 node radial microgrid with RES connected under light load condition and high RES injection	174
Fig.	6.5	Voltage profile of uniform feeder 11 node radial microgrid with RES connected under heavy loading and no RES injection	175
Fig.	6.6	Voltage profile of non-uniform feeder 11 node radial microgrid with RES connected under normal operating conditions	178
Fig.	6.7	Voltage profile of non-uniform feeder 11 node radial microgrid with RES connected under light loading and high RES condition	178
Fig.	6.8	Voltage profile of non-uniform feeder 11 node radial microgrid with RES connected under heavy loading and no RES injection	179

LIST OF TABLES

Table No.	Title	Page No.
Table 3.1	Simulation parameters for voltage regulation of radial microgrid with OLTC transformer as voltage regulator	49
Table 3.2	Simulation parameters for voltage regulation of radial microgrid with STATCOM as voltage regulator	63
Table 3.3	Simulation parameters for voltage regulation of radial microgrid with BESS as voltage regulator	76
Table 3.4	Simulation parameters for voltage regulation of radial microgrid with DVR as voltage regulator	90
Table 3.5	Comparison of different voltage regulators for regulating voltage in radial microgrid	101
Table 4.1	Simulation parameters for voltage regulation of radial microgrid with intermittent RES using OLTC-T and DVR hybrid voltage regulator	115
Table 5.1	Comparison of calculated and simulated data for uniform feeder distribution and normal operating conditions	152
Table 5.2	Comparison of calculated and simulated data for uniform feeder distribution and light loading and high RES injection condition	152
Table 5.3	Comparison of calculated and simulated data for uniform feeder distribution and heavy loading and no RES injection condition	153
Table 5.4	System parameter considered for non-uniform feeder distribution and normal operating condition	155
Table 5.5	ABCD parameter computed for non-uniform feeder distribution and normal operating condition	155
Table 5.6	Comparison of calculated and simulated data for non-uniform feeder distribution and normal operating condition	156
Table 5.7	System parameter considered for non-uniform feeder distribution and light loading and high RES injection condition	157

Table	5.8	ABCD parameter computed for non-uniform feeder distribution and light loading and high RES injection condition	157
Table	5.9	Comparison of calculated and simulated data for non-uniform feeder distribution and light loading and high RES injection condition	158
Table	5.10	System parameters considered for non-uniform feeder distribution and heavy loading and no RES injection condition	158
Table	5.11	ABCD parameter computed for non-uniform feeder distribution and high loading and no RES injection condition	159
Table	5.12	Comparison of calculated and simulated data for non-uniform feeder distribution and heavy loading and no RES injection condition	159
Table	6.1	Difference in nodal voltage from the reference voltage without voltage regulator in uniform distribution feeder	171
Table	6.2	Difference in nodal voltage from the rated voltage with one voltage regulator installed in uniform distribution feeder	172
Table	6.3	Difference in nodal voltage from the rated voltage with two voltage regulators installed in uniform distribution feeder	172
Table	6.4	Difference in nodal voltage from the rated voltage without voltage regulator installed in non-uniform distribution feeder	176
Table	6.5	Difference in nodal voltage from the rated voltage with one voltage regulator installed in non-uniform distribution feeder	177
Table	6.6	Difference in nodal voltage from the rated voltage with two voltage regulator installed in non-uniform distribution feeder	177

ABBREVIATIONS

A	:	Ampere
AC	:	Alternating Current
BESS	:	Battery Energy Storage System
d-axis	:	Direct axis
DC	:	Direct Current
Dq	:	Direct quadrature axis
DSO	:	Distribution System Operator
DVR	:	Dynamic Voltage Restorer
GCI	:	Grid Connecting Inverter
GW	:	Gigawatt
Hz	:	Hertz
kV	:	Kilovolt
kVA	:	Kilo volt-ampere
kW	:	Kilowatt
MATLAB	:	Matrix Laboratory
MPPT	:	Maximum power point tracking
MVA	:	Mega volt-ampere
MW	:	Megawatt
MWh	:	Mega Watt Hour
OLTC	:	On Load Tap Changer
OLTC-T	:	On Load Tap Changing Transformer
PCC	:	Point of common coupling
pf	:	Power factor
PI	:	Proportional Integral
pu	:	Per unit

PV	:	Photovoltaic
PWM	:	Pulse width modulation
q-axis	:	Quadrature axis
RES	:	Renewable Energy Sources
RL	:	Resistive- inductive
rms	:	Root mean square
s	:	Second
SGCI	:	Smart grid connecting inverter
SRF	:	Synchronous reference frame theory
STATCOM	:	Static synchronous compensator
V	:	Volt
VSC	:	Voltage source inverter
W	:	Watt
\bar{U}	:	Mho
Ω	:	Ohm

Chapter 1

INTRODUCTION

1.1 Motivation for the thesis

As the world is increasingly turning to renewable energy sources, it is crucial to explore the effects of integrating renewable energy sources (RES) based generation units into the existing electricity distribution systems. Such RES offer sustainability to the utility grid in curbing electricity price fluctuations and reducing greenhouse gas emissions thereby reducing the environmental impacts.

However, the integration of RES units can also have negative effects on voltage levels and power flow. In traditional distribution systems, the power flows from the utility side to the customer side, which remains unidirectional. With large penetration of RES based generating units, a possibility of bidirectional power flow may exist, thus complicating device operation with the protection system, and, potentially degrading power quality from a voltage level perspective. Moreover, the intermittent nature of RES can cause variable system losses and increased maintenance issues of the devices due to increased switching operations.

As the implementation of renewable energy sources becomes more widespread, the concept of microgrids becomes more adaptable. However, increasing the penetration of renewable energy sources into distribution systems and microgrids can affect voltage levels, making it necessary to study these effects and develop remediation strategies to allow for higher penetration of renewable energy sources.

Therefore, this thesis will explore the effects of high penetration of renewable energy

sources on the voltage profile of the radial distribution systems and micro-grids, providing valuable insights and how it can be improved and can be optimized to allow for greater use of renewable energy sources. By doing so, this research will not only contribute to the development of more sustainable energy solutions but also pave the way for a cleaner and brighter future.

1.2 Glances of the power sector in India

India is the third largest producer of electricity in the world with a power generation of 412 GW as on 31st Jan 2023 [1-2]. In India, the power is generated from a variety of sources which include both conventional sources like fossil fuels and non-conventional sources like solar energy, hydro energy, wind energy etc. The breakdown of power generation from various sources is provided below, and the same information is also displayed in the pie chart in Figure 1.1, illustrating the distribution of different energy sources.

- Coal: 204.435 GW (49.7%)
- Renewable energy sources:
 - Wind: 41.983 GW (10.2%)
 - Solar: 63.894 GW (15.1%)
 - BM Power/Co-gen: 10.21 GW (2.5%)
 - Small hydro: 4.94 GW (1.2%)
 - Waste-to-energy: 0.523 GW (0.1%)
 - Natural gas: 24.824 GW (6.1%)
 - Large hydro: 46.850 GW (11.4%)
 - Nuclear: 6.78 GW (%)

- Diesel: 0.589 GW (0.1%)

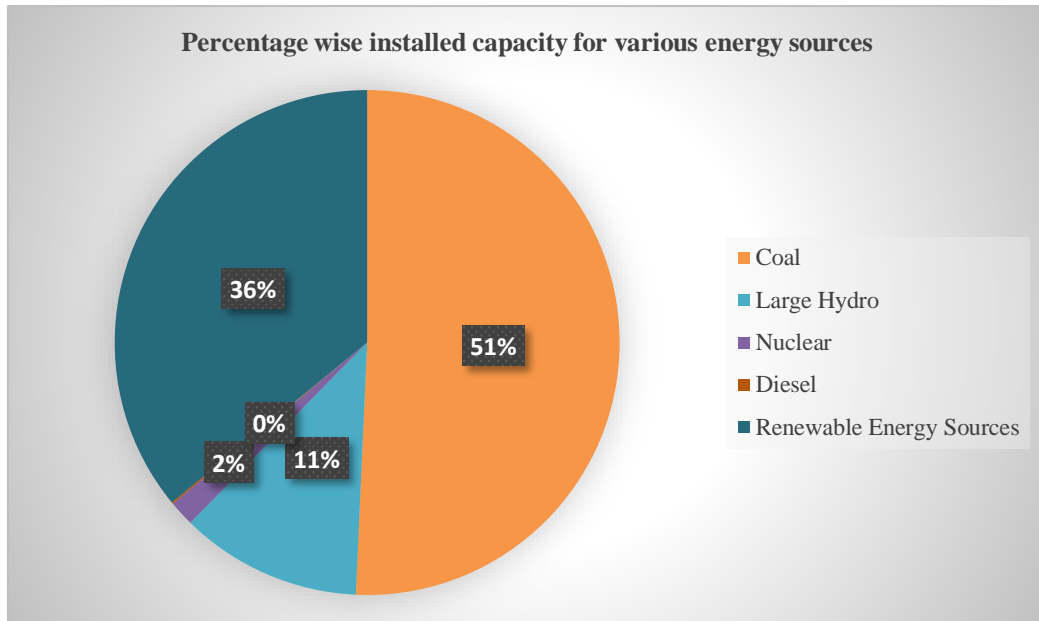


Fig. 1.1: Pie chart showing power share percentage from various sources.

1.3 Changing trend of power generation

Conventional energy sources, including nuclear energy and fossil fuels such as coal, lignite, gas, and diesel, have historically been the primary means of power generation, and still account for approximately 60% of total power generation today. However, these sources are facing limitations and disadvantages that hinder their widespread use for energy generation. These limitations and disadvantages are outlined below.

- **Limited Availability:** Fossil fuels are finite resources, and their reserves are being depleted with the increasing demand for energy. This means that these resources will eventually run out, which makes them unreliable for long-term energy needs.
- **Environmental Impact:** Conventional energy sources contribute significantly

to greenhouse gas emissions, which are major contributors to climate change. The burning of fossil fuels also releases harmful pollutants into the air and water, leading to various health and environmental problems.

- **High Cost:** The extraction and transportation of fossil fuels require significant investment and resources, which add to the overall cost of electricity production. Nuclear energy also involves high upfront costs and requires strict safety measures, which further increases the cost of power generation.
- **Safety Concerns:** Nuclear energy poses risks related to radiation exposure, accidents, and nuclear waste disposal. These risks can have catastrophic consequences and require strict safety protocols and regulations, which add to the cost and complexity of nuclear power generation.
- **Dependence on Imports:** Many countries rely on imported fossil fuels to meet their energy needs, which makes them vulnerable to geopolitical and economic uncertainties. This dependence on imports can also lead to energy insecurity and price volatility.
- **Inflexibility:** Conventional power plants are designed to operate at a certain capacity and cannot easily be ramped up or down to meet changing energy demands. This inflexibility can lead to inefficiencies and wastage of energy.

These limitations and disadvantages are driving the need for alternative and renewable energy sources, which offer greater sustainability, cost-effectiveness, and flexibility for meeting future energy needs. Fig. 1.2 displays a bar graph that depicts the changing trend of energy consumption from conventional and renewable sources in

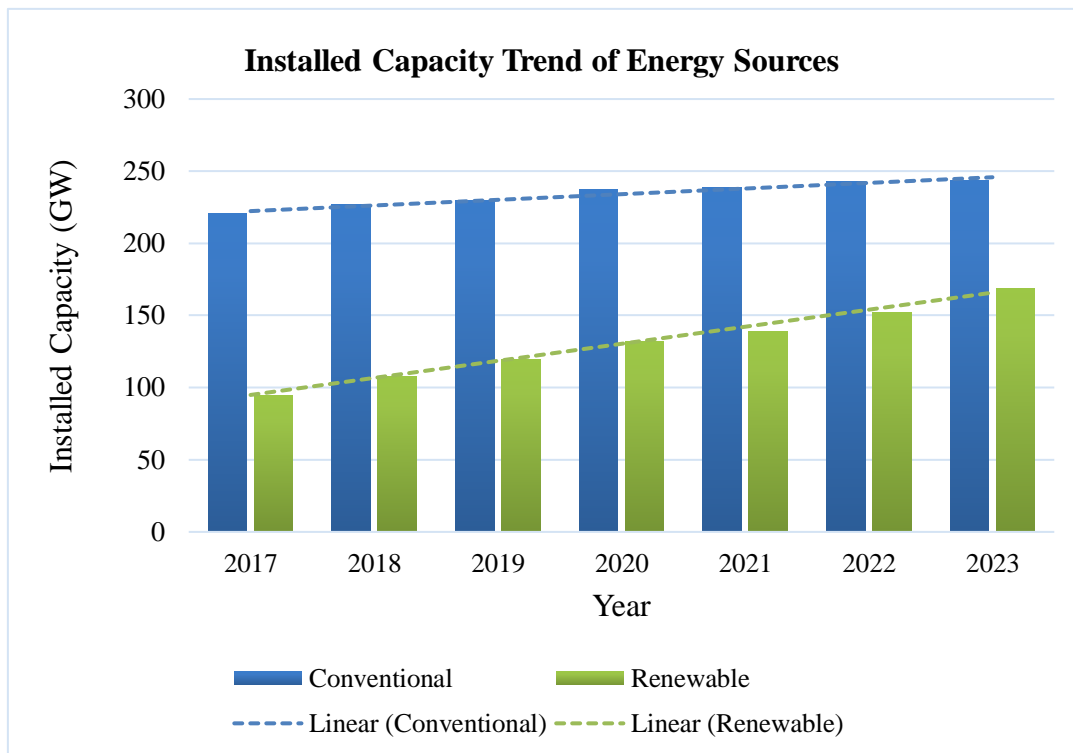


Fig. 1.2: Bar chart showing the trend of various sources of energy.

India over the past few years. The graph indicates that the newer plants being installed in the system are primarily renewable energy sources. Based on the graph, it can be inferred that the share of renewable energy sources in India as well in other countries is growing and is expected to continue to increase in the coming time.

1.4 Renewable Energy Sources and their advantages

Renewable energy is energy from sources that are naturally replenishing but flow-limited; renewable resources are virtually inexhaustible but limited in the amount of energy. RES generally includes solar power, wind power, hydroelectric power, geothermal power, and tidal power. Solar energy is the most widely used renewable energy source, with the installation of solar photovoltaic (PV) panels growing rapidly in recent years. Wind energy is also a significant contributor to renewable energy, with large-scale wind farms being installed in many countries. Hydroelectric power is

generated from the flow of water in rivers, and geothermal energy is generated from the heat of the Earth's core. Biomass energy is derived from organic matter such as wood, crops, and waste materials.

There are several advantages of renewable energy sources, including:

- **Reduced carbon footprint:** Unlike fossil fuels, renewable energy sources do not produce greenhouse gas emissions or other harmful pollutants, which can reduce the carbon footprint and help mitigate climate change.
- **Energy security:** Renewable energy sources are domestically produced and do not rely on imports, which can help increase energy security and reduce dependence on foreign energy sources.
- **Cost savings:** The cost of renewable energy has been decreasing over the years, making it increasingly competitive with traditional energy sources. In some cases, renewable energy sources can even be cheaper than fossil fuels.
- **Job creation:** The renewable energy industry has the potential to create new the jobs in manufacturing, installation, and maintenance of renewable energy systems.
- **Improved public health:** Renewable energy sources do not emit harmful pollutants that can cause respiratory problems, heart disease, and other health issues.
- **Resource Sustainability:** Renewable energy sources such as solar, wind, and hydropower are abundant and will not be depleted like fossil fuels.
- **Increased energy independence:** By diversifying the energy mix and relying

more on renewable energy sources, countries can reduce their dependence on imported oil and gas and improve their energy independence.

1.5 Operating mode of RES

Renewable energy systems (RES) operate in two different modes, Off-Grid and Grid-Connected Mode.

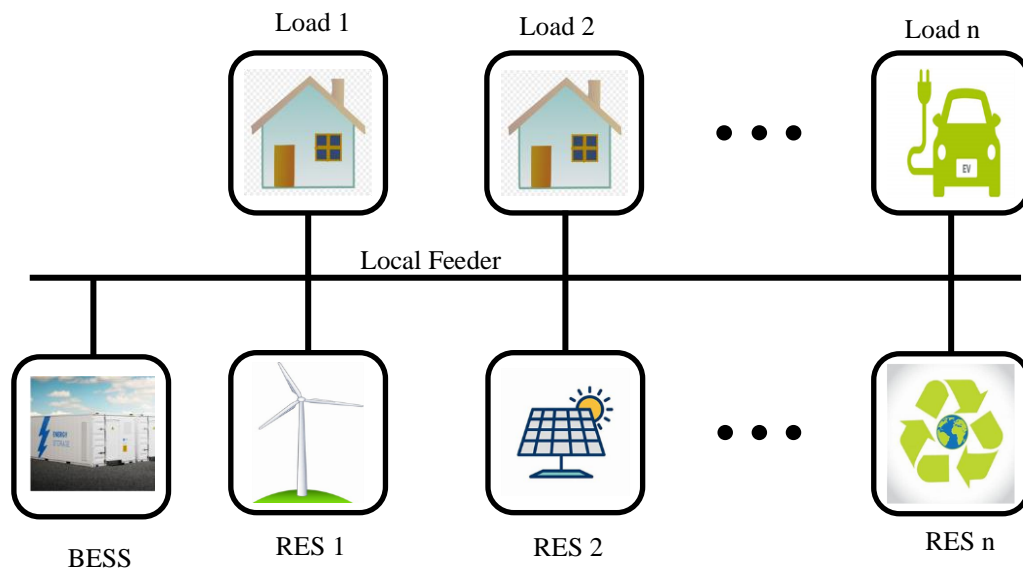


Fig. 1.3: Off-grid mode operation of RES with its local loads

- **Off-Grid Mode:** In the Off-Grid mode, RES systems are not connected to grid mains. Instead, they are designed to supply power to their local loads in a specific location, such as a remote village, island, or a small rural community, which is not connected to the main grid. A block diagram for the isolated mode of operation of RES is shown in Fig. 1.3. In the isolated mode of operation, the RES system must be designed to meet the energy needs of the location it is intended to serve. The system must also be able to provide power continuously, even when there are fluctuations in the renewable energy source, such as

during times when there is no wind or sun. Thus, they are usually supported with battery energy storage to meet the power demand when RES is not supplying power. The operation and control of RES sources are independent of the grid in this mode, and the produced power from RES is solely used to feed the nearby connected load and to the battery.

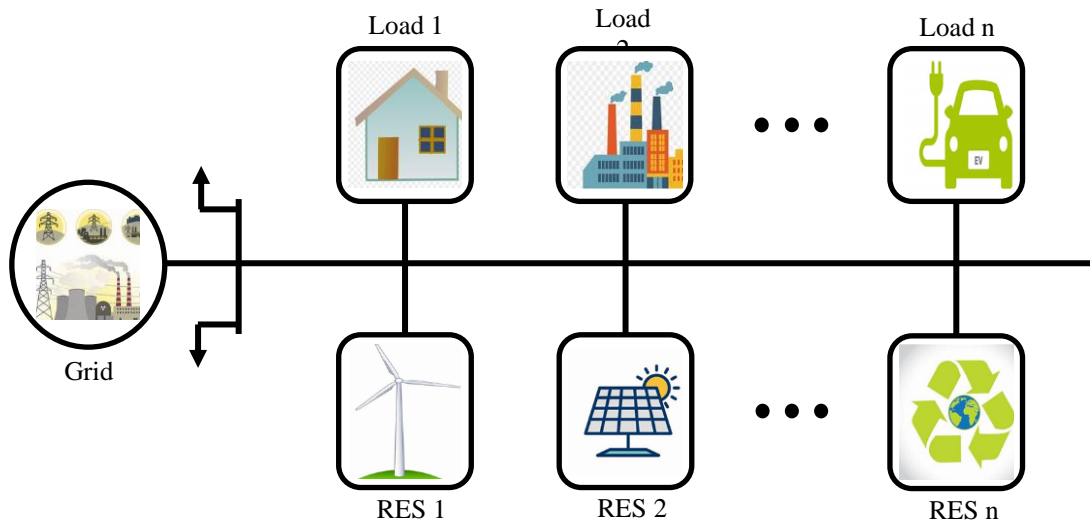


Fig. 1.4: Grid-Connected RES system with loads

- **Grid-Connected mode:** In grid-connected mode, the power generated from the RES system is fed directly into the local electric grid as shown in Fig. 1.4. This allows excess/deficit electricity to be supplied/acquired to/from the grid and can be used by other consumers on the grid.

In the Off-Grid mode the inverters operate either in grid forming mode or at least few inverters operate in grid forming mode and others in grid supportive mode (Master-Slave) configuration. While in Grid-connected RES systems the majority of inverters operate in grid-supportive mode, connecting inverter (GCI) which converts the DC power produced by the solar panels or wind turbines with a converter interface into AC power that is compatible with the grid. The inverter also helps to ensure that the

power being supplied to the grid is synchronized at the point of common coupling (PCC) and frequency and meets the grid's quality standards.

RES typically generate power in the range of a few kilowatts (kW), unless they form large plants and are usually connected to the distribution system or a sub-transmission system. The radial distribution feeder/utility grid is not significantly impacted by the integration of RES when their penetration is low, but the increasing trend of RES installation, visually rooftop photovoltaics, due to government incentives and consumer demand is making their penetration to rise. When a significant portion of the power generated on the grid comes from renewable sources like solar, wind, or hydropower, it is referred to as high penetration of RES in the grid. The percentage threshold for high penetration varies depending on the specific grid, but it is generally considered to be when renewable energy sources account for 20-30% or more of the total power generated. However, as the penetration level of RES increases, the grid faces several challenges, such as voltage and power flow disturbances, equipment's thermal ratings, fault current levels, and protection difficulties [3-5].

1.6 Intermittent nature of RES

The intermittent nature of RES is another detrimental characteristic which may hinder the stable operation of the grid when present in large concentrations. The amount of energy generated by RES varies depending on factors such as weather conditions, time of day, and season. The intermittent nature of RES can create challenges for grid operators, where the balance of electricity supply and demand needs to be struck in real time [3-10].

Here are some examples of the intermittent nature of different RES:

- **Solar power:** The amount of electricity generated by solar panels depends on the amount of sunlight they receive. Cloud cover, time of day, and season can all affect the amount of sunlight available.
- **Wind power:** The amount of electricity generated by wind turbines depends on the strength and consistency of the wind. Wind patterns can vary depending on the time of day and season.
- **Hydropower:** The amount of electricity generated by hydropower plants depends on the water flow and the head of hydro sources. These factors can vary depending on rainfall, snowmelt, and other weather conditions.

1.7 Challenges faced due to intermittent nature and high penetration of RES.

The integration of RES into radial distribution systems presents challenges for distribution system operators (DSO) who must adapt to the traditional passive approach to restrain unidirectional power flow through system control. The conventional distribution system was designed around the idea that electricity flows from the source to the load in a single direction, but the addition of RES has resulted in a more dynamic, bidirectional power flow throughout the radial feeder.

The high penetration of intermittent RES into the distribution system has raised several major issues which are also identified in the literature [3-10]:

- **Reverse power flows in the distribution system:** When local generation exceeds local demand, reverse power flows towards upstream voltage levels, causing voltage rises at most of the nodes in the radial feeder. With a further increase in RES integration, voltage volatility may further worsen.

- **Intermittent power flows in the transmission system:** Reverse power flow may result in intermittent power flows from the distribution system to the transmission system, potentially compromising the protection system.
- **Grid voltage stability:** Abnormal conditions, particularly a high share of RES compared to conventional generation, may lead to frequency instability and the voltage rises if not monitored and controlled.
- **Advanced protection system requirement for radial feeder:** The traditional unidirectional overcurrent protection of the distribution radial feeder must be upgraded to a smart protection system to prevent failure and contingencies.
- **Uneven and dynamically varying voltage in the radial feeder:** Intermittent and unpredictable power injection from RES causes voltage fluctuations throughout the feeder, harming connected motor loads. Further, this may result in a non-uniform voltage profile throughout the radial feeder instead of a drooping voltage profile from the substation to the load.
- **Infrastructure requirements:** To accommodate the variability and intermittency of RES, significant infrastructure investments may be necessary, including energy storage systems, transmission lines, and intervention of smart grid technologies.

Among the various issues discussed voltage disturbance issue is one of the major issues which needs interventions. Voltage variation in the distribution system can cause various problems in electrical systems and equipment, including:

- **Equipment malfunction:** Electrical equipment having AC-DC power supply is vulnerable to voltage fluctuations which are designed to operate within a

specified voltage range. If the voltage deviates too much from the design specifications, it can cause damage to the equipment, reduce its lifespan, or cause it to malfunction.

- **Power quality issues:** Voltage variations can also result in power quality issues such as voltage sags, swells, and interruptions. These power quality issues can cause damage to the equipment or force their shut down, resulting in costly downtime and lost production.
- **Increased energy consumption:** When voltage levels are low, equipment may draw more current to maintain its operation, which leads to increased energy consumption and higher electricity bills.
- **Safety hazards:** Voltage variations can also create safety hazards, particularly when electrical equipment malfunctions or fails to operate correctly. This can result in electrical shocks, fires, and other dangerous situations.
- **Flickering lights:** Variations in voltage can cause lights to flicker or dim. This can be annoying and distracting, especially when it happens frequently.
- **Data loss and corruption:** Sensitive electronic equipment such as computers and servers can be particularly vulnerable to voltage fluctuations. Voltage variations can cause data loss or corruption, which can be costly and disruptive to businesses and organizations.

Thus, the voltage variations in the distribution system can cause various issues, as mentioned, such as equipment malfunction, power quality problems, increased energy consumption, safety hazards, and data loss. The increasing number of renewable energy sources (RES) connected to the distribution system has made voltage level

regulation an even more critical issue. When there is light loading or no demand, the entire local generation is forced to flow back to the substation side and the voltage is bound to rise, which can be severe, well above the permissible level. This situation is more prominent when there are a significant number of RES connected to the distribution system.

To ensure the safe and efficient operation of electrical systems and equipment, it is crucial to monitor and regulate voltage levels within the specified range. It is therefore to prevent voltage variation in presence of RES, various voltage regulation methods need to be used, which may include voltage regulation transformers, voltage control devices, reactive power compensation, and energy storage systems. These methods can regulate voltage levels at different nodes and prevent voltage variations caused by RES integration, improving the efficiency and reliability of the electrical distribution system.

1.8 Scope of Work

The integration of RES into distribution systems and microgrids offers numerous benefits, including reducing greenhouse gas emissions and enhancing energy security. However, the intermittent nature of RES and their high penetration levels present several challenges, such as voltage fluctuations and power quality issues, that must be addressed to ensure a smooth transition from conventional sources to RES. Thus, this opens the scope for the following:

- **Literature Review:** Conduct a comprehensive literature review of the various voltage regulation techniques and their applications in distribution systems and microgrids.

- **Investigation of Preventive Voltage Regulation Approaches:** Explore preventive voltage regulation approaches that can be implemented in new RES systems to mitigate voltage fluctuations and maintain system stability.
- **Analysis of Curative Voltage Regulation Techniques:** Analyze curative or remedial voltage regulation techniques that can be applied to existing RES systems to address power quality issues that may arise.
- **Viability of Hybrid Voltage Regulation Techniques:** Investigate the viability of a hybrid voltage regulation technique that combines preventive and remedial methods to optimize system performance and stability.
- **Integration and Control of Voltage Regulators:** Investigate the integration and control of various voltage regulators in the microgrid/distribution system to ensure smooth operation and minimize disturbances.
- **Placement of Voltage Regulators:** Analyze where voltage regulators should be placed in the microgrid to have a better voltage profile and maintain system stability.

1.9 Organization of Thesis

The thesis is subdivided into several chapters in order to accomplish its goal. The overview of each chapter is as follows:

- **Chapter 2:** It provides a summary of the literature review about the RES and microgrid concepts, as well as the technical difficulties that microgrids face because RESs are intermittent in nature. Then this chapter provides an overview of the various voltage regulator methods and topologies used in microgrid and distribution systems. The scope of the work in various voltage regulation methods, their control and placement in the microgrid are then

described, along with the thesis's objectives.

- **Chapter 3:** This chapter investigated the different voltage regulator options, including on-load tap changing (OLTC) transformers, dynamic voltage restorer (DVR), and static synchronous compensators (STATCOM), for small radial feeders both with and without RES injections. With the use of Matrix laboratory (MATLAB) simulation, their performance is examined for load perturbation, source perturbation, and RES intermittency when RES is connected to the feeder. In this chapter, it is shown how, in microgrids with a number of RESs, employing a single device to regulate voltage is often not an adequate solution.
- **Chapter 4:** This chapter investigates hybrid combinations of two or more voltage regulation devices for maintaining the voltage profile of the feeder for the microgrid and distribution system. The OLTC transformer and DVR duo are the main emphases. The chapter also explains how a grid connection inverter can be used to regulate the power flow from RES into the microgrid so that the voltage at the point of common coupling does not go above the limits specified. The aforementioned concept is mathematically analyzed, and then control schemes for the control of the tap position of the OLTC transformer, the voltage injection of the DVR, and the current injection from the grid-connected inverters (GCI) of the RES are discussed. Later in the chapter, the performance of the duo (OLTC transformer and DVR) and trio (OLTC transformer, DVR, and GCI of RES) is assessed for various types of perturbation and operating conditions.
- **Chapter 5:** This chapter has explored an 11-node radial microgrid with a number of RES connected to it. In this chapter, the impact on voltage levels

brought on by RES's high penetration has been explored, followed by a discussion of how voltage problems can be fixed using series voltage regulators. In addition, an analytical approach for determining the node voltage and branch current based on ABCD characteristics is presented. This technique aids in determining the node where the voltage regulators should be connected and what their capacity will be. A MATLAB simulation is also carried out at the end of the chapter to support and validate the approach.

- **Chapter 6:** The ABCD parameter-based analysis discussed in the preceding chapter is extended in this chapter to determine the number of connected voltage regulators as well as their location within the 11-node radial microgrid under consideration. The MATLAB simulation was used to validate the same, and from the simulation's results, a voltage profile was constructed.
- **Chapter 7:** This chapter summarizes the thesis research work challenges, contributions, and the direction of future work.

Chapter 2

LITERATURE SURVEY

2.1 General

Rooftop RES such as solar and wind power are becoming an integral part of distribution systems as their penetration into the grid is growing by leaps and bounds [11-12]. However, the intermittent nature poses major issues like voltage fluctuations and instability in the distribution system [13-14]. To address the issue, voltage regulation is a necessity for maintaining a uniform, smoother but slightly drooping voltage profile from source to load [15-19]. Various voltage regulation techniques are reported in the literature for distribution feeders having sufficient penetration of intermittent RES. This chapter provides a detailed insight into the survey of literature on the techniques, which include OLTC transformer, STATCOM, DVR etc. The chapter also outlines the objectives of the thesis, which include evaluation and comparison of various voltage regulation techniques to converge on the optimal strategy for voltage regulation in distribution systems and microgrids.

2.2 Need for the voltage regulators.

Voltage regulation becomes essential in distribution feeders/microgrids when a large proportion of intermittent renewable energy sources are connected to the system [15-19]. The voltage regulators are entrusted with the maintenance of a stable voltage level within acceptable limits. Intermittent renewable energy sources, such as wind and solar power, generate electricity inconsistently, depending on the weather conditions [20-21]. As a result, the voltage level in the distribution feeder fluctuates significantly

[22-25]. If the voltage exceeds the acceptable limits, it can damage the connected equipment and cause power outages [25-28]. A voltage regulator helps in mitigating the effects of voltage fluctuations by adjusting the voltage level in the distribution feeder within prescribed limits [29-30] so that the electricity supply becomes more reliable. Additionally, voltage regulation also helps in improving the efficiency of the distribution system [31-33]. By maintaining a stable voltage level, voltage regulation can reduce the losses associated with transmitting and distributing power [31-35]. This, in turn, can help to reduce the cost of power for consumers [34-38].

The solution to the voltage issues which are evolved due to increased penetration of renewable energy sources in the distribution system (or sub-transmission system) can be resolved in two ways: preventive measures and curative measures.

2.3 Preventive Measures for voltage regulation

Preventive measures should be taken for renewable energy sources (RES) that will be integrated into the distribution system in the present times and in future. Two potential solutions include Smart Grid Connecting Inverters (GCI) and Battery Energy Storage Systems (BESS) [38-39].

2.3.1 Smart Grid Connecting Inverter (GCI)

Smart GCIs for RES are networked intelligent inverters capable of having real-time communication with other network stakeholders and other connected inverters. They regulate voltage in the distribution system/ microgrid and lend their hand in maintaining the frequency of the grid by adjusting the output of connected RES [38-43]. When there is excess power generated by the solar panels, smart inverters can

help in regulating the voltage by moving away from the MPPT point and preventing it from exceeding the safe operating limits [38-43]. They can also help in mitigating the voltage fluctuations caused by intermittent renewable energy sources, such as solar and wind [38-43]. Smart inverters use advanced control algorithms to adjust the power output of solar panels in response to changes in the grid voltage. They can also support the grid by providing reactive power, which can help in regulating the voltage levels and maintain a stable power supply [40-43]. In addition, smart inverters can communicate with other devices in the electricity grid, such as energy storage systems and other inverters, to coordinate their actions and optimize their performance [41-43]. This can help in ensuring that the grid is operating efficiently and effectively.

While smart inverters provide many benefits to derive voltage regulation in modern electricity grids, there are also some limitations to their use. Some of the limitations of smart inverters while in service for voltage regulation include:

- **Compatibility issues:** Smart inverters may not be compatible with all types of renewable energy systems or grid configurations, which can limit their effectiveness for voltage regulation [43-49].
- **Lack of standardization:** There is currently no global standard for smart inverter technology, which can create interoperability issues and make it difficult to integrate different systems and devices [43-49].
- **Cost:** Smart inverters are generally more expensive than traditional inverters, which can make them less accessible for some consumers or limit their adoption in certain markets [43-49].
- **Communication and coordination challenges:** Smart inverters rely on communication and coordination with other devices in the grid to optimize

their performance, which can be challenging in large and complex grid systems [43-49].

- **Limited power capacity:** Smart inverters may have limited power capacity compared to traditional inverters, which can limit their effectiveness for voltage regulation in larger solar installations or grids [43-49].

2.3.2 Battery Energy Storage System (BESS)

A battery energy storage system (BESS) offers a viable solution for voltage regulation in a radial distribution system/microgrid with intermittent renewable energy sources. Energy storage refers to the amount of energy that can be stored and discharged with a high level of efficiency.

The BESS can store excess energy generated by intermittent RES during periods of high production and discharge this stored energy during lean periods often referred as peak shaving and valley filling/load shifting [50-57]. This helps in regulating the voltage in the microgrid, which is critical to ensuring the reliable operation of the electrical system.

However, it's important to note that the cost of a BESS is still relatively high, and the economics of using a BESS for voltage regulation in a microgrid will depend on a number of factors, such as the cost of electricity, the size of the microgrid, and the availability of other storage options [50-57].

Overall, a battery energy storage system offers an effective solution for voltage regulation in a microgrid with intermittent RES, but the decision, for their incorporation, should be done after careful evaluation of the specific circumstances of the microgrid.

Typically, both the preventive solutions (GCI and BESS) are installed in conjunction with high-capacity RES, often in the order of MW. Installing them with every small RES would increase the cost of the system. Generally, they are installed with RES to be installed in sub-transmission systems [50-57].

Other preventive measures include proper operational planning for effective energy management and efficacy of controlling energy flow, demand response programs to reduce demand during peak periods, incentivization for the use of renewable energy, and interconnection standards to ensure safe and reliable integration of RES into the grid. However, these solutions require low-latency bidirectional communication, which may prove to be a good solution in the future when the conventional grid fully transitions towards the smart grid.

2.4 Curative Measures for voltage regulation

Curative measures refer to solutions that are implemented to address issues with grid-connected renewable energy sources that are already installed, as well as those that may be installed and connected to the grid in the future. These measures also apply to smaller capacity renewable energy sources, such as rooftop PV systems installed in consumer premises that cannot adequately support the system with battery storage.

To regulate voltage, various devices such as On Load Tap Changing (OLTC) transformers, static synchronous compensators (STATCOMs), dynamic voltage restorers (DVRs) and their hybrid combination are employed as curative measures [58-60].

2.4.1 On-Load Tap Changing Transformer (OLTC-T)

OLTC transformers are a type of transformer that is used to regulate voltage in electrical power systems through changes in the tap positions, in turn changing the turns ratio of the transformer. They are designed to adjust the voltage output of a transformer by changing the position of the transformer's taps while the transformer is still connected to the system and supplying power [61-71]. Fig. 2.1 shows a block diagram of a normal transformer and an OLTC transformer. The OLTC transformer is typically installed in the substation and can be remotely controlled.

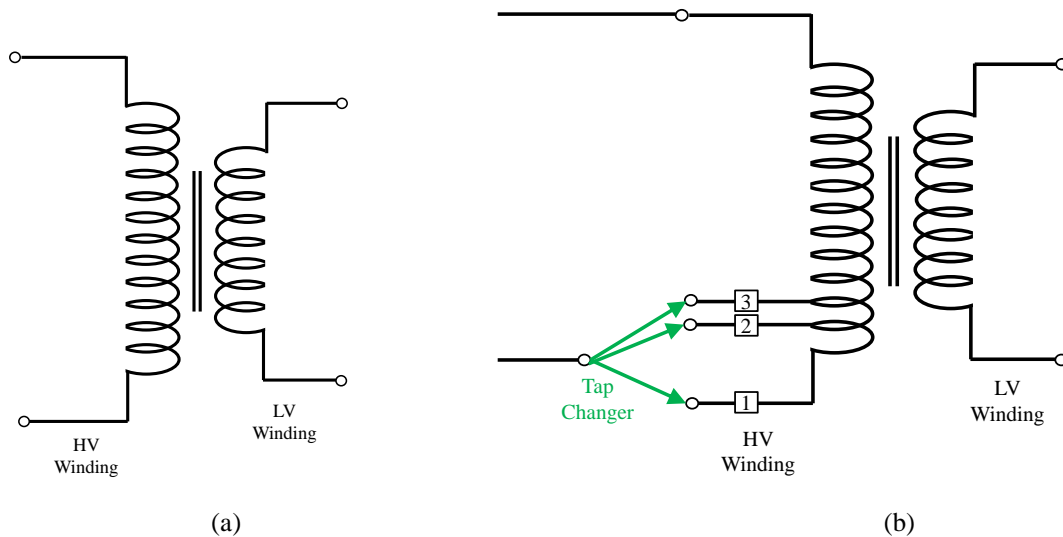


Fig. 2.1: (a) Block diagram of a normal transformer. (b) Block diagram of an OLTC transformer

The effectiveness of OLTC transformers in voltage regulation depends on their control algorithms, which must be able to respond quickly to voltage fluctuations and adjust the taps accordingly [61-71]. Mechanical tap-changers are conventionally used to change taps using mechanical contact switches, but their performance is affected due to long tap changing times and frequent maintenance requirements [63-71]. Recent advancements in the literature have introduced various solid-state devices to change

tap positions more efficiently [64-73]. Advanced control algorithms, such as fuzzy logic and artificial neural networks, have been also proposed in the literature to improve the performance of OLTC transformers.

Intermittency of RES is reportedly addressed by using OLTC transformers in combination with intermittent RES [64-71]. Regulation of voltage levels through adjustment of tap ratio of the transformer in real time allows precise control of voltage levels, even in systems with intermittent RES. OLTC transformers are commonly used in distribution systems with intermittent renewable energy sources (RES) to maintain proper voltage levels and ensure stable operation of the system. The following literature survey presents some major merits/demerits of OLTC transformers and their use in voltage regulation:

- OLTC transformers are an effective means of regulating voltage in distribution systems with intermittent RES sources, such as wind turbines and solar PV systems through the adjustment of the transformer's taps to compensate for fluctuations in voltage caused by these sources [63-66] [71-73].
- In systems with high levels of intermittent RES, multiple OLTC transformers may be needed to ensure proper voltage regulation. Coordination between these transformers and other control devices, such as capacitor banks and voltage regulators, is critical in maintaining stable system operation [61] [63] [67] [71-74].
- The maintenance requirements of OLTC transformers can be significant, particularly in systems with high levels of intermittent RES. Regular inspections and maintenance are needed to ensure proper operation and prevent

equipment failures [75-78].

- The cost of OLTC transformers can be significant, particularly in systems where multiple transformers are needed. However, the cost of OLTC transformers may be justified by their ability to improve system stability and reliability [63] [79].

Some potential challenges that may be faced when using OLTC transformers for voltage regulation in distribution systems with intermittent renewable energy sources (RES):

- **Fast voltage fluctuations:** Intermittent RES sources such as wind turbines and solar PV systems can cause rapid fluctuations in voltage levels. OLTC transformers may not be able to respond quickly enough to these fluctuations, which could result in voltage violations and potential damage to equipment [80-81].
- **Limited control range:** OLTC transformers typically have a limited range of tap positions that they can switch between. In systems with high levels of intermittent RES, the tap positions may need to be adjusted frequently and over a wide range. OLTC transformers may not be able to accommodate these changes, which could result in voltage violations [62-73] [82].
- **Maintenance requirements:** OLTC transformers require regular maintenance to ensure proper operation. In systems with high levels of intermittent RES, the OLTC transformer may need to be adjusted frequently, which could increase maintenance requirements and costs [75-78].

- **Coupled mode voltage regulation:** OLTC transformers regulate voltage by changing the tap position on the transformer, which affects both real and reactive power flow in the system. When renewable energy sources (RES) such as solar or wind power are connected to the system, they typically provide real power without contributing significantly to reactive power. Therefore, when OLTC transformers are used to regulate voltage in a system with RES, the changes in reactive power flow caused by the tap changes can result in unwanted effects such as voltage fluctuations, increased losses, and reduced efficiency. To address this issue, alternative voltage regulation methods involving reactive power compensation or advanced control techniques are requisite for minimizing the impact on real power flow while regulating voltage [83-85].
- **Coordination with other control devices:** OLTC transformers may need to be coordinated with other control devices, such as capacitor banks and voltage regulators, to ensure proper voltage regulation in the system. However, coordinating multiple control devices can be challenging and may require sophisticated control algorithms [86-89].

2.4.2 Static Synchronous Compensator (STATCOM)

Power-electronics converter acting as STATCOM regulates voltage in distribution feeders, while connected in the shunt. It injects current at the point of common coupling (PCC) with an adequate amount of reactive power to regulate the voltage and can be installed near the renewable source in a radial feeder with high penetration of renewable energy sources [90-97]. However, the role of GCI, whose primary objective

is to inject real power into the grid is also entrusted to deal with limited reactive power, depending upon the available capacity of the VSI [92-97]. Particularly, in the night time the role of PV GCI solely shifts to reactive power transactions to regulate the grid voltage. The STATCOM can be controlled to inject or absorb reactive power depending on the voltage level and power flow in the feeder, which helps maintain the voltage within acceptable limits and prevent voltage violations [92-101]. Additionally, it provides other benefits such as improved power factor, increased system stability, and reduced losses [102-108]. However, the installation and operation of a dedicatedly connected STATCOM can be expensive, so its use must be carefully evaluated to ensure that it is cost-effectiveness [109-114].

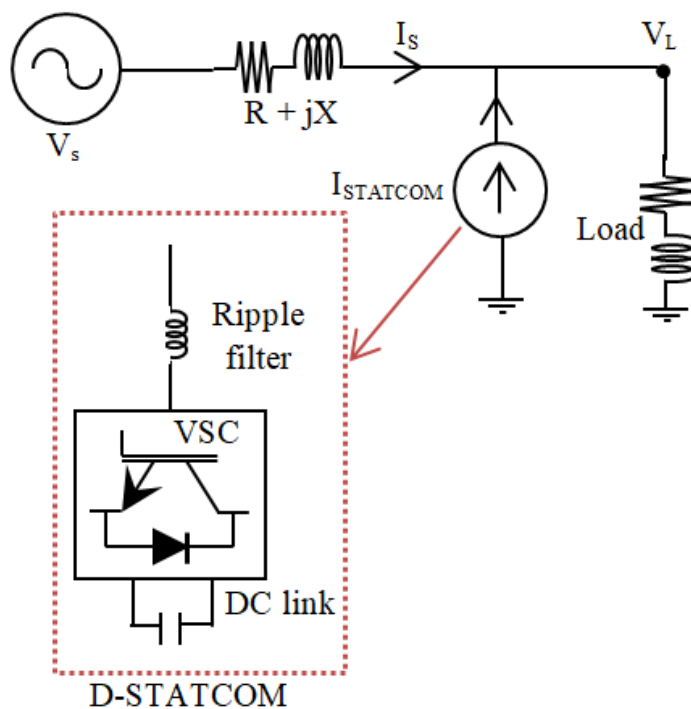


Fig. 2.2: Block diagram of STATCOM

A block diagram for STATCOM connected to a radial feeder is shown in Figure 2.2. STATCOM is composed of several components that work together to regulate voltage

and improve power factors in distribution systems. Power electronic devices, such as IGBTs or GTOs, are switched on and off at PWM switching frequency to generate or absorb reactive power [92-103]. For the use of dedicated STATCOM, the DC capacitor temporarily store energy from source to mitigate the switching and construction losses of power electronic devices, while control systems monitor voltage and power flow in the feeder and adjust the STATCOM output accordingly [93-100]. Filters eliminate harmonics and other high frequency components generated by the switching of the power electronic devices, and power frequency transformers, in case used, match the voltage and impedance levels between the STATCOM and the feeder [95-107]. By working together, these components can regulate voltage, improve power factor, and enhance distribution system stability [98-105].

The capacity of a STATCOM is limited by its power rating, which is determined by the size of the power electronic devices and the DC capacitor [101-108]. The power rating of a STATCOM is typically much smaller than the total power capacity of the feeder it is connected to.

In the systems with high levels of intermittent renewable energy sources (RES), such as solar and wind, the power flow in the feeder can vary significantly over time. During periods of high power flow, the STATCOM may not have enough capacity to absorb all of the reactive power needed to maintain the voltage within acceptable limits [109-114].

This limitation can be exacerbated by the fact that STATCOMs are typically installed at the point of interconnection between the feeder and the renewable source. This means that the STATCOM may have to regulate voltage for a large portion of the

feeder, which can further reduce its capability to regulate the voltage.

To address these limitations, utilities may need to install multiple STATCOMs along the feeder or use other grid stability measures such as energy storage, frequency regulation, and demand response [111-115]. Careful planning and coordination are required to ensure that these measures are integrated effectively and efficiently.

When most of the loads and sources are real power, the reactive power demand in the system is typically low, and the voltage regulation requirements are not as stringent. The decision to use a STATCOM for voltage regulation in a system with primarily real power loads and sources will depend on the specific requirements of the system and the cost-benefit analysis of installing and operating a STATCOM.

2.4.3 Dynamic Voltage Restorer (DVR)

Dynamic Voltage Restorer (DVR) is connected in series and they inject series voltage into the system and by moving the voltage phasor, regulate the voltage. It can be installed at the point of interconnection between the feeder and the renewable source in radial feeders with renewable energy sources. The DVR can be controlled to inject or absorb reactive power by amending the voltage phasor, depending on the voltage level and the power flow in the feeder [116-120]. This will help to maintain the voltage within acceptable limits and prevent voltage violations. The use of DVR in radial feeders with renewable energy sources can provide voltage regulation, improved power factor, increased system stability, and reduced losses [118-123]. DVR is a cost-effective solution compared to the installation and operation of STATCOM [116-123]. The installation of a DVR does not require any additional equipment and can be

installed on the existing system. The only drawback is its short circuit condition and prevention of saturation of its injection transformer.

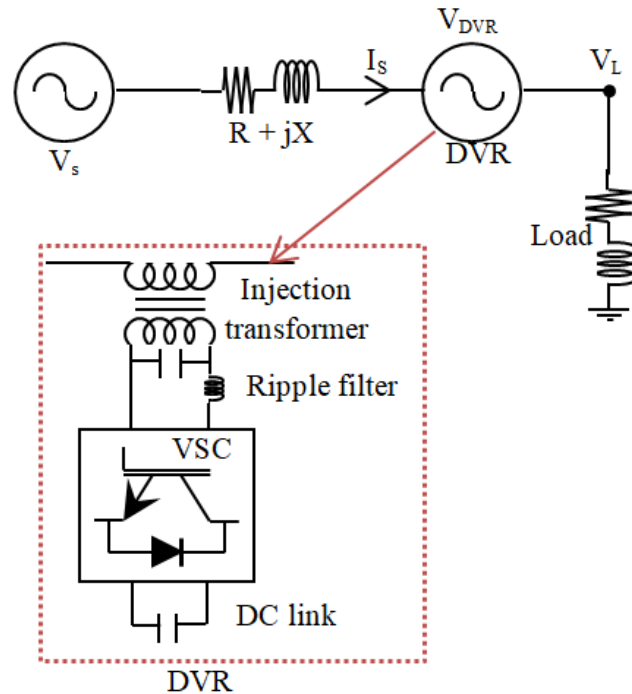


Fig. 2.3: Block diagram of DVR

The DVR comprises of the following components:

- **Voltage source converter (VSC):** It generates an output voltage at an appropriate angle so as to compensate for voltage disturbances. It is composed of a set of power electronic switches and injection transformer that can generate an output voltage of any desired magnitude, angle and frequency.
- **Energy storage device:** Often for reactive power transaction capacitor bank is used to hold the voltage at DC bus and to absorb power from the grid corresponding to switching and construction losses of the VSC, so as to generate the requisite compensating voltage.

- **Injection transformer:** It is used to connect the VSC to the distribution feeder and provides galvanic isolation between them. It can also be used to step-down the voltage as needed. The transformer is an important component of DVR, and it should be designed such that losses in the transformer are minimized besides robust characteristics to avert saturation of the core. For this purpose, often sandwich winding is used.
- **Control system:** It monitors the voltage waveform in the power system and initiates the VSC to inject the compensating voltage when a voltage sag/swell is detected and/or reactive power is transmitted for enabling voltage regulation. It may also include protective features to ensure safe operation of the DVR.
- **Filters:** They are used to suppress high-frequency harmonics or noise generated by the VSC or the power system, ensuring a clean output voltage waveform.

The DVR works by injecting a voltage of the requisite magnitude and with appropriate phase, thus restoring the voltage to its nominal value. The injection of this voltage is achieved using the VSC that is connected to the feeder through the injection transformer. The VSC can quickly and accurately control the voltage to be injected into the feeder, allowing it to regulate the voltage or compensate for voltage disturbances within a few milliseconds.

Regulation strategies for DVR aim to make the load voltage nearly equal to the rated value, using methods such as pre-sag/swell compensation, in-phase compensation, and minimum energy injection [123]. Among these, minimum (optimized) energy injection is the most effective method for voltage regulation, as it compensates for

voltage while minimizing the active power supplied/absorbed by the compensator, with increased depth of compensation [124-128]. The injected voltages are in quadrature with the line/feeder current to provide reactive power-based compensation. The controlling circuit of the VSC of the DVR determines the output voltage supplied by the system. Linear and non-linear control methods are available for the DVR [129]. Linear voltage control methods proposed in the literature include the feed-forward method, feedback method, and multi-loop controller, which are simple and fast approaches [124-128]. In the feed-forward method, the supply voltage is compared with the reference voltage, and the DVR injects the required voltage if the difference exceeds the permissible limit. The feedback control method compares the load voltage with the reference voltage and supplies the difference voltage to the feeder [127] [130-132]. This method offers the advantage of better accuracy than feed-forward control, but it is complex and has a time delay. The multi-loop controller uses two loops to control the DVR voltage, with an additional inner loop controlling the load current, filter capacitor, and/or inductor current [126] [131]. This method combines the strengths of both feed-forward and feedback-control strategies but at the cost of higher complexity and time delay. Non-linear controllers proposed in the literature include artificial neural network (ANN), fuzzy logic (FL), space vector PWM, robust control, sliding mode control, hysteresis control, and repetitive control [132-140].

While the DVR is a useful device for regulating voltage in microgrids or distribution systems with intermittent renewable energy sources, it does have some limitations:

- Limited energy storage: The energy storage device used in the DVR, such as a capacitor bank, has limited energy storage capacity. This limits the duration for which the DVR can regulate the voltage, while dealing with real power the

DVR need even storage support [141-144].

- Limited scalability: The DVR is designed to regulate the voltage at a single point in the distribution system or microgrid. This limits its scalability as it may require multiple DVRs to regulate the voltage across the entire system, increasing its overall cost [135-144].
- High cost: Although DVR is a cost-effective solution compared to the installation and operation of a STATCOM, it is still a relatively expensive device. The cost of the DVR can be a significant barrier to its adoption in some applications [135-144].
- Critical Protection requirements: The DVR since connected in series is sensitive to flow of current through its transformer. Any short circuit appearing on the load side, puts all the voltage drop across it, thus builds very high voltage across the DC bus which could pose threat to the hardware, hence require very fast acting protection/bypass system.

2.4.4 Hybrid Voltage Regulators

Using an individual voltage regulator can have certain drawbacks in a radial microgrid or distribution feeder. A hybrid combination of voltage regulators can be installed in the feeder to overcome their drawbacks and reap their continued benefits [145-151]. The hybrid combination typically may consist of an On-Load Tap-Changing (OLTC) transformer and a dynamic voltage restorer, or OLTC with STATCOM. The OLTC transformer is used for larger voltage adjustments, such as when the voltage is too low or too high. Meanwhile, the dynamic voltage restorer or STATCOM acts in the middle

of the steps to make fine adjustments. Additionally, the dynamic voltage restorer or STATCOM can address fluctuations and harmonics in the system, which further improves power quality.

Combining the OLTC transformer and the dynamic voltage restorer or STATCOM in a hybrid voltage regulator can provide fast, accurate voltage regulation in radial microgrids or distribution feeders. However, the cost of a hybrid voltage regulator can be higher than that of a traditional tap-changing transformer. Therefore, careful consideration must be given to the specific requirements and constraints of the system before choosing a voltage regulation solution.

The literature largely reported the use of OLTC-based transformers in combination with a dynamic shunt regulating device [152-154]. The operation of OLTC transformers with series devices needs further exploration to investigate improvement in performance and regulation in microgrids. Furthermore, as the penetration of renewable energy sources increases into the distribution system, the hybrid combination needs to be studied differently.

2.5 Concept of Microgrid

The increased penetration of Renewable Energy Sources (RES) in distribution systems necessitates the analysis of the radial distribution system with a large penetration of RES. Instead of considering the entire complex distribution system, it is beneficial to fragment it into smaller sections for better analysis. This approach allows for the consideration of a small section of the radial distribution feeder that includes multiple small RES of the order of kW and several distributed loads connected to it, which can

be viewed as a radial grid-connected microgrid with intermittent RES.

Fig. 2.4 and Fig. 2.5 provide a pictorial representation of a typical distribution system and a radial microgrid with numerous RES sources connected to it, respectively. In the considered microgrid, the maximum power generated by RES is around 70-80% of the locally rated load connected.

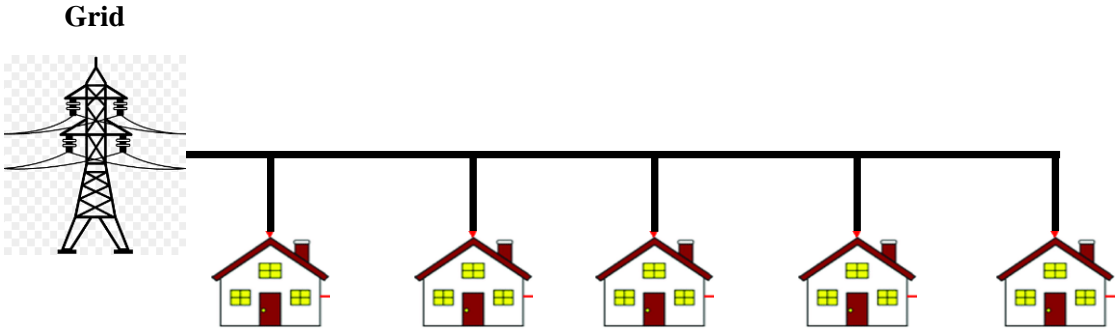


Fig. 2.4: Distribution feeder without RES

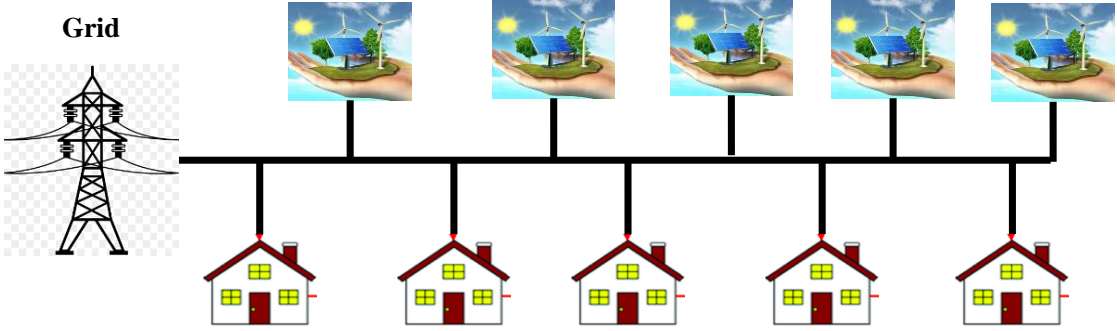


Fig. 2.5: Radial Microgrid/Distribution feeder with RES

2.5.1 Control of Voltage Regulators

Voltage regulation is crucial for the stable and reliable operation of a feeder, and the control of voltage regulators plays a critical role in achieving this. Voltage regulators control the voltage level at their PCC in the feeder by adjusting the transformer taps position in the case of an OLTC transformer or modifying the VSC output in the case

of a power electronics-based voltage regulator.

Without proper control of voltage regulators, the output may not be optimized, and the voltage at their respective PCCs may not be regulated. As the penetration of distributed energy resources increases, a single voltage regulator may not be sufficient to regulate the voltage, and multiple voltage regulators may need to be installed on the feeder. Therefore, it is essential to choose a suitable control method for the voltage regulator.

The simplest way to control voltage regulators is based on local measurements, which do not require data transfer between different devices/components of the microgrid/distribution system [155-159]. The controller performs its action if the voltage exceeds the operational limits at one of the monitored nodes. However, the effectiveness of this control is limited by the network characteristics, such as the different load flow characteristics of the branch where the device is installed. This approach requires a communication infrastructure with limited requirements between selected nodes and the controller [160-165].

On the other hand, coordinated voltage control methods determine their control actions based on information about the whole system, requiring data transfer between network nodes [158-164]. The use of coordinated local control allows solving of conflicts that may appear in the previous approach, where the regulator may not be able to maintain the voltage within the limits in the whole network. The critical nodes and controlled generators must be appropriately selected for this control [159-165]. However, the requirements on the communication infrastructure are higher than for the previous method.

There are various centralized or coordinated voltage control methods in distribution systems that have been developed with different levels of complexity, effectiveness, communication requirements, and investment costs. It is essential to choose the most suitable control method for a particular distribution system to ensure stable and reliable operation.

2.5.2 Location of Voltage regulators

With the high penetration level of RES, a single voltage regulator may not be sufficient to regulate the voltage throughout the feeder/microgrid. Therefore, before installing the system, a proper analysis is required to determine the appropriate number of voltage regulators and their optimal placement in the microgrid [166-171]. The location of a voltage regulator in a microgrid is important because it plays a critical role in maintaining a stable voltage profile throughout the system. In a microgrid, voltage fluctuations can occur due to a variety of factors, including intermittent renewable energy sources (RES), load fluctuations, and faults. A voltage regulator is therefore entrusted to maintain the voltage at a desired level by adjusting the voltage magnitude and/or phase angle.

There are various algorithms and techniques that can be used to determine the optimal placement of voltage regulators in a microgrid. These algorithms typically involve optimization techniques and mathematical models that take into account various system parameters, such as the location of loads, the topology of the microgrid, the type and capacity of the voltage regulators, and the voltage profile requirements [156-171].

2.6 Research Opportunities/ Identified Research Gap

The following opportunities for further research have been identified based on a comprehensive literature review of voltage regulators made for microgrids with intermittent renewable energy sources:

- Investigating both preventive and curative measures for voltage regulation, considering various devices such as OLTC transformers, STATCOM, BESS, DVR, and smart GCI, and selecting a suitable voltage regulator for achieving an optimum voltage profile in the radial microgrid.
- Exploring the effectiveness of using hybrid combinations of two or more regulating devices, since a single voltage regulation device may not effectively regulate voltage in a radial microgrid with a large number of RES.
- Developing a control mechanism for OLTC transformers that takes into account more than just voltage changes while changing tap positions and ensuring that dynamic devices like DVR respond immediately and regulate voltage instantly.
- Examining the role of smart grid connecting inverters of renewable energy sources in controlling the injection of power into the grid to maintain voltage within the limit.
- Analysing the microgrid into smaller sections, connecting smaller rating voltage regulators at certain distances, and investigating the location and capacity of voltage regulators to achieve a better voltage profile in autonomous mode.

These research gaps provide ample opportunities to explore new and uncharted territories in the field of efficient and effective voltage regulation for microgrids with intermittent RES.

2.7 Objectives of Thesis

Based on the research opportunities objective(s) of this research work and thesis are as follows:

- **Investigation of voltage issues in Micro-grid with high penetration of intermittent Renewable energy sources (RES):** The primary objective of this research is to investigate the voltage issues that arise in microgrids with a high penetration of intermittent renewable energy sources. This will involve identifying the key factors that contribute to voltage fluctuations in such systems and understanding the underlying causes of these issues.
- **Study of various solutions available for voltage regulation in micro-grid:** Another objective of this research is to study the various solutions available for voltage regulation in microgrids with high RES penetration. This will involve reviewing the existing literature on voltage regulation techniques and identifying the most promising solutions that can be applied to microgrids.
- **Study for Preventive Measures (for the new system to be inserted) and Curative (already integrated systems) for voltage issues in the microgrid with intermittent RES:** The research will also focus on identifying preventive measures and curative solutions that can be applied to both new and existing microgrid systems to address voltage issues arising from intermittent

renewable energy sources.

- **Analysis, Simulation, Design, Control, and development of a few suitable solutions:** The final objective of this research is to analyse, simulate, design, control, and develop a few suitable solutions for voltage regulation in microgrids with high-RES penetration. This will involve developing and devising several solutions to identify the most effective and efficient techniques that can be applied to microgrid systems. The proposed solutions will be evaluated based on their effectiveness in regulating voltage and maintaining the voltage profile of the microgrid.
- **Identification of the optimal location and capacity of identified voltage regulators in microgrids with high RES penetration:** Another objective of this research is to identify the optimal location and capacity of voltage regulators in microgrids with high RES penetration. This will involve conducting a detailed analysis of the microgrid system, including the RES sources, loads, and network topology, to determine the most effective locations and capacities for voltage regulators. The proposed solutions will be evaluated based on their effectiveness in regulating voltage considering factors such as the size and complexity of the microgrid system in autonomous mode.

Chapter 3

Analysis, Simulation, and Performance Evaluation of Voltage Regulators

3.1 General Overview

The reliable and efficient operation of a radial microgrid or distribution feeder is dependent on a stable and regulated voltage supply. Voltage regulators are essential components of power systems that maintain a constant voltage level and ensure a smooth and uninterrupted flow of electricity. With the increasing demand for electricity and the populous integration of renewable energy sources, voltage regulators play an even more critical role in maintaining the voltage profile of the radial microgrid or distribution feeder.

To ensure efficient and reliable operation, it is often essential to analyze, simulate, and evaluate the performance of voltage regulators. Analytical and simulation tools provide a powerful platform for studying the behaviour of voltage regulators under different operating conditions and evaluating their performance in real-time. Performance evaluation helps in identifying the strengths and weaknesses of voltage regulators, providing insights into their design and operation.

Moreover, voltage regulators have a significant impact on the power quality of the microgrid or distribution feeder. Poor voltage regulation can result in voltage fluctuations, voltage sags, and voltage surges, which can affect the performance of connected sensitive electrical equipment. Therefore, it is crucial to regularly evaluate the performance of voltage regulators to ensure the maintenance of stability and

regulation of voltage supply for and meeting out the required power quality standards.

3.2 OLTC Transformer

An On-Load Tap Changing Transformer (OLTC-T) is commonly utilized in radial microgrids or distribution feeders that feature intermittent renewable energy sources (RES) to regulate the voltage supply. These transformers have multiple taps on their high voltage winding, and a tap changer mechanism to enable voltage adjustments while the transformer remains in operation. This feature makes it possible to compensate for voltage fluctuations that may arise from the variability of RES such as solar or wind power. The tap changer mechanism is typically controlled by a voltage regulation control that monitors the voltage on the grid and adjusts the transformer taps accordingly. OLTCs are primarily installed on the high voltage winding of the transformer, as it typically experiences lower current levels.

3.2.1 Analysis of OLTC transformer

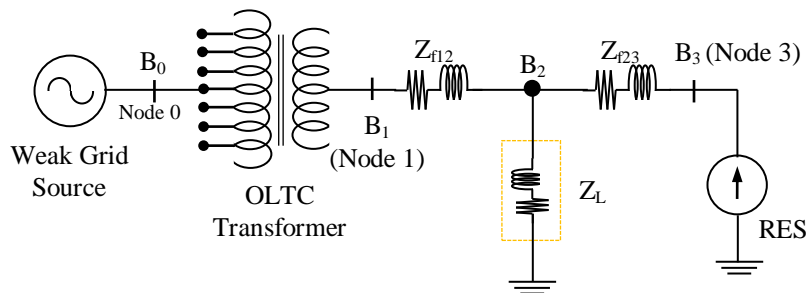


Fig. 3.1: Single line diagram of OLTC transformer for voltage regulation in radial microgrid with RES penetration

Fig. 3.1 shows a block diagram of OLTC transformer connected in a radial microgrid/distribution feeder with intermittent RES. The source is regarded as a weak power source, being very far off from the generator which witnessing substantial line impedance OLTC-T, intermittent RES distributed line impedance, and loads. The

power extracted from the weak source is designed to cater only to the base load in the feeder. The primary responsibility of OLTC-T is to regulate the voltage on the output side of the nodes in order to maintain a unidirectional downward power flow. This is achieved by regulating the voltage within a range of $\pm 10\%$, with a step size of $\pm 0.2\%$. The load comprises of 3-phase series RL loads, which consume both real and reactive power. Feeder line impedances are considered present at two different locations, one between OLTC-T and load, and the other between the load and RES for analysis, simulation, and performance evaluation of the current case. The RES is considered as a variable current-controlled source representing current-controlled GCI, which is located towards the end of the feeder, representing the worst-case scenario for voltage regulation and power reversal for the considered circuit in Fig 3.1. The interfacing inverter (GCI) for RES is controlled to provide the maximum power output from the RES duly tracked by MPPT controller representing the PV-fed GCI.

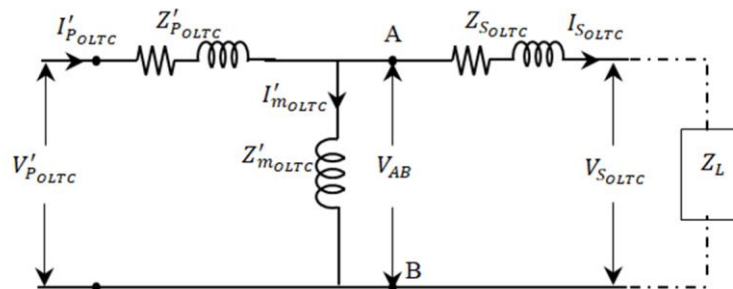


Fig. 3.2(a) Equivalent circuit of OLTC transformer referred on secondary side of transformer

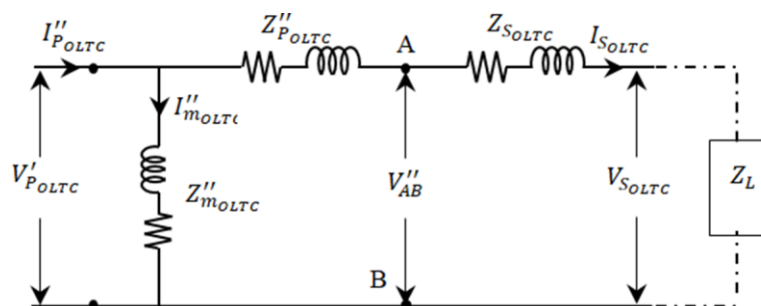


Fig. 3.2(b): Simplified equivalent circuit of OLTC transformer referred on the secondary side of transformer

Analysis of OLTC-T is seen from its equivalent circuit referred to the secondary side shown in Fig. 3.2(a). Since the taps are only present on the primary side of the OLTC-T, changes in tap positions only affect the impedance of the primary winding, resulting in the change in referred impedance of the primary winding on the secondary side of the OLTC-T ($Z'_{P_{OLTC}}$), while the impedance of the secondary winding of the OLTC-T ($Z'_{S_{OLTC}}$), reflect negligible variations. The equivalent circuit shown in Fig. 3.2(a) is further simplified across terminal AB for clear observation of the differences in voltage and impedances with changes in the tap positions, and the resulting simplified equivalent circuit is shown in Fig. 3.2(b). The system parameters such as primary side referred voltage and current and secondary side voltage and current are expected to be the same in the new transformed circuit, i.e.

- $V'_{P_{OLTC}} = V''_{P_{OLTC}}$;
- $I'_{P_{OLTC}} = I''_{P_{OLTC}}$;
- $V_{S_{OLTC}} = V''_{S_{OLTC}}$;
- $I_{S_{OLTC}} = I''_{S_{OLTC}}$.

The no load current for the simplified equivalent circuit as seen from Fig. 3.2(b) is given by:

$$I''_{m_{OLTC}} = I''_{P_{OLTC}} - I_{S_{OLTC}}.$$

$$\text{But } I'_{P_{OLTC}} \cong I''_{P_{OLTC}}$$

Therefore,

$$I''_{m_{OLTC}} \cong I'_{P_{OLTC}} - I_{S_{OLTC}}$$

$$\Rightarrow I''_{m_{OLTC}} \cong I'_{m_{OLTC}}$$

Voltage across terminal AB in Fig. 3.2(a) is:

$$V_{AB_{OLTC}} = V'_{P_{OLTC}} - Z'_{P_{OLTC}} I'_{P_{OLTC}}$$

and voltage across terminal AB in Fig. 3.2(b) is:

$$V''_{AB_{OLTC}} = V''_{P_{OLTC}} - Z''_{P_{OLTC}} I_{S_{OLTC}} = V'_{P_{OLTC}} - Z''_{P_{OLTC}} I_{S_{OLTC}}.$$

However, the voltage across terminal AB is assumed to be approximately equal before (Fig. 3.2(a)) and after (Fig. 3.2(b)) transformation. Therefore,

$$\begin{aligned} V_{AB} &\cong V''_{AB} \\ \Rightarrow V'_{P_{OLTC}} - Z'_{P_{OLTC}} I'_{P_{OLTC}} &= V'_{P_{OLTC}} - Z''_{P_{OLTC}} I_{S_{OLTC}} \\ \Rightarrow Z''_{P_{OLTC}} &= Z'_{P_{OLTC}} \left(\frac{I'_{P_{OLTC}}}{I_{S_{OLTC}}} \right) = Z'_{P_{OLTC}} \left(\frac{I'_{m_{OLTC}} + I_{S_{OLTC}}}{I_{S_{OLTC}}} \right) \\ \Rightarrow Z''_{P_{OLTC}} &= Z'_{P_{OLTC}} \left(1 + \frac{I'_{m_{OLTC}}}{I_{S_{OLTC}}} \right) \end{aligned} \quad (3.1)$$

The magnetizing current $I'_{m_{OLTC}}$ and secondary winding current $I_{S_{OLTC}}$ when computed on the basis from Fig. 3.2(a) can be expressed as:

$$\begin{aligned} I'_{m_{OLTC}} &= I'_{P_{OLTC}} \left(\frac{Z_{S_{OLTC}} + Z_L}{Z_{S_{OLTC}} + Z_L + Z_{m_{OLTC}}} \right) \text{ and} \\ I_{S_{OLTC}} &= I'_{P_{OLTC}} \left(\frac{Z_{m_{OLTC}}}{Z_{S_{OLTC}} + Z_L + Z_{m_{OLTC}}} \right) \end{aligned}$$

To simplify $Z''_{P_{OLTC}}$, expressions for $I'_{m_{OLTC}}$ and $I_{S_{OLTC}}$ are substituted in equation (3.1).

Thus,

$$\therefore Z''_{P_{OLTC}} = Z'_{P_{OLTC}} \left(1 + \frac{I'_P \left(\frac{Z_{S_{OLTC}} + Z_L}{Z_{S_{OLTC}} + Z_L + Z_{m_{OLTC}}} \right)}{I'_P \left(\frac{Z_{m_{OLTC}}}{Z_{S_{OLTC}} + Z_L + Z_{m_{OLTC}}} \right)} \right) \quad (3.2)$$

Equation (3.2) is simplified to obtain the value of $R''_{P_{OLTC}}$ and $X''_{P_{OLTC}}$.

$$R''_{P_{OLTC}} = \frac{\left(R_{S_{OLTC}} X'_{P_{OLTC}} + R_L X'_{P_{OLTC}} + R'_{P_{OLTC}} X_{S_{OLTC}} + R'_{P_{OLTC}} X_L + R'_{P_{OLTC}} X'_{m_{OLTC}} \right)}{X'_{m_{OLTC}}} \quad (3.3)$$

$$X''_{POLTC} = \frac{\left(\begin{array}{c} X'_{POLTC}X_{SOLTC} + X'_{POLTC}X_L \\ + X'_{POLTC}X'_{mOLTC} - R'_{POLTC}R_L - R'_{POLTC}R_{SOLTC} \end{array} \right)}{X'_{mOLTC}} \quad (3.4)$$

Further in the equivalent circuit shown in Fig. 3.2(a), the magnetizing current is given

by: $I'_{mOLTC} = \frac{V_{AB}}{Z'_{mOLTC}}$ and in the simplified equivalent circuit shown in Fig. 3.2(b),

the magnetizing current is given by: $I''_{mOLTC} = \frac{V'_{POLTC}}{Z''_{mOLTC}}$. Now, as the magnetizing

current in both the circuit is almost same. Therefore,

$$\begin{aligned} \frac{V_{AB}}{Z'_{mOLTC}} &= \frac{V'_{POLTC}}{Z''_{mOLTC}} \\ \Rightarrow Z''_{mOLTC} &= \left(\frac{V'_{POLTC}}{V_{AB}} \right) Z'_{mOLTC} \end{aligned} \quad (3.5)$$

As depicted from Fig. 3.2(a)

$$V_{AB} = V_{POLTC} \frac{Z'_{mOLTC}(Z_{SOLTC} + Z_L)}{(Z'_{mOLTC}(Z_{SOLTC} + Z_L) + (Z'_{mOLTC} + Z_{SOLTC} + Z_L)Z'_{POLTC})}$$

Putting this value of V_{AB} in equation (3.5).

$$Z''_{mOLTC} = \frac{Z'_{mOLTC} \left(Z'_{mOLTC}(Z_{SOLTC} + Z_L) + Z'_{POLTC}(Z_{SOLTC} + Z_L + Z'_{mOLTC}) \right)}{Z'_{mOLTC}(Z_{SOLTC} + Z_L)}$$

R''_{mOLTC} and X''_{mOLTC} can be obtained by simplifying the preceding equation and separating the Real and Imaginary components as follows:

$$R''_{mOLTC} = \frac{(R_{SOLTC} + R_L)(A) + (X_{SOLTC} + X_L)(B)}{(R_{SOLTC} + R_L)^2 + (X_{SOLTC} + X_L)^2} \quad (3.6)$$

$$X''_{mOLTC} = \frac{(R_{SOLTC} + R_L)(B) - (X_{SOLTC} + X_L)(A)}{(R_{SOLTC} + R_L)^2 + (X_{SOLTC} + X_L)^2} \quad (3.7)$$

Where,

$$A = R_{S_{OLTC}} R'_{P_{OLTC}} + R'_{P_{OLTC}} R_L - X'_{m_{OLTC}} X_{S_{OLTC}} - X'_{m_{OLTC}} X_L - X'_{P_{OLTC}} X_{S_{OLTC}} \\ - X'_{P_{OLTC}} X_L - X'_{P_{OLTC}} X_{m_{OLTC}}$$

and

$$B = R_{S_{OLTC}} X'_{m_{OLTC}} + R_L X'_{m_{OLTC}} + R'_{P_{OLTC}} X'_{m_{OLTC}} + R_{S_{OLTC}} X'_{P_{OLTC}} + R'_{P_{OLTC}} X_{S_{OLTC}} \\ + R'_{P_{OLTC}} X_L + R_L X'_{P_{OLTC}}$$

In the simplified equivalent circuit shown in Fig. 3.2 (b), the output voltage at the OLTC terminals is:

$$V_{S_{OLTC}} = V'_{P_{OLTC}} - I_{S_{OLTC}} (Z''_{P_{OLTC}} + Z_{S_{OLTC}}) \quad (3.8)$$

V'_P and Z_S do not change as the taps of the OLTC-T change; nevertheless, $I_{S_{OLTC}}$ varies depending on the impedance and loading state in the transformer; on the other hand, Z''_P varies depending on the tap position of the OLTC-T and can be expressed as:

$$Z''_{P_{OLTC}} = x^2 R''_{P_{OLTC}} + jx^2 X''_{P_{OLTC}} \quad (3.9)$$

Where, $R''_{P_{OLTC}}$ and $X''_{P_{OLTC}}$ are nominal values at 1:1ratio and x is the turn ratio at current tap position.

Thus, the output voltage of the OLTC-T at current tap position can be expressed as:

$$V_{S_{OLTC}_x} = V'_{P_{OLTC}} - I_{S_{OLTC}} [(x^2 R''_{P_{OLTC}} + jx^2 X''_{P_{OLTC}}) + Z_{S_{OLTC}}] \quad (3.10)$$

The OLTC-T's output terminal voltage at the terminal is therefore expressed in terms of direct axis (d-axis) and quadrature axis (q-axis) components in equation (3.11) for simplicity of further analysis regarding the study of OLTC-T interaction.

$$\begin{bmatrix} V_{OLTC_d} \\ V_{OLTC_q} \end{bmatrix} = \begin{bmatrix} \cos(\theta) & \cos\left(\theta - \frac{2\pi}{3}\right) & \cos\left(\theta + \frac{2\pi}{3}\right) \\ -\sin(\theta) & -\sin\left(\theta - \frac{2\pi}{3}\right) & -\sin\left(\theta + \frac{2\pi}{3}\right) \end{bmatrix} \begin{bmatrix} V_{OLTC_a} \\ V_{OLTC_b} \\ V_{OLTC_c} \end{bmatrix} \quad (3.11)$$

3.2.2 Control of OLTC transformer

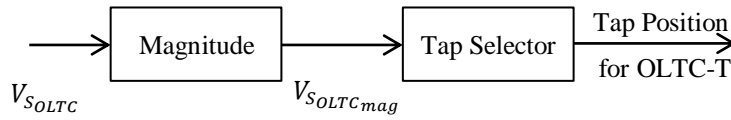


Fig. 3.3: Tap position controller of OLTC Transformer

The main objective of this control is to maintain the voltage at the terminal of the OLTC-T within a set range. To achieve this, the OLTC-T's tap position is adjusted based on the measured value of the magnitude V_{SOLTC} . If the measured value falls outside the set range, the tap controller of the OLTC-T adjusts its tap position to the right position. This will increase or decrease the voltage at the OLTC-T's terminal, bringing it back to the desired range.

Overall, the block diagram shown in Fig. 3.3 provides a high-level representation of the control mechanism used to regulate the voltage at the OLTC-T's terminal. It may include various components such as sensors, controllers, and actuators, which work together to ensure that the OLTC-T operates within the desired range and maintains the required voltage levels.

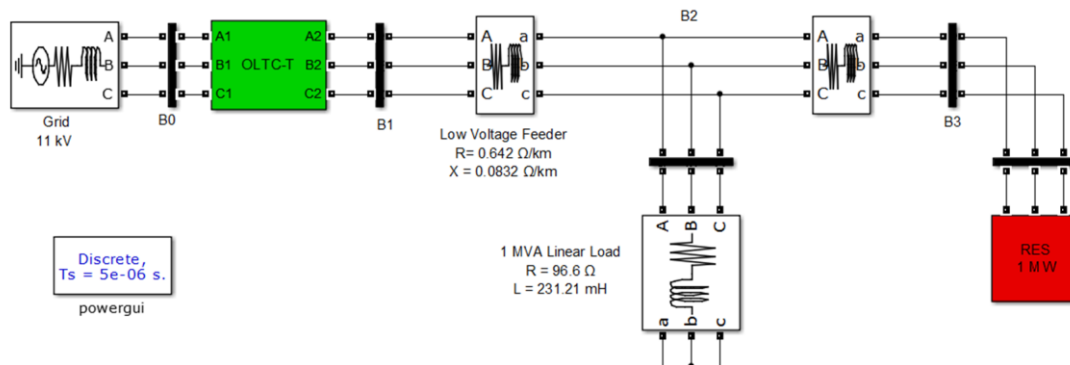


Fig. 3.4: MATLAB simulation diagram of radial microgrid with OLTC transformer as voltage regulator

3.2.3 Simulation Diagram of OLTC transformer

The performance of an OLTC transformer is being evaluated using a simulation model developed in the MATLAB/SIMULINK environment with the SimPowerSystems toolbox. The simulation diagram for the same is shown in Fig. 3.4. The simulation model includes various components, such as a weak source implemented using a three-phase source and a series RL branch to represent the feeder drop, a three-phase OLTC transformer with multiple taps, a balanced linear load with a power factor of 0.8 lagging and a rating of 1 MVA, and 0.67 MW intermittent RES source implemented as a current-controlled GCI. To simulate the worst-case scenario, the RES module is positioned at the end of the feeder, where there is the highest fluctuation in terminal voltage and reversal of power flow. The component parameters used in the simulation model are listed in Table 3.1.

Table 3.1: Simulation parameters for voltage regulation of radial microgrid with OLTC transformer as voltage regulator

System Parameter	Values
Source Voltage (V_s)	33kV, 50Hz
OLTC Transformer	33/11kV, 2.5 MVA
Feeder impedance (Z_f)	$0.642 + j 0.083 \Omega/\text{km}$ [172]
RES power rating	0.67 MW during normal injection
Load	1 MVA, 0.8 pf lagging, linear and balanced Load $Z_L = 96.8 + j 72.64 \Omega$

3.2.4 Performance Evaluation of OLTC transformer

The performance of the OLTC-T for voltage regulation is enhanced in the radial microgrid under challenging conditions, including the intermittent nature of renewable energy sources (RES), load perturbations, and source voltage perturbations such as under voltage and overvoltage.

RES Intermittency

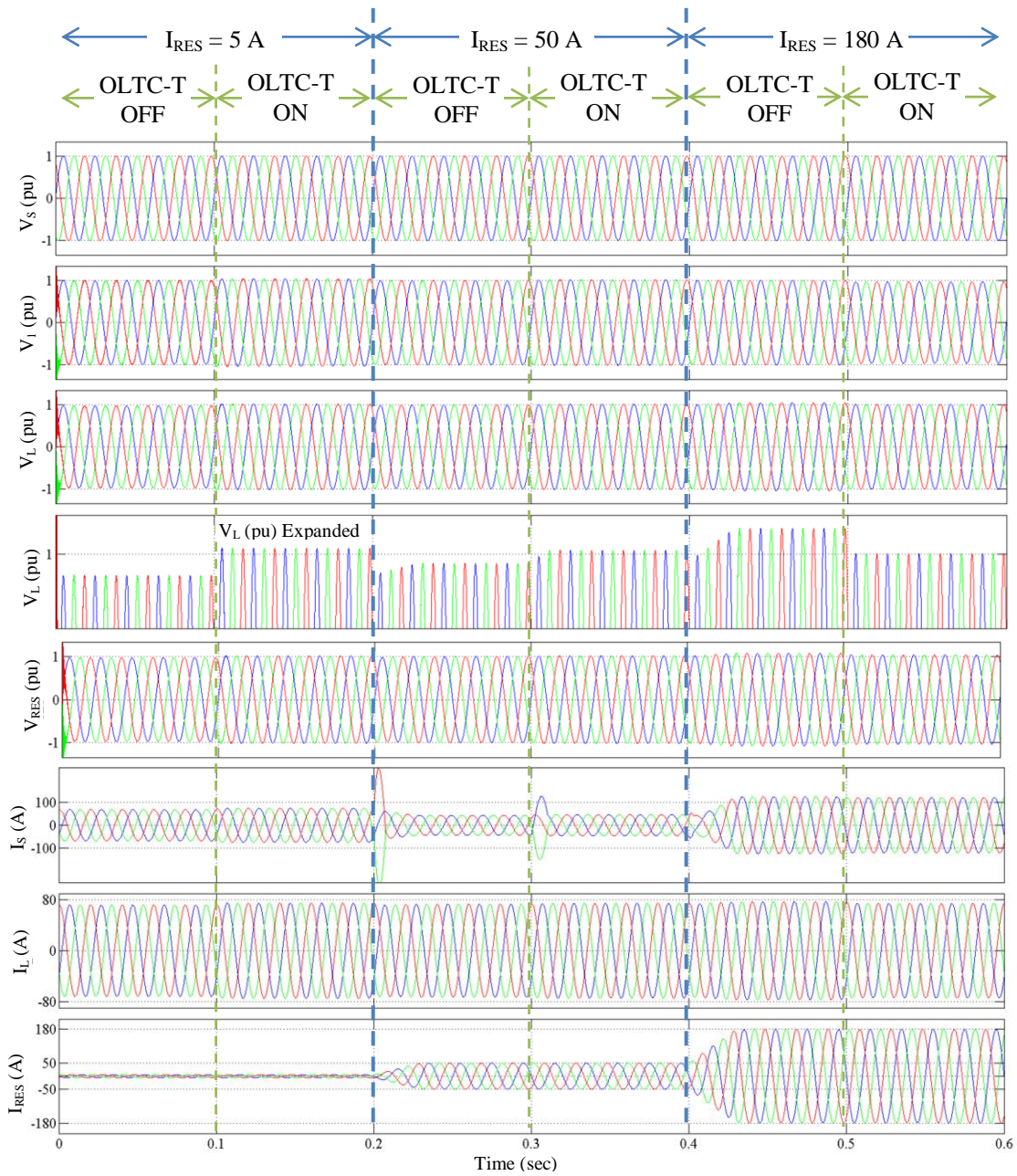


Fig. 3.5: Voltage and current waveforms in radial microgrid with OLTC transformer as voltage regulator during RES intermittency

V_S : Source Voltage (in per units), V_1 : Voltage at secondary terminal of OLTC-T (in pu), V_L/V_{PCC} : Voltage at load terminal (in pu), V_{RES} : Voltage at the terminal of RES (in pu), I_S : Source current (in A), I_L : Load Current (in A), I_{RES} : RES current (in A),

Since the Renewable energy sources (RES) are intermittent by nature, accordingly variable power is injected into the system which can result in voltage fluctuations.

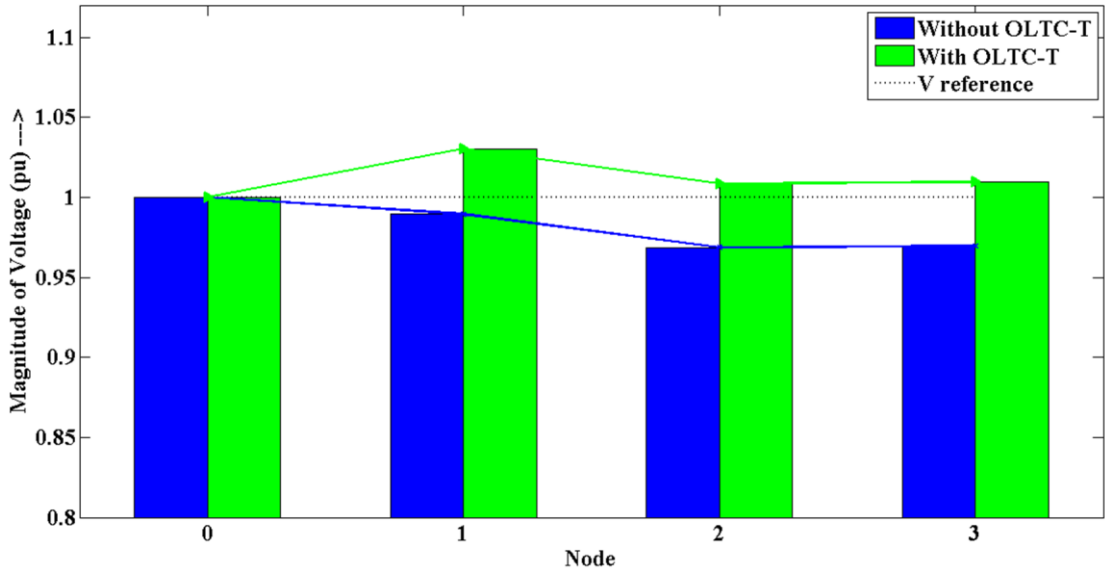


Fig. 3.6: Voltage profile of radial microgrid with OLTC transformer as voltage regulator during RES intermittency at $I_{RES} = 5 A$

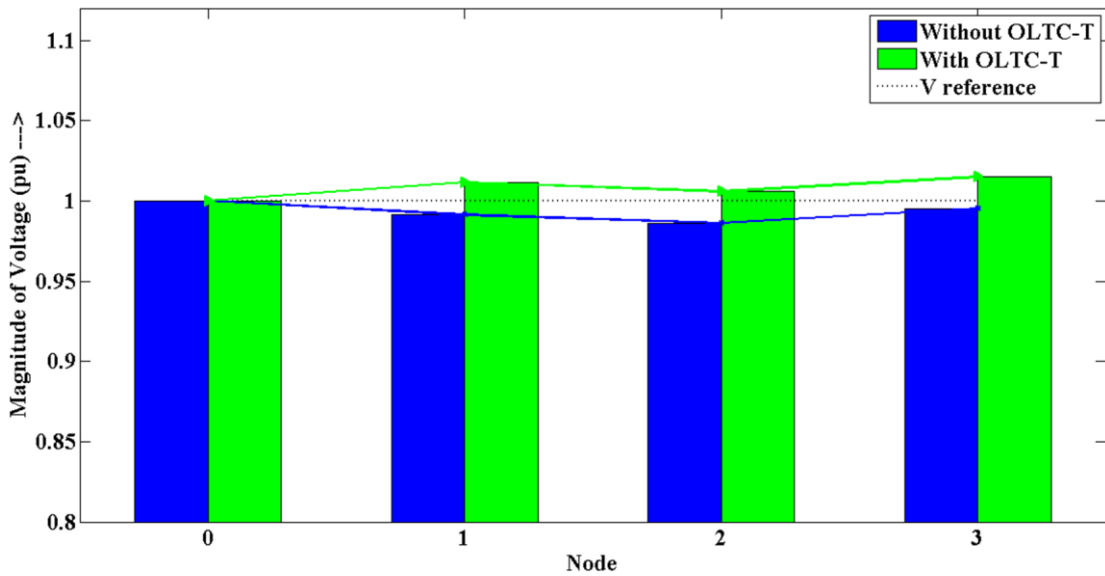


Fig. 3.7: Voltage profile of radial microgrid with OLTC transformer as voltage regulator during RES intermittency at $I_{RES} = 50 A$

However, the on-load tap changer transformer (OLTC-T), through changing taps, regulates the voltage at its secondary terminal (PCC), by adjusting its tap position and also restricts the reverse flow of power. The waveforms depicting voltage regulation during RES intermittency are shown in Fig. 3.5. At the initial stage, RES penetration is

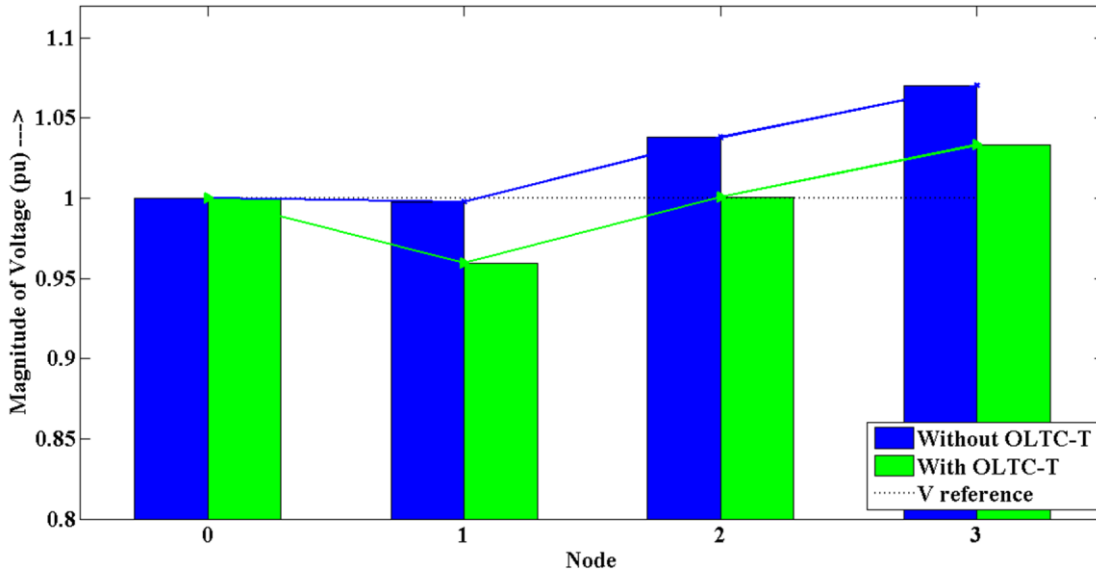


Fig. 3.8: Voltage profile of radial microgrid with OLTC transformer as voltage regulator during RES intermittency at $I_{RES} = 180$ A

low with $I_{RES} = 5$ A, from $t = 0$ to $t = 0.2$ sec. The OLTC transformer starts to regulate the voltage from $t = 0.1$ sec to $t = 0.2$ sec, while, it continue with 1:1 turn ratio, from $t = 0$ to $t = 0.1$ sec and switches its tap position to regulate the output/load voltage at $t = 0.1$ sec

From $t = 0.2$ sec to $t = 0.4$ sec, when the RES injection increases to $I_{RES} = 50$ A, OLTC-T adjusts its tap position at 0.3 sec to regulate the voltage. When the RES injection further increases to $I_{RES} = 180$ A, at 0.4 sec, the OLTC-T encounters the worst penetration level and switches to new tap position and starts voltage at $t = 0.5$ sec. It may be observed that in all the three cases, the OLTC transformer has regulated the voltage to a great extent, but the value does not meet the exact rated value requirements at any of the nodes in the microgrid feeder. The results are further elaborated by charting the voltage profiles for each intermittency level without and with the OLTC transformer, as seen from Fig. 3.6, Fig. 3.7 and Fig. 3.8.

Load Perturbation

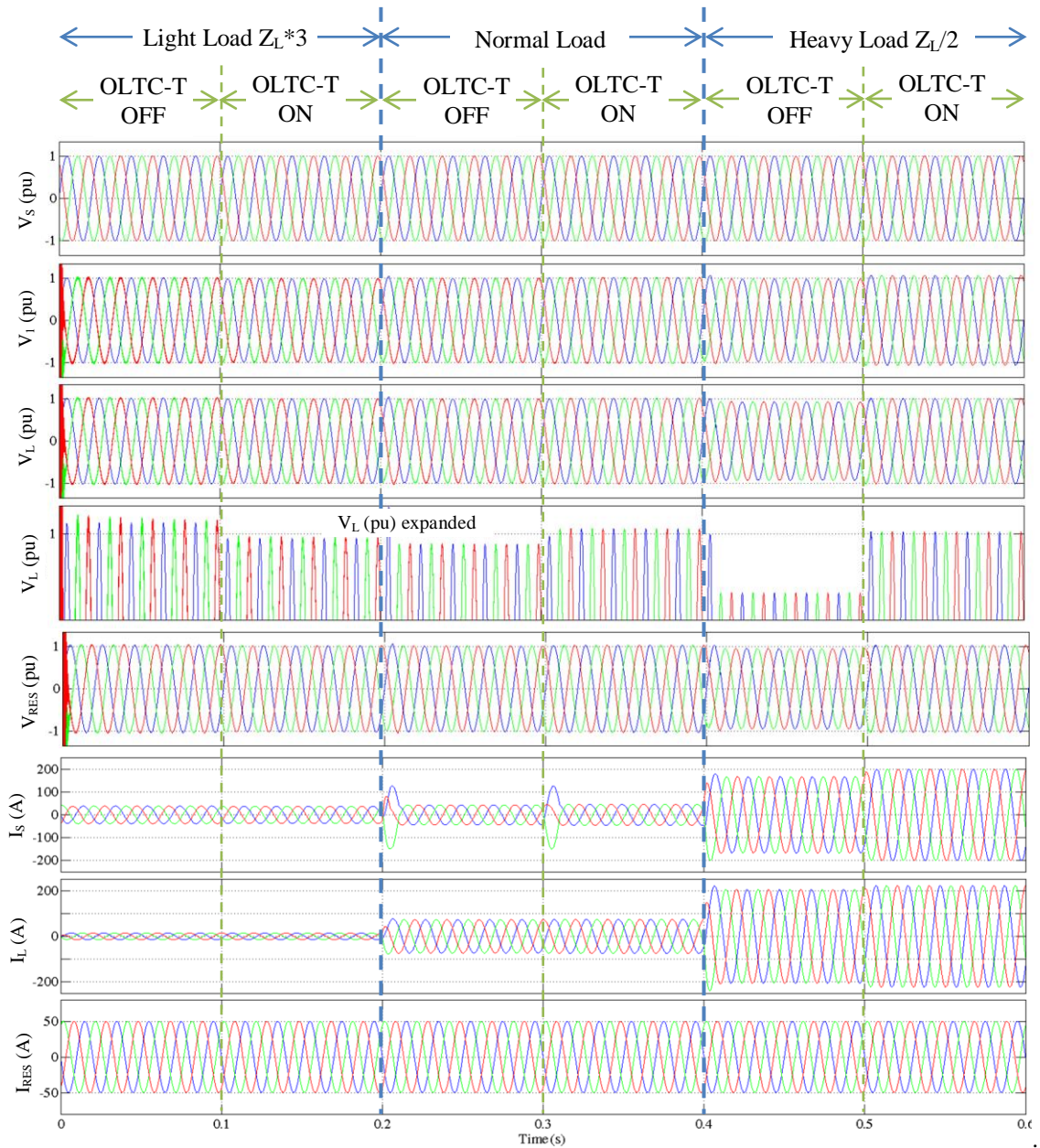


Fig. 3.9: Voltage and current waveform for voltage regulation in considered radial microgrid with OLTC as voltage regulator during load perturbation condition.

V_S : Source Voltage (in per units), V_1 : Voltage at secondary terminal of OLTC-T (in pu), V_L/V_{PCC} : Voltage at load terminal (in pu), V_{RES} : Voltage at the terminal of RES (in pu), I_s : Source current (in A), I_L : Load Current (in A), I_{RES} : RES current (in A),

The load perturbation is explored as the second perturbation condition to evaluate the performance of OLTC-T waveforms for this case are illustrated in Fig. 3.9. This condition assumes that the RES has normal levels of injection into the microgrid.

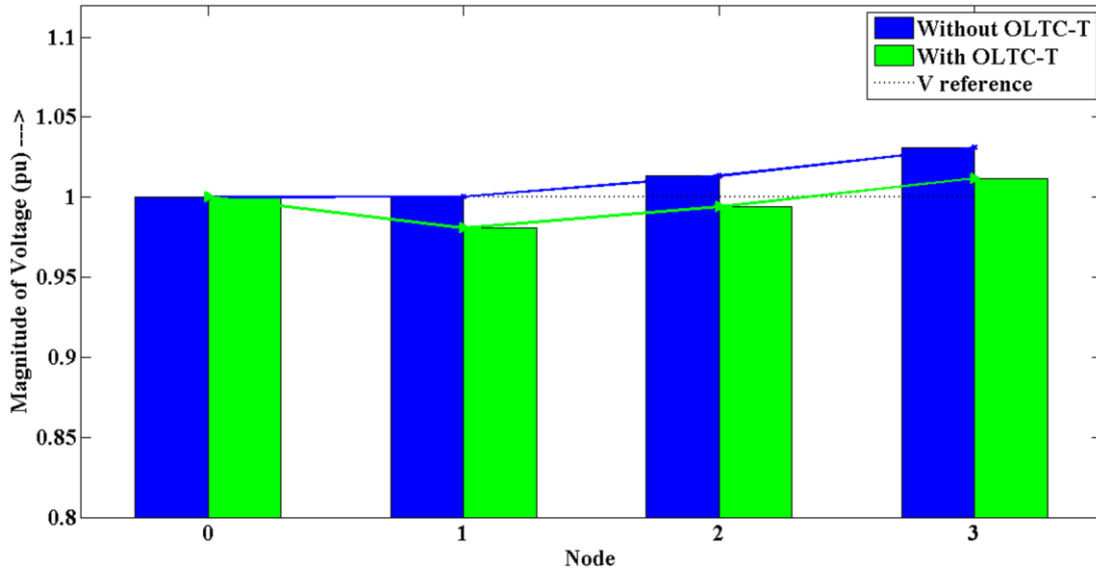


Fig. 3.10: Voltage Profile of radial microgrid with OLTC transformer as voltage regulator during load perturbation at light loading condition

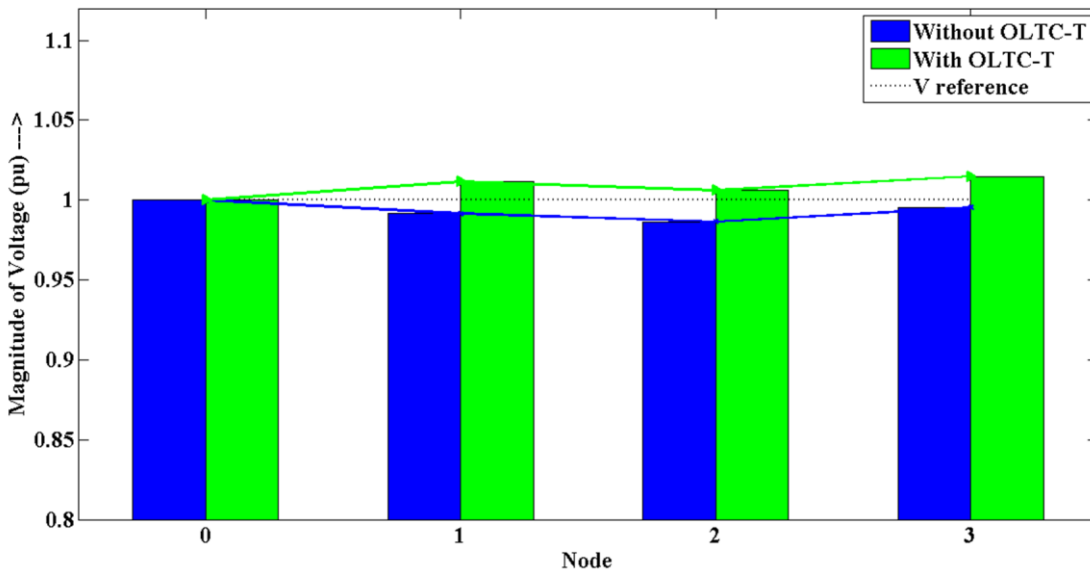


Fig. 3.11: Voltage Profile of radial microgrid with OLTC transformer as voltage regulator during load perturbation at rated loading condition

Initially, from $t = 0$ the system operates at light load condition 20% of the rated load value, causing an overvoltage condition seems to arise due to reversal of power flow in the microgrid feeder. OLTC transformer regulates the voltage at $t = 0.2$ sec as seen from voltage profile in Fig. 3.10. At $t = 0.2$ sec, the load is returns to the rated load

value, Fig. 3.11, and the OLTC transformer shifts its tap position to 1:1 turns ratio. Then at $t = 0.4$ sec, the load is increased to 150% of the rated load value, and the OLTC transformer regulates the voltage within a certain range by changing its tap position at $t = 0.5$ sec. Voltage profile for this is shown in Fig. 3.12. The OLTC-T regulates the voltage at its PCC within the range of 2%.

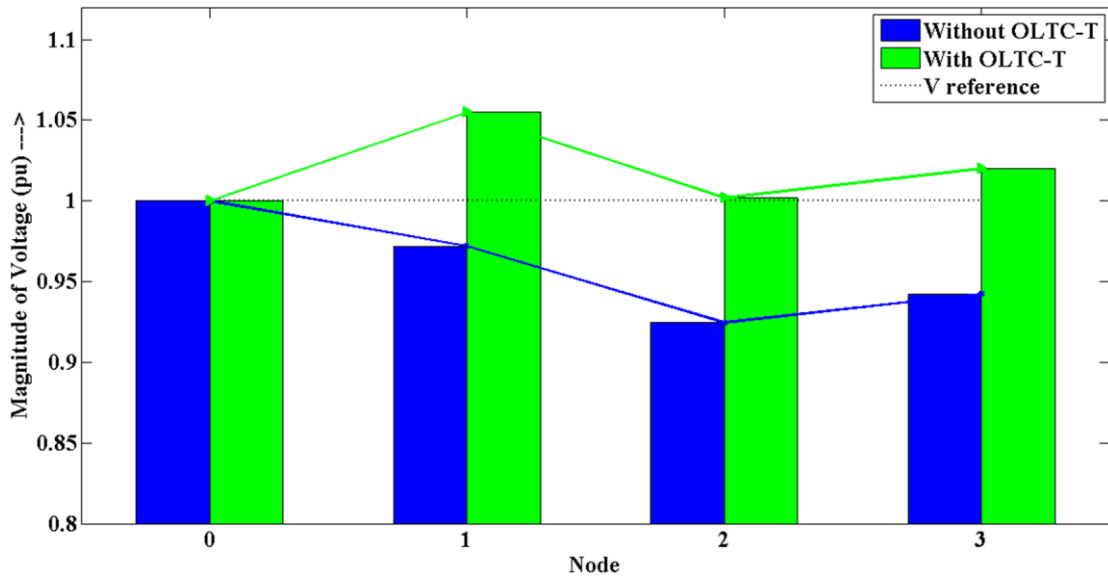


Fig. 3.12: Voltage Profile of radial microgrid with OLTC transformer as voltage regulator during load perturbation at heavy loading condition

Source Perturbations

This scenario demonstrates how voltage variations can affect the grid and how the OLTC-T regulates voltage at the end of the feeder. The waveform for this transient is displayed in Fig. 3.13. From $t = 0$ sec to $t = 0.2$ sec, the supply voltage will remain close to the nominal voltage, with a small loss due to feeder impedance. At $t = 0.2$ sec, an undervoltage condition occurs in the grid, prompting the OLTC-T to adjust its tap position to regulate the voltage at its terminal. This situation lasts until $t = 0.4$ sec, after which the grid voltage experiences an overvoltage issue from the grid side at $t =$

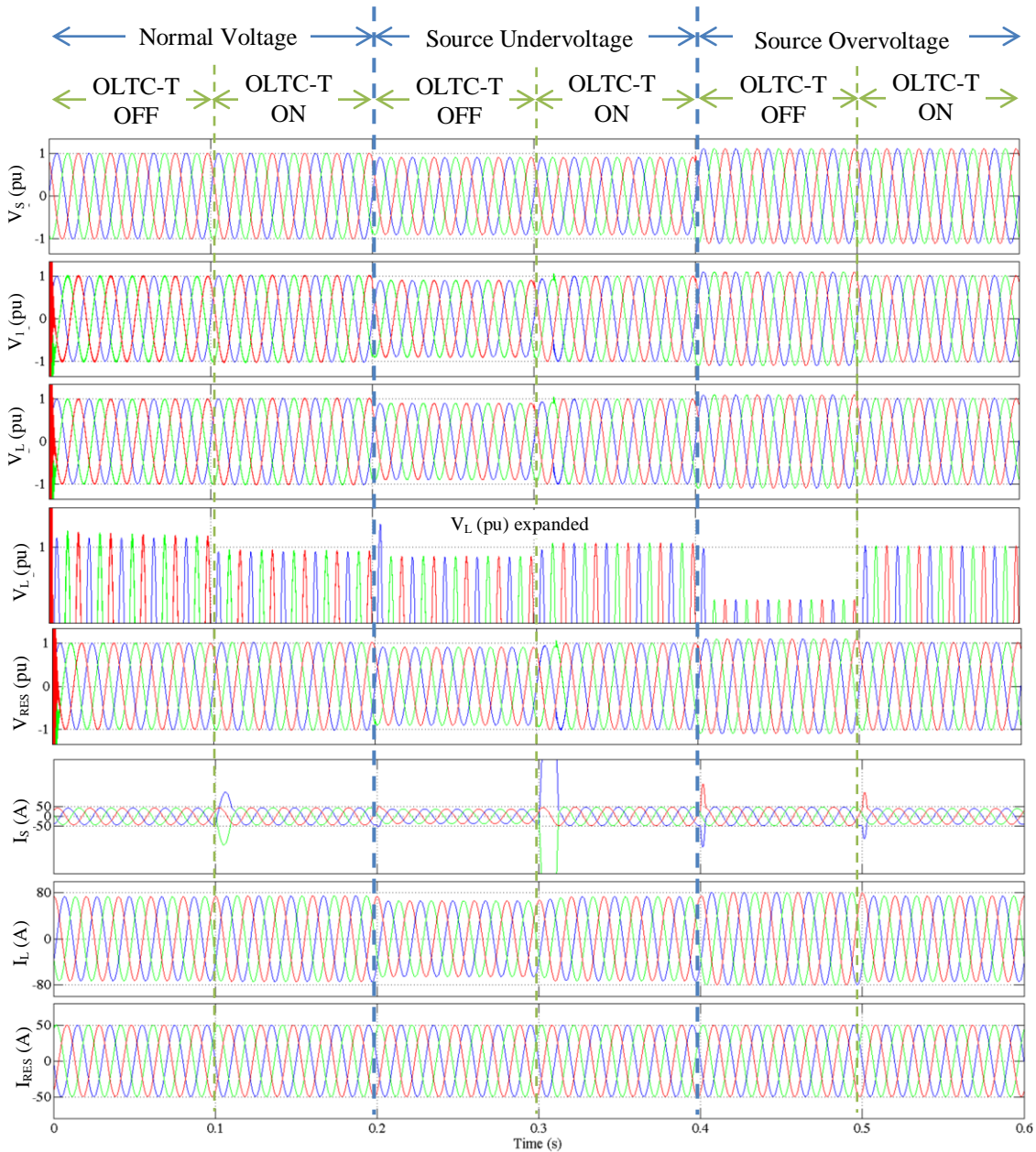


Fig. 3.13: Voltage and current waveform for voltage regulation in considered radial microgrid with OLTC as voltage regulator during source perturbation condition.

V_S : Source Voltage (in per units), V_1 : Voltage at secondary terminal of OLTC-T (in pu), V_L/V_{PCC} : Voltage at load terminal (in pu), V_{RES} : Voltage at the terminal of RES (in pu), I_S : Source current (in A), I_L : Load Current (in A), I_{RES} : RES current (in A),

0.4 sec. The OLTC-T's tap changer function maintains the voltage within the limits at its terminal at $t = 0.5$ sec. The voltage profile for rated voltage, undervoltage and overvoltage at the grid, shown in Fig. 3.14, Fig. 3.15 and Fig. 3.16, respectively, provides further insight into the performance of the OLTC-T.

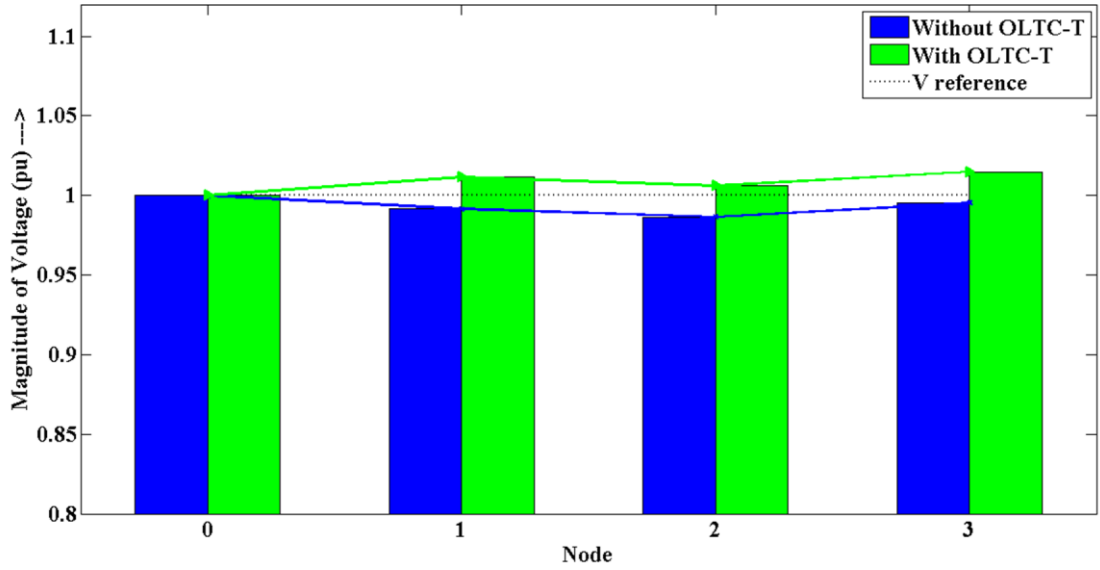


Fig. 3.14: Voltage Profile of radial microgrid with OLTC transformer as voltage regulator during source perturbation at rated voltage from source side

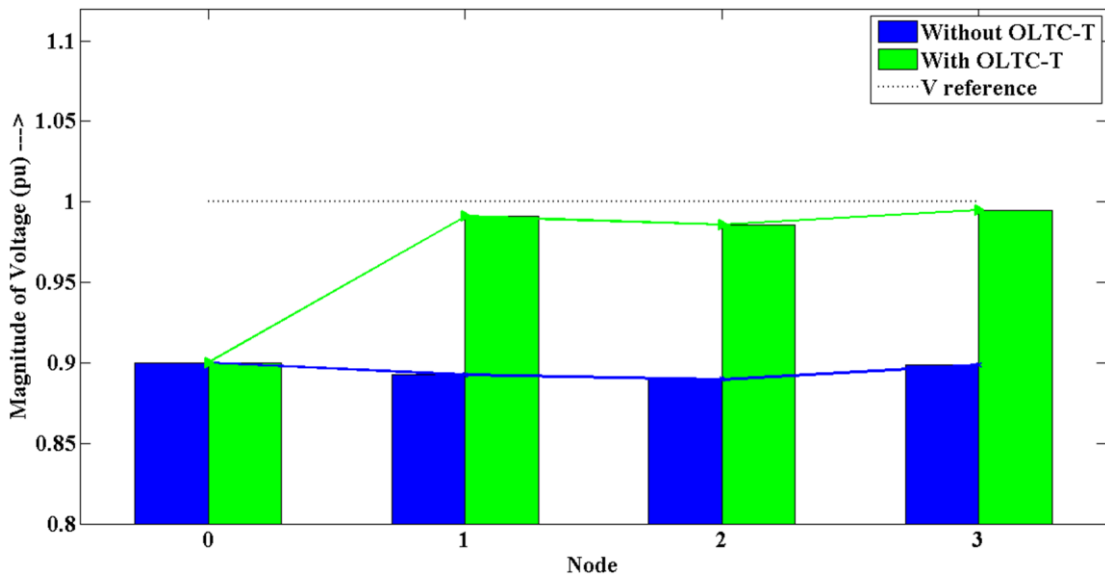


Fig. 3.15: Voltage Profile of radial microgrid with OLTC transformer as voltage regulator during source perturbation at undervoltage from source side

3.3 Static Synchronous Compensator (STATCOM)

In the event of a current disturbance or voltage fluctuation in the system, the STATCOM can supply or absorb reactive current to balance the system and ensure a stable voltage.

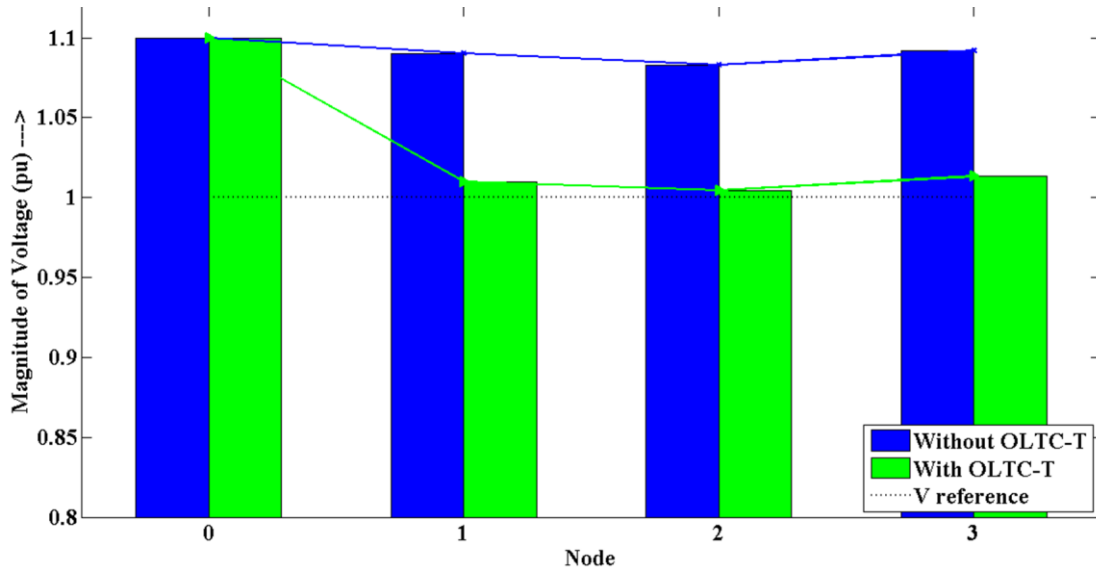


Fig. 3.16: Voltage Profile of radial microgrid with OLTC transformer as voltage regulator during source perturbation at overvoltage from source side

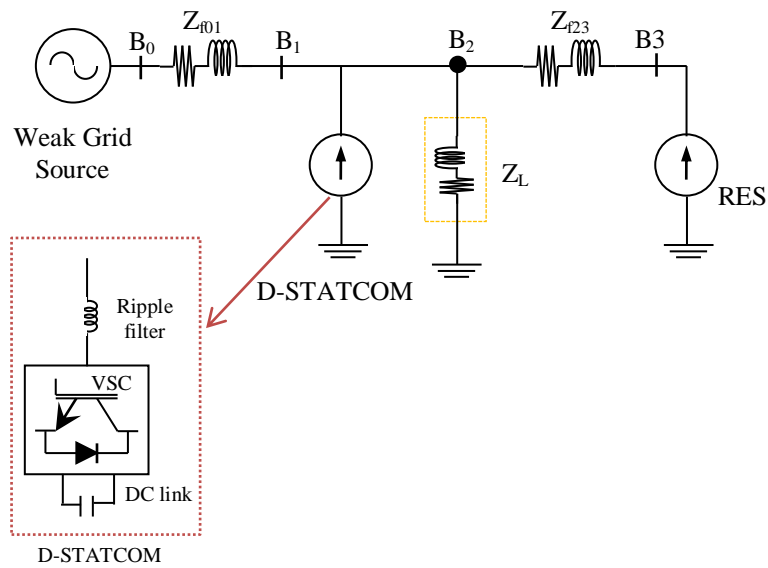


Fig. 3.17: Single line diagram of STATCOM for voltage regulation in radial microgrid with RES penetration

3.3.1 Analysis of STATCOM

The block diagram shown in Fig. 3.17 illustrates a STATCOM connected in a radial microgrid or distribution feeder with intermittent Renewable Energy Sources (RES). The microgrid system consists of a weak power source, STATCOM, intermittent RES,

distributed line impedance, and loads. The weak power source provides power exclusively to the base load in the feeder. The load is a simple three-phase linear load that consumes both real and reactive power. The distributed line impedance is located in two areas: between the source and the load, and between the load and RES. The RES is a variable current-controlled source located near the end of the feeder, designed to evaluate the worst-case scenario for voltage regulation and power reversal.

The STATCOM is responsible for supplying or absorbing current to meet the reactive power demand of the load, and for regulating the voltage by supplying or absorbing reactive current into the feeder.

Before the placement of STATCOM, the grid solely catered to the demand of load current, and the relationship between the load current (I_L) and the grid current (I_S) can be expressed as:

$$I_L = I_S \quad (3.12)$$

Rewriting the same in a d-axis and q-axis component using synchronous reference frame (SRF) theory:

$$I_{L_d} + j I_{L_q} = I_{S_d} + j I_{S_q} \quad (3.13)$$

Voltage at the PCC without placement of the STATCOM into the feeder is calculated as:

$$\begin{aligned} V_L &= V_S - I_S * (R_f + jX_f) \\ \Rightarrow V_{L_d} + j V_{L_q} &= V_{S_d} + j V_{S_q} - (I_{S_d} + j I_{S_q}) * (R_f + jX_f) \end{aligned} \quad (3.14)$$

The STATCOM is connected in shunt with the grid, and it tries to regulate the voltage at its terminal by injecting/absorbing reactive power into the microgrid. Now, the load current is equal to the sum of source current (I_S) and STATCOM current (I_{STATCOM}),

given by:

$$I_L = I_{STATCOM} + I_S \quad (3.15)$$

$$I_{Ld} + jI_{Lq} = I_{Sd} + jI_{Sq} + I_{STATCOMd} + jI_{STATCOMq} \quad (3.16)$$

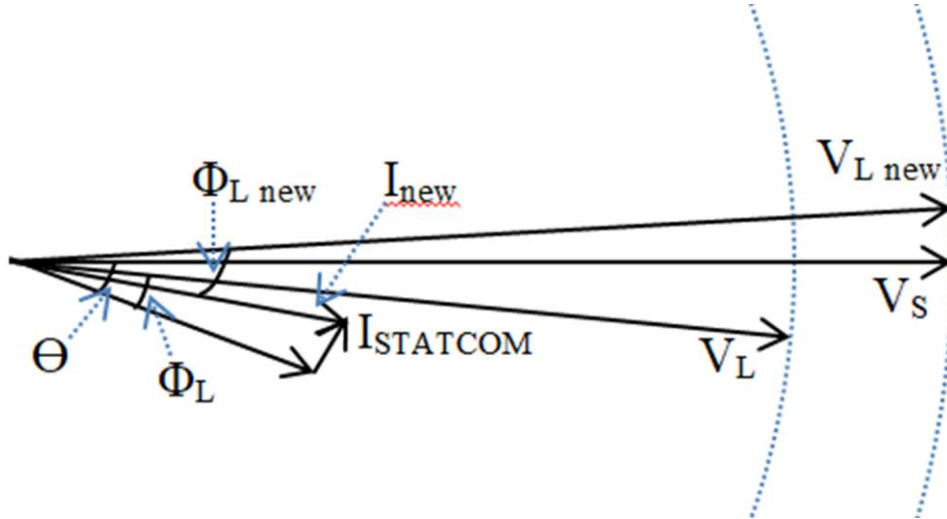


Fig. 3.18: Phasor diagram of STATCOM for voltage regulation at its PCC

With the STATCOM's involvement in managing reactive power, the grid no longer supplies reactive power but only the real component. As a result, the voltage drop across the feeder is reduced, and the voltage at the PCC is increased. If the STATCOM's reactive compensation is increased, a certain amount of reactive power flows towards the grid, further increasing the PCC voltage and regulating it to the rated value. If the PCC voltage is too high, the STATCOM regulates it by absorbing reactive current. This concept is illustrated with a phasor diagram shown in Fig. 3.18.

Considering that STATCOM is regulating voltage by injecting only the reactive current demand of load, and the real component of load current is solely catered by the grid, Equation (3.16) can be rewritten as:

$$I_{Ld} + jI_{Lq} = jI_{STATCOM} + I_{Sd} \quad \text{with } I_{Sq} = 0; \quad (3.17)$$

The voltage at PCC after the placement of STATCOM can be expressed in the dq frame as:

$$V_{Ld} + j V_{Lq} = V_S - (I_{sd}) * (R_f + jX_f) \quad (3.18)$$

Comparing Equation (3.14) and Equation (3.18), considering the feeder impedance is the same in both cases, it is clear that V_{PCC} in the second case, with STATCOM, is appreciably higher than the first case, without STATCOM.

3.3.2 Control of STATCOM

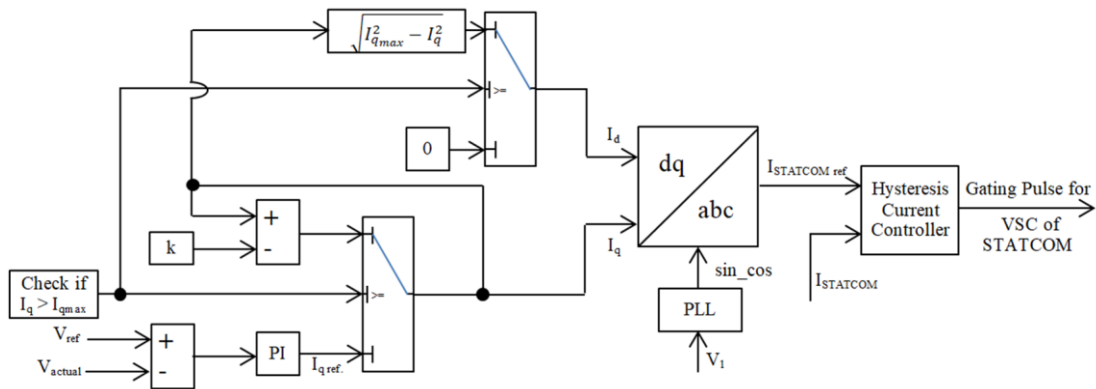


Fig. 3.19: Block diagram for gating pulse control for STATCOM

The current control of the VSC of STATCOM is achieved through synchronous reference frame theory. The control block diagram for generating gating pulses for the VSC of STATCOM is shown in Fig. 3.19. The controller senses the voltage at the terminal and generates the q-axis component of the current (I_q) by passing the difference between the sensed voltage and the reference voltage through the PI controller thereby contributing towards reactive power for regulating the voltage. When the STATCOM approaches its reactive power limit, the q-axis component is saturated, and the d-axis component (I_d) is increased simultaneously to generate the reference STATCOM current ($I_{STATCOMrefdq}$), thereby resorting to real power based

control. The reference values of I_d and I_q are transformed into abc reference signals through reverse PARK's transformation. The gating pulses for the VSC switches are generated by passing the reference current ($I_{STATCOMref}$) and the actual current ($I_{STATCOM}$) through a hysteresis current controller. The hysteresis current controller generates gating pulses for switching the VSC of STATCOM, resulting in the required regulation of voltage through injection of reactive and real power as aforesaid.

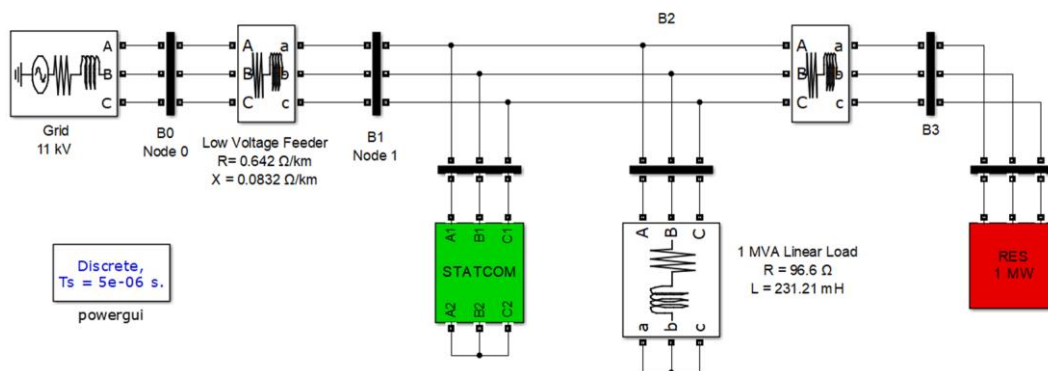


Fig. 3.20: MATLAB simulation diagram of radial microgrid with STATCOM as voltage regulator

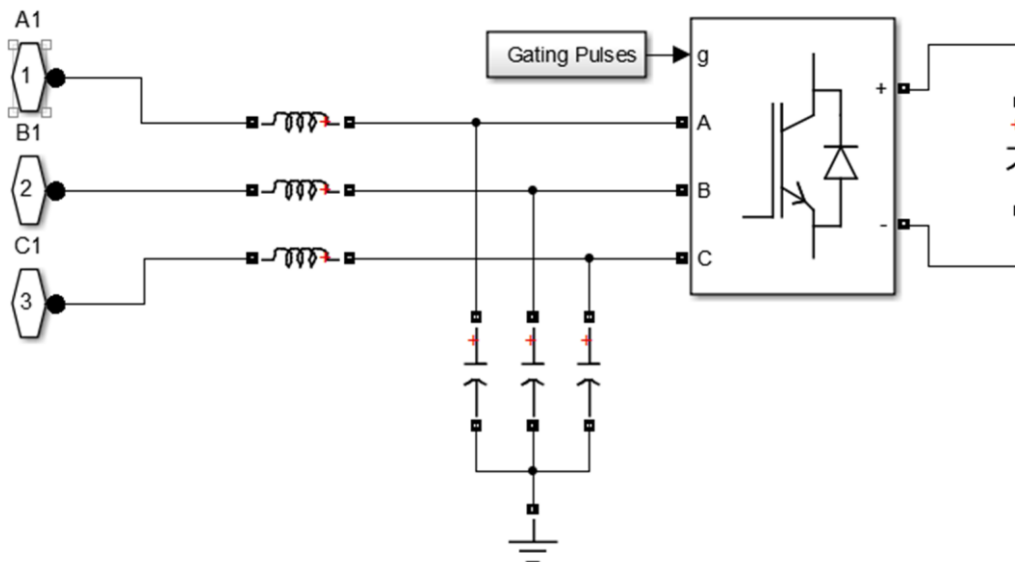


Fig. 3.21: Expanded simulation diagram for STATCOM

3.3.3 Simulation Diagram of STATCOM

The performance of STATCOM as voltage regulator is evaluated using a simulation model developed in the MATLAB/SIMULINK environment. Fig. 3.20 shows the simulation diagram developed on MATLAB/SIMULINK platform using PowerSystem toolbox for the evaluation and Fig. 3.21 shows the expanded simulation diagram for STATCOM. The simulation model comprises of several components, including a weak source implemented using a three-phase source and a series RL branch to represent the feeder drop, a STATCOM, a balanced linear load with a power factor of 0.8 lagging and a rating of 1 MVA, and an intermittent RES source implemented as a current-controlled inverter. The STATCOM is realized through a VSC with a capacitor on the DC link. The output of the VSC is connected in shunt with the feeder after passing through a LC filter. To simulate the worst-case scenario, the RES module is placed at the end of the feeder, where the highest fluctuation in

Table 3.2: Simulation parameters for voltage regulation of radial microgrid with STATCOM as voltage regulator

System Parameter	Values
Source Voltage (V_s)	11kV, 50Hz
STATCOM	11kV, 2 MVA
Feeder impedance (Z_f)	$0.642 + j 0.083 \Omega/\text{km}$
RES power rating	0.67 MW during normal injection
Load	1 MVA, 0.8 pf lagging, linear and balanced Load $Z_L = 96.8 + j 72.64 \Omega$

terminal voltage and reversal of power flow maybe observed. The simulation parameters used in the simulation model are listed in Table 3.2.

3.3.4 Performance Evaluation of STATCOM

The performance of STATCOM for voltage regulation is evaluated based on simulation results of a radial microgrid under different conditions. These conditions

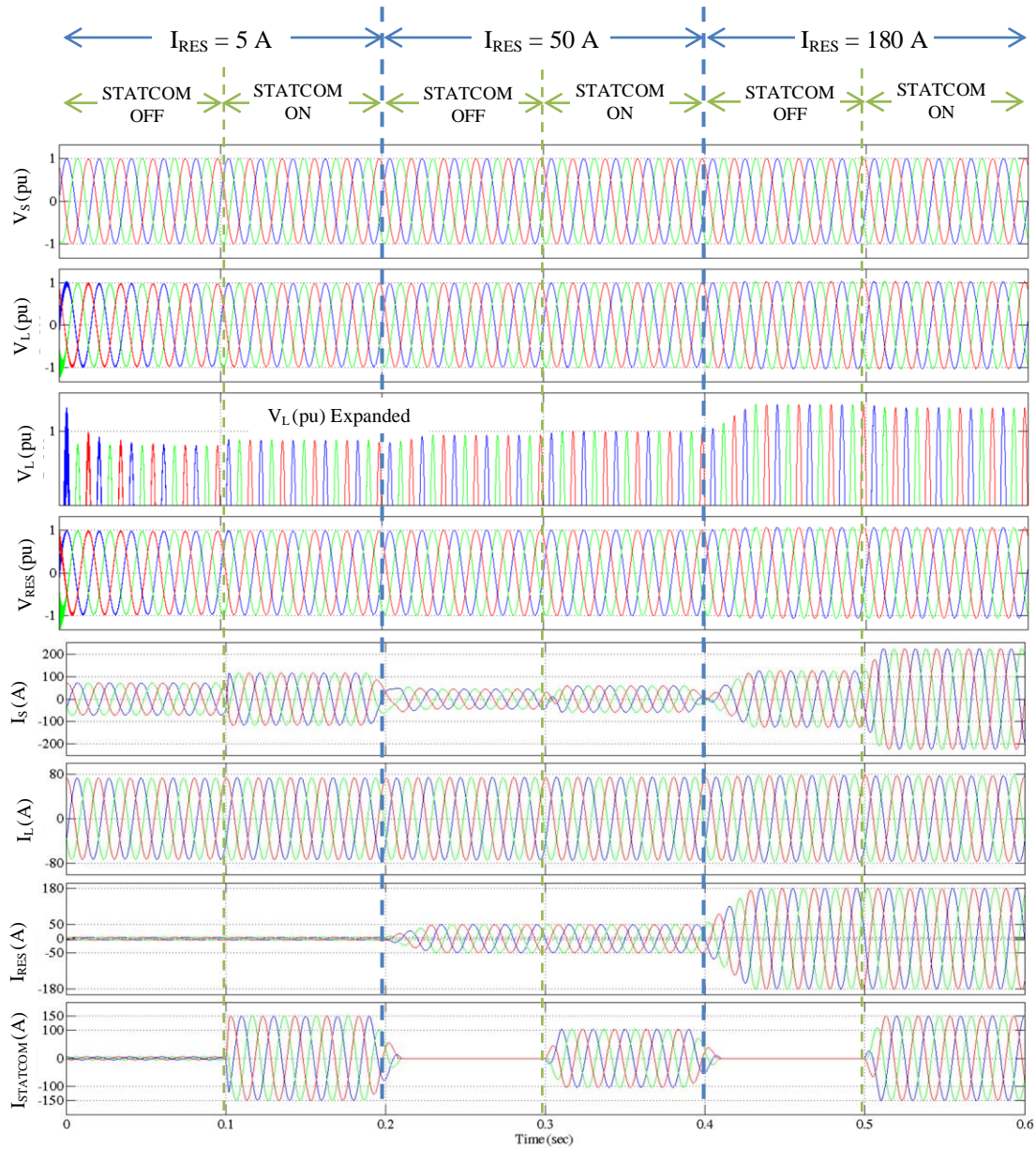


Fig. 3.22: Voltage and current waveform for voltage regulation in considered radial microgrid with STATCOM as voltage regulator during RES intermittency condition.

V_S : Source Voltage (in per units), V_L/V_{PCC} : Voltage at load terminal (in pu), V_{RES} : Voltage at the terminal of RES (in pu), I_s : Source current (in A), I_L : Load Current (in A), I_{RES} : RES current (in A), $I_{STATCOM}$: Current supplied/absorbed by STATCOM (in A)

include the intermittent nature of RES, load perturbations, and source voltage perturbations such as undervoltage and overvoltage.

RES Intermittency

The performance of STATCOM is tested for the intermittent nature of RES connected to the feeder. The results, as seen in Fig. 3.22, the perturbation in power injection from

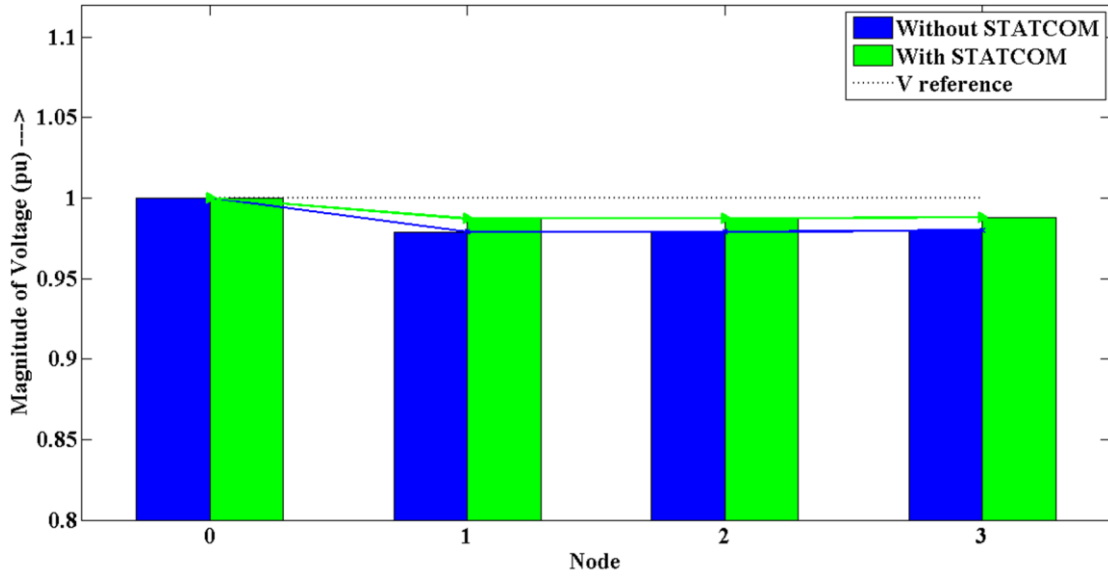


Fig. 3.23: Voltage profile of radial microgrid with STATCOM as voltage regulator during RES intermittency at $I_{RES} = 5$ A

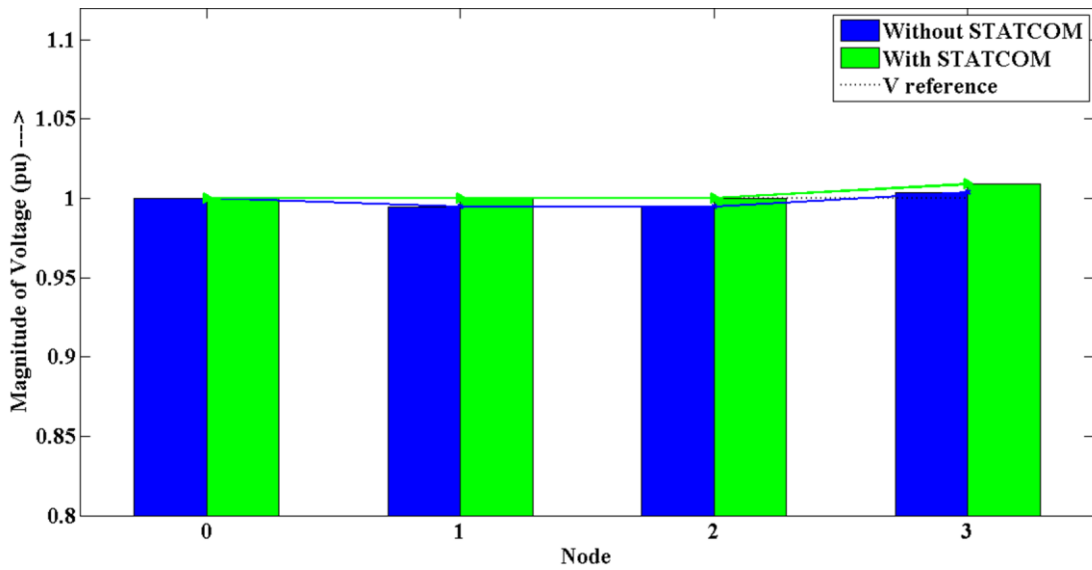


Fig. 3.24: Voltage profile of radial microgrid with STATCOM as voltage regulator during RES intermittency at $I_{RES} = 50$ A

$t = 0$ to $t = 0.2$ sec, I_{RES} is kept at 5 A (light generation), from $t = 0.2$ to 0.4 sec, I_{RES} is made to 50 A regarding normal generation and from $t = 0.4$ sec to 0.6 sec, RES current injection is high with $I_{RES} = 180$ A, depicting over generation. In all three cases, STATCOM tries to regulate the voltage during $t = 0.1$ to 0.2 sec, $t = 0.3$ sec to $t = 0.4$ sec for second level of current injection by RES, and during $t = 0.5$ sec to $t = 0.6$ sec

corresponding to third level of injection. However, it may be observed that the STATCOM can only regulate the voltage when the RES injection is nominal ($I_{RES} = 50$ A). In the other two cases, STATCOM provides only a marginal shift. This is due to the fact that STATCOM regulates the voltage by compensating for the reactive current demand, but in the considered system, the reactive power demand is very low, and the voltage variations are mainly due to real power variations. Moreover, the

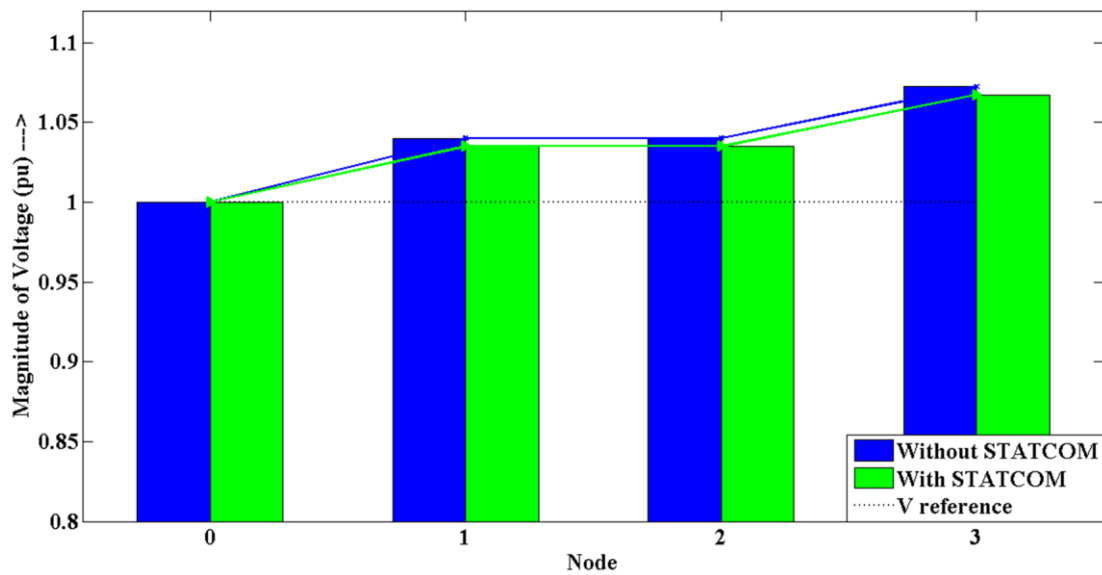


Fig. 3.25: Voltage profile of radial microgrid with STATCOM as voltage regulator during RES intermittency at $I_{RES} = 180$ A

regulation of voltage indirectly by controlling or compensating current requires either a very high capacity STATCOM or real power support. These results are further supported by the voltage profiles drawn for different levels of RES injection as shown in Fig. 3.23, Fig. 3.24, and Fig. 3.25 respectively.

Load Perturbation

Similar current level patterns are used to evaluate the performance of STATCOM under load perturbation and the same is illustrated in Fig. 3.26. These conditions assume that the RES has sufficient input power therefore generating constant power,

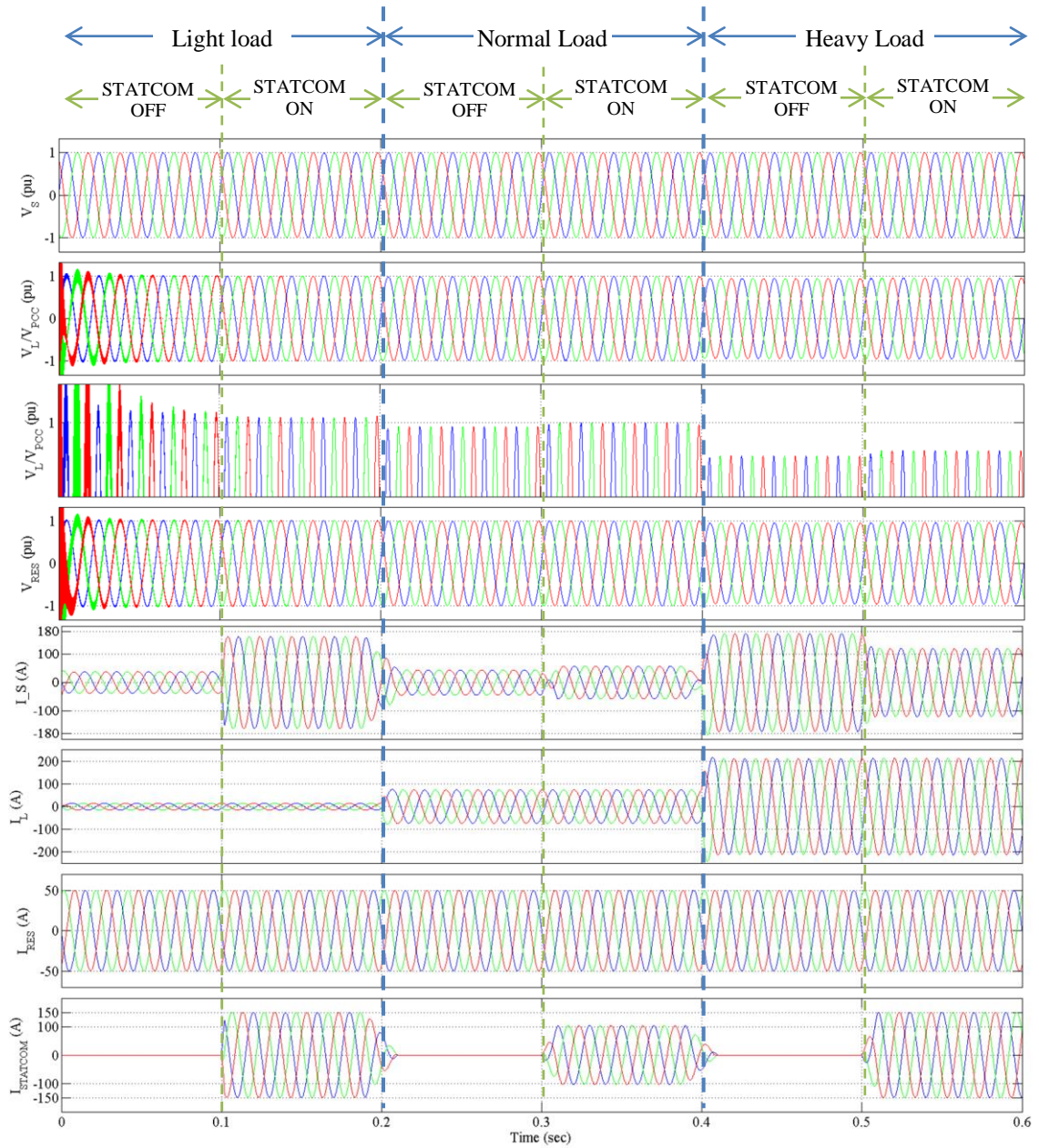


Fig. 3.26: Voltage and current waveforms for voltage regulation in considered radial microgrid with STATCOM as voltage regulator during load perturbation condition.

V_S : Source Voltage (in per units), V_L/V_{PCC} : Voltage at load terminal (in pu), V_{RES} : Voltage at the terminal of RES (in pu), I_s : Source current (in A), I_L : Load Current (in A), I_{RES} : RES current (in A), $I_{STATCOM}$: Current supplied/absorbed by STATCOM (in A)

approximately equivalent to the rated load. Initially, the system operates in a light loading condition. STATCOM tries to regulate the voltage at $t = 0.1$ sec but is unable to meet the desired voltage range, and the system ends up with a rising voltage profile as seen from Fig. 3.27. At $t = 0.2$ sec, the load reaches the rated load value, Fig. 3.28,

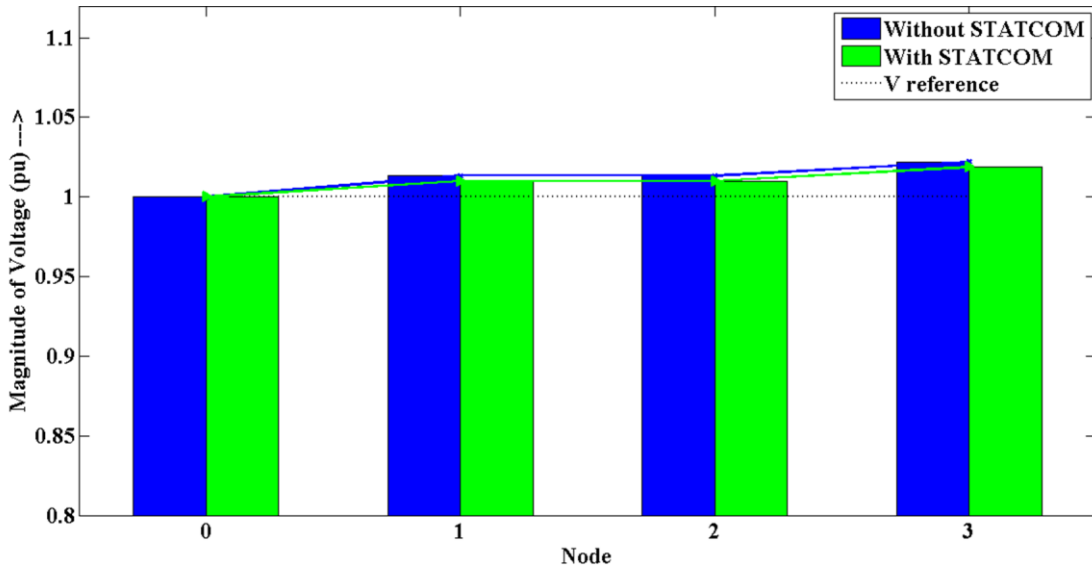


Fig. 3.27: Voltage Profile of radial microgrid with STATCOM as voltage regulator during load perturbation at light loading condition.

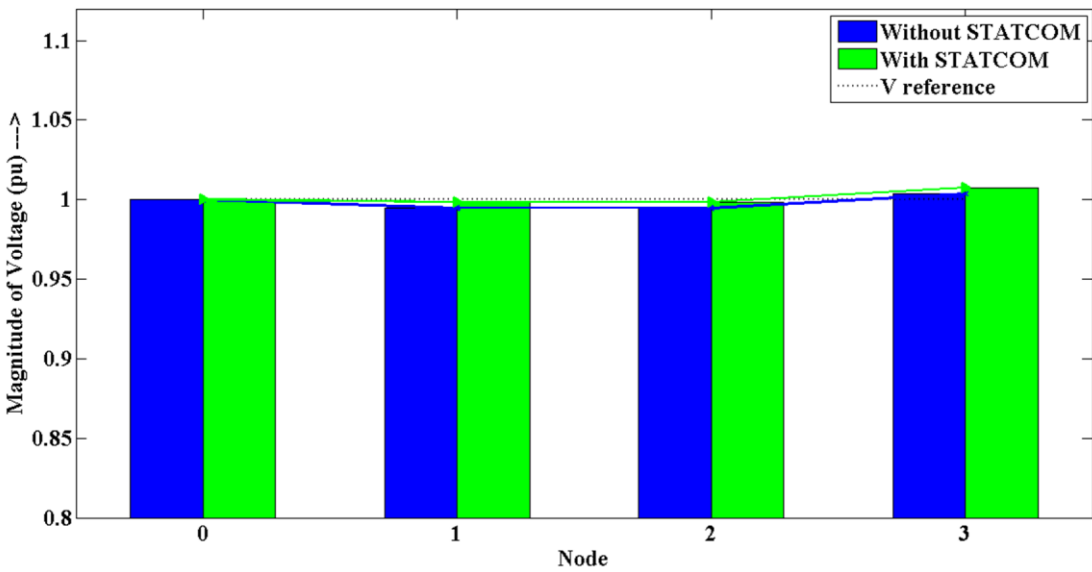


Fig. 3.28: Voltage Profile of radial microgrid with STATCOM as voltage regulator during load perturbation at rated loading condition

and STATCOM's switched in at $t = 0.3$ sec to regulate the voltage. It may be assumed that STATCOM cannot justify the regulation as desired. At $t = 0.4$ sec when the load is increased to 150% of the rated load value, and STATCOM is switched in to regulate the voltage at $t = 0.5$ sec, it fails to regulate the voltage, and the system ends up with an undervoltage or drooping voltage profile as seen from Fig. 3.29.

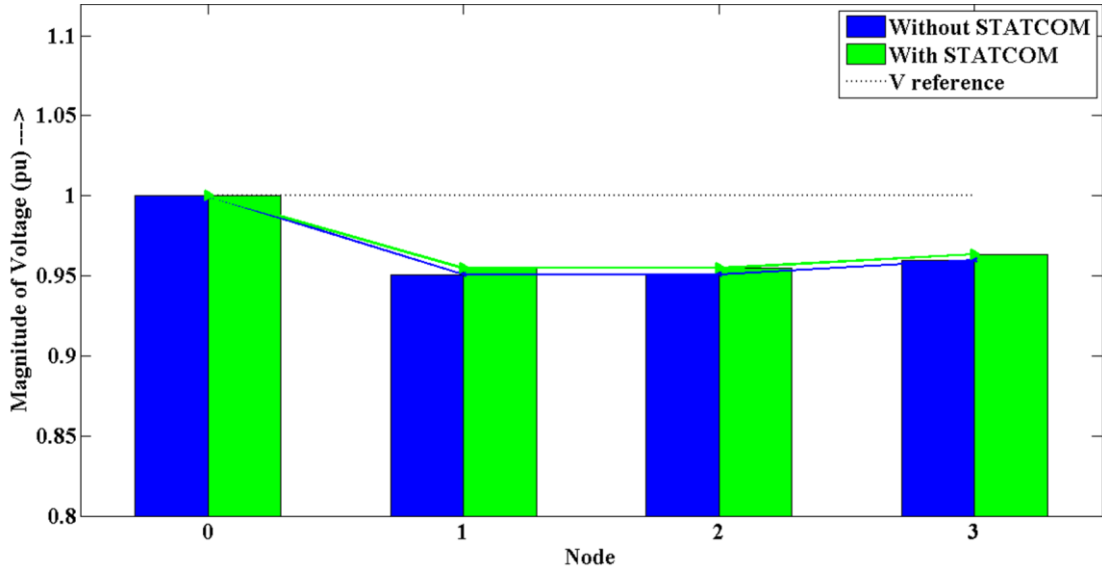


Fig. 3.29: Voltage Profile of radial microgrid with STATCOM as voltage regulator during load perturbation at heavy loading condition

Source Perturbations

The case of undervoltage and overvoltage perturbations from the source side is considered to evaluate the performance of STATCOM in regulation of voltage. The waveforms obtained from the simulation are shown in Fig. 3.30. The cases are studied in three different time periods. Time $t = 0$ sec to $t = 0.2$ sec deals with normal voltage condition, Fig. 3.31. During such condition STATCOM, does not interface at all. After the transient period, when STATCO is switched in, voltage returns to normal.

While from $t = 0.2$ sec to $t = 0.4$ sec, when feeder experiences under voltage conditions, STATCOM fail to regulate the voltage. The voltage profile shown is in Fig. 3.32, provides a clearer picture. Similarly, during overvoltage from the source side, duly observed from $t = 0.4$ sec to $t = 0.6$ sec, and at $t = 0.5$ sec STATCOM is switched in the voltage profile is slightly improved, but it cannot regulate it fully. The results are further supported by the voltage profile shown in Fig. 3.33.

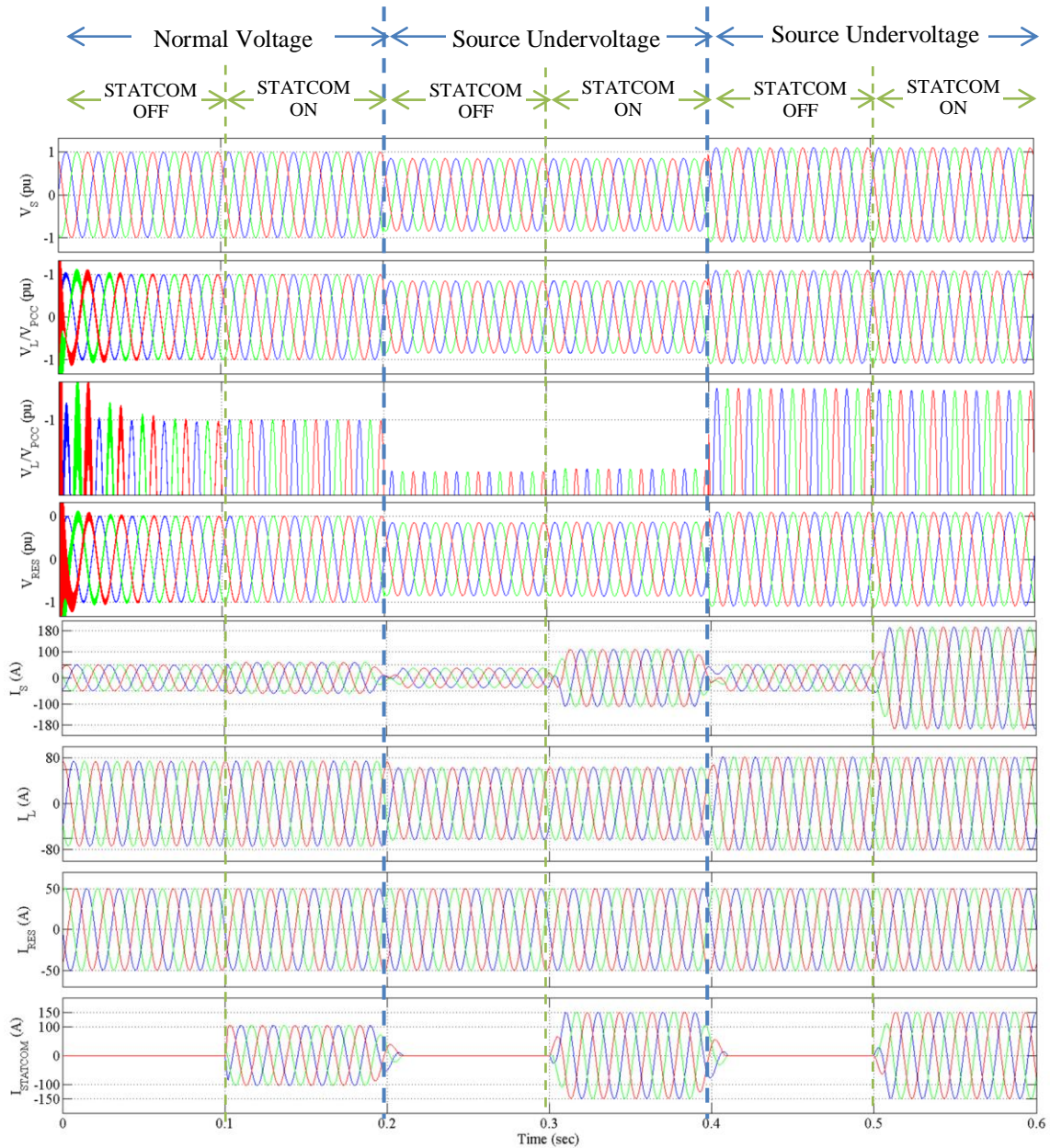


Fig. 3.30: Voltage and current waveforms for voltage regulation in considered radial microgrid with STATCOM as voltage regulator during source perturbation condition.

V_S : Source Voltage (in per units), V_L/V_{PCC} : Voltage at load terminal (in pu), V_{RES} : Voltage at the terminal of RES (in pu), I_S : Source current (in A), I_L : Load Current (in A), I_{RES} : RES current (in A), $I_{STATCOM}$: Current supplied/absorbed by STATCOM (in A)

3.4 Battery Energy Storage System (BESS)

BESS is a type of energy storage system that uses batteries to store energy and release it when needed to regulate the voltage of the power system based on transaction of real

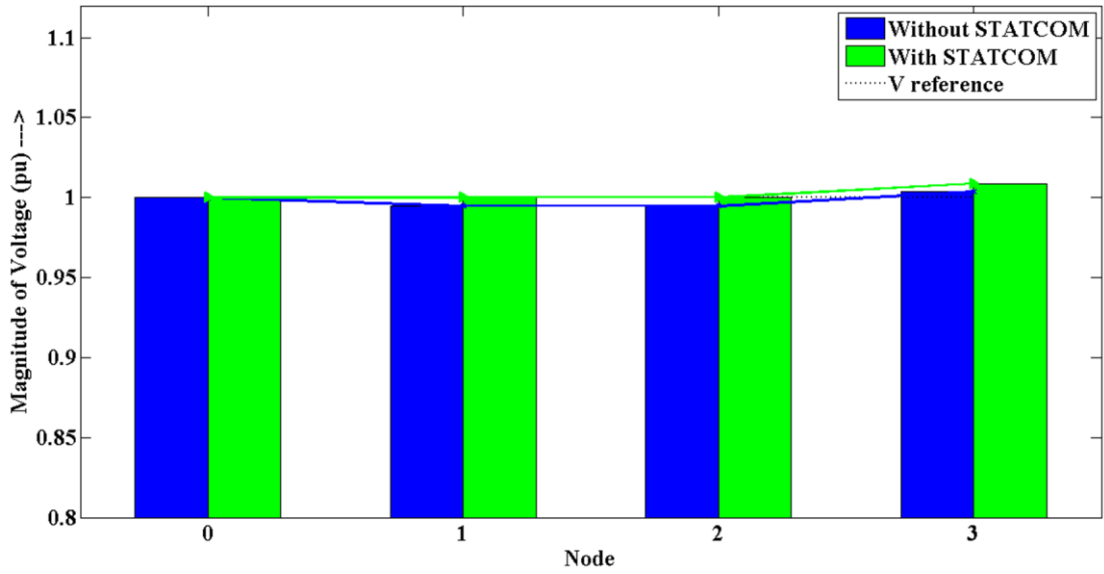


Fig. 3.31: Voltage Profile of radial microgrid with STATCOM as voltage regulator during source perturbation at rated voltage from source side

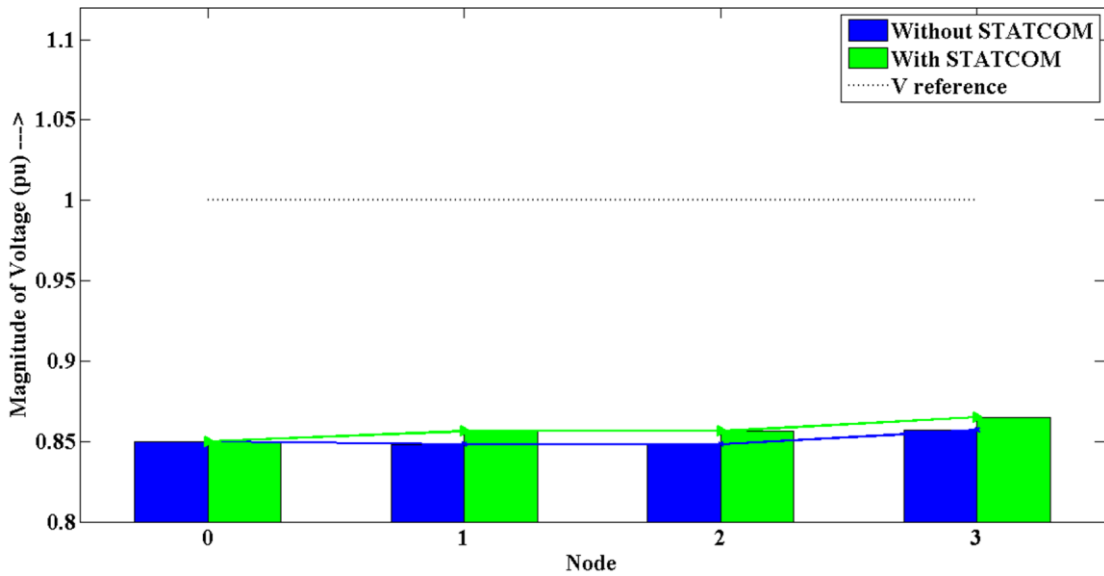


Fig. 3.32: Voltage Profile of radial microgrid with STATCOM as voltage regulator during source perturbation at undervoltage from source side

power. BESS can be connected in parallel or in series with the power system to compensate for voltage fluctuations and maintain a stable voltage level at the load. Block diagram of BESS connected in a radial microgrid is shown in Fig. 3.34.

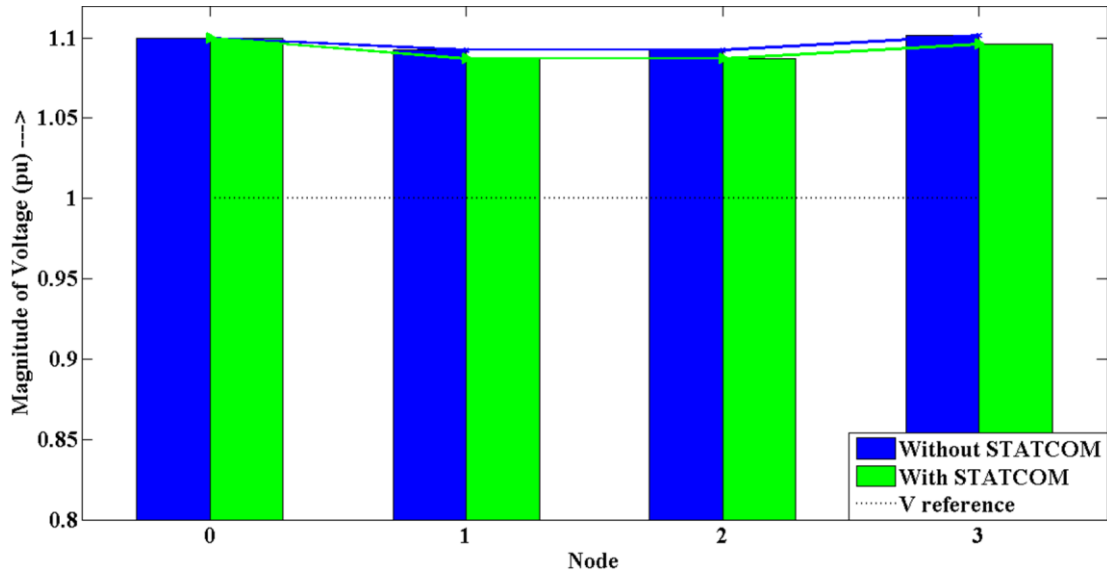


Fig. 3.33: Voltage Profile of radial microgrid with STATCOM as voltage regulator during source perturbation at overvoltage from source side

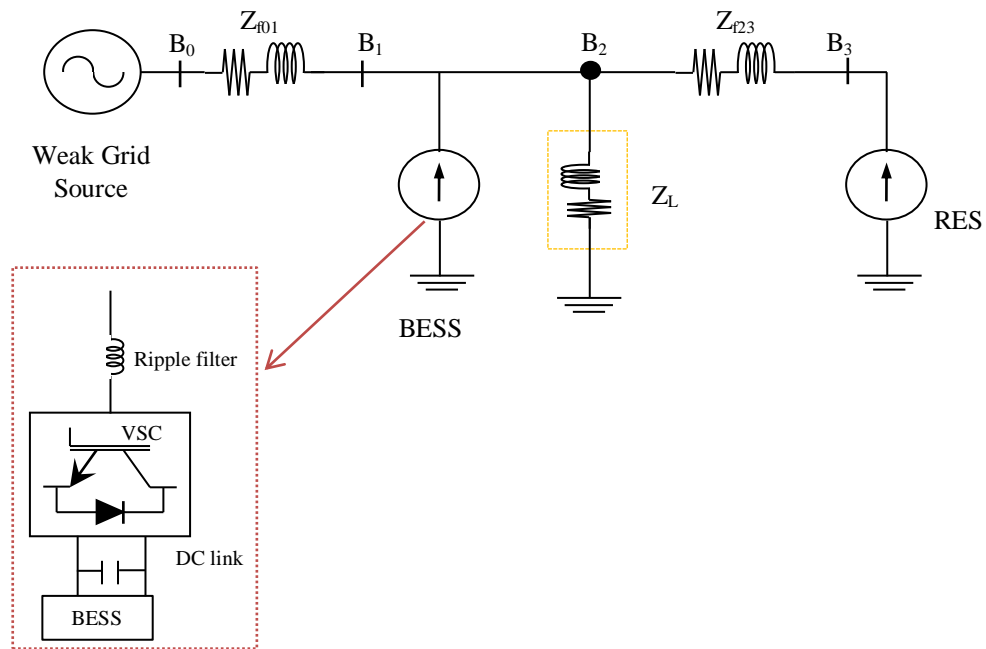


Fig. 3.34: Single line diagram of BESS for voltage regulation in radial microgrid with RES penetration

3.4.1 Analysis of BESS

The modelling equation for BESS can be derived based on the principle of energy balance in the power system. BESS is typically modelled as a voltage source in series

with a reactance (X_s) and a resistance (R_s). The voltage source represents the energy stored in the battery, while the reactance and resistance account for the voltage drop across the device. The energy stored in the battery is given by:

$$E = 0.5 C V^2 \quad (3.19)$$

Where,

E is the energy stored in the battery,

C is the capacitance of the battery, and

V is the voltage of the battery.

The voltage of the BESS, V_{BESS} , can be expressed as:

$$V_{BESS} = V_{PCC} + R_s I_{BESS} + j X_s I_{BESS} \quad (3.20)$$

Where,

V_{PCC} is the terminal voltage of the power system,

R_s and X_s are the series resistance and reactance of the BESS, and

I_{BESS} is the current flowing through the BESS.

The power flow into the BESS, P , can be expressed as:

$$P = V_{BESS} I_{BESS} \quad (3.21)$$

The rate of change of energy stored in the battery can be expressed as:

$$\frac{dE}{dt} = P$$

Substituting the value of V_{BESS} in the expression for P :

$$P = (V_{PCC} + R_s I_{BESS}) I_{BESS}$$

Substituting the value of P in the expression for rate of change of energy dE/dt ,

$$\frac{dE}{dt} = (V_{PCC} + R_s I_{BESS})I_{BESS} \quad (3.22)$$

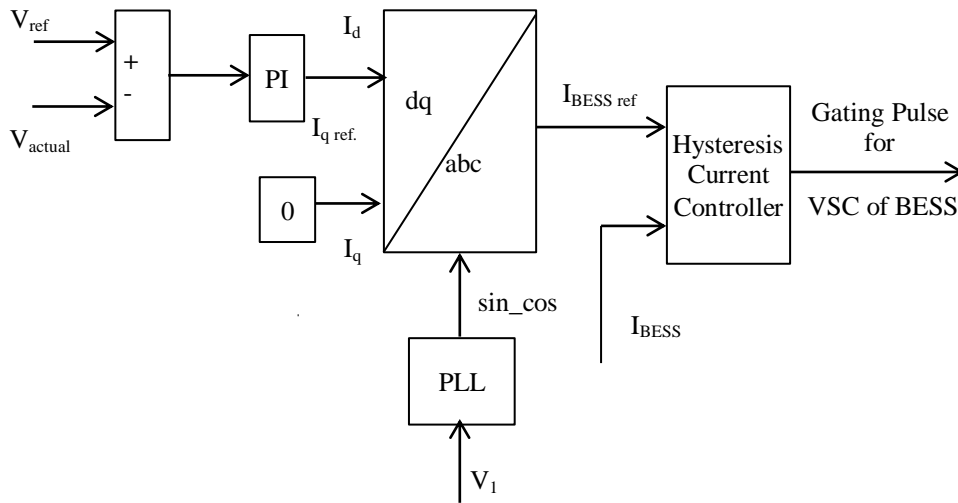


Fig. 3.35 Block diagram for gating pulse control for BESS

The voltage regulation, relates to the rate of change of energy stored in the battery to the terminal voltage of the power system and the current flowing through the BESS. The equation can be used to analyse the performance of the BESS in various power system scenarios and optimize its design and operation for maximum efficiency and reliability.

3.4.2 Control of BESS

The control of the VSC for BESS is similar to that of STATCOM, with a few differences as seen from Fig. 3.35. In BESS, the PI controller output produces only the d-axis reference current, and it does not provide any q-axis component. The output of the PI controller generates the reference d-axis current (I_d) for BESS. The reference I_d , with $I_q = 0$, undergoes reverse park transformation to produce the reference BESS current signal ($I_{BESSref}$). The difference between $I_{BESSref}$ and the actual BESS current (I_{BESS}) is then passed through the hysteresis current controller, as in the case of

STATCOM. The hysteresis current controller generates the gating pulses for switching the VSC of BESS, resulting in the required charge or discharge of the battery. Therefore, the basic control principle of BESS is similar to that of STATCOM, but the control strategy for BESS is modified to meet the requirements of battery charging and discharging.

3.4.3 Simulation Diagram of BESS

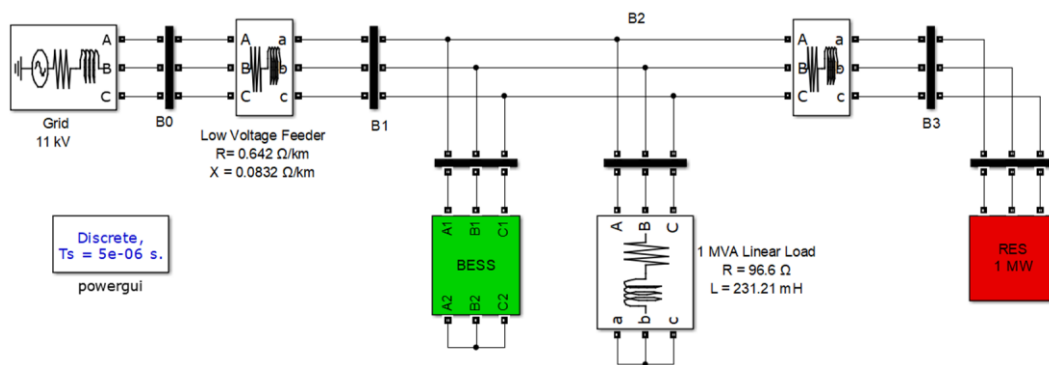


Fig. 3.36: MATLAB simulation diagram of radial microgrid with BESS as voltage regulator

The performance of BESS as a voltage regulator is evaluated using a simulation model developed in the MATLAB/SIMULINK environment. Fig. 3.36 shows the simulation diagram used for the evaluation. The simulation model includes several components, such as a weak source implemented using a three-phase source and a series RL branch to represent the feeder drop, a BESS, a balanced linear load with a power factor of 0.8 lagging and a rating of 1 MVA, and an intermittent RES source implemented as a current-controlled inverter. The BESS is realized through a VSC with a capacitor and battery tank on the DC link, and the output of the VSC is connected in shunt with the feeder after passing through a ripple filter. The simulation parameters used in the simulation model are listed in Table 3.3.

Table 3.3: Simulation parameters for voltage regulation of radial microgrid with BESS as voltage regulator

System Parameter	Values
Source Voltage (V_s)	33kV, 50Hz
BESS	11 kV, 1.6 MWh
Feeder impedance (Z_f)	$0.642 + j 0.083 \Omega/\text{km}$
RES power rating	0.67 MW at normal injection
Load (Between OLTC-T and RES)	1 MVA 0.8 pf lagging, Linear and Balanced Load $Z_L = 96.8 + j 72.64 \Omega$

3.4.4 Performance Evaluation of BESS

The performance of BESS is also evaluated for RES intermittency, load perturbation, and source perturbation with the simulation results done in MATLAB.

RES Intermittency

During RES intermittency, Battery Energy Storage Systems (BESS) can be used to regulate the voltage in the microgrid. Fig. 3.37 shows the voltage regulation waveform during RES intermittency. At the initial stage, the microgrid operates with low RES injection, where $I_{RES} = 5 \text{ A}$ from $t = 0$ to $t = 0.2 \text{ sec}$. During this period, BESS regulates the voltage by supplying real power from $t = 0.1 \text{ sec}$ to $t = 0.2 \text{ sec}$, as shown in Fig. 3.38. When the RES injection increases to $I_{RES} = 50 \text{ A}$ from $t = 0.2 \text{ sec}$ to $t = 0.4 \text{ sec}$, BESS again regulates the voltage from $t = 0.3 \text{ sec}$ to $t = 0.4 \text{ sec}$ as shown in Fig. 3.39. During this period, the voltage is regulated by BESS by supplying or absorbing real power as needed.

At $t = 0.4 \text{ sec}$, the RES injection increases significantly with $I_{RES} = 180 \text{ A}$, causing voltage variations in the microgrid. BESS responds to this by regulating the voltage from $t = 0.5 \text{ sec}$ to $t = 0.6 \text{ sec}$, as shown in Fig. 3.40. During this period, BESS

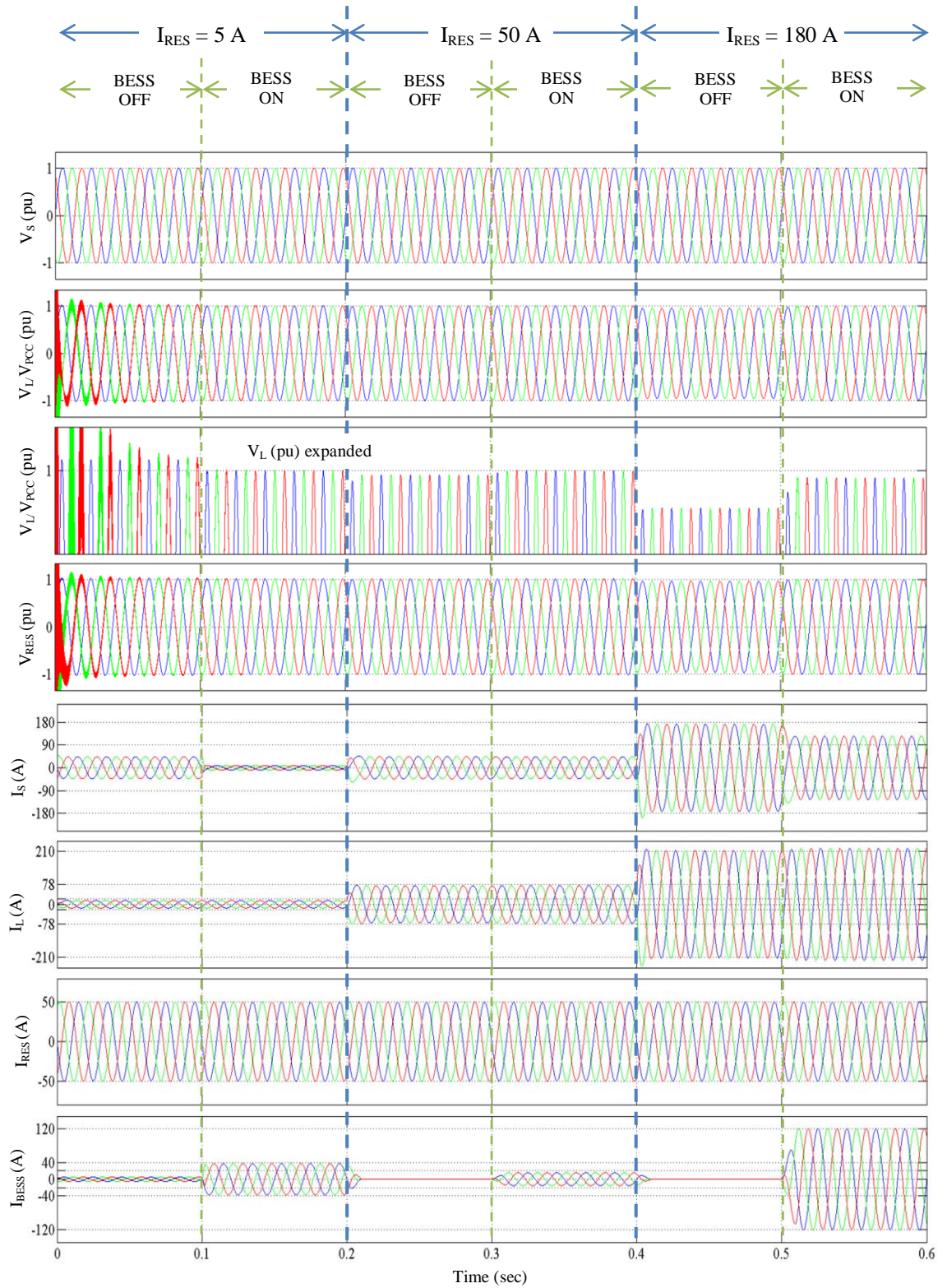


Fig. 3.37: Voltage and current waveforms for voltage regulation in considered radial microgrid with BESS as voltage regulator during RES intermittency condition.

V_s : Source Voltage (in per units), V_L/V_{PCC} : Voltage at load terminal (in pu), V_{RES} : Voltage at the terminal of RES (in pu), I_s : Source current (in A), I_L : Load Current (in A), I_{RES} : RES current (in A), $I_{STATCOM}$: Current supplied/absorbed by BESS (in A)

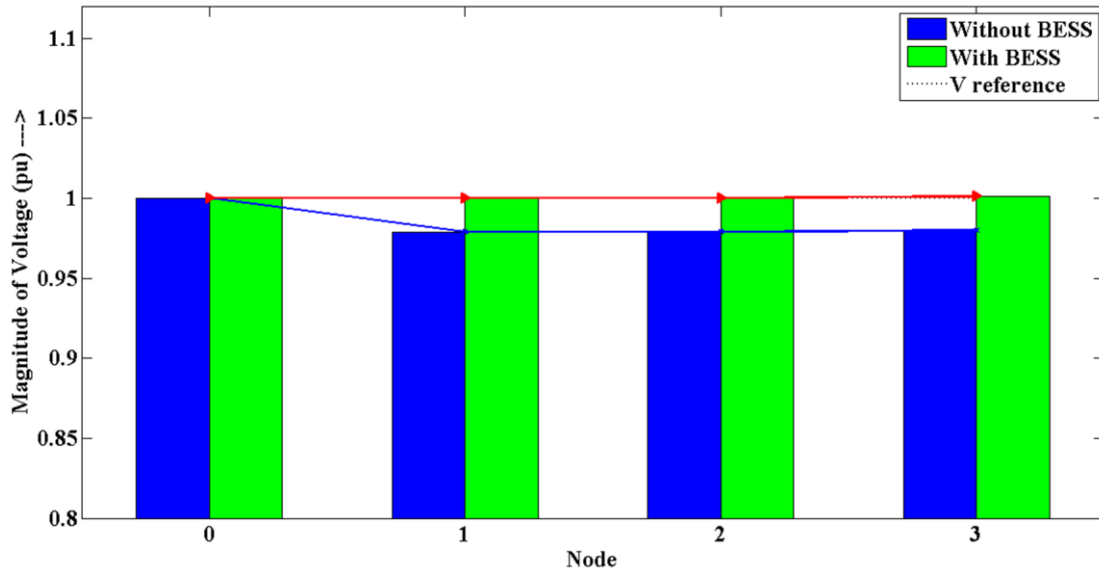


Fig. 3.38: Voltage profile of radial microgrid with BESS as voltage regulator during RES intermittency at $I_{RES} = 5 \text{ A}$

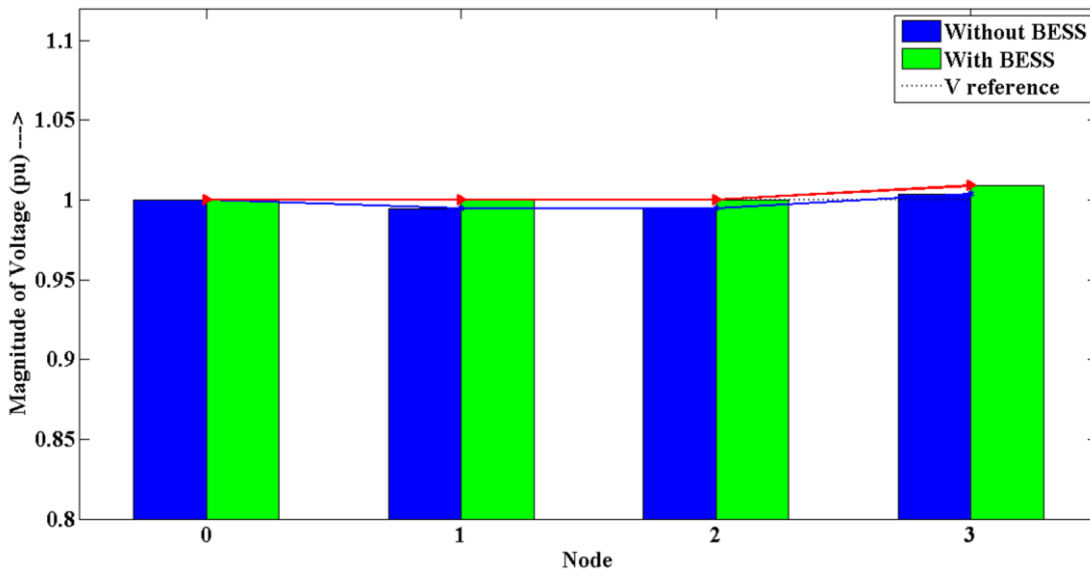


Fig. 3.39: Voltage profile of radial microgrid with BESS as voltage regulator during RES intermittency at $I_{RES} = 50 \text{ A}$

voltage variations in the microgrid. BESS responds to this by regulating the voltage from $t = 0.5 \text{ sec}$ to $t = 0.6 \text{ sec}$, as shown in Fig. 3.40. During this period, BESS regulates the voltage by supplying or absorbing real power to ensure that the voltage remains within acceptable limits.

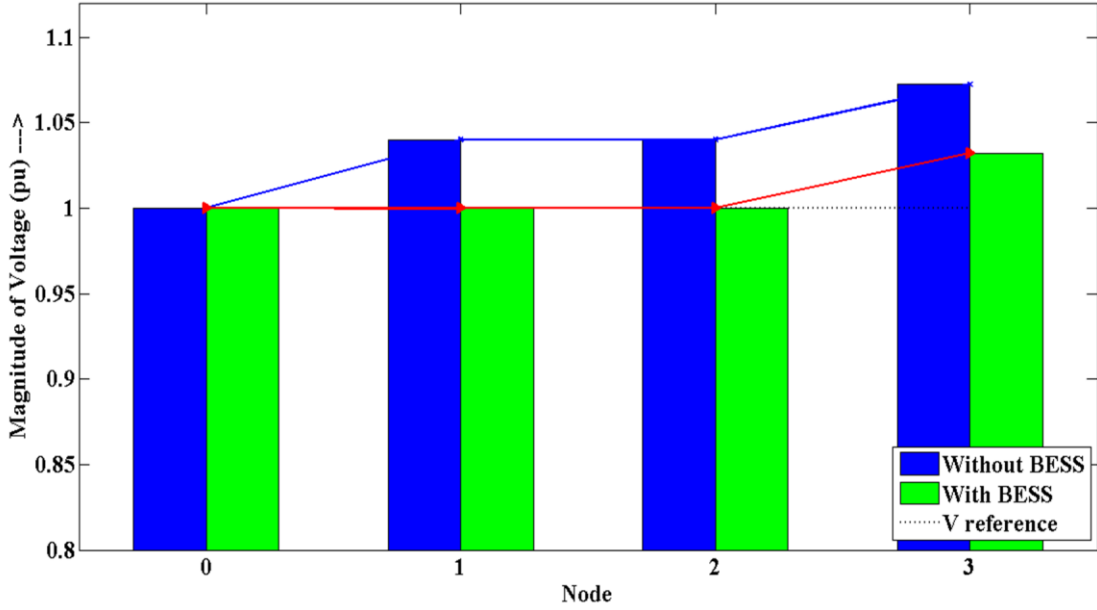


Fig. 3.40: Voltage profile of radial microgrid with BESS as voltage regulator during RES intermittency at $I_{RES} = 180$ A

Load Perturbation

The load perturbation result waveforms are shown in Fig. 3.41. At $t = 0$ to $t = 0.2$ sec, the load is in light loading condition, i.e. 20% of the rated load. The BESS regulates the voltage from $t = 0.1$ sec to $t = 0.2$ sec by supplying real power, and the voltage profile is shown in Fig. 3.42.

From $t = 0.2$ to $t = 0.4$ sec, the load is in rated loading condition with nominal RES injection, Fig. 3.43. Also at $t = 0.2$ sec BESS is switched off to show its effectiveness and later switched into the circuit at $t = 0.3$ sec. The BESS regulates the voltage from $t = 0.3$ sec to $t = 0.4$ sec.

Similarly, from $t = 0.4$ sec to $t = 0.6$ sec, the load is in heavy loading condition, i.e. 150% of the rated value. The BESS attempts to regulate the voltage from $t = 0.5$ sec to $t = 0.6$ sec but is not fully able to regulate the voltage due to limited capacity, and the voltage profile is shown in Fig. 3.44.

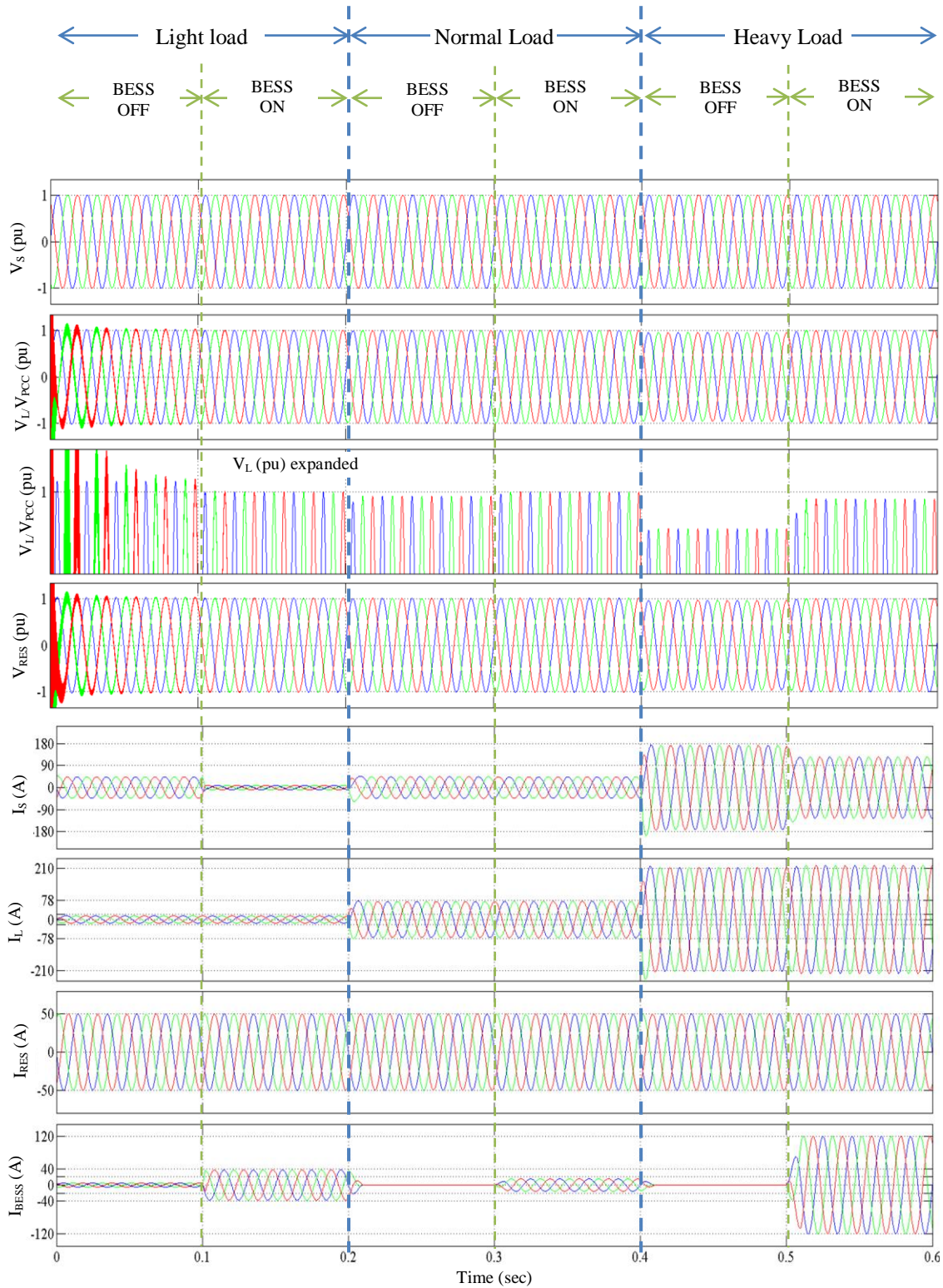


Fig. 3.41: Voltage and current waveforms for voltage regulation in considered radial microgrid with BESS as voltage regulator during load perturbation condition.

V_S : Source Voltage (in per units), V_L/V_{PCC} : Voltage at load terminal (in pu), V_{RES} : Voltage at the terminal of RES (in pu), I_s : Source current (in A), I_L : Load Current (in A), I_{RES} : RES current (in A), I_{BEES} : Current supplied/absorbed by BESS (in A)

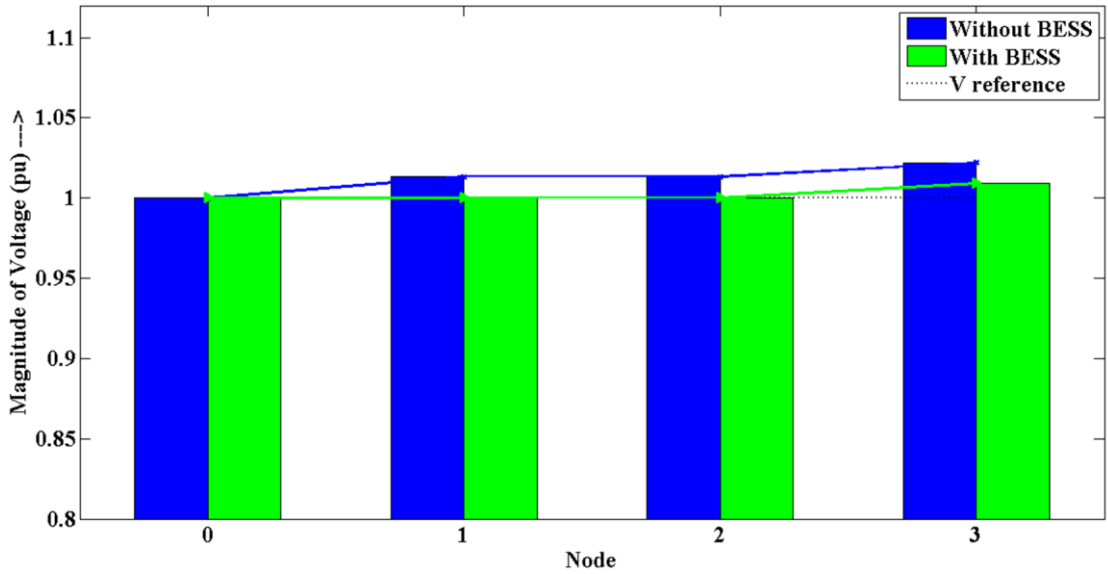


Fig. 3.42: Voltage Profile of radial microgrid with BESS as voltage regulator during load perturbation at light loading condition

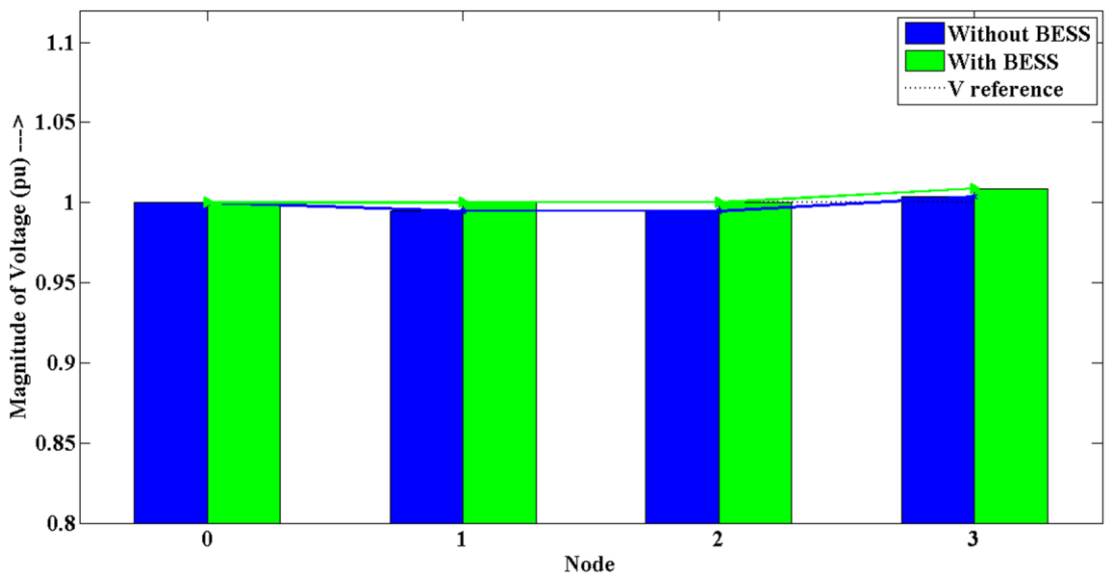


Fig. 3.43: Voltage Profile of radial microgrid with BESS as voltage regulator during load perturbation at rated loading condition

Source Perturbations

Source perturbation result waveform is shown in Fig. 3.45. At $t = 0$ to $t = 0.2$ sec, rated source voltage is maintained at the source, Fig. 3.46, and BESS regulates voltage from $t = 0.1$ sec to $t = 0.2$ sec. From $t = 0.2$ to $t = 0.4$ sec, there is an under voltage condition.

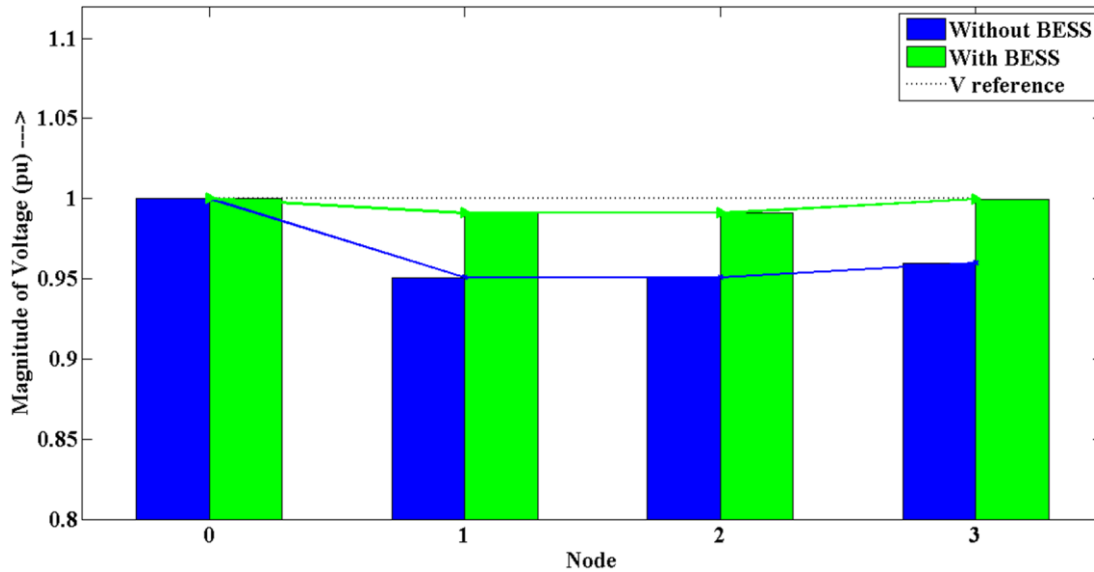


Fig. 3.44: Voltage Profile of radial microgrid with BESS as voltage regulator during load perturbation at heavy loading condition

BESS tries to regulate voltage from $t = 0.3$ sec to $t = 0.4$ sec, but it is not fully able to regulate the voltage, possibly due to limited capacity. The voltage profile is shown in Fig. 3.47. From $t = 0.4$ sec to $t = 0.6$ sec, there is an over voltage condition at the source. BESS tries to regulate voltage from $t = 0.5$ sec to $t = 0.6$ sec, but in this condition also BESS is not fully able to regulate the voltage, possibly due to its limited capacity. The voltage profile for the same is shown in Fig. 3.48.

3.5 Dynamic Voltage Restorer (DVR)

A Dynamic Voltage Restorer (DVR) is a power quality device used to mitigate voltage sags, swells, and interruptions in an electrical power system. It is a type of power electronic device that is capable of injecting a series voltage of the same magnitude and opposite polarity as the voltage sag or swell in the power system. The injected voltage restores the voltage to its normal value, thereby preventing damage to sensitive equipment.

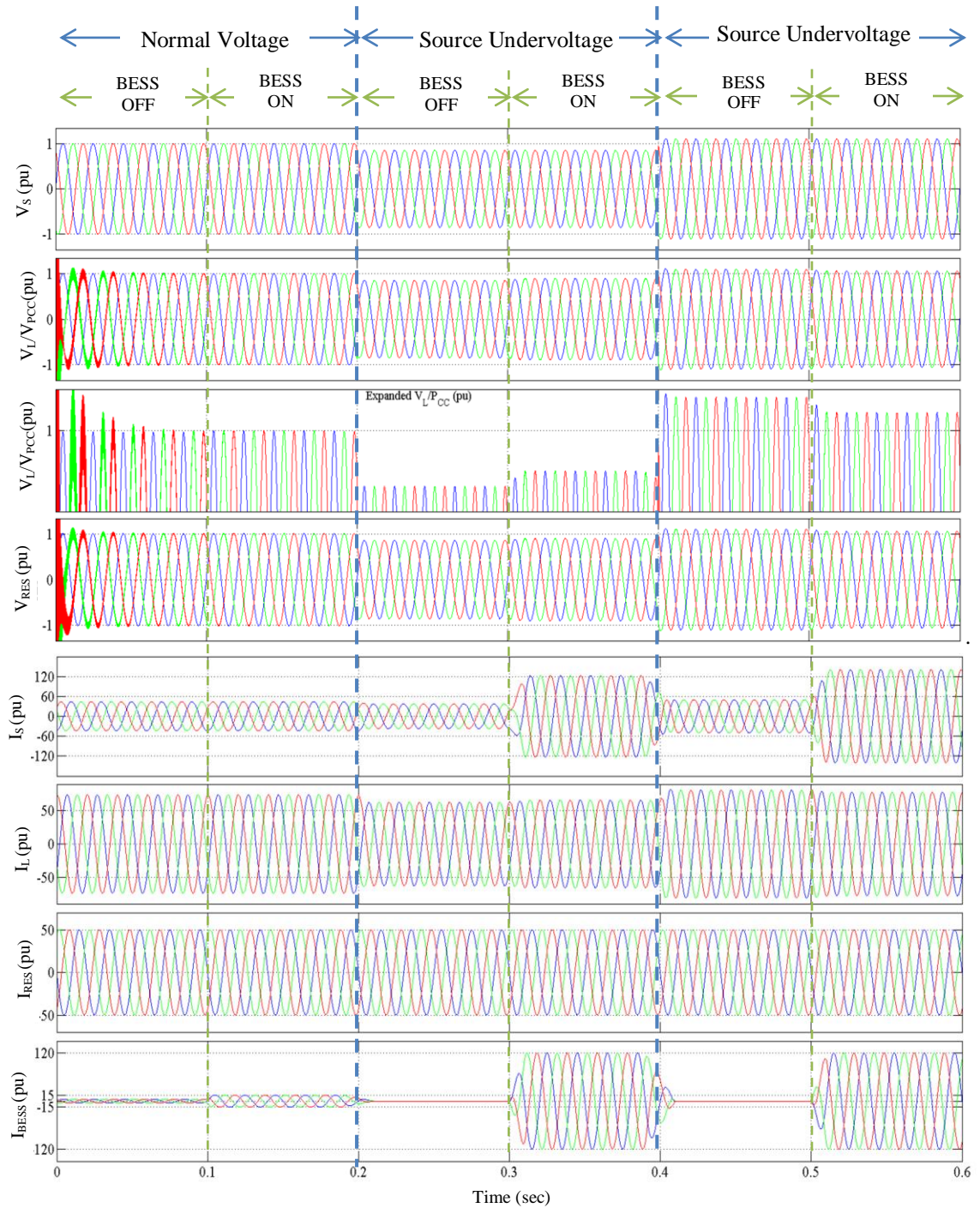


Fig. 3.45: Voltage and current waveforms for voltage regulation in considered radial microgrid with BESS as voltage regulator during source perturbation condition.

V_s : Source Voltage (in per units), V_L/V_{PCC} : Voltage at load terminal (in pu), V_{RES} : Voltage at the terminal of RES (in pu), I_s : Source current (in A), I_L : Load Current (in A), I_{RES} : RES current (in A), I_{BESS} : Current supplied/absorbed by BESS (in A)

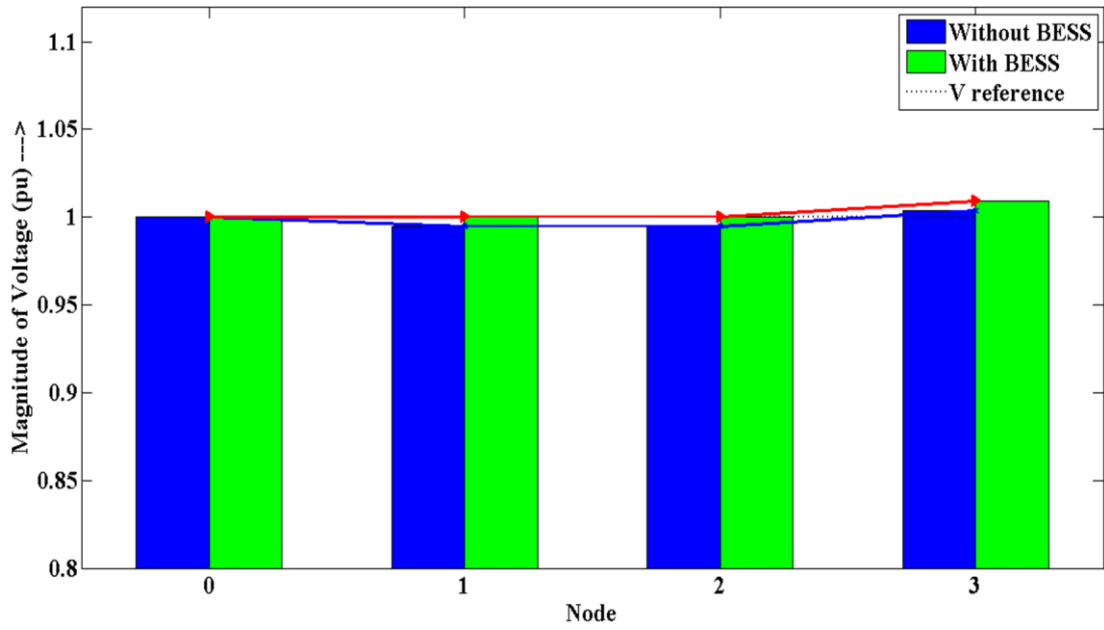


Fig. 3.46: Voltage Profile of radial microgrid with BESS as voltage regulator during source perturbation at rated voltage from source side

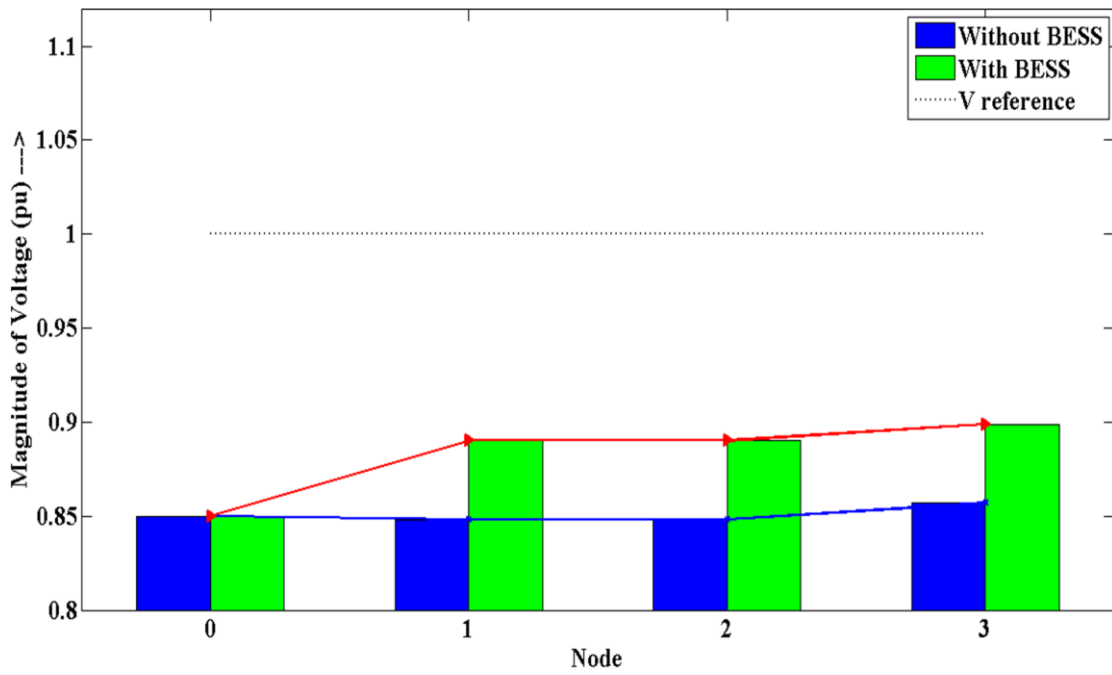


Fig. 3.47: Voltage Profile of radial microgrid with BESS as voltage regulator during source perturbation at undervoltage from source side

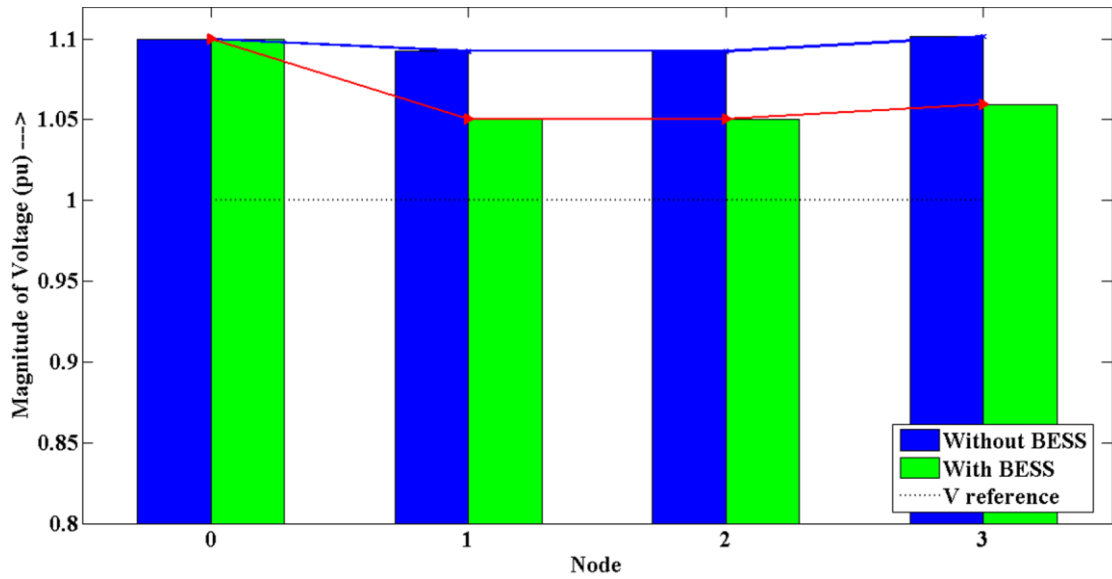


Fig. 3.48: Voltage Profile of radial microgrid with BESS as voltage regulator during source perturbation at overvoltage from source side

3.5.1 Analysis of DVR

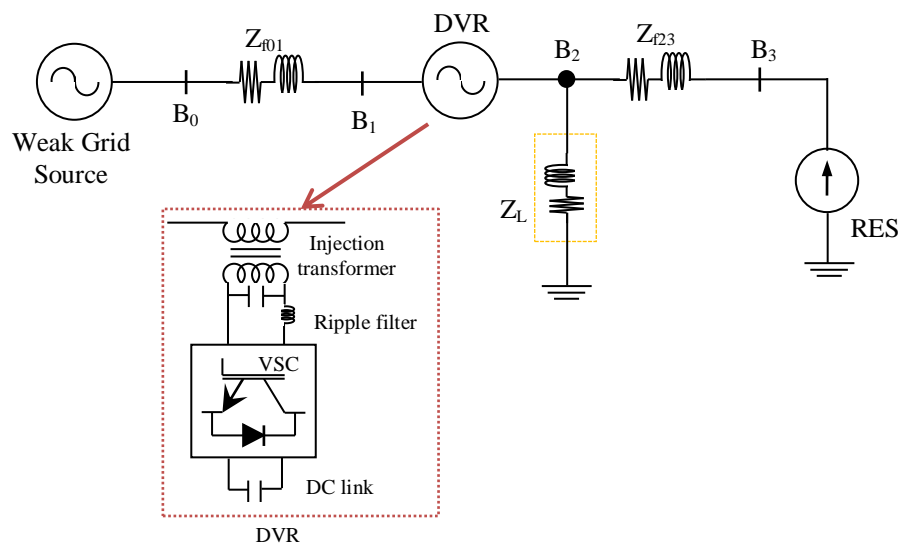


Fig. 3.49: Single line diagram of DVR for voltage regulation in radial microgrid with RES penetration

The block diagram shown in Fig.3.49 illustrates a DVR connected in a radial microgrid or distribution feeder with intermittent RES. The microgrid system consists of a weak power source, DVR, intermittent RES, distributed line impedance, and

loads. The weak power source provides power exclusively to the base load in the feeder. The load is a simple three-phase linear load that consumes both real and reactive power. The distributed line impedance is located in two areas: between the source and the load, and between the load and RES. The RES is a variable current-controlled source located near the end of the feeder, designed to evaluate the worst-case scenario for voltage regulation and power reversal. The DVR is responsible for supplying or absorbing voltage for regulating the voltage by supplying or absorbing reactive voltage at point of common coupling.

Before the placement of DVR, the grid solely catered to the demand of load current, and the relationship between the load current (I_L) and the grid current (I_S) can be expressed as:

$$I_L = I_S \quad (3.23)$$

Rewriting the same in a d-axis and q-axis component using synchronous reference frame theory:

$$I_{Ld} + j I_{Lq} = I_{Sd} + j I_{Sq} \quad (3.24)$$

Voltage at the PCC without placement of the DVR into the feeder is calculated as:

$$\begin{aligned} V_L &= V_S - I_S * (R_f + jX_f) \\ \Rightarrow V_{Ld} + j V_{Lq} &= V_{Sd} + j V_{Sq} - (I_{Sd} + j I_{Sq}) * (R_f + jX_f) \end{aligned} \quad (3.25)$$

The DVR is connected in series with the grid, and it tries to regulate the voltage at its terminal by injecting/absorbing reactive voltage into the microgrid. Now, the voltage at load voltage at the terminals of DVR is given by equation (3.26).

$$V_{Ld} + j V_{Lq} = V_{Sd} + j V_{Sq} - (I_{Sd} + j I_{Sq}) * (R_f + jX_f) + V_{DVRd} + j V_{DVRq} \quad (3.26)$$

With the DVR's involvement in managing reactive voltage, the grid no longer supplies reactive voltage but only the real component. As a result, the voltage drop across the

feeder is reduced, and the voltage at the PCC is increased. When the DVR's reactive compensation is increased, there is further increase in the PCC voltage and regulating it to the rated value. If the PCC voltage is too high, the DVR regulates it by absorbing reactive voltage. This concept is illustrated with a phasor diagram shown in Fig. 3.50.

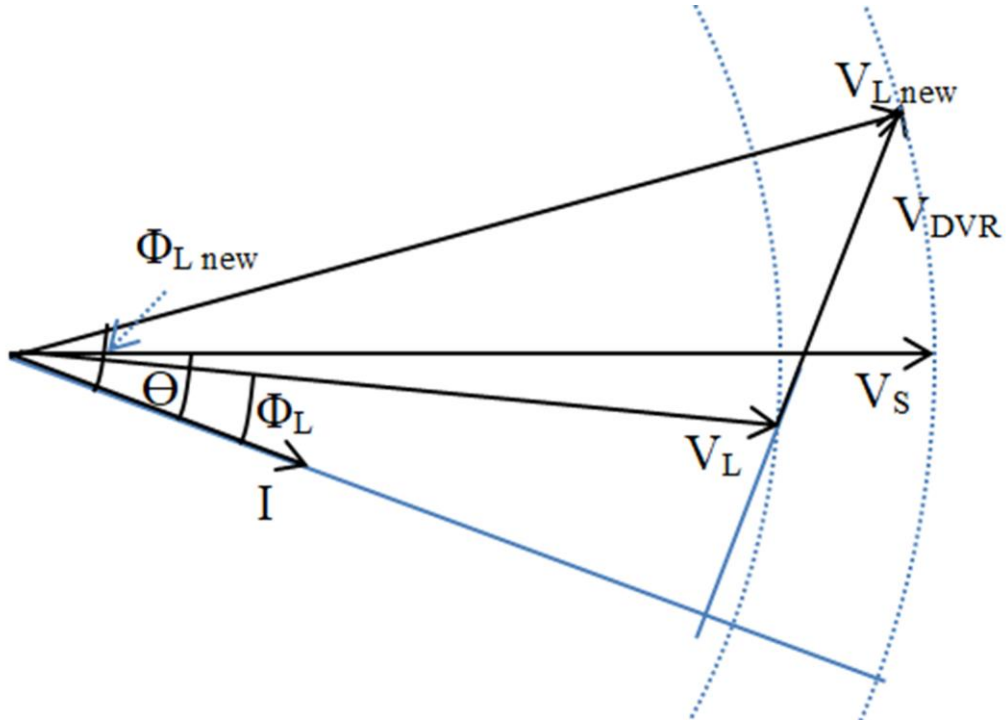


Fig. 3.50: Phasor diagram of DVR for voltage regulation at its PCC

If the DVR is involved in managing real voltage, the load burden on grid is reduced. As a result, the voltage drop across the feeder is reduced, and the voltage at the PCC is increased. When the DVR's real compensation is increased, there is further increase in the PCC voltage and regulating it to the rated value.

Considering that DVR is regulating voltage by injecting only the reactive voltage demand of load, and the real component of voltage is solely catered by the grid, Equation (3.25) can be rewritten as:

$$V_{Ld} + j V_{Lq} = (V_{Sd} + jV_{Sq}) - (I_{Sd}) * (R_f + jX_f) \pm j V_{DVRq} \quad (3.27)$$

Comparing equation (3.25) with equation (3.27), considering the feeder impedance same in both cases, it is clear that V_{PCC}/V_L is improved and the value of the resultant load voltage depends whether the DVR is injecting or absorbing voltage.

3.5.2 Control of DVR

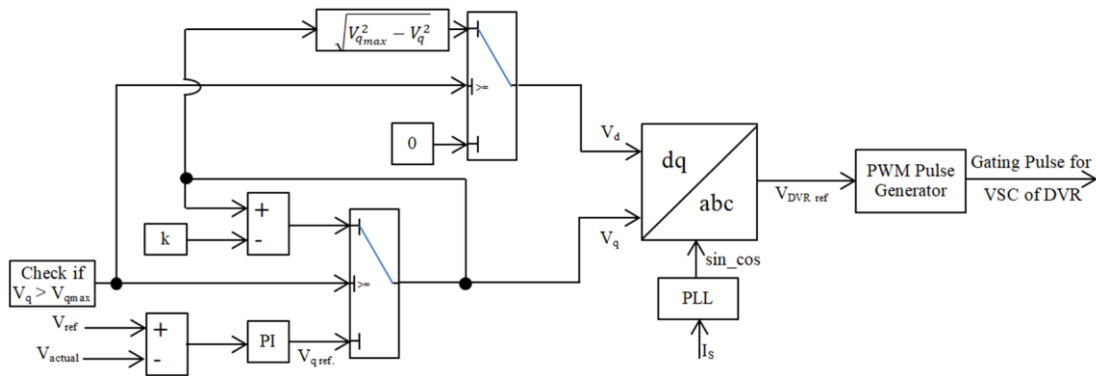


Fig. 3.51: Block diagram for gating pulse control for DVR

The control scheme utilized in the simulation also utilizes SRF theory to manage the gating pulses of VSC in the DVR. This scheme can precisely control the injection of the necessary voltage, as shown in Fig. 3.51 block diagram of the control scheme. To generate the required DVR reference voltage, a proportional-integral (PI) controller accurately measures the difference between the rated voltage and the measured voltage from the DVR terminals. Typically, the control scheme employs the q-axis component (V_q) to generate the DVR reference voltage, i.e., through the reactive power component only. However, the control scheme also has the flexibility to adjust the reference voltage by modifying both the q-axis and d-axis components if the DVR's reactive capacity is insufficient to regulate the terminal voltage. This adjustment is accomplished by increasing the d-axis component (V_d) slowly and simultaneously decreasing V_q , which ensures that the voltage remains within a specified range.

Later, the reverse park transformation is utilized to transform the reference V_d and V_q into a reference V_{abc} signal. Then, the abc reference signal is passed through the pulse width modulator (PWM) block to generate gating pulses of VSC that controls the switching of VSC switches. This regulates the voltage at the terminal of the DVR.

3.5.3 Simulation Diagram of DVR

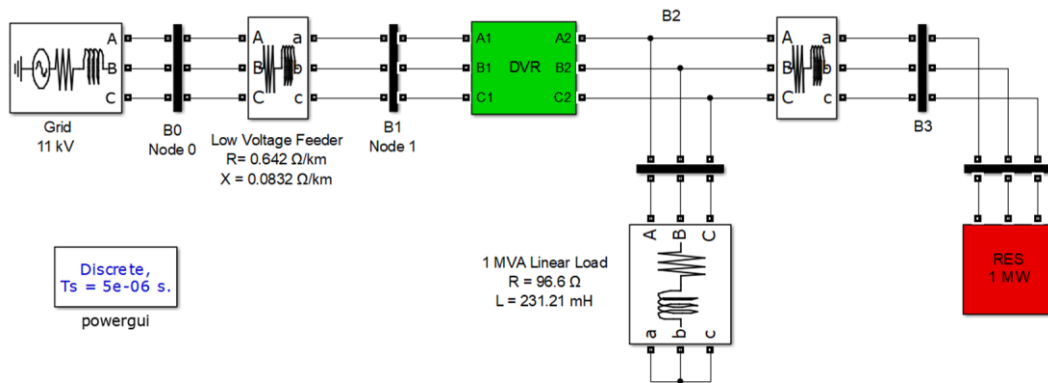


Fig. 3.52(a): MATLAB simulation diagram of radial microgrid with DVR as voltage regulator

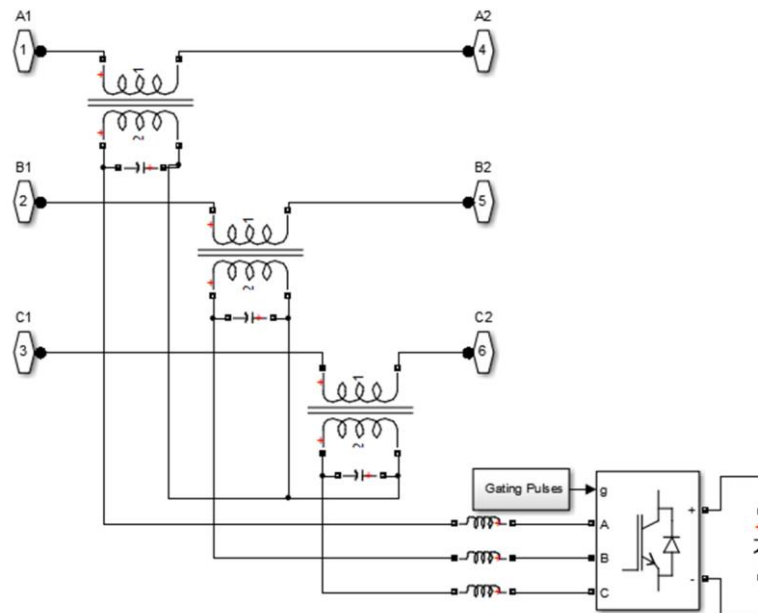


Fig. 3.52(b): Expanded simulation diagram for DVR

Similarly, the performance of DVR as voltage regulator is evaluated using a simulation model developed in the MATLAB/SIMULINK environment. Fig. 3.52(a)

shows the simulation diagram used for the evaluation and Fig. 3.52(b) shows the expanded diagram of DVR. The simulation model includes several components, such as a weak source implemented using a three-phase source and a series RL branch to represent the feeder drop, a DVR, a balanced linear load with a power factor of 0.8 lagging and a rating of 1 MVA, and an intermittent RES source implemented as a current-controlled inverter. The DVR is realized through a VSC with a capacitor on the DC link, and the output of the VSC is connected in series with the feeder through an injection transformer after passing through a ripple filter. The simulation parameters used in the simulation model are listed in Table 4.3.

Table 3.4: Simulation parameters for voltage regulation of radial microgrid with DVR as voltage regulator

System Parameter	Values
Source Voltage (V_s)	33kV, 50Hz
DVR	33/11kV, 0.5 MVA
Feeder impedance (Z_f)	$0.642 + j 0.083 \Omega/\text{km}$
RES power rating	0.67 MW at normal injection
Load (Between OLTC-T and RES)	1 MVA, 0.8 pf lagging, Linear and Balanced Load $Z_L = 96.8 + j 72.64 \Omega$

3.5.4 Performance Evaluation of DVR

The performance of the Dynamic Voltage Restorer (DVR) is evaluated in a radial microgrid under different conditions to evaluate its performance. These conditions include the intermittent nature of renewable energy sources (RES), load perturbations, and source voltage perturbations such as under-voltage and overvoltage.

RES Intermittency

During RES intermittency, the DVR compensates for voltage variations in the microgrid caused by the variable power injection of RES. Fig. 3.53 illustrates the

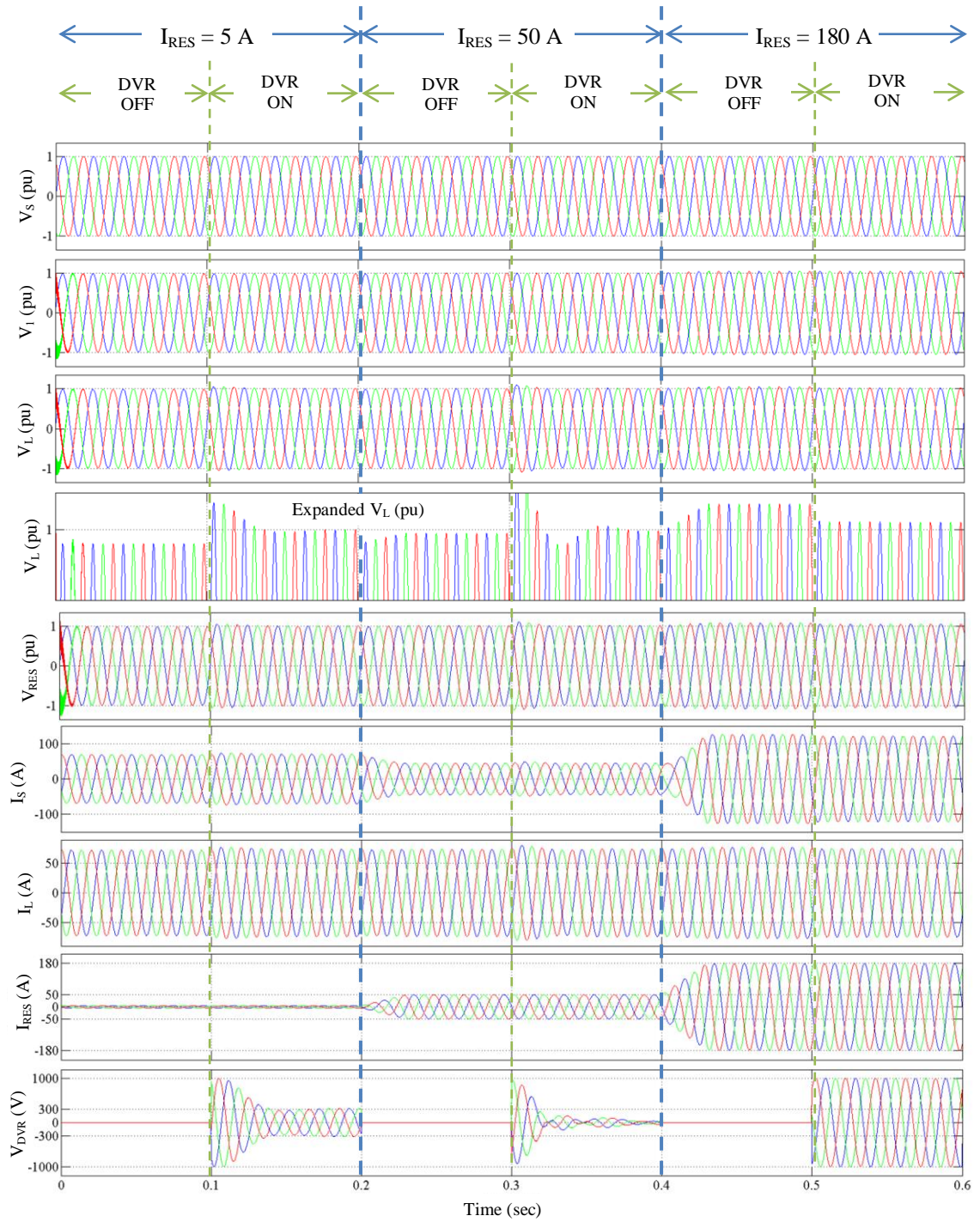


Fig.3.53: Voltage and current waveforms for voltage regulation in considered radial microgrid with DVR as voltage regulator during RES intermittency condition.

V_S : Source Voltage (in per units), V_1 : Voltage at source side terminal of DVR, V_L/V_{PCC} : Voltage at load terminal (in pu), V_{RES} : Voltage at the terminal of RES (in pu), I_S : Source current (in A), I_L : Load Current (in A), I_{RES} : RES current (in A), V_{DVR} : Voltage supplied/absorbed by DVR (in V)

voltage regulation waveform during RES intermittency. Initially, the DVR is in standby mode, and the system operates with low RES injection, with $I_{RES} = 5$ A. At $t =$

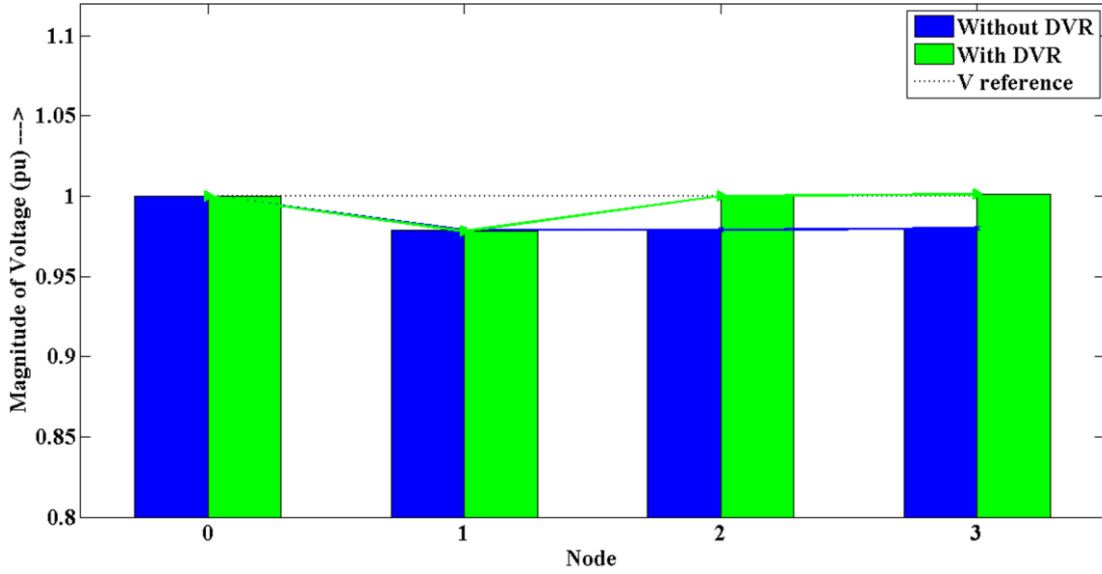


Fig. 3.54: Voltage profile of radial microgrid with DVR as voltage regulator during RES intermittency at $I_{RES} = 5 \text{ A}$

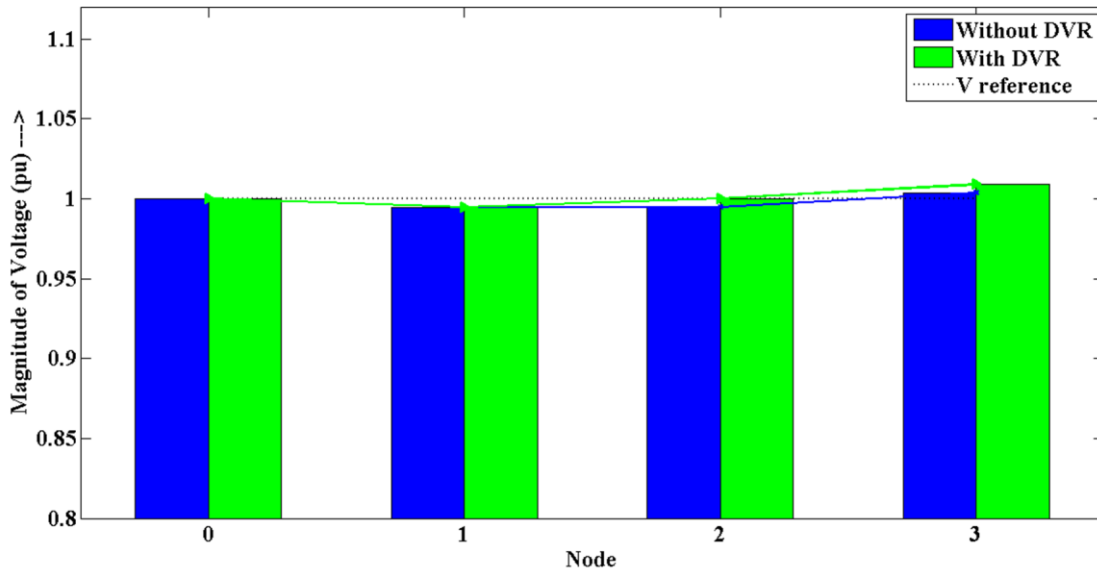


Fig. 3.55: Voltage profile of radial microgrid with DVR as voltage regulator during RES intermittency at $I_{RES} = 50 \text{ A}$

0.1 sec, the DVR starts injecting voltage and regulates the voltage profile as seen in Fig. 3.54. When RES injection becomes normal at $t = 0.2 \text{ sec}$, the DVR goes back to standby mode. The voltage profile of the system shows very little variation, which is also regulated by the DVR at its terminal at $t = 0.3 \text{ sec}$ as seen from Fig. 3.55. At $t =$

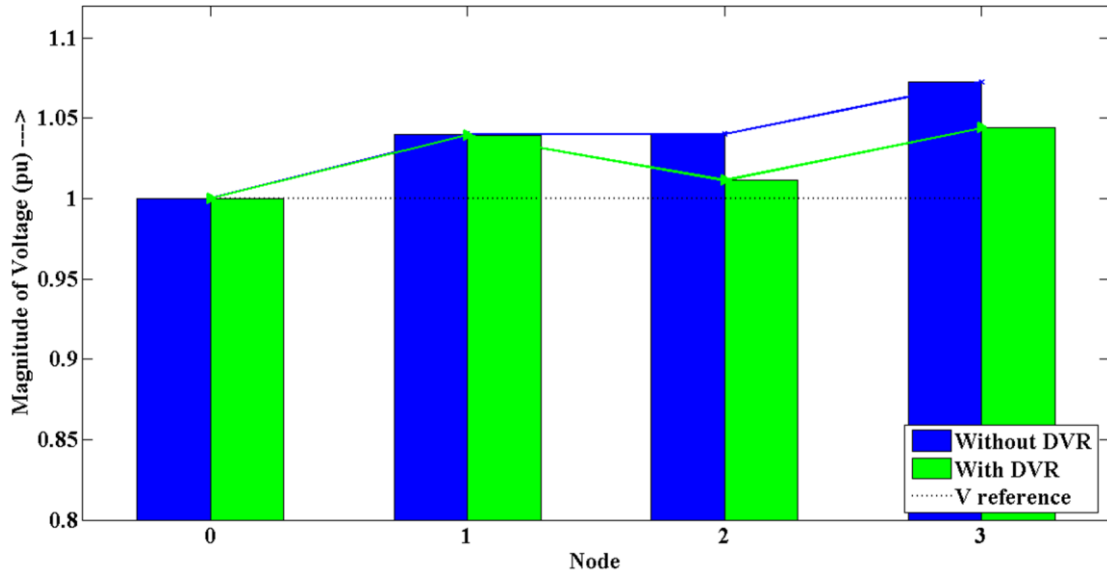


Fig. 3.56: Voltage profile of radial microgrid with DVR as voltage regulator during RES intermittency at $I_{RES} = 180$ A

0.4 sec, when the RES injection drastically increases with $I_{RES} = 180$ A. The DVR is switched in at $t = 0.5$ sec and it may be observed that DVR tries to regulate the voltage at its terminal. Although the voltage shows a huge improvement, despite of the fact that the DVR only regulates through reactive power, it is not been able to fully regulate the voltage. The observation is duly supported further by voltage profile shown in Fig. 3.56.

Load Perturbation

Under the load perturbation condition, the DVR mitigates voltage variations caused by sudden changes in the loading conditions. Fig. 3.57 illustrates the voltage regulation waveform during load perturbations. Initially, the system operates at a light loading condition, causing overvoltage at the terminal. The DVR absorbs reactive power from the feeder by switching into the circuit at $t = 0.1$ sec and regulates the voltage as seen from the voltage profile shown in Fig. 3.58. When the loading comes back to the rated

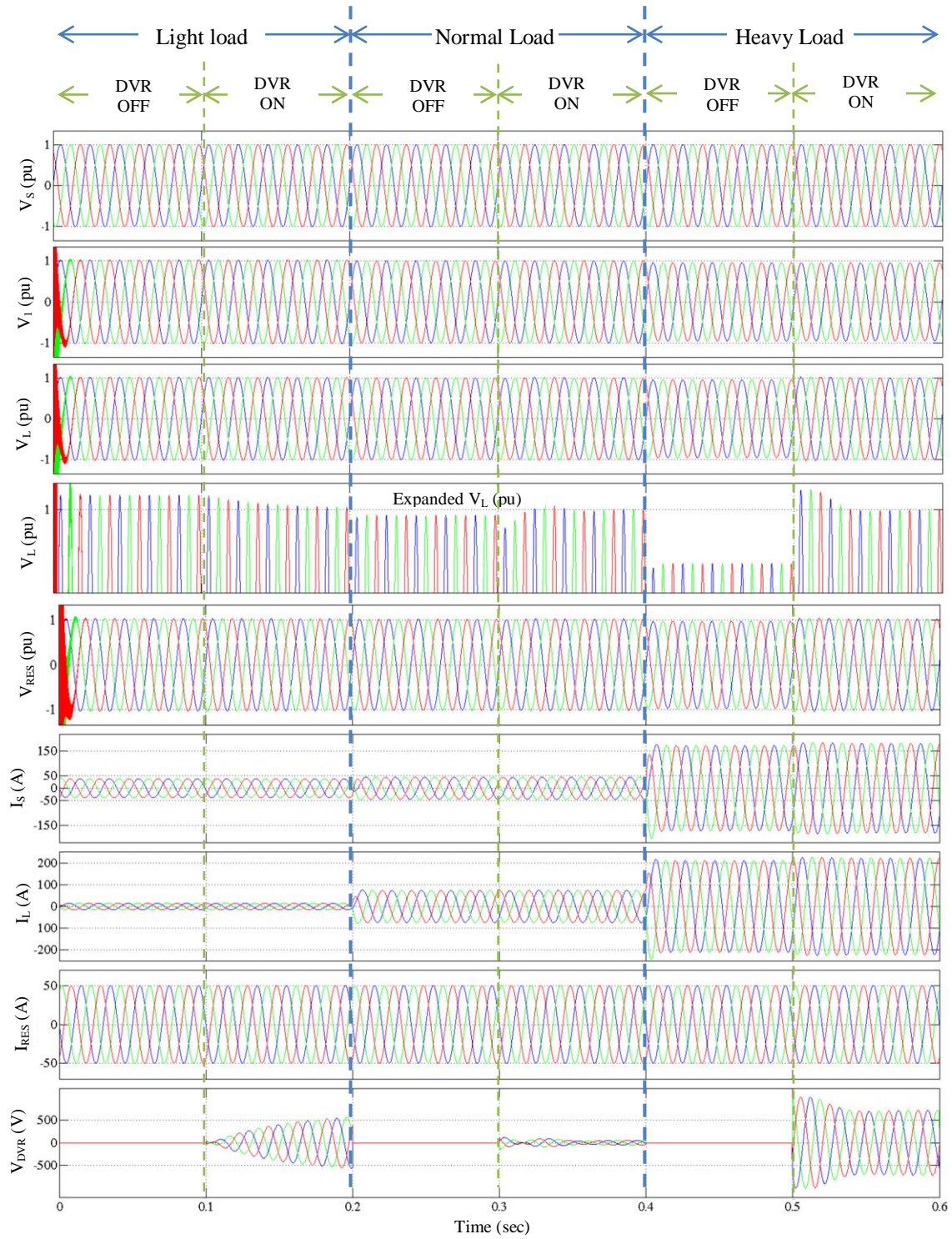


Fig. 3.57: Voltage and current waveforms for voltage regulation in considered radial microgrid with DVR as voltage regulator during load perturbation condition.

V_S : Source Voltage (in per units), V_1 : Voltage at source side terminal of DVR, V_L/V_{PCC} : Voltage at load terminal (in pu), V_{RES} : Voltage at the terminal of RES (in pu), I_S : Source current (in A), I_L : Load Current (in A), I_{RES} : RES current (in A), V_{DVR} : Voltage supplied/absorbed by DVR (in V)

value at $t = 0.2$ sec, the system returns to normal, Fig. 3.59. Later, at $t = 0.4$ sec, the

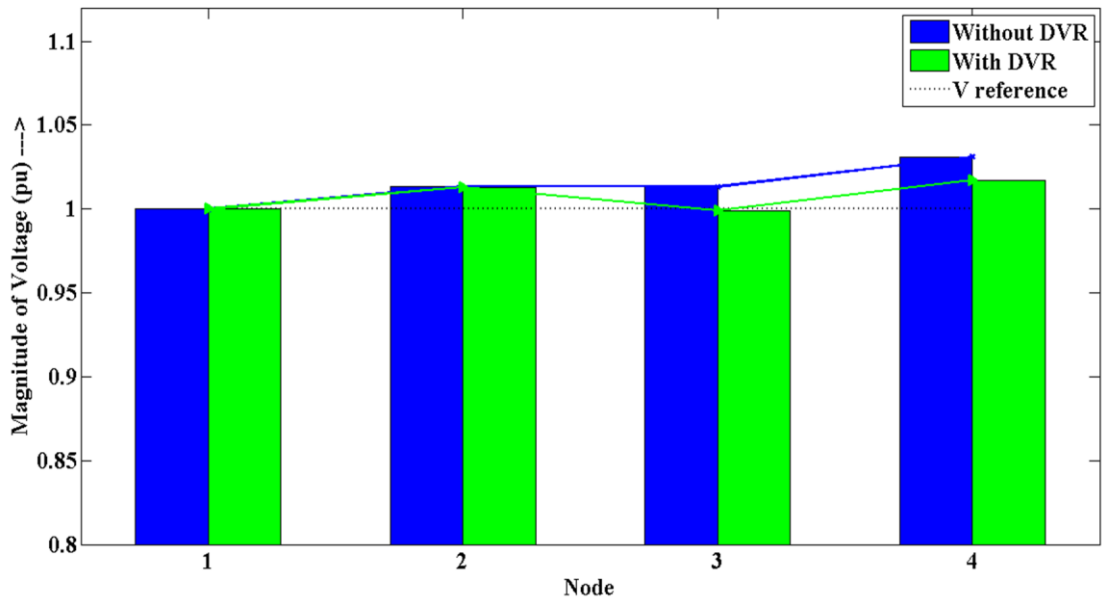


Fig. 3.58: Voltage Profile of radial microgrid with DVR as voltage regulator during load perturbation at light loading condition.

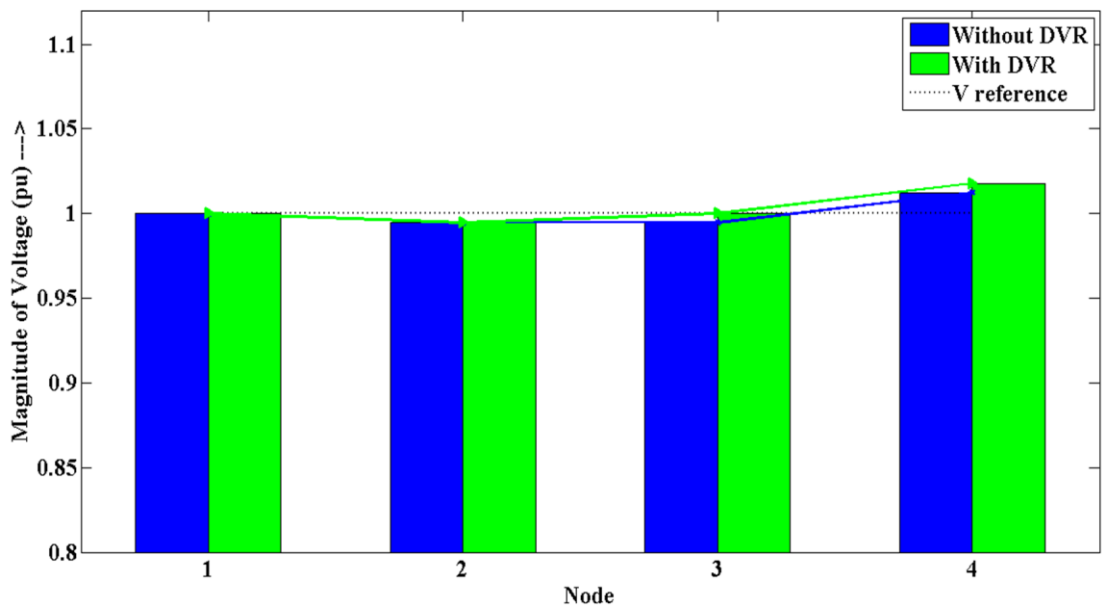


Fig. 3.59: Voltage Profile of radial microgrid with DVR as voltage regulator during load perturbation at rated loading condition

feeder undergoes a heavy loading condition, causing undervoltage at the load terminal. The DVR regulates the voltage to the rated value by switching into the circuit at $t = 0.5$ sec, as shown in Fig. 3.60.

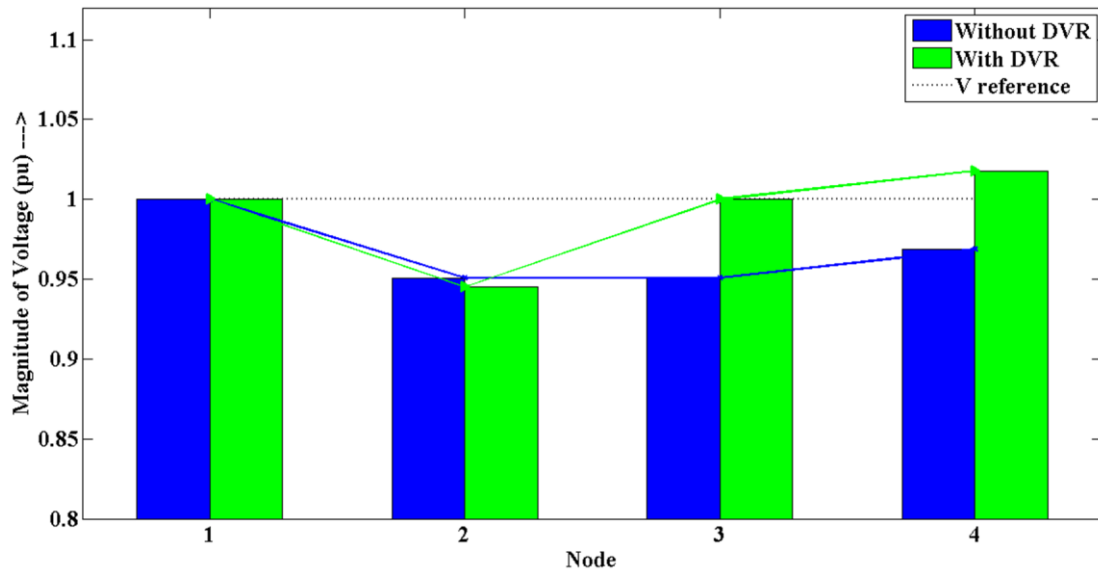


Fig. 3.60: Voltage Profile of radial microgrid with DVR as voltage regulator during load perturbation at heavy loading condition

Source Perturbations

The source perturbation conditions are explored for undervoltage and overvoltage conditions, where the DVR mitigates voltage variations caused by grid-side voltage fluctuations. Fig. 3.61 illustrates the voltage regulation waveforms during source perturbations. At the initial stage, the grid voltage remains close to the nominal value, even if the DVR is turned ON at $t = 0.1$ sec, its output seizes to low value and the implication is null and void, Fig 3.62. At $t = 0.2$ sec, an undervoltage condition occurs in the grid, and when the DVR injects the required reactive power at $t = 0.3$ sec, a substantial improvement in voltage regulation is witnessed. Although the DVR significantly increases the voltage, the voltage is not fully regulated, as shown in the voltage profile in Fig. 3.63. Similarly, when the source is perturbed, at $t = 0.4$ sec, for an overvoltage condition, the DVR regulates the voltage by absorbing the excess reactive power just after its switching in into the circuit at $t = 0.5$ sec, as shown in Fig. 3.64.

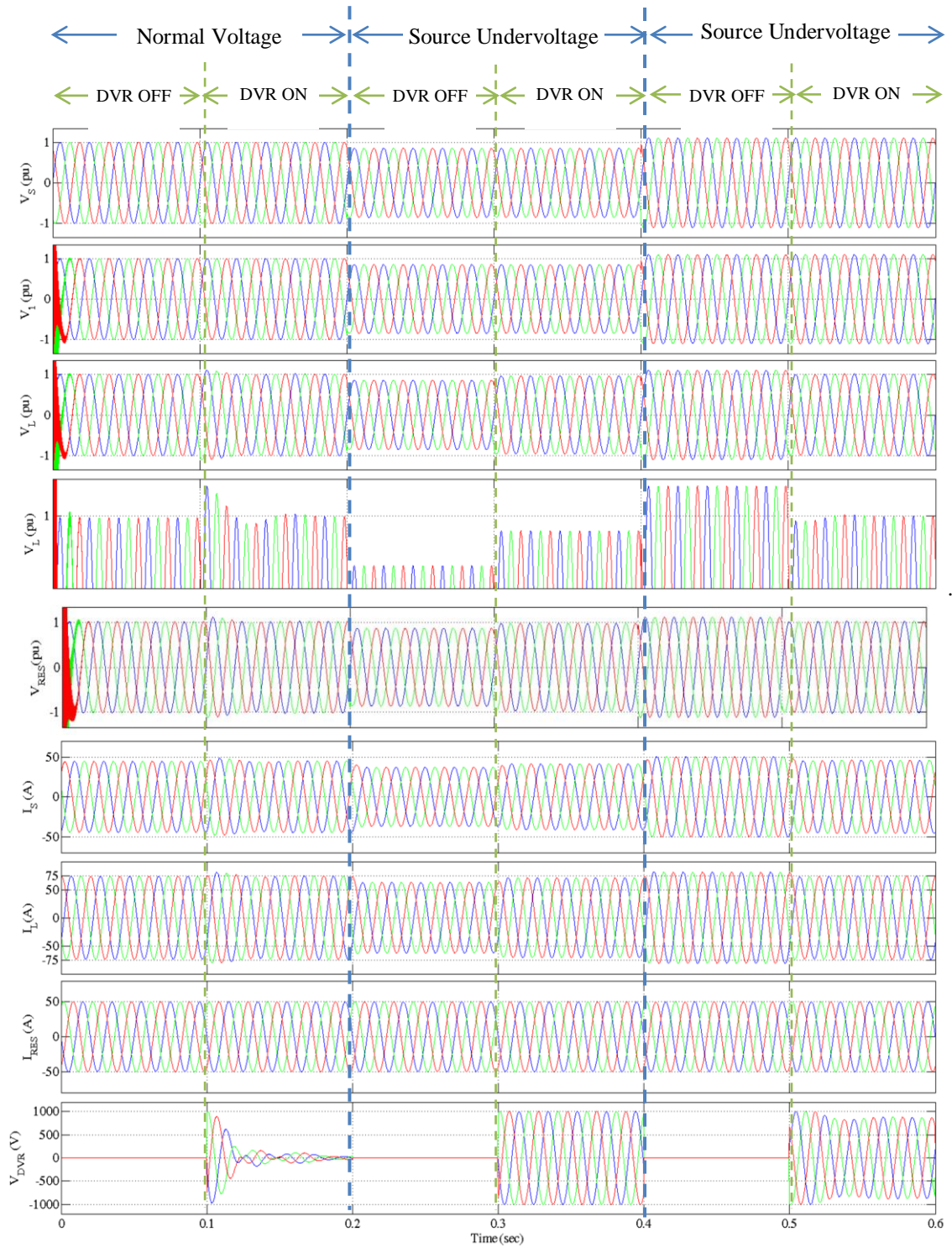


Fig. 3.61: Voltage and current waveform for voltage regulation in considered radial microgrid with DVR as voltage regulator during source perturbation condition.

V_S : Source Voltage (in per units), V_1 : Voltage at the source side terminal of DVR, V_L/V_{PCC} : Voltage at load terminal (in pu), V_{RES} : Voltage at the terminal of RES (in pu), I_S : Source current (in A), I_L : Load Current (in A), I_{RES} : RES current (in A), V_{DVR} : Voltage supplied/absorbed by DVR (in V)

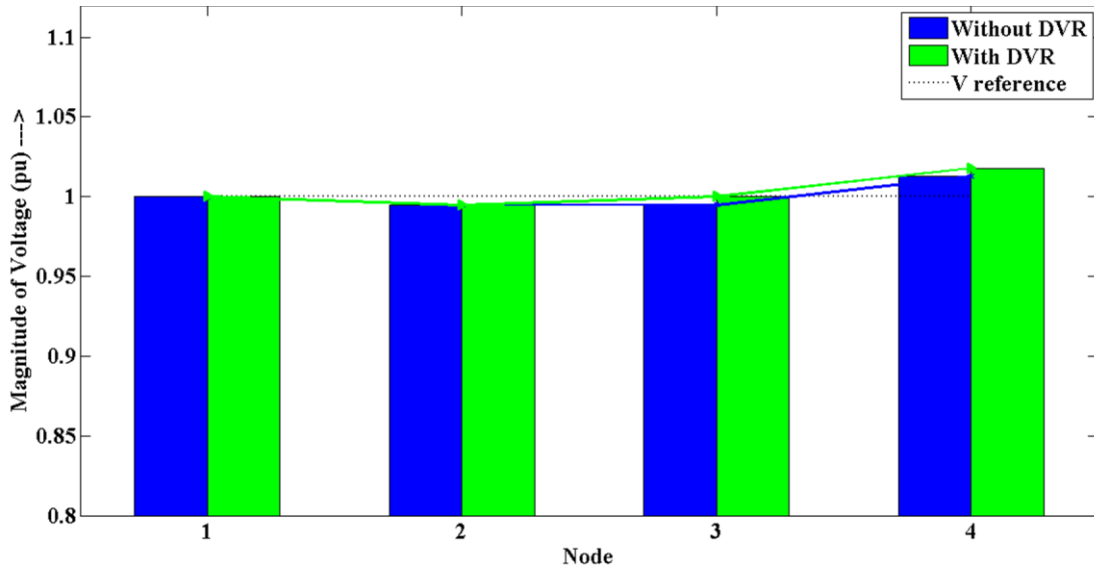


Fig. 3.62: Voltage Profile of radial microgrid with DVR as voltage regulator during source perturbation at rated voltage from source side

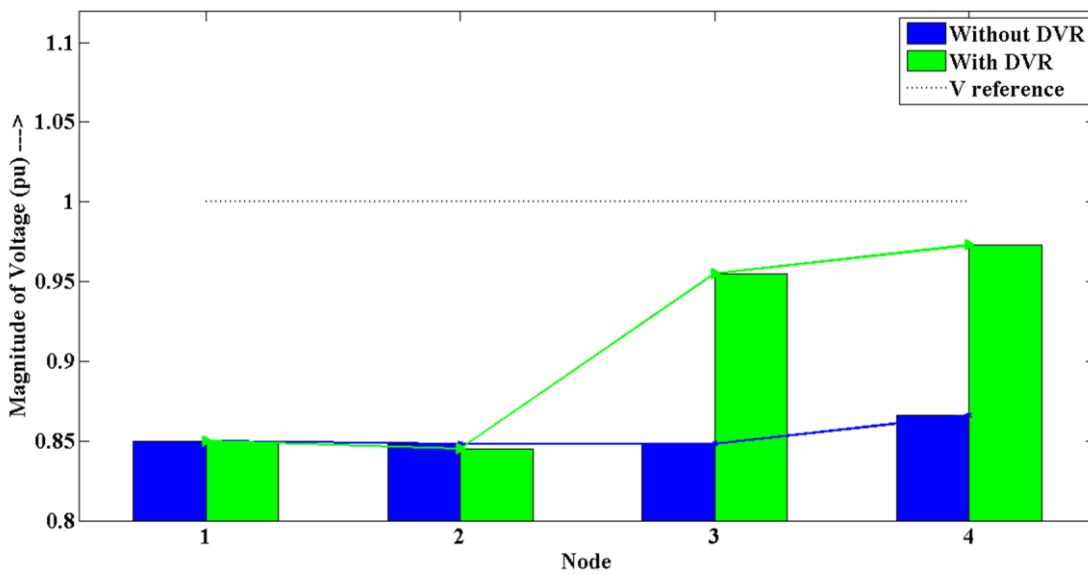


Fig. 3.63: Voltage Profile of radial microgrid with DVR as voltage regulator during source perturbation at undervoltage from source side

3.6 Comparison of different voltage regulators for radial microgrid/distribution fed with RES

A comparison of different voltage regulators based on simulation results and voltage profile for voltage regulation in grid-connected radial microgrids/distribution feeders

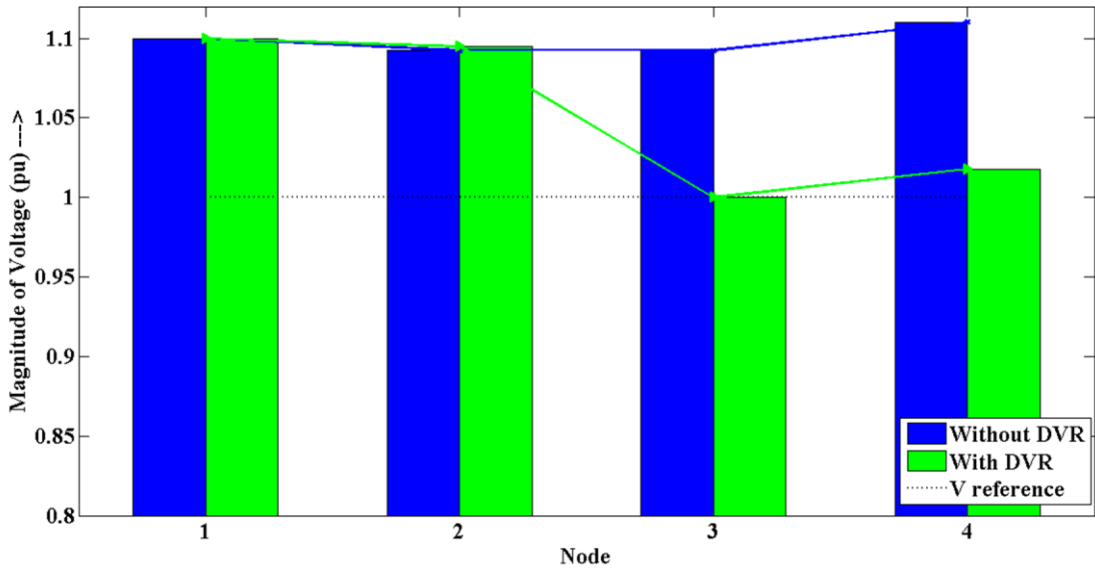


Fig. 3.64: Voltage Profile of radial microgrid with DVR as voltage regulator during source perturbation at overvoltage from source side

for different types of variations like RES intermittency, load perturbation, and source perturbation has been performed. The following has been discussed below and also in Table 3.5:

- DVR (Dynamic Voltage Restorer): DVR is an effective voltage regulator that can maintain the voltage near the regulated value in most conditions. It can also regulate the voltage in situations where the variation exceeds its limit, such as during low grid voltages and high RES injection. Additionally, since it is connected through an injection transformer, it can be installed anywhere throughout the feeder without requiring significant circuit changes.
- OLTC (On-Load Tap Changer) Transformer: OLTC is a good choice for voltage regulation as it is located near the substation and can regulate the voltage to a great extent in different conditions. It maintains the voltage near the substation, which prevents the reversal of power flow towards the grid, and

also eliminates the need for instant upgrades to the protection system based on unidirectional power flow. However, OLTC is a slow device that cannot undergo many changes instantly, and sudden changes like clouds appearing and disappearing can result in instantaneous tap changing, which is not favorable. It works better when a dynamic device is associated with it.

- BESS (Battery Energy Storage System): BESS can regulate the voltage in many cases and shows a significant improvement in others. However, it is not advisable to use BESS all the time as the capacity of the battery required is high, and it is not always feasible to install such a high-capacity battery system everywhere. It can be a good option for peak shaving, but it should not always be used as a voltage regulator because as the number of distributed voltage regulators requirement increases installation of BESS is going to be a complex and costly affair.
- STATCOM (Static Synchronous Compensator): STATCOM is a suitable device for the regulation of voltage in conventional distribution feeders, as it can regulate the voltage easily by injecting/absorbing reactive current at the point of common coupling of the network. However, in the case of a microgrid where real perturbations by connected RES are more frequent, STATCOM does not respond well even with their full capacity. Thus, it is not seen as a suitable choice of voltage regulator for maintaining the voltage in microgrids with high penetration of intermittent RES.

Table 3.5 (a): Comparison of different voltage regulators for regulating voltage in radial microgrid

Voltage Regulator	Principle	Depth of Compensation	Effectiveness
DVR	Uses power electronics to inject a voltage in series with the grid voltage, which compensates for voltage fluctuations	Can provide voltage regulation up to 100% of the nominal voltage and can regulate for major disturbances	Effective in regulating voltage
STATCOM	Uses power electronics to inject a voltage in parallel with the grid voltage, which compensates for voltage fluctuations	Cannot be able to contribute much to regulation as the system mainly comprises real power components. Thus, STATCOM limits are exhausted in most of the cases	Not much effective in the radial microgrids
BESS	Uses batteries to store energy and inject a voltage in parallel with the grid voltage, which compensates for voltage fluctuations	Can provide voltage regulation up to a great extent. But the limitation is that it is able to regulate only upto the times its capacity is not exhausted fully.	Effective in mitigating voltage disturbances and maintaining voltage stability, but limited in the depth of compensation and capacity
OLTC-transformer	Uses a transformer with multiple taps to adjust the voltage level based on the load demand	Can provide voltage regulation up to 10-20% of the nominal voltage and can compensate for voltage sags and swells to some extent, but with a delay	Effective in maintaining voltage stability, but limited in the depth of compensation and capacity

Table 3.5 (b): Comparison of different voltage regulators for regulating voltage in radial microgrid

Voltage Regulator	Ease of Operation	Installation Cost	Speed of Operation	Cost of installation
DVR	Requires specialized personnel for operation and maintenance, but can be remotely controlled through a supervisory control and data acquisition (SCADA) system	High installation cost due to the requirement of power electronics	Fast	High
STATCOM	Requires specialized personnel for operation and maintenance, but can be remotely controlled through a supervisory control and data acquisition (SCADA) system	High installation cost due to the requirement of power electronics	Fast	Very high
BESS	Relatively easy to operate and maintain, but may require periodic battery replacements and disposal	Moderate to high installation cost depending on the battery technology and number of distributed voltage regulators	Fast	High
OLTC-transformer	Relatively easy to operate and maintain, and does not require a continuous power supply	Moderate installation cost but may require additional transformer and switchgear.	Slow	Low

3.7 Conclusion

From the comprehensive investigation of different voltage regulators in the chapter, it appears that DVR and OLTC transformer are the most effective voltage regulation options for microgrids, while BESS and STATCOM may have limitations in the given scenarios. DVR and OLTC transformer can maintain the voltage near the regulated value in most conditions and are relatively simple and low-cost options. BESS can regulate the voltage in many cases but requires a high-capacity battery system, and STATCOM is suitable for conventional distribution feeders but may not respond well in microgrids with high penetration of intermittent RES. It is suggested that a combination of OLTC transformer and DVR should be studied as a potential solution for voltage regulation in microgrids.

Chapter 4

Hybrid Configurations for Voltage Regulation

4.1 General Overview

In the context of radial microgrids with intermittent renewable energy sources (RES), voltage regulation is a crucial issue that requires careful consideration. The study conducted in Chapter 3 reveals comprehensive comparison of various configurations of voltage regulators and it is identified that the on-load tap changer (OLTC) transformer and dynamic voltage restorer (DVR) are the potential solutions for regulating voltage in most situations, where one does the coarse changes and the other does fine changes. However, these regulators also have their limitations. For example, the OLTC transformer regulates voltage in discrete steps, leading to quantum jumps in both the phase and magnitude of voltage at the point of common coupling (PCC). To address such limitation, a hybrid combination of DVR with OLTC control of transformer could bring step-less voltage regulation over an extended range. The chapter presents comprehensive study dealing with analysis and a simple and fast control strategy for hybrid control of both OLTC and DVR for regulation of voltage in radial feeders under RES intermittency, load perturbations and source side disturbances. The proposed control strategy is simple and easily implementable, enabling step less operation of the combination. Additionally, the application of smart grid-connected inverter (SGCI) is also explored to connect the RES to the microgrid through it, which further extends the range of voltage regulation by marginally adjusting the RES power injection by moving away from MPPT. Simulated results

under the MATLAB environment are presented to validate the effectiveness of the proposed control scheme.

4.2 OLTC Transformer and DVR Hybrid for Voltage Regulation

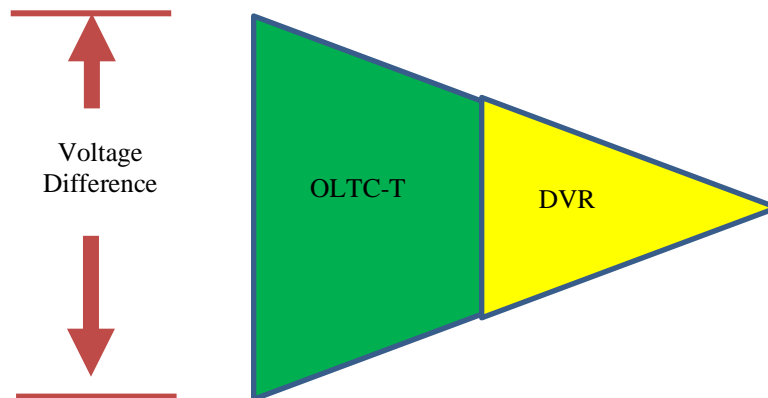


Fig. 4.1: Pictorial representation of voltage regulation range of OLTC transformer and DVR in radial microgrid

The implementation of the OLTC transformer supported by a dynamic voltage regulation device (DVR) is explored in this chapter for regulating voltage in the radial microgrid/distribution feeder. The OLTC-T primarily regulates the coarse voltage, while the DVR provides fine seamless regulation, as illustrated in Fig. 4.1. Together, these devices efficiently regulate voltage in the radial microgrid/distribution feeder, ensuring stable and reliable voltage profile of the microgrid.

4.2.1 System Considerations for OLTC-T and DVR Hybrid

The block diagram representation of the system used to study the regulation of voltage and aversion of reverse power flow towards the grid with the hybrid control of OLTC-T and DVR is shown in Fig. 4.2. The system includes a weak source, OLTC-T, DVR,

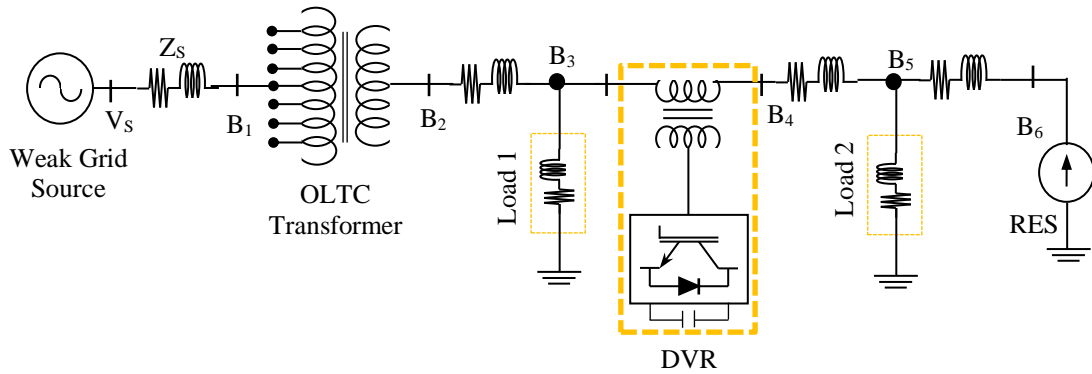


Fig. 4.2: Single diagram of OLTC transformer and DVR hybrid for voltage regulation in radial microgrid with RES penetration

RES, distributed line impedance, and other loads. The power extracted from the weak source is designed to cater only for the base load in the feeder. The OLTC-T is primarily responsible for regulating the voltage on the output side of nodes to enable unidirectional downward power flow. It maintains voltage within a range of $\pm 10\%$ with a step size of ± 0.02 pu. The DVR, on the other hand, is required to maintain the voltage of the nodes downstream of power flow from the output node to which it is connected. The system also includes two 3-phase RL loads consuming both demanding both real and reactive power, lumped line impedance at different locations as shown in Fig. 4.2. The RES is considered as a variable current controlled source and is connected towards the end of the radial feeder/microgrid to present the worst-case scenario for voltage regulation and may result in complete reversal of power from RES upstream directed towards the grid side.

4.2.2 Analysis for OLTC-T and DVR Hybrid

A simplified analysis is presented to understand the coordinated operation of OLTC-T and DVR for regulating voltage in radial microgrids with intermittent RES. The analysis is divided into two parts. The first part deals with the major regulation issue, which is curated by the OLTC-T by altering, tap positions, presented as "inter-turn

regulation." The second part deals with the minor regulation/differential regulation handled by the DVR, which works between the tap positions, presented as "intra-turn regulation."

Inter-turn Analysis

In the inter-turn analysis, the OLTC-T is considered from its equivalent circuit referred to on the secondary side, as discussed in Chapter 3 section 3.2.1. The output voltage of the OLTC-T at the current tap position is given by an equation that includes resistance, reactance, and impedance terms:

$$V_{S_{OLTC_x}} = V'_{P_{OLTC}} - I_{S_{OLTC}} [(X^2 R''_{P_{OLTC}} + jX^2 X''_{P_{OLTC}}) + Z_{S_{OLTC}}] \quad (4.1)$$

The output terminal voltage of the OLTC-T is expressed in terms of d-axis and q-axis components for further analysis of the OLTC-T-DVR interaction.

$$\begin{bmatrix} V_{OLTC_d} \\ V_{OLTC_q} \end{bmatrix} = \begin{bmatrix} \cos(\theta) & \cos\left(\theta - \frac{2\pi}{3}\right) & \cos\left(\theta + \frac{2\pi}{3}\right) \\ -\sin(\theta) & -\sin\left(\theta - \frac{2\pi}{3}\right) & -\sin\left(\theta + \frac{2\pi}{3}\right) \end{bmatrix} \begin{bmatrix} V_{OLTC_a} \\ V_{OLTC_b} \\ V_{OLTC_c} \end{bmatrix} \quad (4.2)$$

Intra-turn Analysis

In the intra-turn analysis, it is observed that inter-turn regulation of OLTC-T provides regulation within a certain range but is unable to achieve the exact voltage. Therefore, DVR is required to provide fine regulation between tap positions with intra-turn regulation. The intra-turn regulation deals with the operation of DVR, which is responsible for regulating voltage between different tap positions of OLTC-T. Equivalent circuit so obtained for the hybrid combination of OLTC transformer and DVR hybrid is shown in Fig. 4.3. The output voltage of the OLTC-T and DVR

combination at the terminal of DVR is given by an equation (4.3) that includes OLTC-T and DVR output voltages.

$$V_L = V_{OLTC} + V_{DVR} \quad (4.3)$$

Where,

- V_{OLTC} ($V_{OLTC} = V_{OLTC_d} + jV_{OLTC_q}$) is the output voltage of OLTC-T obtained from the previous sub-section.
- V_{DVR} is the voltage injected/absorbed by the DVR

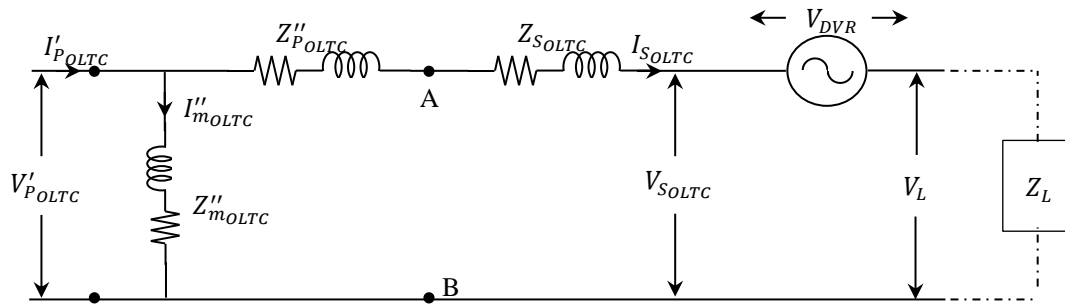


Fig. 4.3: Equivalent circuit system having both OLTC transformer and DVR

The DVR is primarily used to inject voltage that corresponds to the requisite reactive power for regulation. This voltage injection is in quadrature with the line current, which is treated as the reference phase. Therefore, the output voltage of the DVR, with the current as the reference phase, can be expressed in a complex form

$$V_{DVR} = V_{DVR_d} + jV_{DVR_q}$$

Where,

- V_{DVR_d} represents the real part of the voltage injection, and
- V_{DVR_q} represents the imaginary part of the voltage injection.

Since the current is the reference phase, the real part of the DVR voltage injection is set to zero ($V_{DVR_d} = 0$), and only the imaginary part is considered. Thus, the output voltage of the DVR with the current as the reference phase can be written as:

$$V_{DVR} = V_{DVRq} \quad (4.4)$$

Thus, the resultant output load voltage when DVR is utilizing the reactive power alone is given by:

$$V_L = V_{OLTCd} + j(V_{OLTCq} + V_{DVRq}) \quad (4.5)$$

The analysis for voltage regulation with incorporation of OLTC-T and DVR provides insight into the compensation range of DVR and OLTC-T, and the modelled response helps in tap selection of OLTC-T and DVR sizing.

4.2.3 Control of OLTC-T and DVR Hybrid

The genesis of control lies first in identification of inter-turn/intra-turn control and accordingly either changing the tap of the transformer or to manage the voltage regulation with the DVR. Such demarcation is based on sudden change experienced in voltage, which marks changes in both real and reactive power of the node. In synchronous reference frame the OLTC current ($I_{S_{OLTC}}$) is broken into $I_{S_{d_{OLTC}}}$ and $I_{S_{q_{OLTC}}}$ which pertains to real power and reactive power respectively such that,

$$P_{OLTC} \propto I_{S_{d_{OLTC}}} \quad \text{and} \quad Q_{OLTC} \propto I_{S_{q_{OLTC}}}.$$

It is therefore,

$$\frac{P_{OLTC}}{Q_{OLTC}} = \frac{I_{S_{d_{OLTC}}}}{I_{S_{q_{OLTC}}}} \quad (4.6)$$

The ($I_{S_{d_{OLTC}}}/I_{S_{q_{OLTC}}}$) ($= I_d/I_q$) ratio can be used to portray any significant change in real and reactive power that may occur as a result of transients and perturbations in the system. If the I_d/I_q ratio is substantial changed (beyond $\pm 2\%$), it means there are major voltage variations that demand major voltage regulation, and this calls for voltage regulation to range the inter-turn regulation mode (OLTC-T). If the ratio is

small, it means there are requirements for minor voltage variation and for that intra-turn regulation mode would suffice. Two hybridized autonomous control involving OLTC-T and DVR for voltage regulation in the distribution feeder is coordinated by observing the ratio of d-axis and q-axis component of current i.e. I_d/I_q and determination of the capacity exhaustion of DVR and OLTC-T together. The comprehensive coordinated control is performed in the following order: mode identification (Fig. 4.4(a)), mode implementation: inter-turn regulation control (Fig. 4.4(b) and/or intra-turn regulation control (Fig. 4.4(c)).

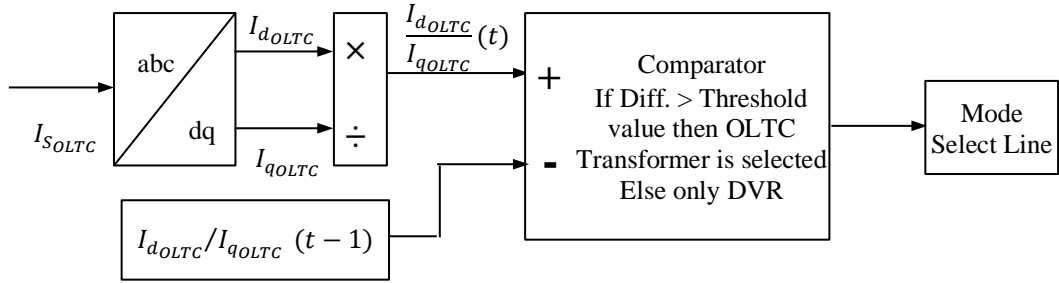


Fig. 4.4(a): Block diagram for mode select line for hybrid voltage regulator in radial microgrid

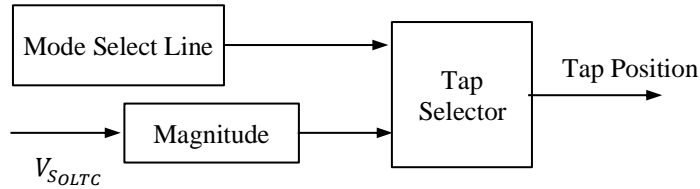


Fig. 4.4(b): Inter-turn regulation: Tap position controller for OLTC transformer

Mode identification: It involves identification of ‘inter-turn/intra-turn regulation’ mode by utilizing the OLTC-T output current in synchronous reference frame as shown in Eq. 4.7.

$$\begin{bmatrix} I_{S_{d_{OLTC}}} \\ I_{S_{q_{OLTC}}} \end{bmatrix} = \begin{bmatrix} \cos(\omega t) & \cos\left(\omega t - \frac{2\pi}{3}\right) & \cos\left(\omega t + \frac{2\pi}{3}\right) \\ -\sin(\omega t) & -\sin\left(\omega t - \frac{2\pi}{3}\right) & -\sin\left(\omega t + \frac{2\pi}{3}\right) \end{bmatrix} \begin{bmatrix} I_{S_{a_{OLTC}}} \\ I_{S_{b_{OLTC}}} \\ I_{S_{c_{OLTC}}} \end{bmatrix} \quad (4.7)$$

With $V_{S_{OLTC}}$ (V_{B2}) as a temporary reference, the $I_{S_{d_{OLTC}}}$ ($= I_d$) and $I_{S_{q_{OLTC}}}$ ($= I_q$)

components of current provide an estimate of the real and reactive power involved. Whereas, the synchronous reference frame for DVR is designed with respect to current as reference phasor thus phase displacement need to be evaluated from decomposition of load side voltage of DVR is dq frame to facilitate quadrature voltage (V_{qDVR}) for computation. As noted in the preceding section, the values of $I_{S_{dOLTC}}$ and $I_{S_{qOLTC}}$ are utilised to determine the ratio I_d/I_q , which pertains to ratio of real to reactive power. If the ratio reaches a specific threshold, it means that power injection from RES has changed significantly, a substantial load has been inserted/ disserted from the system and/or the grid side voltage is altered significantly.

The basic block diagram for control in inter turn regulation mode is shown in Fig. 4.4 (b). This mode envisages the controlling of the OLTC-T's tap position. If the magnitude ($V_{S_{OLTC}}$) does not fall within this range, the tap controller of the OLTC-T adjusts its tap position to the right tap position, allowing the voltage at its terminal to be regulated within a set range.

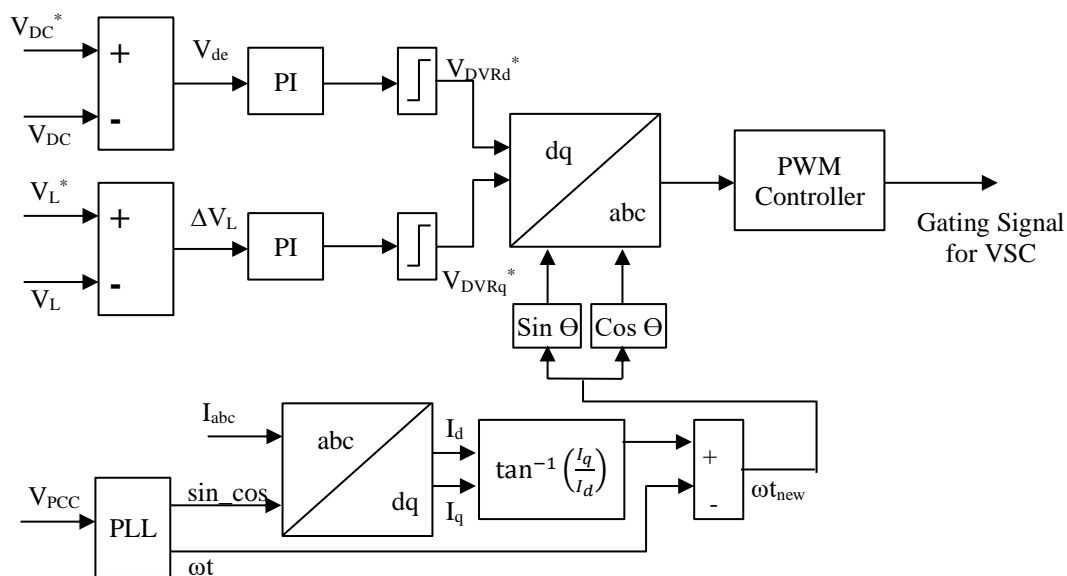


Fig. 4.4(c): Block diagram for controlling VSC of DVR

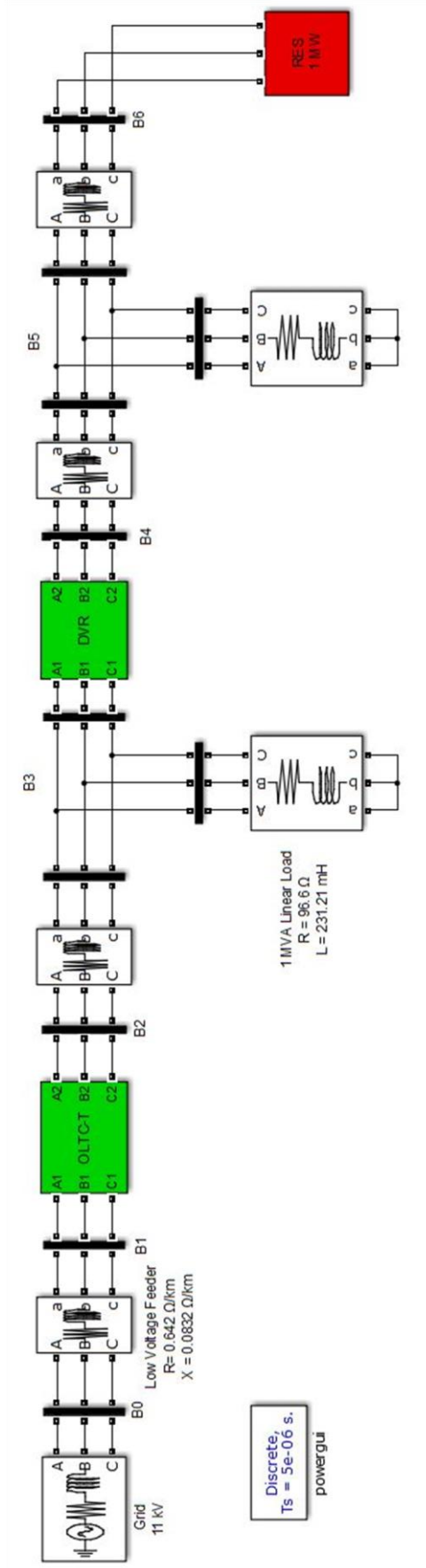


Fig. 4.5: MATLAB Simulink diagram for testing of OLTC transformer and DVR hybrid for voltage regulation in radial microgrid

When the ratio $I_{S_{dOLTC}}/I_{S_{qOLTC}}$ is within the threshold limit, the control exercises the intra-turn regulation mode. In this mode the OLTC remain unperturbed and instead DVR responds to the change in voltage at its terminal. In fact, DVR regulates the voltage between the tap points of OLTC-T (inter-turn regulation mode). It measures its terminal voltage and compares it to the reference value before passing the error through a PI controller, which forces to control to keep the voltage difference to a base minimum. Because the DVR is primarily concerned with reactive power, its control allows it to provide a q-axis component that regulates the voltage at its terminal to the required value. The reference DVR voltage is the voltage required to exercise the control is in quadrature with the feeder current, as determined by the q-axis component.

$$V_{qDVR}(n) = V_{qDVR}(n-1) + K_P \left(\Delta V_{Lmag}(n) + \Delta V_{Lmag}(n-1) \right) + K_I \Delta V_{Lmag}(n) \quad (4.8)$$

Where, $\Delta V_{Lmag} = V_{Lmag}^* - V_{Lmag}$; and, K_P and K_I are the proportional and integral gain of the PI controller. The block diagram representation of the control of DVR is shown in Fig. 4.4 (c).

4.2.4 Simulation Diagram for OLTC-T and DVR Hybrid

The considered radial microgrid is simulated using the SimPowerSystems toolbox in a MATLAB/SIMULINK environment. The simulation model comprises a three-phase source to represent the weak source, a series RL branch as to depict the lumped feeder drop, a 3- Φ OLTC-T multi-tap transformer, two balanced linear loads of a prescribed rating with 0.8 power factor lagging, a DVR, and an intermittent RES source implemented as a current-controlled inverter, as shown in Fig. 4.5. The RES module is positioned at the end of the feeder to demonstrate the worst-case scenario in terms of

fluctuations in terminal voltage and reversal of power flow. The component parameters of the simulation model are listed in Table 4.1.

Table 4.1: Simulation parameters for voltage regulation of radial microgrid with intermittent RES using OLTC-T and DVR hybrid voltage regulators

System Parameter	Values
Source Voltage (V_s)	33kV, 50Hz
OLTC transformer	33/11kV, 50Hz, 5 MVA, $\pm 10\%$ range, 2% step size
Feeder impedance (Z_f)	$0.642 + j 0.083 \Omega/\text{km}$
RES power rating	1.5 MW for normal injection condition
Load	1 MVA, 0.8 pf lagging, Linear and balanced three phase load
DVR	0.5 MVA

4.2.5 Performance Evaluation of OLTC-T and DVR Hybrid

The effectiveness of the OLTC-T and DVR system in regulating voltage is tested under various operating conditions in the radial microgrid. This includes the intermittent nature of RES, load and source voltage perturbations such as under voltage and overvoltage.

RES Intermittency

The performance of OLTC-T and DVR hybrid is evaluated under different current injections at various intervals of time. Prima-facia I_d/I_q ratio is monitored for distinguishing the control for inter turn and intra turn operation and/or both. Lesser than the threshold value duly average for two-three fundamental cycles (toward different transients) OLTC-T does not react to the situation and the responsibility is left to distributed DVRs for taking care of voltage regulation and maintenance of voltage profile.

The current and voltage waveforms at different nodes for this scenario are displayed in

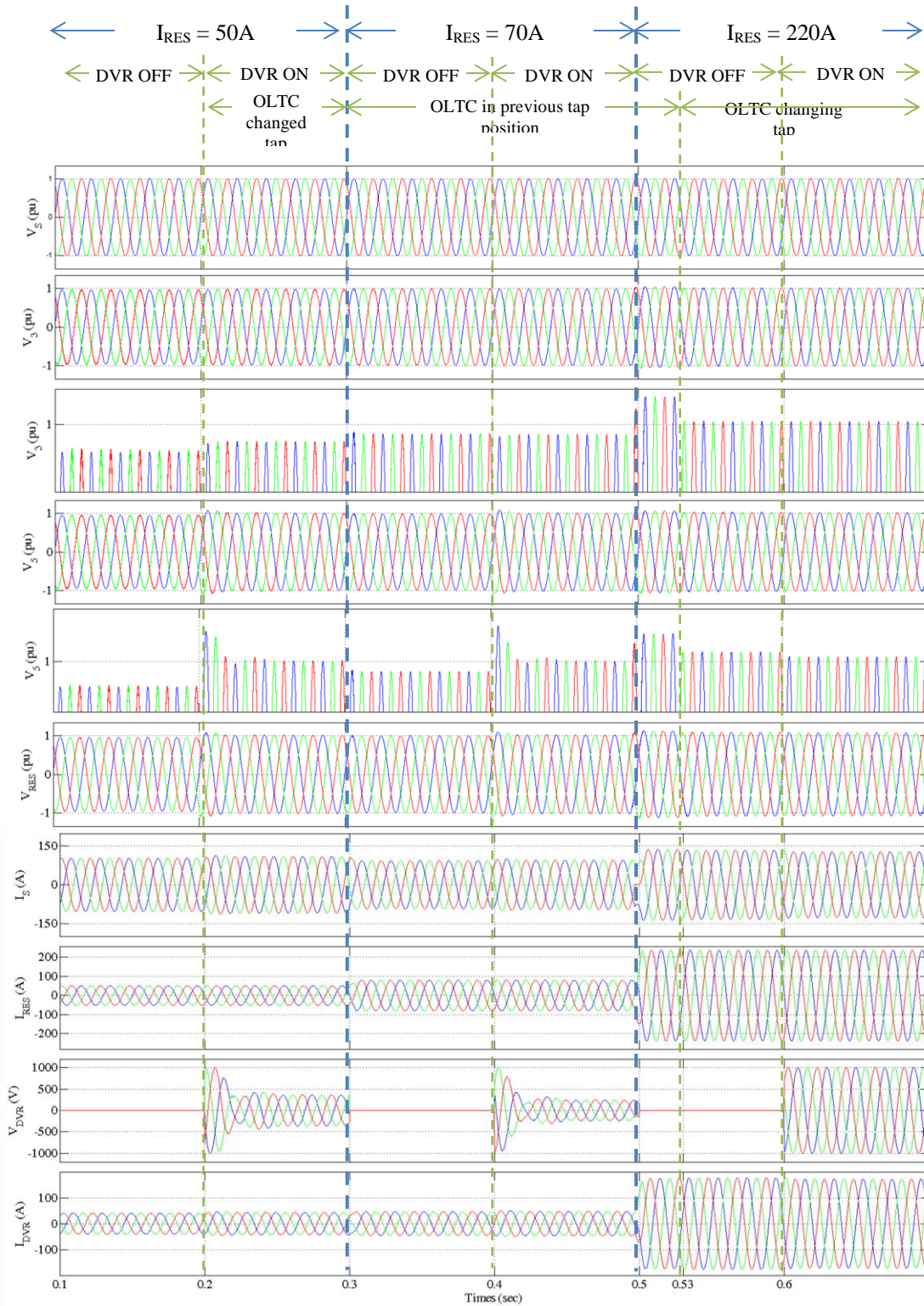


Fig. 4.6: Voltage and current waveforms in radial microgrid with OLTC transformer and DVR as voltage regulator during RES intermittency.

V_s : source voltage (pu), V_3 : voltage at the secondary terminal of the OLTC transformer (in pu), V_5 : voltage at the output terminal of DVR (in pu), V_{RES} : Voltage at the terminal of RES (in pu), I_s : Source current (in A), I_{RES} : RES current (in A), V_{DVR} : Voltage supplied/absorbed by DVR (in V)

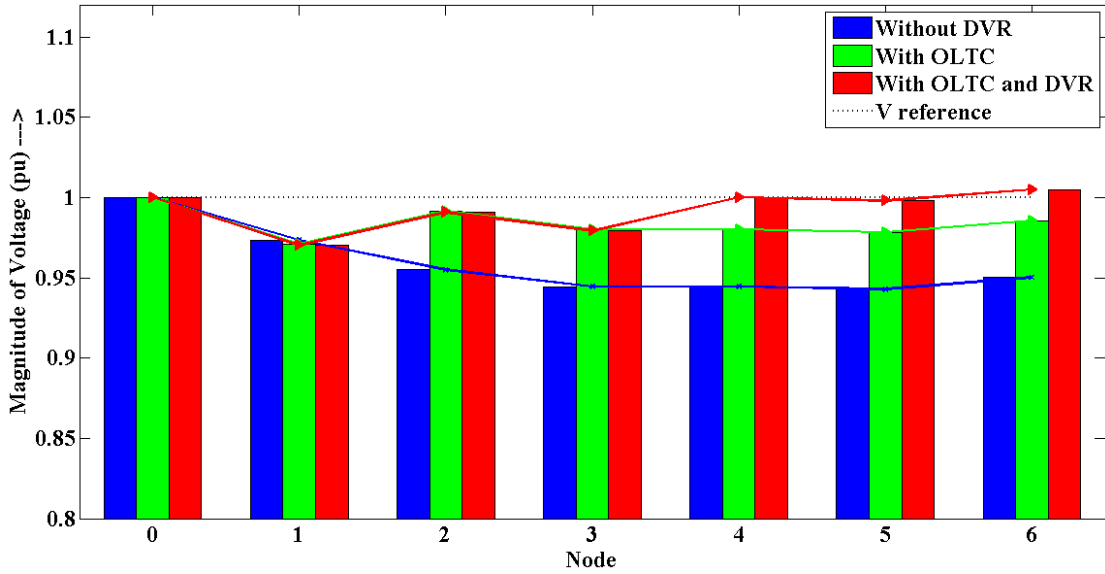


Fig. 4.7: Voltage profile of radial microgrid with OLTC transformer and DVR as voltage regulator during RES intermittency at $I_{RES} = 50$ A

Fig. 4.6. Initially, from $t = 0$ to $t = 0.3$ sec, $I_{RES} = 50$ A is injected by RES, which is inadequate to meet the local loads connected to the grid, resulting in a drooping voltage profile depicted in Fig. 4.7. The OLTC transformer is kept at a 1:1 voltage ratio (normal condition) to enable a clear depiction of the voltage profile changes that occur within the microgrid when the tap position is altered. It may be observed for voltage at node 3 (V_3) the situation calls for regulation. The control enables the tap changing process at $t = 0.2$ sec, where it may be observed that the OLTC transformer alters its tap position, to next higher tap position and the DVR also comes to action, which is evident from V_5 , leading to a significant improvement in the voltage profile, which is regulated to the rated value at the DVR terminal (V_5), is also reflected in the waveforms and voltage profiles.

At $t = 0.3$ sec, the RES injection into the feeder increases to $I_{RES} = 70$ A. As the difference in current is minor, the system needs to undergo only minimal changes, and it is therefore, the I_d/I_q ratio does not see breakoff the threshold from earlier improved situation, restricting any change of tap of the OLTC transformer, thus maintaining the

same tap position. In order to demonstrate the efficacy of DVR into the system, the

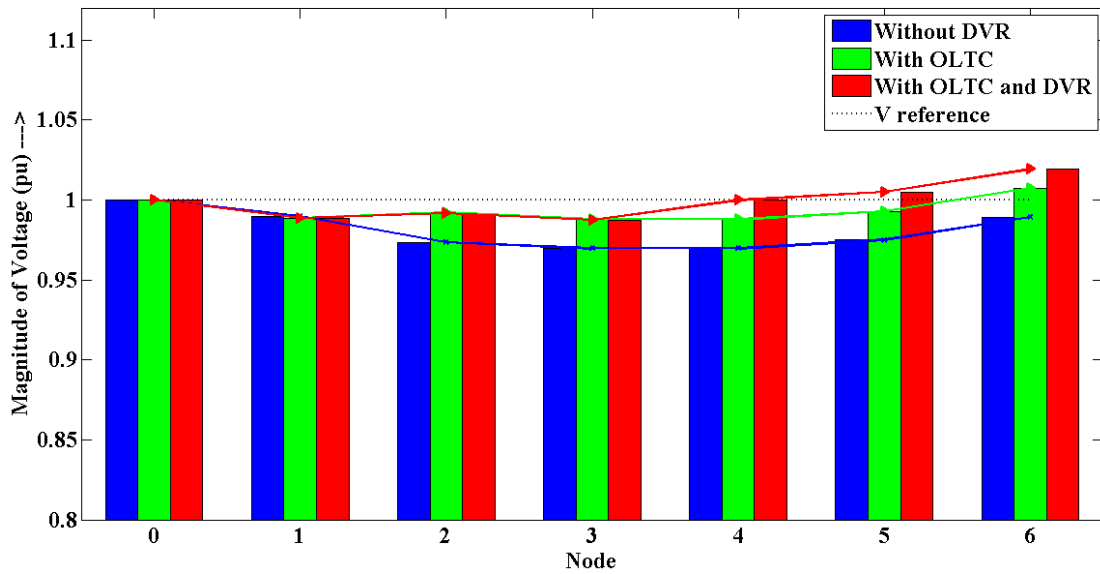


Fig. 4.8: Voltage profile of radial microgrid with OLTC transformer and DVR as voltage regulator during RES intermittency at $I_{RES} = 70$ A

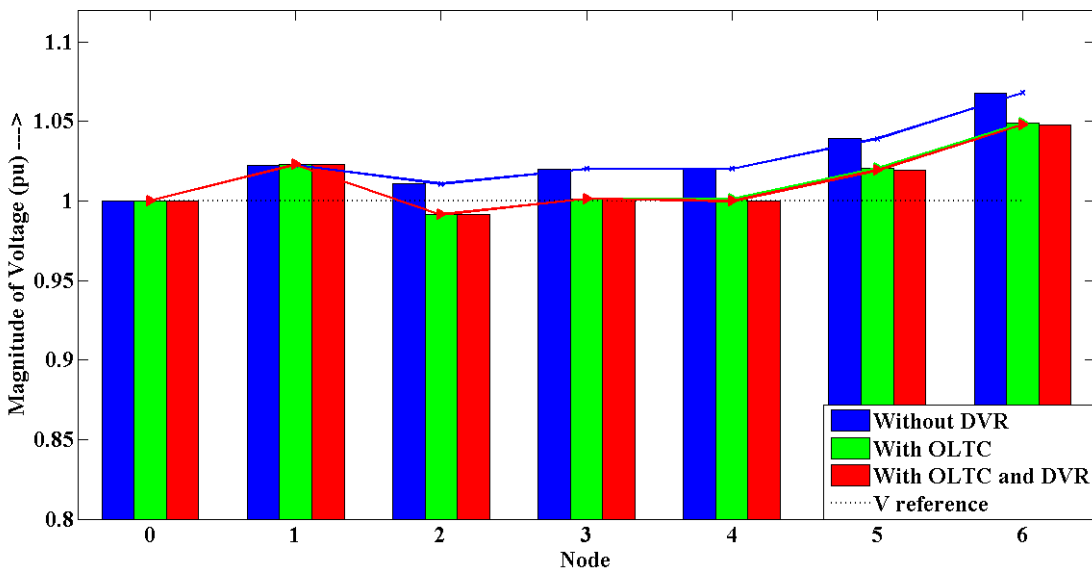


Fig. 4.9: Voltage profile of radial microgrid with OLTC transformer and DVR as voltage regulator during RES intermittency at $I_{RES} = 220$ A

operation of DVR is disabled again at $t = 0.3$ sec, resulting in drop of voltage at node 5 (V_5). At $t = 0.4$ sec, the DVR is re-introduced into the circuit, it may be observed that V_5 is again regulated through reactive power support, dually evident by the jump in voltage observed at V_5 and V_{RES} . As depicted in Fig. 4.8, the voltage is maintained at node '5' by the DVR, and the overall voltages at all nodes in the microgrid fall within

an acceptable range.

Later, at $t = 0.5$ sec, the RES injection increases substantially, resulting in a rising voltage profile as shown in Fig. 4.9. The OLTC transformer mode controller detects a large change in the I_d/I_q ratio, leading to a three tap down change in the OLTC transformer, which is executed at $t = 0.53$ sec, for clarity. It may be observed that with three tap down position, the OLTC transformer has successfully regulated the voltage at its secondary terminal (V_3) to a great extent, as demonstrated by the voltage profile depicted in Fig. 4.9 (node 3). Then at $t = 0.6$ sec, the DVR is reactivated and the voltage at terminal V_5 and V_{RES} through absorbing the reactive power from the feeder (intra turn regulation). The hybrid operation of the OLTC transformer and DVR has significantly regulated the voltage variations at all the nodes caused by extreme generation conditions in the radial microgrid.

Load Perturbation between OLTC transformer and DVR

The second transient condition examined in this study involves a load perturbation for the load situated between the OLTC transformer and DVR. It was assumed that the RES injected sufficient power $I_{RES} = 100$ A to cater to the load, while the grid supplied either reactive power or minimal real power when rated load was demanded. The voltage and current waveforms for this condition were presented in Fig. 4.10, where the initial transient situation was not shown.

During the first 0.3 seconds, the load was maintained at a low level, close to one third of the rated load, resulting in an overvoltage condition at the terminal and feeder as all the power from RES moved towards the grid main. The OLTC transformer maintained a 1:1 ratio without any variation, while DVR voltage regulation started from $t = 0.2$

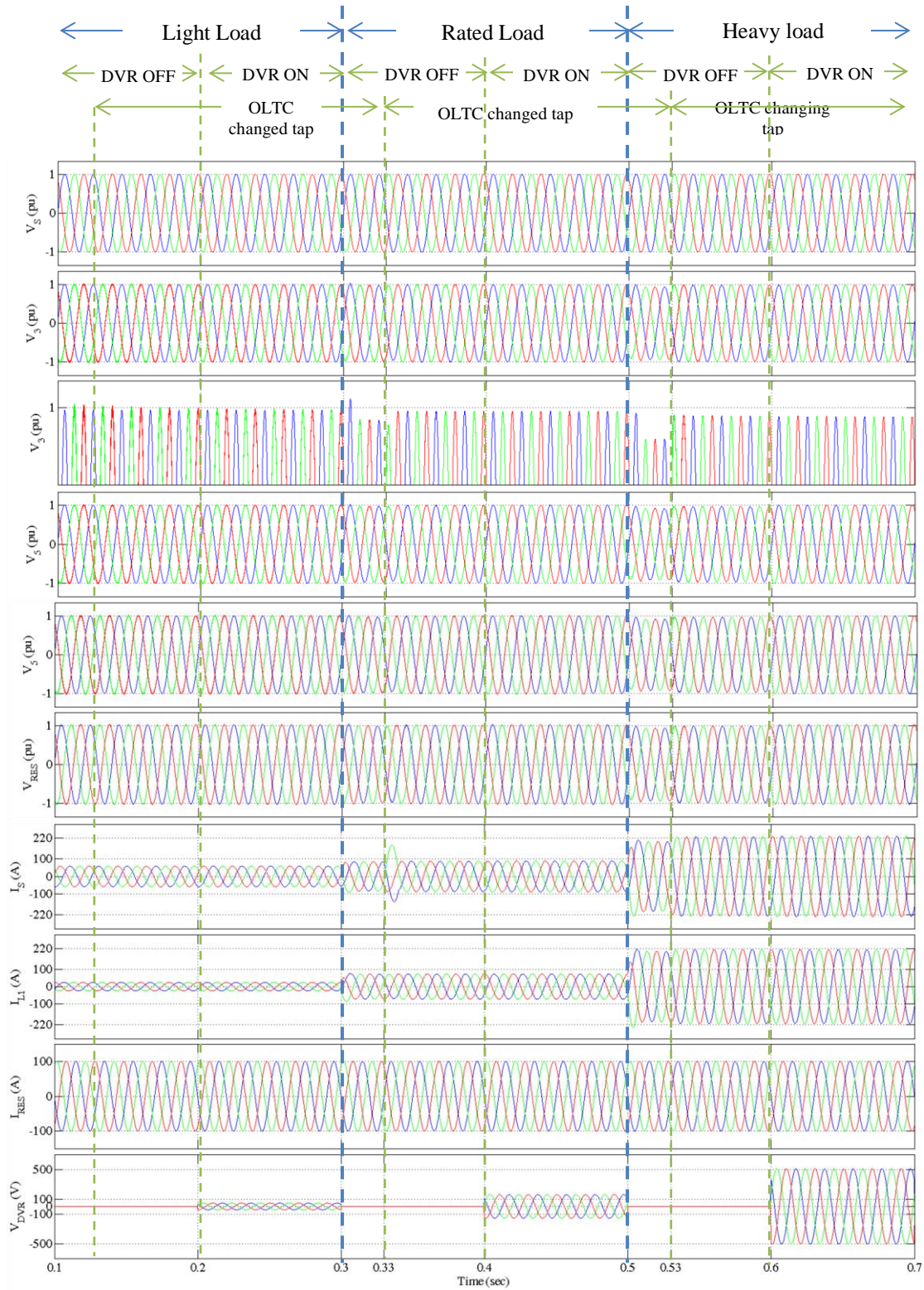


Fig. 4.10: Voltage and current waveforms in radial microgrid with OLTC transformer and DVR as voltage regulator during Load Perturbation (Load between OLTC transformer and DVR).

V_S : source voltage (pu), V_3 : voltage at the secondary terminal of the OLTC transformer (in pu), V_5 : voltage at the output terminal of DVR (in pu), V_{RES} : Voltage at the terminal of RES (in pu), I_S : Source current (in A), I_{L1} : Load 1 current (A), I_{RES} : RES current (in A), V_{DVR} : Voltage supplied/absorbed by DVR (in V)

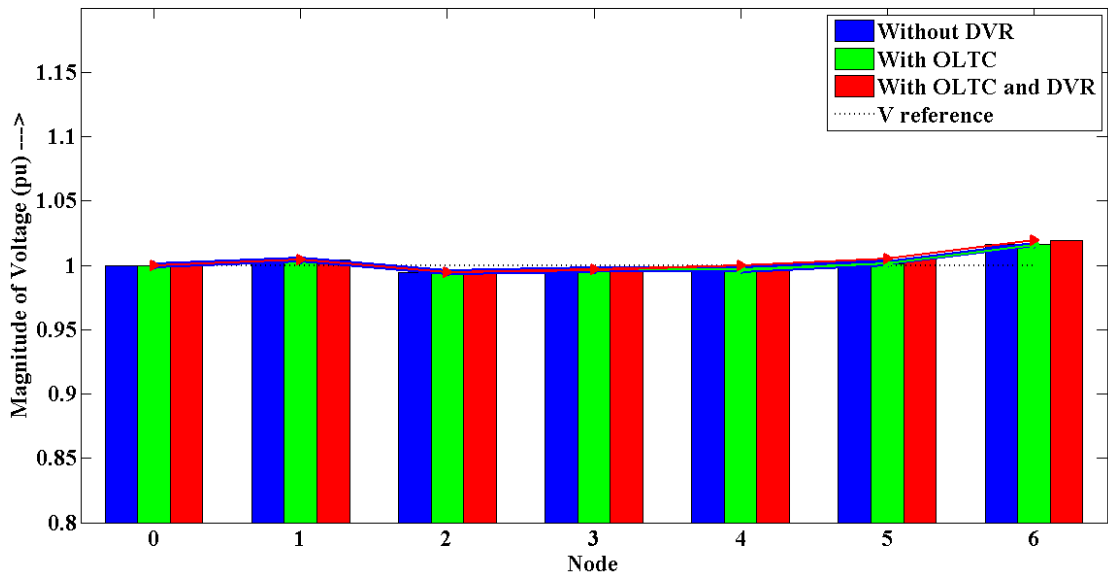


Fig. 4.11: Voltage profile of radial microgrid with OLTC transformer and DVR as voltage regulator during Load Perturbation (Load between OLTC transformer and DVR) at light loading condition

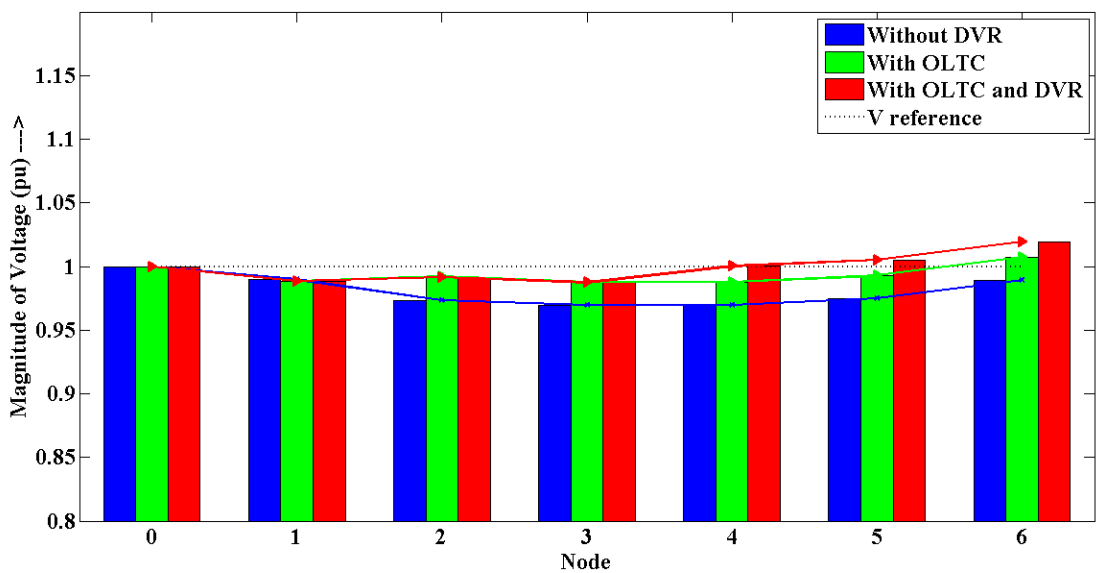


Fig. 4.12: Voltage profile of radial microgrid with OLTC transformer and DVR as voltage regulator during Load Perturbation (Load between OLTC transformer and DVR) at rated loading condition

sec and improved the voltage profile of the microgrid, as evident from the voltage profile in Fig. 4.11.

At $t = 0.3$ sec, the load returned to rated loading condition, and the I_d/I_q ratio remained relatively unchanged. Thus, the tap position of the OLTC transformer did not change, while the DVR started regulating the voltage profile of the microgrid at

t=0.4 sec, as evident from the waveforms and voltage profile shown in Fig. 4.12.

Subsequently, at t = 0.5 sec, the system underwent heavy loading condition, and the OLTC transformer responded almost instantaneously in a few cycles to regulate the major share of voltage. The DVR fine-tuned the voltage at its terminal at t = 0.6 sec, resulting in significant improvement in the voltage profile of the system, as supported by the voltage profile shown in Fig. 4.13.

Overall, the actions of the OLTC transformer and DVR significantly improved the voltage profile of the microgrid system under both transient conditions.

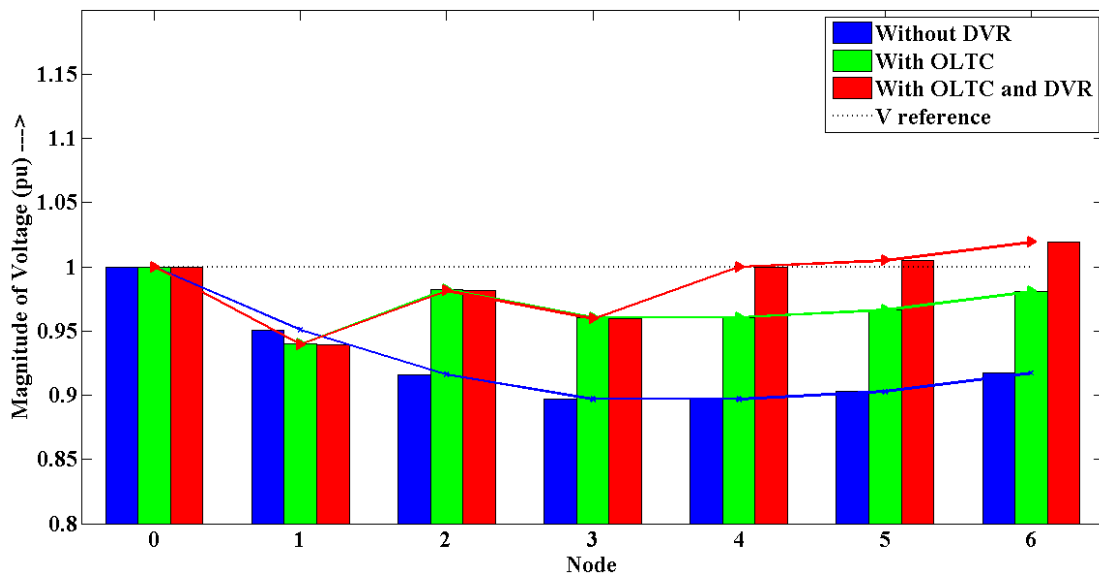


Fig. 4.13: Voltage profile of radial microgrid with OLTC transformer and DVR as voltage regulator during Load Perturbation (Load between OLTC transformer and DVR) at heavy loading condition

Load Perturbation between DVR and RES

In the third condition, where the load perturbation is done between the DVR and RES, the OLTC transformer and DVR combination exhibit a behavior similar to the previous case. They have successfully regulated the voltage at their respective terminals, resulting in an improved voltage profile along the feeder. This can be observed from the waveforms and voltage profiles presented in Fig. 4.14 to Fig. 4.17.

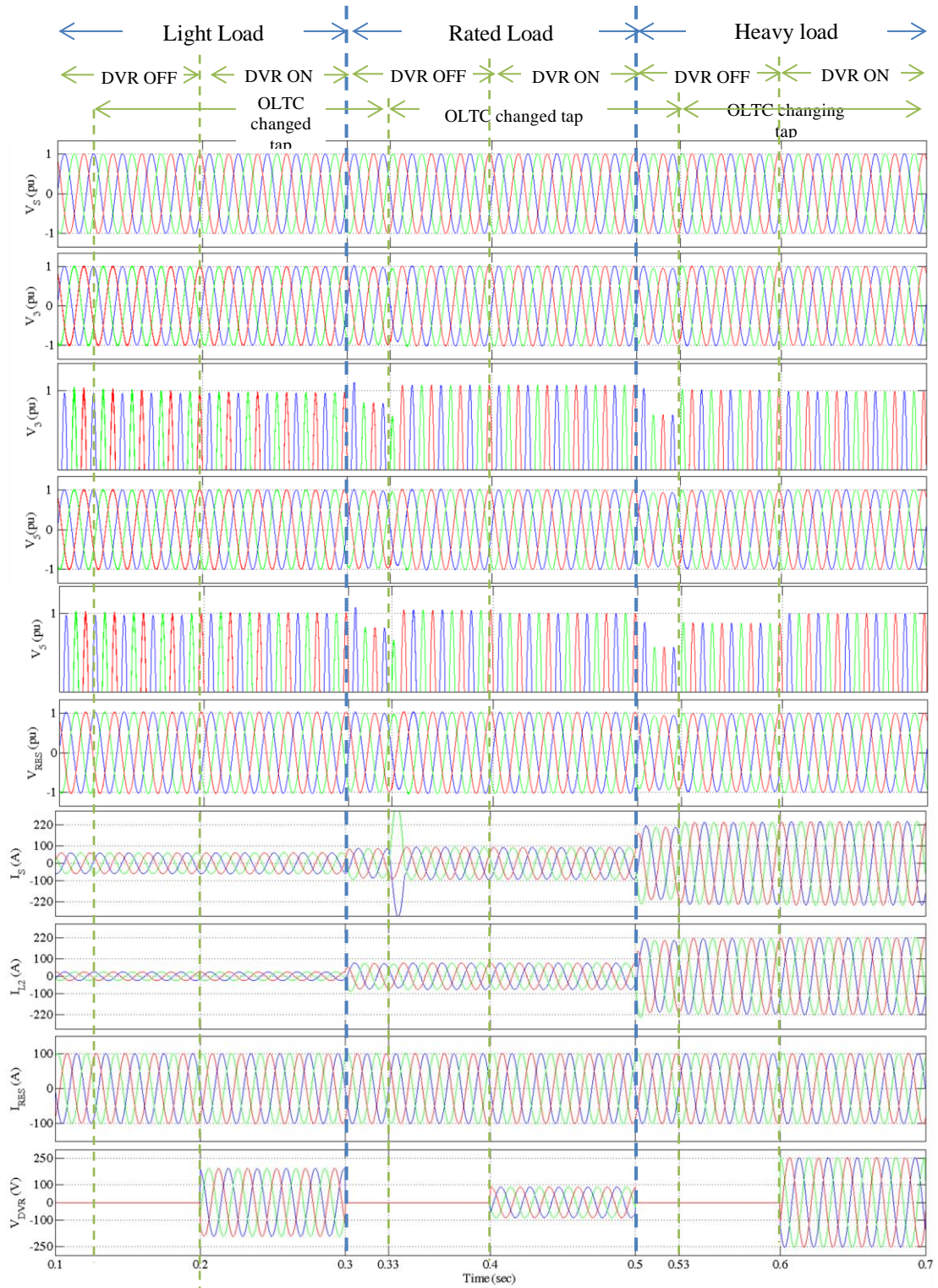


Fig. 4.14: Voltage and current waveforms in radial microgrid with OLTC transformer and DVR as voltage regulator during Load Perturbation (Load between DVR and RES).

V_S : source voltage (pu), V_3 : voltage at the secondary terminal of the OLTC transformer (in pu), V_5 : voltage at the output terminal of DVR (in pu), V_{RES} : Voltage at the terminal of RES (in pu), I_s : Source current (in A), I_{L2} : Load 2 current (A), I_{RES} : RES current (in A), V_{DVR} : Voltage supplied/absorbed by DVR (in V)

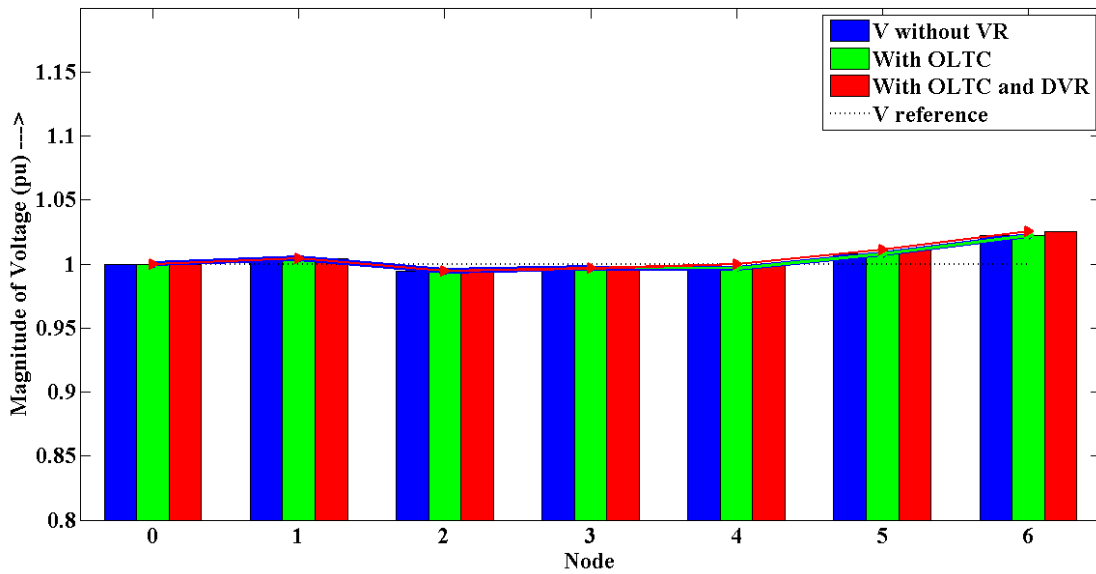


Fig. 4.15: Voltage profile of radial microgrid with OLTC transformer and DVR as voltage regulator during Load Perturbation (Load between DVR and RES) at light loading condition

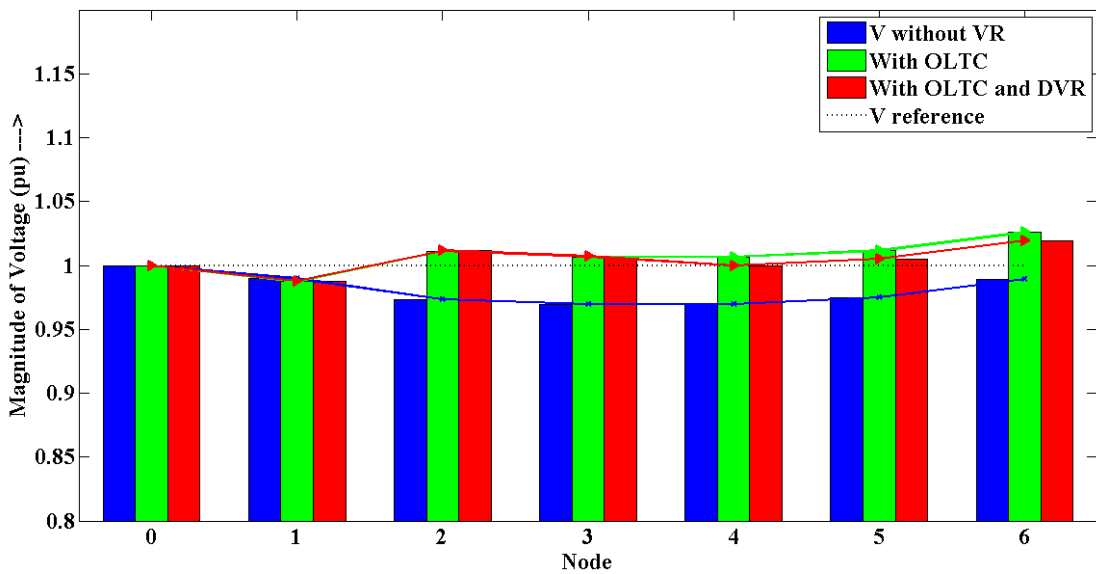


Fig. 4.16: Voltage profile of radial microgrid with OLTC transformer and DVR as voltage regulator during Load Perturbation (Load between DVR and RES) at rated loading condition

Source Perturbations

The fourth scenario analyzes the effect of voltage variations on the microgrid due to changes in the grid side voltage, and evaluates the effectiveness of the OLTC transformer and DVR combination in regulating voltage. The waveforms presented in

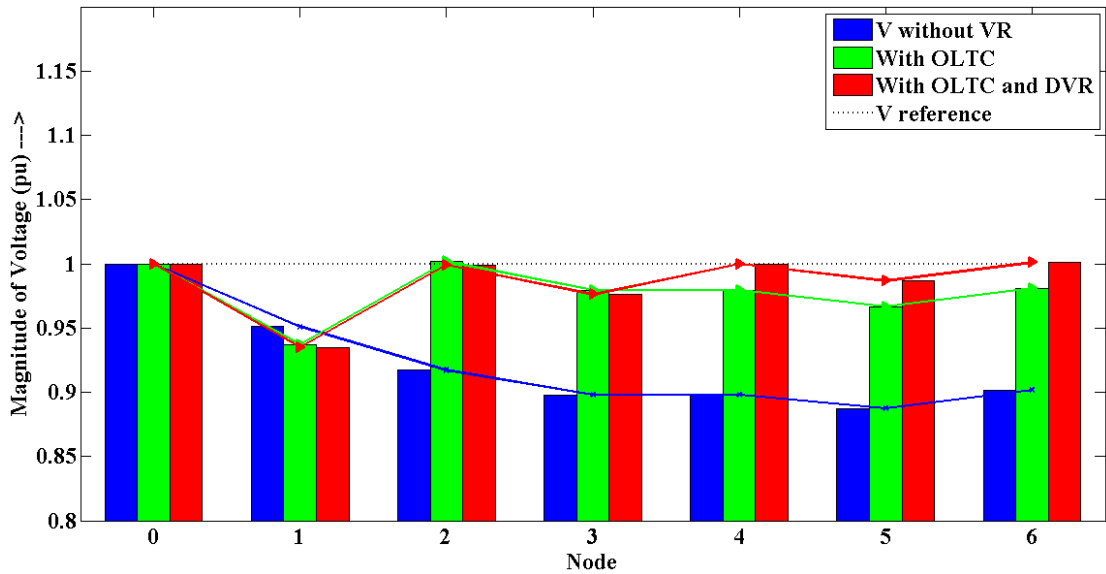


Fig. 4.17: Voltage profile of radial microgrid with OLTC transformer and DVR as voltage regulator during Load Perturbation (Load between DVR and RES) at heavy loading condition

Fig. 4.18 illustrate the current and voltage variations for this case. During the initial period, from $t = 0$ sec to $t = 0.3$ sec, the grid voltage remains close to the nominal value, and the voltage throughout the feeder is well-regulated, with some loss attributed to the feeder impedance. The DVR effectively regulates the voltage at its terminal, as observed from the voltage profile depicted in Fig. 4.19.

At $t = 0.3$ sec, an undervoltage condition occurs on the grid, leading to the OLTC transformer adjusting its tap position at $t = 0.33$ sec due to a significant change in the I_d/I_q ratio. The DVR simultaneously provides the necessary reactive power at $t = 0.4$ sec to regulate the voltage at its terminal. The combined action of the OLTC transformer and DVR substantially improves the voltage profile, as evident from Fig. 4.20. This situation persists until $t = 0.5$ sec, after which the grid voltage rises, causing an overvoltage problem in the microgrid from $t = 0.5$ sec to $t = 0.7$ sec. The OLTC transformer responds almost instantaneously and changes its tap position at $t = 0.53$ sec, and the DVR absorbs reactive power to regulate the voltage and keep it within acceptable limits. The voltage profile displayed in Fig. 4.21 supports this assertion.

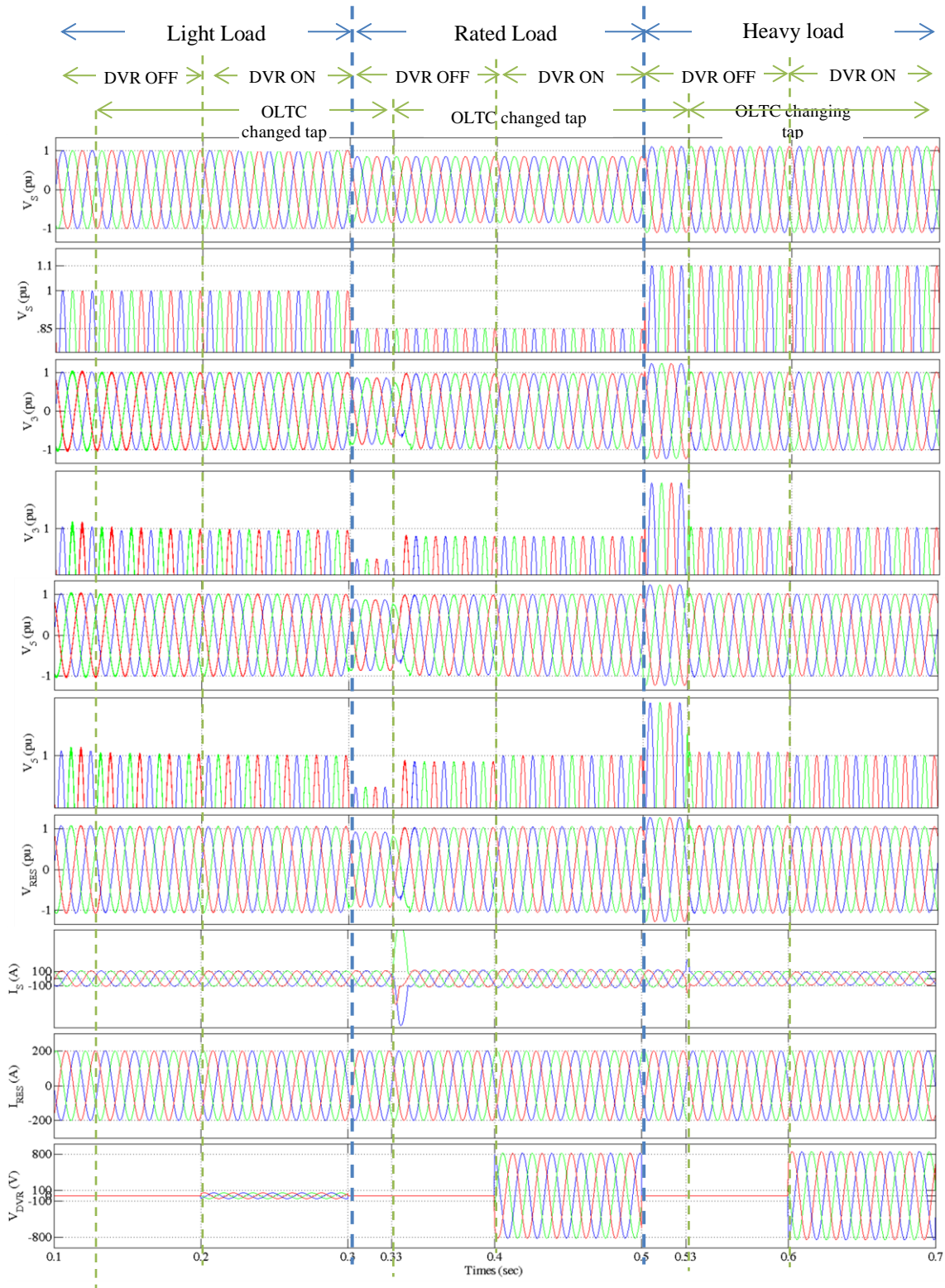


Fig. 4.18: Voltage and current waveforms in radial microgrid with OLTC transformer and DVR as voltage regulator during source perturbation

V_s : source voltage (pu), V_3 : voltage at the secondary terminal of the OLTC transformer (in pu), V_5 : voltage at the output terminal of DVR (in pu), V_{RES} : Voltage at the terminal of RES (in pu), I_s : Source current (in A), I_{RES} : RES current (in A), V_{DVR} : Voltage supplied/absorbed by DVR (in V)

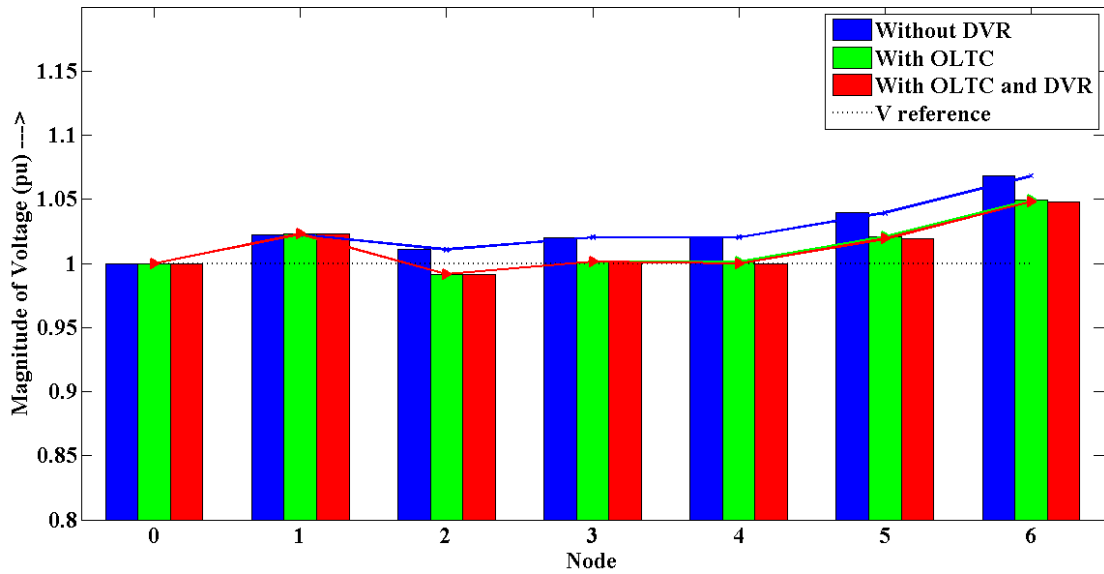


Fig. 4.19: Voltage profile of radial microgrid with OLTC transformer and DVR as voltage regulator during source perturbation at rated voltage from source side

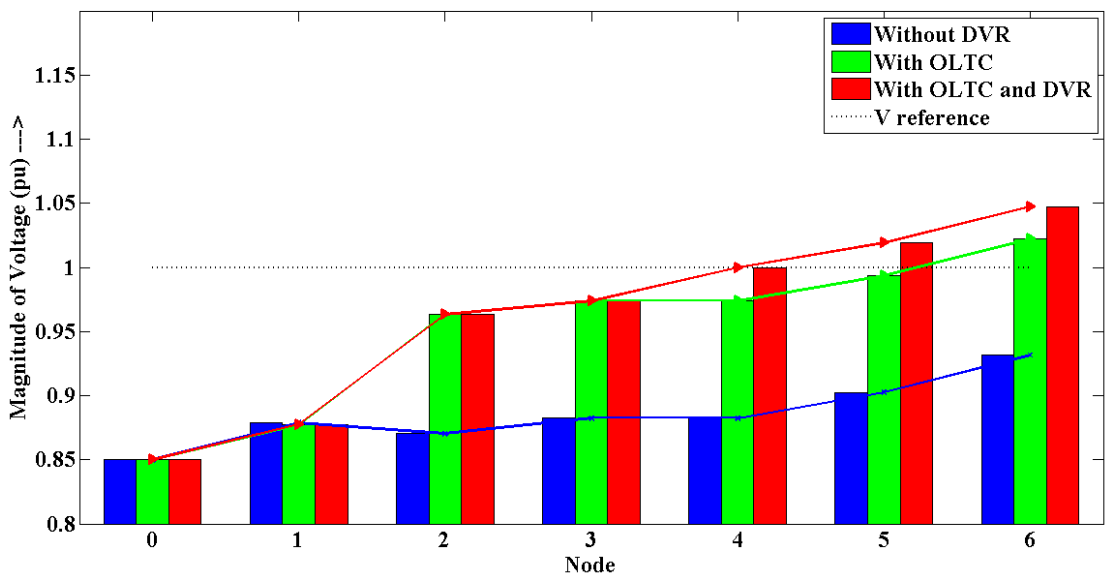


Fig. 4.20: Voltage profile of radial microgrid with OLTC transformer and DVR as voltage regulator during source perturbation at undervoltage from source side

4.3 OLTC Transformer and DVR Hybrid duo supported by smart GCI for Voltage Regulation

The combination of OLTC-T and DVR effectively maintains voltage control at their terminals across a wide range of operating conditions, leading to a notable

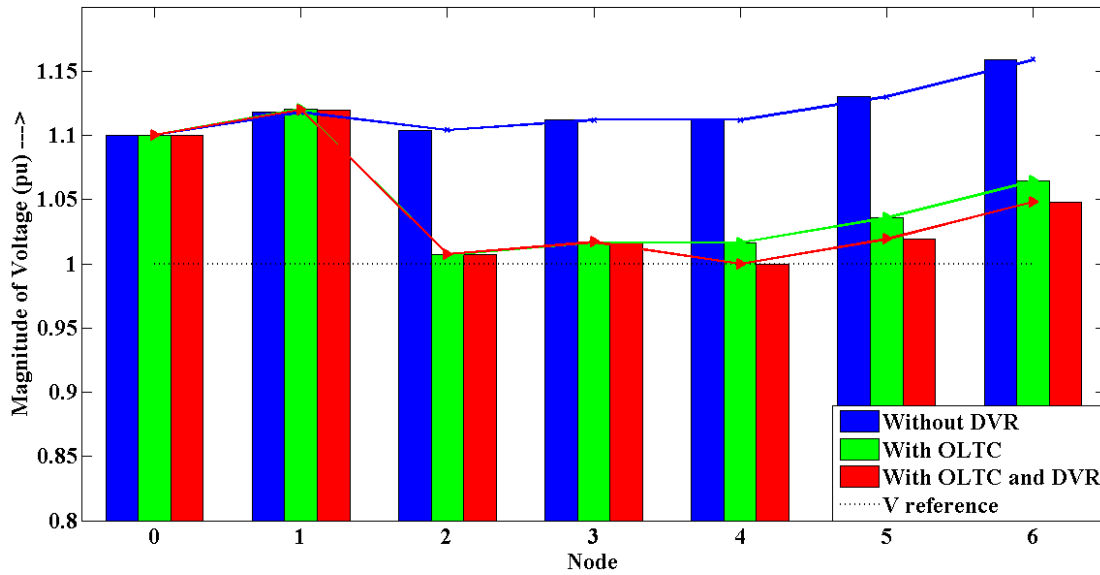


Fig. 4.21: Voltage profile of radial microgrid with OLTC transformer and DVR as voltage regulator during source perturbation at overvoltage from source side

improvement in the voltage profile. However, in few instances where multiple disruptive events occur simultaneously, even with both OLTC-T and DVR operating at their maximum capacity, it may not be possible to fully regulate the voltage. In such complex scenarios, the smart GCI connected to RES within the microgrid plays a crucial role. It can dynamically adjust the power injection into the feeder, thereby further enhancing the voltage profile. This system mirrors the one discussed earlier in this chapter, which covered the hybrid application of OLTC-T and DVR for voltage regulation. The only difference is that the GCI is capable of marginally controlling the power output from the RES.

4.3.1 Control of trio for voltage regulation

The OLTC-T and DVR work in tandem to regulate voltage under normal operating conditions, with the same control mechanism as discussed in the previous case. However, when the penetration of renewable energy increases and the load on the microgrid decreases, the OLTC-T and DVR may not be able to maintain the voltage at

its reference value. In this situation, an inverter coupling RES to the microgrid can switch from MPPT mode to a deloaded condition. This allows only the necessary power to be supplied to the load, bringing the voltage at the terminals back within acceptable limits. Once the load returns to normal, the GCI control enters the MPPT mode again, and the OLTC-T and DVR take over the voltage regulation process.

4.3.2 Analysis of Smart GCI

There are several ways that inverters can be used for voltage regulation in microgrids, including:

- Voltage droop control: Inverters can be programmed to respond to changes in voltage by adjusting their power output. This is known as voltage droop control, where the output power decreases as the voltage increases.
- Power curtailment: Inverters can also curtail their power output to regulate voltage during times of high generation or low load. This can help to prevent overvoltage or undervoltage conditions that can damage equipment or disrupt power supply.
- Inverters can also be controlled by advanced algorithms and communication systems that enable real-time monitoring and management of power flows. This allows for more precise and efficient voltage regulation in microgrids.

Here the analysis is presented for the power curtailment method for voltage regulation has been utilised. The power output of an inverter can be curtailed to regulate the voltage and this is basically that the RES has been shifted from MPPT mode to the deloading mode of generation. When the PCC voltage exceeds the rated voltage, the

maximum power output of the RES can be reduced to prevent overvoltage conditions.

The power curtailment equation is as follows:

$$P_{max} = P_{base} \left(\frac{V_{PCC}}{V_{rated}} \right)^2$$

Where,

- P_{max} is the maximum power output,
- P_{base} is the base power output.
- V_{PCC} is the measured voltage at PCC, and
- V_{rated} is the base voltage.

The power curtailment equation shows how the maximum power output of RES has been reduced as the PCC voltage is increased above the rated voltage. This helps to prevent overvoltage conditions that can damage equipment.

4.3.3 Control of Smart GCI

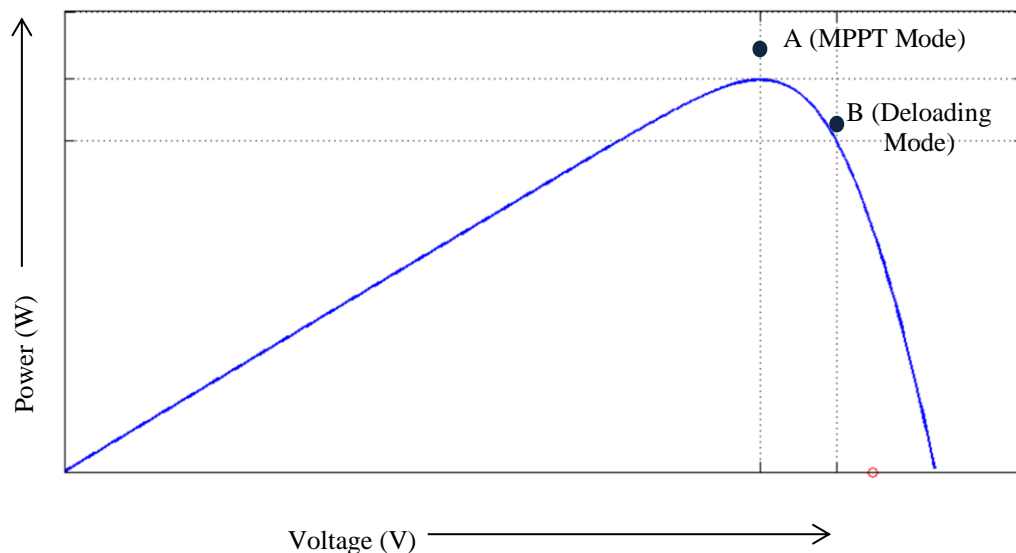


Fig. 4.22: Power shifting curve for RES

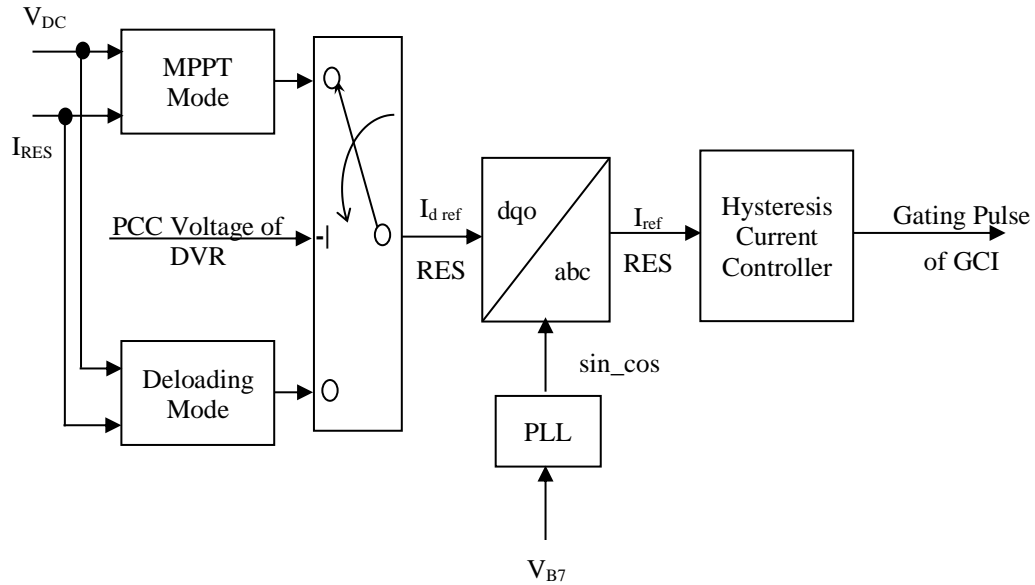


Fig. 4.23: Block diagram for mode control of smart GCI

The Smart GCI control strategy involves switching between Maximum Power Point Tracking (MPPT) mode and deloading mode as seen from Fig. 4.22 to ensure that the RES only pumps in the required power and the voltage at the terminals is maintained within limits. The control block of the interface inverter measures the voltage at the point of common coupling, and if it exceeds a certain level, the control of the GCI is switched to deloading mode. The GCI's reference current is then decreased, lowering the power injected into the system. The block diagram for the control block is shown in Fig. 4.23. The power variation range is typically limited to 5-10% to ensure that power utilization from RES does not suffer much. As soon as the loading returns to normal, the GCI control enters the MPPT mode. The switching between MPPT mode and deloading mode is a critical aspect of the GCI control strategy, as it ensures that the power injected into the system is regulated, and the voltage at the terminals is maintained within safe limits. This helps in the stable operation of the grid and ensures the optimal utilization of RES.

4.3.4 Performance Evaluation of OLTC-T, DVR and SGCI trio

The performance of the trio is evaluated under specific conditions: instances where overvoltage occurs during light loading and undervoltage occurs during heavy loading. These are crucial scenarios to assess as they present challenges that require the trio to regulate the voltage accurately.

However, in the majority of cases, the OLTC-T and DVR duo are capable of regulating the voltage effectively. Therefore, these cases are comparable to the aforementioned scenarios and are not discussed in detail. It's essential to note that the ability of the trio to handle the specified scenarios highlights its capacity to operate efficiently even under challenging circumstances.

Performance evaluation of the trio in overvoltage and light loading conditions

Performance of trio is evaluated under condition of overvoltage on the grid side and operating load at 20% of the rated condition. In this scenario, the system experiences a significant rise in voltage throughout, as illustrated by the voltage and current waveforms in Fig. 4.24 and voltage profiles in Fig. 4.25.

Without any regulation from $t = 0$ to $t = 0.2$ sec, overvoltage is observed at all terminal points, indicating the difficulty in maintaining system stability under this condition. However, the OLTC transformer, which is designed to regulate the voltage by adjusting the transformer's tap position, takes action at $t = 0.2$ sec, substantially improving the voltage profile of the system. This observation highlights the effectiveness of the OLTC transformer in regulating voltage and maintaining system

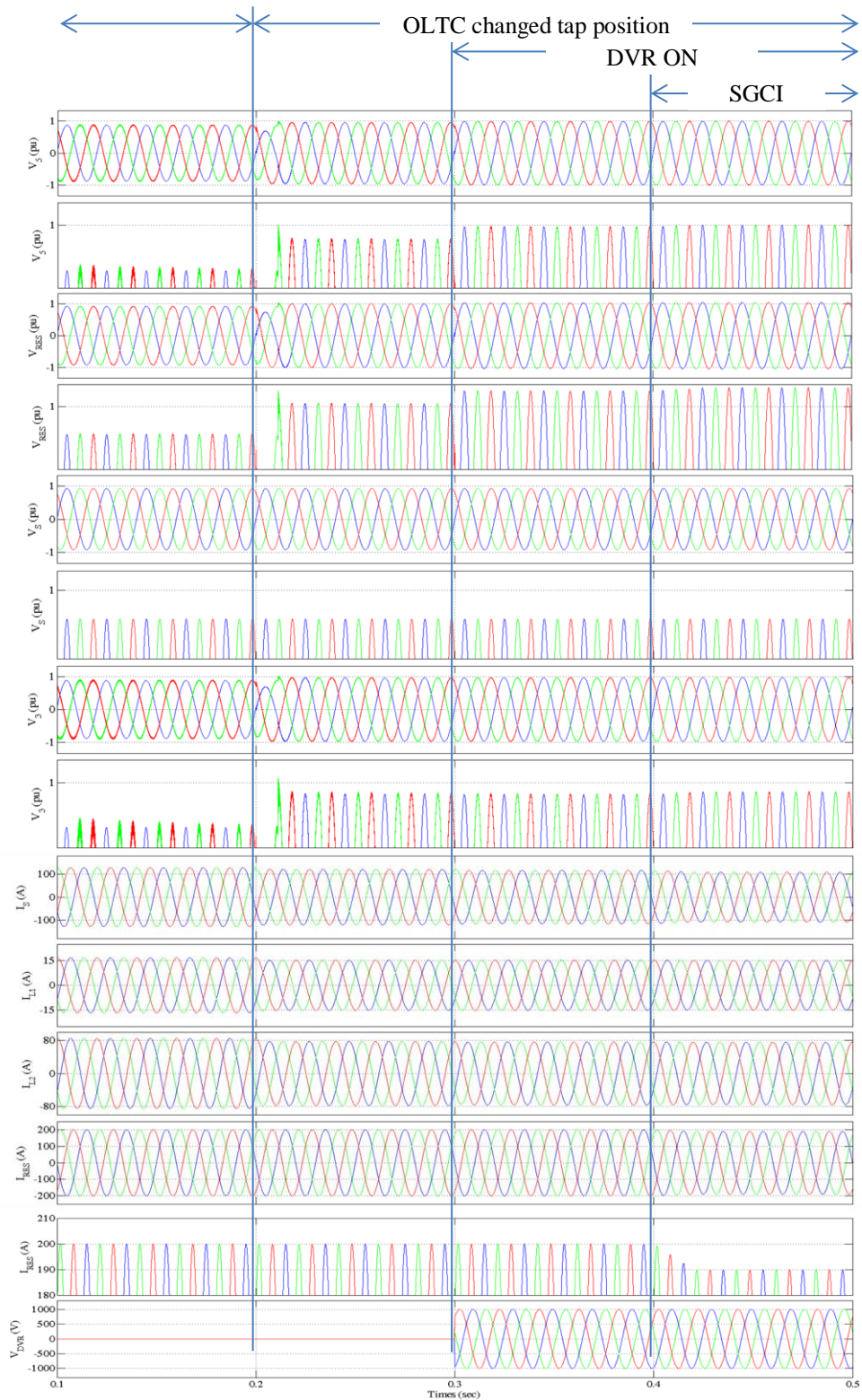


Fig. 4.24: Voltage and current waveforms in radial microgrid with OLTC transformer, DVR and smart GCI as voltage regulator during overvoltage and light loading condition

V_S : source voltage (pu), V_3 : voltage at the secondary terminal of the OLTC transformer (in pu), V_5 : voltage at the output terminal of DVR (in pu), V_{RES} : Voltage at the terminal of RES (in pu), I_S : Source current (in A), I_{L1} and I_{L2} : Load currents (A), I_{RES} : RES current (in A), V_{DVR} : Voltage supplied/absorbed by DVR (in V)

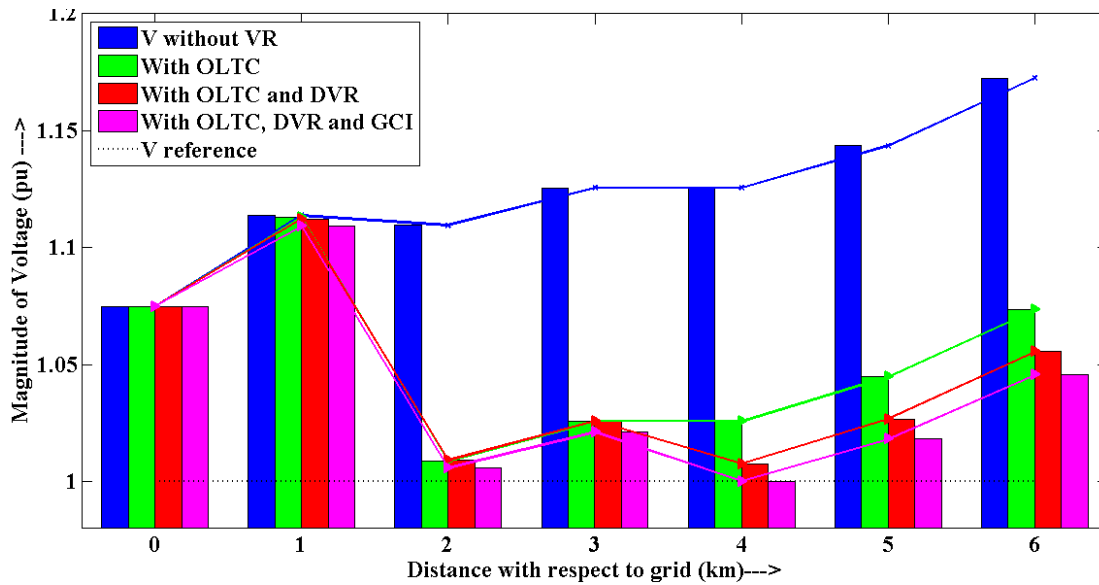


Fig. 4.25: Voltage profile of radial microgrid with OLTC transformer, DVR and smart GCI as voltage regulator during overvoltage and light loading condition

stability under challenging conditions.

The DVR, a device designed to regulate voltage by absorbing/supplying reactive power, also plays a critical role in improving the system's voltage profile. At $t = 0.3$ sec, the DVR starts absorbing reactive power, further enhancing the system's voltage profile. However, even with the DVR's contribution, the voltage at the DVR terminal does not reach the rated value.

At $t = 0.4$ sec, the smart GCI inverter comes into play, causing the RES to shift its operating point from MPPT to deloading mode, reducing I_{RES} and regulating the voltage at terminal of DVR and improved marginally at its PCC. This shift in operating point is crucial as it allows the smart GCI inverter to regulate the voltage and ensure the system's stability, as shown in Fig. 4.25.

Overall, this highlights the role of the OLTC transformer, DVR, and smart GCI inverter in maintaining system stability and regulating voltage under challenging overvoltage and light loading conditions.

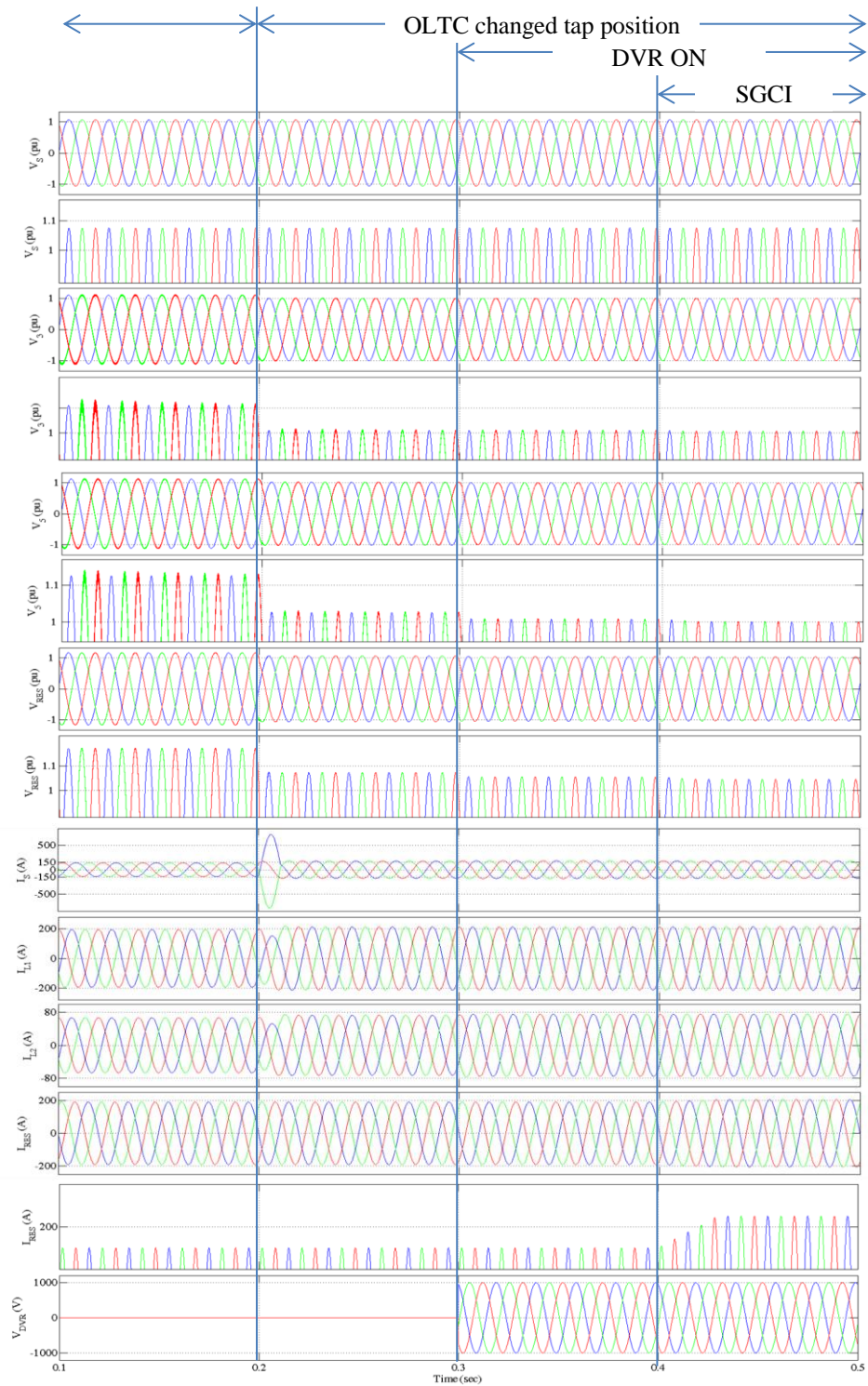


Fig. 4.26: Voltage and current waveforms in radial microgrid with OLTC transformer, DVR and smart GCI as voltage regulator during undervoltage and heavy loading condition

V_S : source voltage (pu), V_3 : voltage at the secondary terminal of the OLTC transformer (in pu), V_5 : voltage at the output terminal of DVR (in pu), V_{RES} : Voltage at the terminal of RES (in pu), I_S : Source current (in A), I_{L1} and I_{L2} : Load currents (A), I_{RES} : RES current (in A), V_{DVR} : Voltage supplied/absorbed by DVR (in V)

Performance evaluation of the trio in undervoltage and heavy loading conditions

This scenario involves undervoltage on the grid side and the load operating at 150% of the rated condition. The voltage and current waveforms are shown in Fig. 4.26, and voltage profiles are presented in Fig. 4.27. A significant drop in voltage throughout the microgrid can be observed without any regulation from $t = 0$ to $t = 0.2$ sec, and undervoltage is observed at all terminal points (nodes), highlighting the difficulty in maintaining system stability.

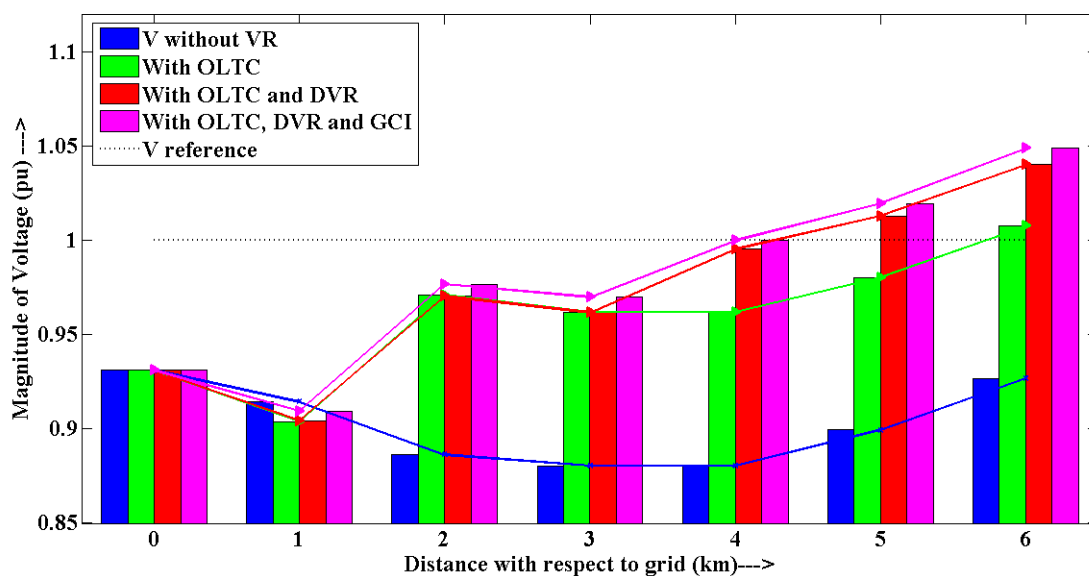


Fig. 4.27: Voltage profile of radial microgrid with OLTC transformer, DVR and smart GCI as voltage regulator during undervoltage and heavy loading condition

The OLTC transformer takes action at $t = 0.2$ sec, substantially improving the voltage profile. The DVR also plays a critical role in enhancing the system's voltage profile by supplying reactive power at $t = 0.3$ sec. However, even with the DVR's contribution, the voltage at its terminal does not reach the rated value.

At $t = 0.4$ sec, the smart GCI inverter shifts the RES operating point from deloading mode to the MPPT mode, increasing IRES and improving the voltage at its terminal.

This shift in operating point allows the smart GCI inverter to regulate voltage and maintain system stability, as shown in Fig. 4.27. The critical role of the OLTC transformer, DVR, and smart GCI inverter in maintaining system stability and regulating voltage under challenging undervoltage and heavy loading conditions is highlighted.

4.4 Conclusion

This chapter has explored the hybrid voltage regulators, specifically the OLTC transformer and DVR duo, which offer their respective benefits in regulating voltages. The OLTC-T provides major voltage regulation, while the DVR handles minor and small disturbances. By introducing an additional control element to the OLTC transformer that considers the I_d/I_q ratio before operating, the two devices operate autonomously, yet their coordinated control strategy enhances their effectiveness.

The MATLAB simulation results and voltage profile graphs demonstrate the ability of the OLTC transformer and DVR to regulate voltage at their respective terminals and significantly improve the voltage profile of the microgrid in most cases. Moreover, the smart GCI of RES also contributes to voltage regulation by complementing the duo voltage regulation, providing a preventive approach.

Overall, their ability to work in unison improves the microgrids performance and ensures efficient power distribution. The hybrid voltage regulators discussed in this chapter offer a promising solution for voltage regulation in microgrids.

Chapter 5

Analysis of Radial Microgrid with High Penetration of RES

5.1 General Overview

RES has become increasingly important in recent years, resulting in their greater penetration in the distribution system and microgrid. With a large number of RES distributed throughout the microgrid, efficient and effective operation is required without disrupting the existing protection scheme. The intermittent nature of RES further exacerbates the challenge, as fluctuations in voltage levels at the PCC can breach voltage regulation limits. In this chapter, the proposed work envisages the whole microgrid fragmented into multiple controlled sections having multiple RES in each section when seen from the distribution transformer. An analytical method for the estimation of nodal voltage and branch current based on ABCD parameters across each such controlled section has been investigated. The analytical results presented in this chapter are further verified through MATLAB simulations.

5.2 Radial Microgrid Configuration and Analysis

Fig. 5.1 depicts the block diagram of a proposed radial microgrid system designed to investigate the effects of voltage at different nodes or terminals of the radial microgrid due to the intermittent penetration of RES. In this proposed method, a reference node (n_0) is selected from the distribution feeder close to the distribution substation and represented as a voltage source (V_S). For the sake of development of concept for analysing RES sources (I_{RES_i}) and loads (Z_{L_i}) are connected alternately throughout the

radial micro-grid, to strive symmetry initially, where 'i' represents the node number with respect to the reference node.

The RES sources are assumed to be connected to even nodes from the reference node (n_2, n_4, n_6 and so on), while the loads are assumed connected to odd nodes from the reference node (n_1, n_3, n_5 and so on). By employing this approach, the impact of intermittent RES on the voltage levels at different nodes or terminals of the radial microgrid can be analysed effectively. The proposed system presents a typical configuration for studying the effects of intermittent RES penetration in radial micro-grid systems.

In this proposed system, the RES sources are considered to be connected to the microgrid as a current source to represent current-controlled VSC, while the loads are three-phase balanced RL loads. Both RES sources and loads are placed at certain distances within the microgrid, which are represented by the sectional impedance ($Z_{i,j}$). Since the microgrid is a part of the distribution network, the microgrid sectional impedance also have a high R/X ratio (approximately 8). This high R/X ratio results in significant voltage drops, which can affect the overall voltage levels within the microgrid at low voltage level. By taking into account the sectional impedance and their associated R/X ratios, the proposed system provides a more accurate representation of the effects of high penetration of intermittent RES in radial microgrid systems.

In the proposed system, the loads are represented by lumped impedance (Z_{L_i}), given by equation (5.1):

$$Z_{L_i} = \frac{V_{n_i} (rated)}{P_{L_i} + Q_{L_i}} \quad (5.1)$$

Here, $V_{n_i} (rated)$ represents the rated voltage at the node and $P_{L_i} + Q_{L_i}$ represents the rated power of the load (i.e., the power consumed by the load at the rated voltage). While there may be other types of loads present in the microgrid, for the purpose of simplification, only constant impedance type of loads are considered for the current study.

To study the effect of high penetration of renewable energy sources (RES) on a microgrid, an ABCD parameter-based method is developed to estimate nodal voltages and branch currents throughout the microgrid. The ABCD parameters are commonly used to describe two-port networks and are defined as follows:

- A: The voltage gain when the input current is zero
- B: The input/output impedance when the output voltage is zero
- C: The output/input admittance when the input current is zero
- D: The current gain when the output voltage is zero

Using the ABCD parameters, the nodal voltages and branch currents of the microgrid can be estimated. Here is a step-by-step description of the analysis is presented below:

Step 1: Considering first section of the radial micro-grid

Simplify the microgrid by considering a segment between two nodes, labelled as n_0 and n_2 in Fig. 5.2(a). This segment is denoted as Section '02'. The ABCD parameters of Section '02' can be calculated using the basic two-port network equations:

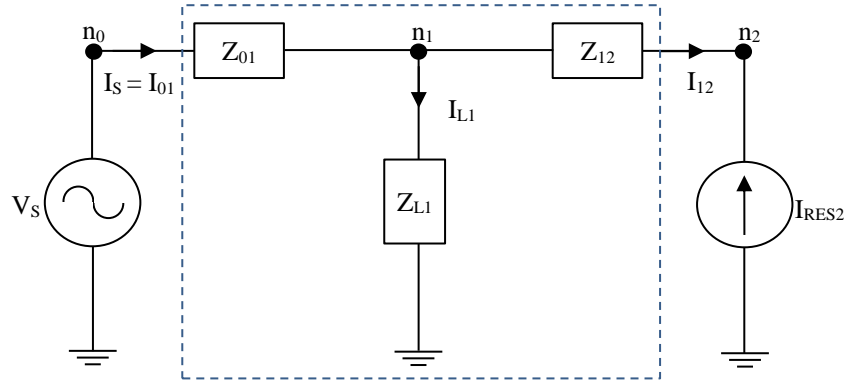


Fig. 5.2(a): Single Line Diagram of Section between nodes '0' and '2'

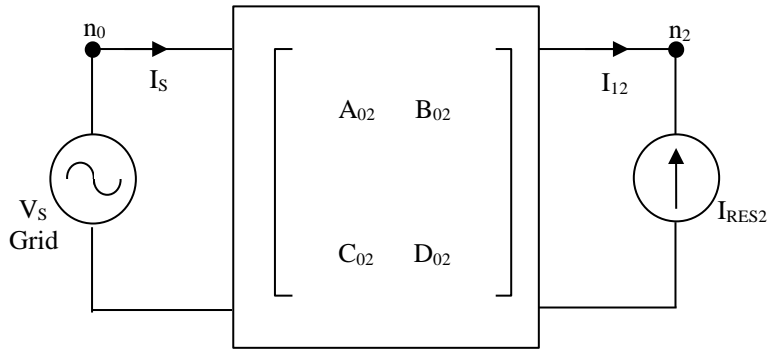


Fig. 5.2(b): ABCD parameter equivalent of Section between nodes '0' and '2'

$$A_{02} = \left. \frac{V_{n_0}}{V_{n_2}} \right|_{I_{12}=0} = 1 + \frac{Z_{01}}{Z_{L1}} \quad (5.2)$$

$$B_{02} = \left. \frac{V_{n_0}}{I_{12}} \right|_{V_{n_2}=0} = Z_{01} + Z_{12} + \frac{Z_{01}Z_{12}}{Z_{L1}} \quad (5.3)$$

$$C_{02} = \left. \frac{I_{01}}{V_{n_2}} \right|_{I_{12}=0} = \frac{1}{Z_{L1}} \quad (5.4)$$

$$D_{02} = \left. \frac{I_{01}}{I_{12}} \right|_{V_{n_2}=0} = 1 + \frac{Z_{12}}{Z_{L1}} \quad (5.5)$$

The equivalent circuit for section '02', represented by its ABCD parameter, is shown in Fig. 5.2(b).

Step 2: Considering the radial micro-grid in terms of ABCD parameters, with equivalent circuit diagram presented in Fig. 5.3

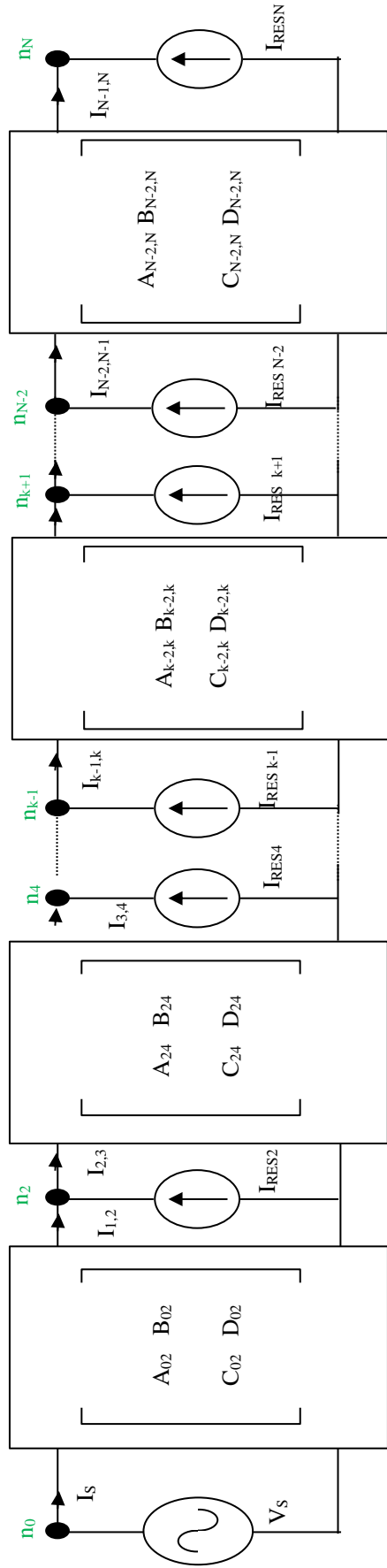


Fig 5.3: ABCD Equivalent circuit of considered 'N' node radial microgrid

Whereas, the ABCD parameters, for each subsequent sections, between any two consecutive RES can be formulated in terms of equation(5.6) to equation (5.9), and are represented in the equivalent circuit diagram of the entire microgrid, as shown in Fig.

5.3. ABCD parameters for any section, between two even nodes ‘i’ and ‘i+2’ are:

$$A_{i,i+2} = \left. \frac{V_{n_i}}{V_{n_{i+2}}} \right|_{I_{i+1,i+2}=0} = 1 + \frac{Z_{i,i+1}}{Z_{L_{i+1}}} \quad (5.6)$$

$$B_{i,i+2} = \left. \frac{V_{n_i}}{I_{i+1,i+2}} \right|_{V_{n_{i+2}}=0} = Z_{i,i+1} + Z_{i+1,i+2} + \frac{Z_{i,i+1}Z_{i+1,i+2}}{Z_{L_{i+1}}} \quad (5.7)$$

$$C_{i,i+2} = \left. \frac{I_{i,i+1}}{V_{n_{i+2}}} \right|_{I_{i+1,i+2}=0} = \frac{1}{Z_{L_{i+1}}} \quad (5.8)$$

$$D_{i,i+2} = \left. \frac{I_{i,i+1}}{I_{i+1,i+2}} \right|_{V_{n_{i+2}}=0} = 1 + \frac{Z_{i+1,i+2}}{Z_{L_{i+1}}} \quad (5.9)$$

Step 3:

From Fig. 5.3, the basic equations of ABCD parameters for two-port networks for the section between node ‘0’ and node ‘2’ (‘02’) can be expressed as:

$$V_S = A_{02}V_{n_2} + B_{02}I_{12} \quad (5.10)$$

$$I_S = C_{02}V_{n_2} + D_{02}I_{12} \quad (5.11)$$

Where,

V_S is the voltage of reference nodes,

$I_S(= I_{01})$ is the source current

V_{n_2} is the voltage of node n_2

I_{12} is the current leaving section '02'.

Likewise, the equations for section between node ‘2’ and node ‘4’ (‘24’) are represented as:

$$V_{n_2} = A_{24}V_{n_4} + B_{24}I_{34} \quad (5.12)$$

$$I_{23} = C_{24}V_{n_4} + D_{24}I_{34}$$

$$\Rightarrow I_{12} = C_{24}V_{n_4} + D_{24}I_{34} + I_{RES_2} \quad (5.13)$$

Similarly, generalized equations for section between node 'i' and node 'i+2' are given by:

$$V_{n_i} = A_{i,i+2}V_{n_{i+2}} + B_{i,i+2}I_{i+1,i+2} \quad (5.14)$$

$$I_{i,i+1} = C_{i,i+2}V_{n_{i+2}} + D_{i,i+2}I_{i+1,i+2}$$

$$\Rightarrow I_{i-1,i} = C_{i,i+2}V_{n_{i+2}} + D_{i,i+2}I_{i+1,i+2} + I_{RES_i} \quad (5.15)$$

Comprehensively, the complete micro-grid can be considered for any location with the assumption that the current of RES's at all the nodes are known under smart grid environment. The combined matrix equation for the micro-grid can be expressed by equation (5.16).

$$\begin{bmatrix} A_{02} & 0 & \dots & 0 & 0 & 0 & B_{02} & 0 & 0 & 0 \\ -I & A_{24} & \dots & 0 & 0 & 0 & 0 & B_{24} & 0 & \dots \\ 0 & -I & \dots & 0 & \dots & 0 & \dots & 0 & \dots & 0 \\ 0 & \dots & \dots & A_{N-4,N} & 0 & \dots & \dots & 0 & 0 & B_{N-2,N} \\ 0 & 0 & \dots & -I & A_{N-2,i} & 0 & 0 & \dots & 0 & 0 \\ \hline C_{02} & 0 & \dots & 0 & 0 & I & D_{02} & 0 & 0 & 0 \\ 0 & C_{24} & 0 & 0 & 0 & 0 & -I & D_{24} & 0 & 0 \\ 0 & \dots & \dots & 0 & 0 & 0 & 0 & \dots & \dots & 0 \\ 0 & 0 & 0 & C_{N-4,N} & 0 & \dots & 0 & 0 & I & D_{N-2,N} \\ 0 & 0 & 0 & 0 & C_{N-2,i} & 0 & 0 & \dots & 0 & -I \end{bmatrix} \cdot \begin{bmatrix} V_{n_2} \\ V_{n_4} \\ \dots \\ V_{n_{N-2}} \\ V_{n_N} \\ I_S \\ I_{12} \\ I_{34} \\ \dots \\ I_{N-4,N} \end{bmatrix} = \begin{bmatrix} V_S \\ 0 \\ \dots \\ 0 \\ B_{N-2,N}I_{RES_N} \\ 0 \\ I_{RES_2} \\ \dots \\ I_{RES_{N-2}} \\ I_{RES_{N-2}} \\ + D_{N-4,N-2}I_R \end{bmatrix} \quad (5.16)$$

This equation is of the form $AX = B$, where $X = A^{-1}B$. Solving this matrix equation can help estimate the voltage at different nodes and the currents flowing in/out of

different sections where RESs are connected to the micro-grid. Later other branch parameters can also be found out using the backward sweep method and general equation for this is given by equation (5.17).

$$V_{n_{i+1}} = V_{n_{i+2}} + I_{i+1,i+2} \cdot Z_{i+1,i+2} \quad (5.17)$$

These estimated values of voltage along the length of the microgrid can allow the distribution system operator to draw the voltage profile of the microgrid.

5.3 Validation of Analysis with MATLAB Simulation

The reliability and suitability of the analytical method used to calculate sectional parameters in microgrids have been confirmed through extensive MATLAB simulations of an 11-node radial microgrid. Fig. 5.4(a) shows the microgrid's single-line diagram, while Fig. 5.4(b) presents the ABCD reduced network. The simulation diagram is depicted in Fig. 5.5. Node 0 (n_0) acts as the reference node, with RES sources connected at nodes 2, 4, 6, 8, and 10, and loads connected at nodes 1, 3, 5, 7, and 9. The proposed analytical method calculates nodal voltages, which are then compared with the simulated values to validate the proposed mathematical analysis and its suitability for better size, control and operate from micro-grid with high penetration of RES.

To evaluate the proposed analytical method, the ABCD analysis was performed on the considered system under two cases:

- Case 1: Uniform distribution of the loads and RES on the microgrid feeder and
- Case 2: non-uniform distribution of the loads and RES on the microgrid feeder.

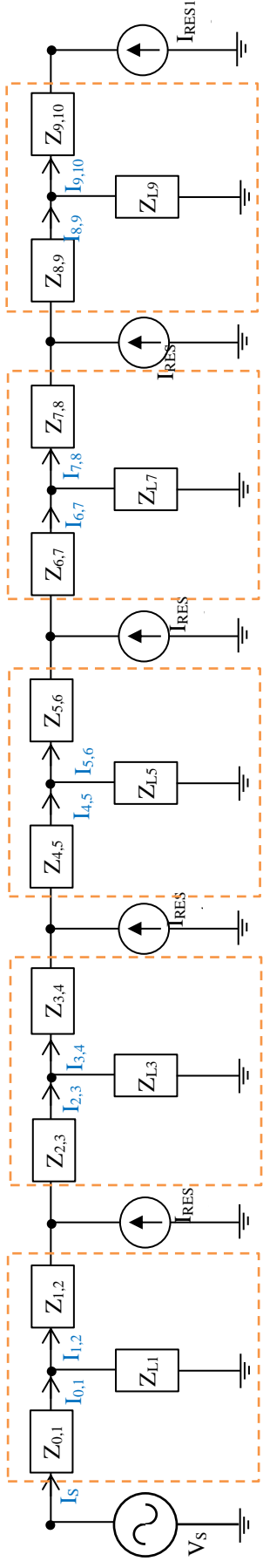


Fig. 5.4(a): Single line diagram of 11 node radial microgrid

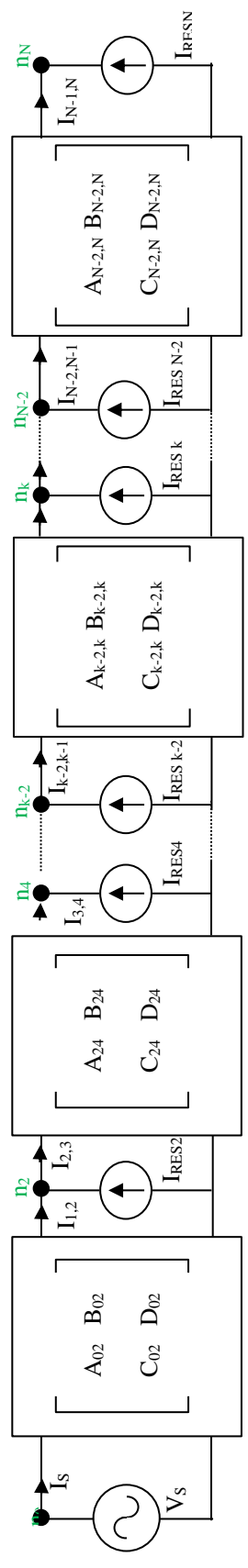


Fig 5.4(b): ABCD Equivalent circuit of considered 11 node radial microgrid

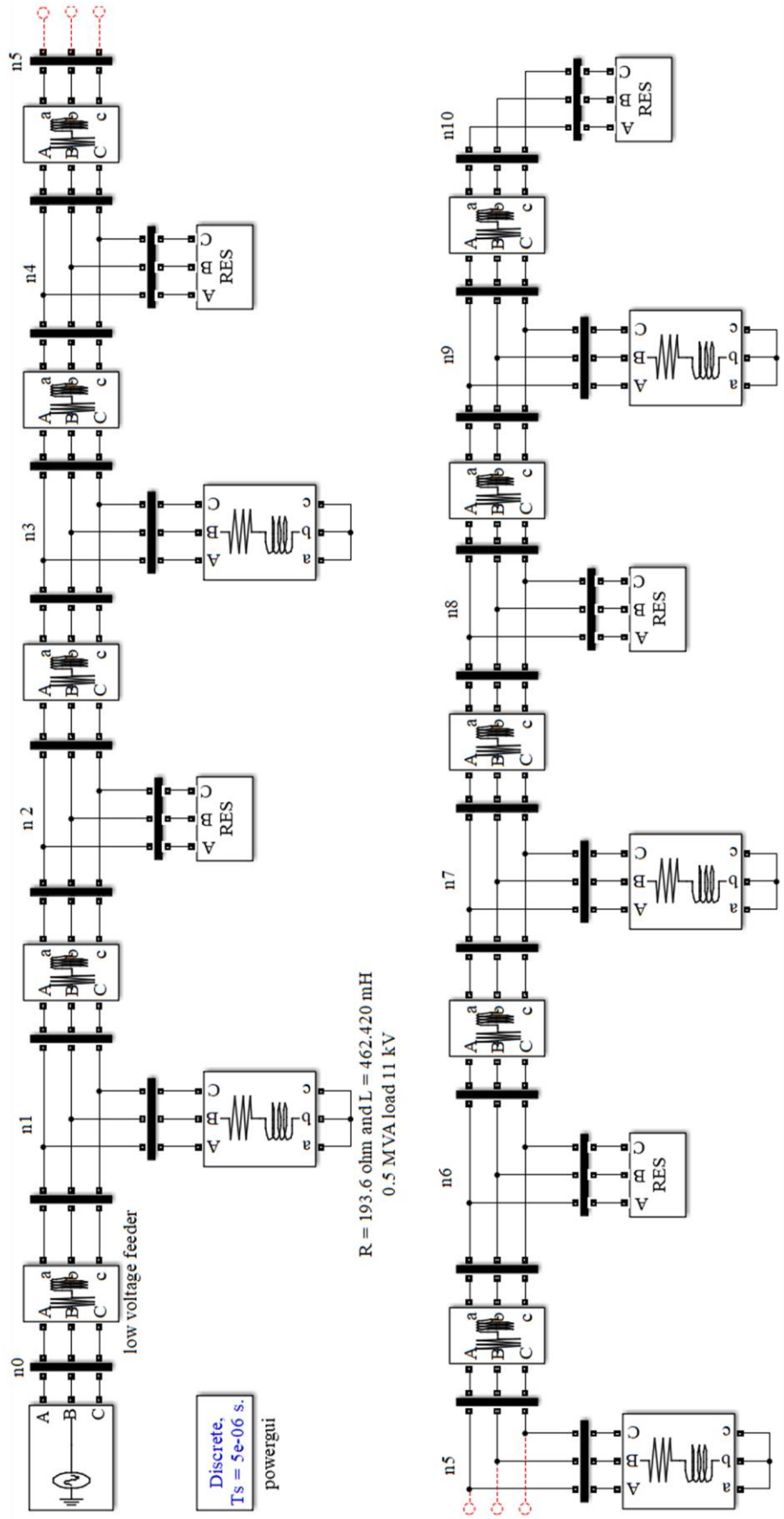


Fig. 5.5: Simulation diagram of 11 node radial microgrid

Each case was then tested under three different conditions to assess the microgrids behaviour under various scenarios, including normal and worst-case scenarios of renewable energy sources (RES) power injection. These conditions includes:

- (1) Rated load and normal RES injection,
- (2) Light load (one third of rated loading condition $Z_L = Z_{L3}$) and high RES current injection ($I_{RES} = I_{RES} X 2$), and
- (3) Heavy load (twice the rated loading condition $Z_L = Z_L/2$) and no RES injection.

Case 1: Uniform Distribution of loads and RES on the radial Microgrid Feeder

A uniform feeder distribution is considered for the first case, with each node separated by a feeder of 1 km having an impedance of $Z_f = 0.642 + j0.083 \Omega/km$ [172]. Rated loads are connected at all nodes, with $S = 0.5 MVA$ and $Z_L = 193.6 + j145.273 \Omega$. Normal injection of RES is considered as $S_{RES} = 0.25 MVA$ and $I_{RES\ peak} = 20 A$. ABCD parameters of each section are calculated using equation (5.6) to equation (5.9), and are given as:

$$A_{i,i+2} = 1 + \frac{Z_{i,i+1}}{Z_{L_{i+1}}} = 1 + \frac{0.642 + j 0.083}{193.6 + j 145.273} = 1.0023 - j 0.0013$$

$$B_{i,i+2} = Z_{i,i+1} + Z_{i+1,i+2} + \frac{Z_{i,i+1}Z_{i+1,i+2}}{Z_{L_{i+1}}}$$

$$B_{i,i+2} = (0.642 + j0.083) + (0.642 + j0.083) + \left(\frac{0.642 + j0.083}{193.6 + j 145.273} \right)$$

$$B_{i,i+2} = 1.2856 + j 0.1653 \Omega$$

$$C_{i,i+2} = \frac{1}{Z_{L_{i+1}}} = \frac{1}{193.6 + j 145.273} = 0.0033 - j 0.0025 \text{ U}$$

$$D_{i,i+2} = 1 + \frac{Z_{i+1,i+2}}{Z_{L_{i+1}}} = 1 + \frac{0.642 + j 0.083}{193.6 + j 145.273} = 1.0023 - j 0.0013$$

Further the equation (5.16) and equation (5.17) to calculate the nodal voltages are modified as set of equation mentioned below:

$$\begin{bmatrix}
 A_{02} & 0 & 0 & 0 & 0 & 0 & B_{02} & 0 & 0 & 0 \\
 -1 & A_{24} & 0 & 0 & 0 & 0 & 0 & B_{24} & 0 & 0 \\
 0 & -1 & A_{46} & 0 & 0 & 0 & 0 & 0 & B_{46} & 0 \\
 0 & 0 & -1 & A_{68} & 0 & 0 & 0 & 0 & 0 & B_{68} \\
 0 & 0 & 0 & -1 & A_{8,10} & 0 & 0 & 0 & 0 & 0 \\
 C_{02} & 0 & 0 & 0 & 0 & - & D_{02} & 0 & 0 & 0 \\
 & & & & & I & & & & \\
 0 & C_{24} & 0 & 0 & 0 & 0 & -1 & D_{24} & 0 & 0 \\
 0 & 0 & C_{46} & 0 & 0 & 0 & 0 & -1 & D_{46} & 0 \\
 0 & 0 & 0 & C_{68} & 0 & 0 & 0 & 0 & -1 & D_{68} \\
 0 & 0 & 0 & 0 & C_{8,10} & 0 & 0 & 0 & 0 & -1
 \end{bmatrix} \cdot \begin{bmatrix}
 V_{n_2} \\
 V_{n_4} \\
 V_{n_6} \\
 V_{n_8} \\
 V_{n_{10}} \\
 I_S \\
 I_{12} \\
 I_{34} \\
 I_{56} \\
 I_{78}
 \end{bmatrix} = \begin{bmatrix}
 V_S \\
 0 \\
 0 \\
 0 \\
 B_{8,10} I_{RES_{10}} \\
 0 \\
 I_{RES_2} \\
 I_{RES_4} \\
 I_{RES_6} \\
 I_{RES_8} \\
 + D_{8,10} I_{RES_6}
 \end{bmatrix} \quad (5.18)$$

$$V_{n_1} = V_{n_2} + I_{12} \cdot Z_{12} \quad (5.19)$$

$$V_{n_3} = V_{n_4} + I_{34} \cdot Z_{34} \quad (5.20)$$

$$V_{n_5} = V_{n_6} + I_{56} \cdot Z_{56} \quad (5.21)$$

$$V_{n_7} = V_{n_8} + I_{78} \cdot Z_{78} \quad (5.22)$$

$$V_{n_9} = V_{n_{10}} + I_{9,10} \cdot Z_{9,10} \quad (5.23)$$

The calculated nodal voltage magnitude values are compared to the simulated nodal voltage magnitude values, and the results are shown in Table 5.1. The analytical method is in close agreement with the simulated data, conforming its validity and accuracy.

For the light load and high RES penetration condition, load and RES current injection are modified to: $Z_L = 580.8 + j435.819 \Omega$ and $I_{RES\ peak} = 40 A$. ABCD parameters are

Table 5.1: Comparison of calculated and simulated data for uniform feeder distribution and normal operating conditions

Node Voltage (in kV)	Calculated Data		Simulation Data	Error (in %)
	Voltage	Voltage Magnitude	Voltage Magnitude	
V ₀	8.980	8.982	8.982	0.000
V ₁	8.940 + 0.064i	8.941	8.941	0.000
V ₂	8.921 + 0.117i	8.922	8.922	0.001
V ₃	8.889 + 0.168i	8.890	8.891	0.002
V ₄	8.878 + 0.207i	8.880	8.880	0.002
V ₅	8.853 + 0.245i	8.856	8.857	0.003
V ₆	8.850 + 0.272i	8.854	8.854	0.004
V ₇	8.833 + 0.297i	8.838	8.839	0.004
V ₈	8.838 + 0.311i	8.843	8.844	0.005
V ₉	8.855 + 0.327i	8.836	8.862	0.297
V ₁₀	8.843 + 0.325i	8.849	8.849	0.006

Table 5.2: Comparison of calculated and simulated data for uniform feeder distribution and light loading and high RES injection condition

Node Voltage (in kV)	Calculated Data		Simulation Data	Error (in %)
	Voltage	Voltage Magnitude	Voltage Magnitude	
V ₀	8.982	8.982	8.982	0.000
V ₁	9.073 + 0.0366i	9.073	9.073	-0.002
V ₂	9.172 + 0.0693i	9.173	9.172	-0.002
V ₃	9.245 + 0.0986i	9.246	9.246	-0.003
V ₄	9.326 + 0.1240i	9.327	9.326	-0.005
V ₅	9.381 + 0.1459i	9.382	9.382	-0.003
V ₆	9.442 + 0.1640i	9.444	9.444	-0.003
V ₇	9.479 + 0.1787i	9.481	9.481	-0.005
V ₈	9.523 + 0.1894i	9.525	9.525	-0.005
V ₉	9.592 + 0.2034i	9.595	9.543	-0.544
V ₁₀	9.567 + 0.2001i	9.569	9.569	-0.005

Table 5.3: Comparison of calculated and simulated data for uniform feeder distribution and heavy loading and no RES injection condition

Node Voltage (in kV)	Calculated Data		Simulation Data	Error (in %)
	Voltage	Voltage Magnitude	Voltage Magnitude	
V_0	8.980	8.980	8.982	0.017
V_1	$8.783 + 0.102i$	8.784	8.784	0.000
V_2	$8.627 + 0.181i$	8.629	8.628	-0.007
V_3	$8.470 + 0.260i$	8.474	8.474	-0.004
V_4	$8.353 + 0.318i$	8.359	8.359	0.001
V_5	$8.237 + 0.376i$	8.245	8.245	-0.002
V_6	$8.159 + 0.414i$	8.170	8.169	-0.009
V_7	$8.082 + 0.453i$	8.094	8.094	0.001
V_8	$8.043 + 0.471i$	8.057	8.057	-0.004
V_9	$8.005 + 0.489i$	8.020	8.019	-0.009
V_{10}	$8.005 + 0.489i$	8.020	8.019	-0.009

calculated from equation (5.6) to equation (5.9) are given as:

$$A_{i,i+2} = 1.0008 - 0.0004i$$

$$B_{i,i+2} = 1.2845 + 0.1658i\Omega$$

$$C_{i,i+2} = 0.0011 - 0.0008i \text{ } \bar{V}$$

$$D_{i,i+2} = 1.0008 - 0.0004i$$

Nodal voltages for the uniform case are calculated, and the results are compared to the simulated values in Table 5.2. The proposed analytical method closely resembles the simulated data, confirming its accuracy.

With the heavy load condition and no RES injection condition, the computed values and comparison of simulated results and analytical computations are drawn is also analysed using the same process. Here,

$Z_L = 580.8 + j435.819 \Omega$ and $I_{RES\ peak} = 0 A$. ABCD parameters are computed and tabulated in table 5.3 along with simulated results kept side by side.

$$A_{i,i+2} = 1.0047 - 0.0026i$$

$$B_{i,i+2} = 1.2872 + 0.1647i \Omega$$

$$C_{i,i+2} = 0.0066 - 0.0050i \text{ U}$$

$$D_{i,i+2} = 1.0047 - 0.0026i$$

The nodal voltage values for calculated and simulated results are shown in Table 5.3.

Case 2: Non-Uniform Distribution of Microgrid Feeder

The second scenario investigates a non-uniform feeder distribution in a microgrid, where each section has unique characteristics such as varying line lengths, loading values, and different power injections from renewable energy sources. This case is analysed for similar conditions as has been done for uniform distribution condition case.

Under the normal operating condition (Condition 1), the system parameters specified in Table 5.4 are used to calculate the ABCD parameter values for each section by applying equations (5.6) to (5.9). Due to the variations in section length and loads, the ABCD parameter values differ for each section, as shown in Table 5.5. The nodal voltages are then calculated using equations 5.18 to 5.23. These values are compared with the simulation results obtained from MATLAB Simulink, and the comparison is presented in Table 5.6. The results demonstrate close agreement between the proposed analytical method and simulated values.

Table 5.4: System parameter considered for non- uniform feeder distribution and normal operating condition

Section		length of section (in km)	Feeder impedance		S_L (in MVA) / P_{RES} (in MW)	Z_L (in Ω)/ I_{RES} (in A)
02	Z_{f01}	0.5	$0.3210 + 0.0415i$	Z_{L1}	0.625	$154.88+116.218i$
	Z_{f12}	1.2	$0.7704 + 0.0996i$	I_{RES2}	0.343	18
24	Z_{f23}	0.8	$0.5136 + 0.0664i$	Z_{L3}	0.417	$232.32+174.328i$
	Z_{f34}	1	$0.6420 + 0.0830i$	I_{RES4}	0.419	22
46	Z_{f45}	1.5	$0.9630 + 0.1245i$	Z_{L5}	0.500	$193.6+145.273i$
	Z_{f56}	0.8	$0.5136 + 0.0664i$	I_{RES6}	0.381	20
68	Z_{f67}	1.2	$0.7704 + 0.0996i$	Z_{L7}	0.417	$232.32+174.328i$
	Z_{f78}	0.8	$0.5136 + 0.0664i$	I_{RES8}	0.419	22
8,10	Z_{f89}	1.2	$0.7704 + 0.0996i$	Z_{L9}	0.625	$154.88+116.218i$
	$Z_{f9,10}$	1	$0.6420 + 0.0830i$	I_{RES10}	0.343	18

Table 5.5: ABCD parameter computed for non- uniform feeder distribution and normal operating condition

A_{02}	$1.0015 - 0.0008i$	B_{02}	$1.0926 + 0.1406i$
C_{02}	$0.0041 - 0.0031i$	D_{02}	$1.0035 - 0.0020i$
A_{24}	$1.0016 - 0.0009i$	B_{24}	$1.1567 + 0.1490i$
C_{24}	$0.0028 - 0.0021i$	D_{24}	$1.0019 - 0.0011i$
A_{46}	$1.0035 - 0.0020i$	B_{46}	$1.4785 + 0.1901i$
C_{46}	$0.0033 - 0.0025i$	D_{46}	$1.0019 - 0.0011i$
A_{68}	$1.0023 - 0.0013i$	B_{68}	$1.2853 + 0.1655i$
C_{68}	$0.0028 - 0.0021i$	D_{68}	$1.0016 - 0.0009i$
$A_{8,10}$	$1.0035 - 0.0020i$	$B_{8,10}$	$1.4148 + 0.1816i$
$C_{8,10}$	$0.0041 - 0.0031i$	$D_{8,10}$	$1.0029 - 0.0016i$

Table 5.6: Comparison of calculated and simulated data for non- uniform feeder distribution and normal operating condition

Node Voltage (in kV)	Calculated Data		Simulation Data	Error (in %)
	Voltage	Voltage Magnitude	Voltage Magnitude	
V_0	$8.9800 + 0.0000i$	8.982	8.982	0.000
V_1	$8.9601 + 0.0333i$	8.960	8.960	-0.007
V_2	$8.9401 + 0.0956i$	8.941	8.939	-0.024
V_3	$8.9176 + 0.1359i$	8.919	8.916	-0.036
V_4	$8.9069 + 0.1768i$	8.909	8.904	-0.050
V_5	$8.8696 + 0.2354i$	8.873	8.866	-0.072
V_6	$8.8665 + 0.2577i$	8.870	8.863	-0.084
V_7	$8.8464 + 0.2891i$	8.851	8.842	-0.101
V_8	$8.8470 + 0.3028i$	8.852	8.843	-0.105
V_9	$8.8525 + 0.3239i$	8.858	8.826	-0.367
V_{10}	$8.8409 + 0.3224i$	8.847	8.838	-0.104

In addition, the proposed analytical method is also applied to the light loading and high renewable energy source (RES) injection condition and also for the heavy loading with no RES injection condition in a non-uniformly distributed microgrid feeder. Feeder impedance for all the conditions are assumed same. For the system under consideration, Tables 5.7 and 5.8 provide the system parameters and corresponding ABCD values for light loading with high RES injection, while Tables 5.10 and 5.11 present the same information for heavy loading without RES injection. The nodal voltages obtained from the proposed analytical method are compared with the simulation results and are shown in Tables 5.9 and 5.12, respectively. The results demonstrate that the proposed analytical method shows close agreement with the simulated values, conforming its suitability for analysing microgrids even with non-uniform feeder distributions.

Table 5.7: System parameter considered for non-uniform feeder distribution and light loading and

high RES injection condition

Section		S_L (in MVA) / P_{RES} (in MW)	Z_L (in Ω) / I_{RES} (in A)
02	Z_{L1}	0.208	464.64+348.6564i
	I_{RES2}	0.686	36
24	Z_{L3}	0.139	696.96+522.9846i
	I_{RES4}	0.838	44
46	Z_{L5}	0.167	580.8+435.8205i
	I_{RES6}	0.762	40
68	Z_{L7}	0.139	696.96+522.9846i
	I_{RES8}	0.838	44
8,10	Z_{L9}	0.208	464.64+348.6564i
	I_{RES10}	0.686	36

Table 5.8: ABCD parameter computed for non-uniform feeder distribution and light loading and high RES injection condition

A₀₂	1.0005 - 0.0003i	B₀₂	1.0918 + 0.1409i
C₀₂	0.0014 - 0.0010i	D₀₂	1.0012 - 0.0007i
A₂₄	1.0005 - 0.0003i	B₂₄	1.1560 + 0.1493i
C₂₄	0.0009 - 0.0007i	D₂₄	1.0006 - 0.0004i
A₄₆	1.0012 - 0.0007i	B₄₆	1.4772 + 0.1906i
C₄₆	0.0011 - 0.0008i	D₄₆	1.0006 - 0.0004i
A₆₈	1.0008 - 0.0004i	B₆₈	1.2844 + 0.1658i
C₆₈	0.0009 - 0.0007i	D₆₈	1.0005 - 0.0003i
A_{8,10}	1.0012 - 0.0007i	B_{8,10}	1.4132 + 0.1823i
C_{8,10}	0.0014 - 0.0010i	D_{8,10}	1.0010 - 0.0005i

Table 5.9: Comparison of calculated and simulated data for non-uniform feeder distribution and light loading and high RES injection condition

Node Voltage (in kV)	Calculated Data		Simulation Data	Error (in %)
	Voltage	Voltage Magnitude	Voltage Magnitude	
V₀	8.9800 + 0.0000i	8.982	8.982	0.000
V₁	9.0281 + 0.0188i	9.028	9.027	-0.015
V₂	9.1506 + 0.0580i	9.151	9.146	-0.048
V₃	9.2138 + 0.0818i	9.214	9.208	-0.070
V₄	9.2987 + 0.1082i	9.299	9.290	-0.097
V₅	9.3838 + 0.1422i	9.385	9.372	-0.137
V₆	9.4350 + 0.1572i	9.436	9.421	-0.158
V₇	9.4810 + 0.1757i	9.483	9.465	-0.190
V₈	9.5167 + 0.1853i	9.519	9.499	-0.208
V₉	9.5794 + 0.2010i	9.582	9.515	-0.696
V₁₀	9.5563 + 0.1980i	9.558	9.539	-0.208

Table 5.10: System parameter considered for non-uniform feeder distribution and heavy loading and no RES injection condition

Section		S_L (in MVA) /P_{RES} (in MW)	Z_L(in Ω)/I_{RES} (in A)
02	Z _{L1}	1.250	77.44+58.1094i
	I _{RES2}	0.000	0
24	Z _{L3}	0.833	116.16+87.1641i
	I _{RES4}	0.000	0
46	Z _{L5}	1.000	96.8+72.63675i
	I _{RES6}	0.000	0
68	Z _{L7}	0.833	116.16+87.1641i
	I _{RES8}	0.000	0
8,10	Z _{L9}	1.250	77.44+58.1094i
	I _{RES10}	0.000	0

Table 5.11: ABCD parameter computed for non-uniform feeder distribution and high loading and no RES injection condition

A₀₂	1.0029 - 0.0016i	B₀₂	1.0938 + 0.1401i
C₀₂	0.0083 - 0.0062i	D₀₂	1.0070 - 0.0040i
A₂₄	1.0031 - 0.0018i	B₂₄	1.1577 + 0.1485i
C₂₄	0.0055 - 0.0041i	D₂₄	1.0039 - 0.0022i
A₄₆	1.0070 - 0.0040i	B₄₆	1.4804 + 0.1893i
C₄₆	0.0066 - 0.0050i	D₄₆	1.0037 - 0.0021i
A₆₈	1.0047 - 0.0026i	B₆₈	1.2866 + 0.1650i
C₆₈	0.0055 - 0.0041i	D₆₈	1.0031 - 0.0018i
A_{8,10}	1.0070 - 0.0040i	B_{8,10}	1.4172 + 0.1806i
C_{8,10}	0.0083 - 0.0062i	D_{8,10}	1.0058 - 0.0033i

Table 5.12: Comparison of calculated and simulated data for non-uniform feeder distribution and heavy loading and no RES injection condition

Node Voltage (in kV)	Calculated Data		Simulation Data	Error (in %)
	Voltage	Voltage Magnitude	Voltage Magnitude	
V₀	8.980	8.982	8.982	0.000
V₁	8.9034 + 0.0413i	8.904	8.903	-0.001
V₂	8.7628 + 0.1144i	8.764	8.763	-0.002
V₃	8.6690 + 0.1632i	8.671	8.670	-0.001
V₄	8.5773 + 0.2103i	8.580	8.580	-0.002
V₅	8.4398 + 0.2809i	8.445	8.444	-0.004
V₆	8.3905 + 0.3060i	8.396	8.396	-0.005
V₇	8.3164 + 0.3437i	8.324	8.323	-0.004
V₈	8.2869 + 0.3587i	8.295	8.295	0.007
V₉	8.2426 + 0.3811i	8.251	8.252	0.007
V₁₀	8.2426 + 0.3811i	8.251	8.252	0.007

5.4 Conclusion

In summary, the chapter presents a detailed discussion on the new ABCD parameter based method for analysing the voltage profile of microgrids and different loading conditions and/or different RES injection conditions. The method has been validated through analytical calculations and simulations using MATLAB Simulink on a small scale radial microgrid with multiple RES and load connections. The comparison of the calculated and simulated values of nodal voltages for different cases and conditions demonstrates the accuracy and efficiency of the presented new analytical method in analysing microgrids with both uniform and non-uniform feeder distributions, as well as various loading and RES injection conditions.

The results of this study indicate that the ABCD parameter-based method can be a valuable tool for researchers and practitioners in the field of microgrid analysis. This method provides an effective approach for predicting nodal voltage and voltage profile in a reliable and efficient manner to operate the microgrid properly, allowing for a high penetration of RES in the existing radial feeder while making minimal alterations in the protection system and avoiding reverse power flow. Future research can expand on this method, applying it to larger and more complex microgrids, contributing to the advancement of microgrid technology and its applications.

Chapter 6

Analysis and Evaluation of Voltage Regulator Quantity and Placement in Radial Microgrid

6.1 General

The nodal voltages and voltage profile of the system have been meticulously analysed for various feeder sectional parametric variations, uniform and non-uniform distributions, loading conditions, and RES injection into the grid. However, due to the different voltage levels at different terminals, it is crucial to regulate and maintain a consistent voltage range throughout the feeder for better voltage profile. The developed analytical tool can further extend direction for location of the installation of the voltage regulator(s) in particular, the DVR. The pressing issue becomes, determining the number of the voltage regulator(s) necessary, their optimal locations, and the required capacity to ensure that the requisite voltage profile and keeping them within a specific limit/range. This chapter delves deeper further into the analysis to identify the suitable course of action to achieve the desired outcomes.

6.2 Location and Number of the voltage regulator(s)

In a microgrid, the optimal location of a voltage regulator is crucial in maintaining a stable voltage profile. This is achieved by considering various factors such as load centres, distance of loads from the regulator, and the voltage profile of the system.

The proposed approach for voltage regulation in a radial microgrid has been identified by using a hybrid combination of OLTC transformers and series voltage regulators, specifically DVRs. OLTC transformers are typically located near the substation to

regulate the voltage at the main feeder. In contrast, DVRs are placed throughout, in a distributed manner, in the feeder to maintain a stable voltage profile.

Keeping in mind the fixed location of the OLTC transformer near the substation the algorithm for finding the location of DVRs, their capacity, and their number is developed. The approach ensures that the voltage profile of the system remains within acceptable limits and reduces the voltage drop, resulting in an efficient and reliable microgrid system.

6.2.1 Algorithm to find the location of the voltage regulator(s)

The proposed approach for determining the suitable number and location of voltage regulators in a distribution system involves the following steps:

Step 1: Calculation of the nodal voltages and branch currents for different conditions, including normal operating condition, light loading and high RES injection condition, and heavy loading and no RES injection condition, using ABCD parameter-based analysis (as discussed in chapter 5).

Step 2: Calculation of the difference between the calculated value of nodal voltage and the rated value of voltage for all these conditions.

Step 3: Starting from the reference node, comparison of the differences with the acceptable difference range is drawn. If the voltage lies within the acceptable range, no further action is needed, but if it falls outside the acceptable range, need for voltage regulator is flagged.

Step 4: Counting the number of conditions for which a voltage regulator is required for each node. If two or more conditions are required to be satisfied, a voltage regulator at that particular node is recommended for the installation. When all the nodes are monitored the algorithm may be terminated for further iterations.

Step 5: After installation of DVR, as per the recommendation and repeating steps 1-4

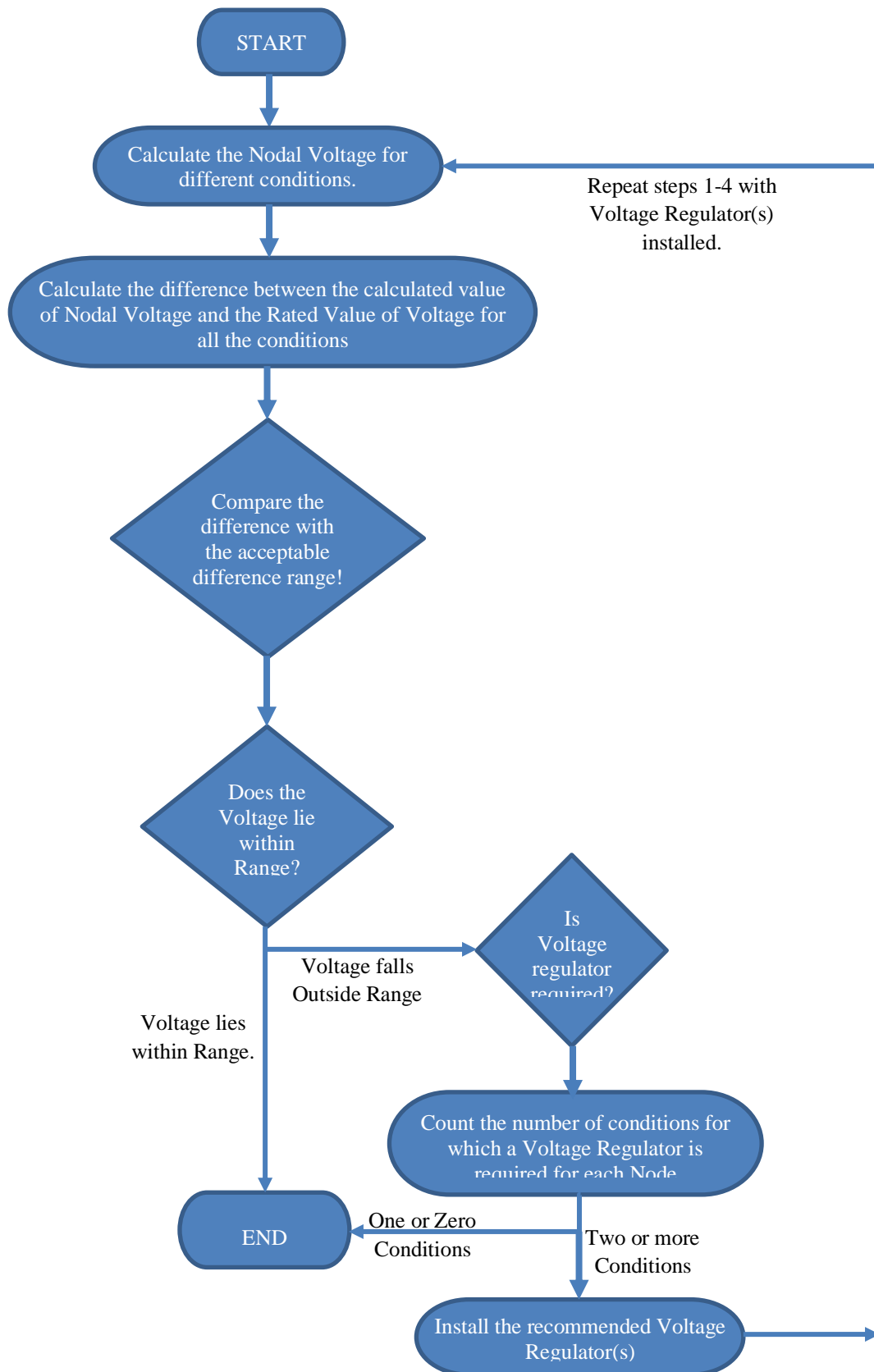


Fig. 6.1: Flowchart to show the location and number of voltage regulator to be installed.

keeping the installation of voltage regulator(s), if the voltage at most of the nodes lies within the acceptable range, and the requirement of the voltage regulator has decreased to one or zero number, the algorithm stands terminated. Otherwise, it goes back to step 1 and repeat the process until the voltage at most of the nodes lies within the acceptable range.

A pictorial representation of the algorithm is shown in Fig. 6.1. By following these steps, the proposed approach can determine the optimal number and location of voltage regulators in a distribution system to maintain a stable voltage profile and ensure efficient and reliable operation under different conditions.

6.3 Capacity of voltage regulator

The capacity of a series connected voltage regulator in a microgrid is an important consideration that should be carefully evaluated to ensure its capability of operating in odds and adequately meeting the voltage regulation requirements of the system. Algorithm involving following steps are considered to determine the capacity of a voltage regulator in service:

Step 1: Determining the maximum and minimum voltage levels permissible in the microgrid. This can be done through a power flow analysis or by measuring the voltage levels at various points in the system. In the considered scenario ABCD based analysis has been used to determine the maximum and minimum voltage range in the microgrid.

Step 2: Calculating the voltage drop/rise that occurs at the node under consideration during the occurrence of maximum and minimum voltage levels. This gives an idea about the range of voltage regulation required to maintain a stable and reliable voltage at the terminal and also in the microgrid.

Step 3: Capability of voltage regulator by regulating the voltage levels within the desired range and is sufficient to handle the maximum expected load and/or any voltage/current fluctuations in the system.

Capacity of OLTC transformer is calculated in similar way as the capacity of the distribution transformer and does not require much special attention. However, the finer are the number of steps the capacity of DVR will accordingly be reduced. The capacity of a distribution transformer is typically expressed in terms of its kVA/MVA rating. To determine the appropriate rating for a distribution transformer, following key factors are to be considered:

- **Load demand:** The rating of the distribution transformer should be sufficient to meet the expected load demand of the electrical system it is serving. This can be estimated based on factors such as the number and type of electrical devices that will be connected to the system, as well as their power ratings and usage patterns.
- **Voltage drop:** The rating of the distribution transformer should also take into account to avert the voltage drop that may occur across the electrical system due to their switching into and out of the circuit. This can be estimated based on factors such as the length of the distribution lines and the resistance and impedance of the system components.
- **Power factor:** The rating of the distribution transformer is also considered for the operating power factor of the connected electrical load.

Once these factors are considered, the appropriate kVA/MVA rating for the distribution transformer is determined using standard formulas and guidelines for power system design. It is typically recommended to oversize the rating of the distribution transformer by a certain percentage (e.g. 10-20%) to provide additional

capacity for future load growth and to ensure reliable operation of the electrical system.

Since number of DVRs are to be installed throughout the feeder, in distributed manner, their capacity calculation is designed very much required before their installation. It should be such that they regulate the voltage at their output terminals. With already known maximum voltage range deviation that may occur at the node where voltage regulator is to be installed, the compensation is derived accordingly, and capacity may thus be drawn.

Let V_i be the voltage at the terminal and V_{DVR} be the voltage injected or absorbed by the DVR. The new resultant voltage at the terminal (PCC of DVR) is given by equation (6.1):

$$V_{i_{new}} = V_i + V_{DVR} \quad (6.1)$$

Assuming the DVR maintains the voltage to the rated value after regulation, the magnitude of the new terminal voltage is equal to the rated voltage magnitude, which can be expressed as:

$$\begin{aligned} |V_{i_{new}}| &= V_{rated} \\ \Rightarrow |V_{i_{new}}| &= |V_i + V_{DVR}| \end{aligned} \quad (6.2)$$

This equation can be transformed into d-axis and q-axis components by synchronous reference frame theory, resulting in Equation (6.3):

$$\left| (V_{i_d} + jV_{i_q}) + (V_{DVR_d} + jV_{DVR_q}) \right| = V_{rated} \quad (6.3)$$

To determine the voltage injected or absorbed by the DVR, the next step is to apply the appropriate control strategy. Usually, the DVR can only inject or absorb reactive power, although certain control schemes may also involve real power injection or absorption. The actual amount of injection or absorption will vary depending on the

specific type of control utilized.

Computation of DVR voltage through injection/absorption of reactive power alone:

As voltage regulation is mainly achieved through the reactive power by the DVR, the d-axis component of the voltage regulator becomes zero ($V_{VRd} = 0$). Therefore, equation (6.3) is modified as:

$$\left| (V_{i_d} + jV_{i_q}) + (jV_{DVRq}) \right| = V_{rated} \quad (6.4)$$

To compute the value of voltage required by the voltage regulator to regulate the voltage, equation (6.4) can be solved as follow:

$$\sqrt{(V_{i_d})^2 + (V_{i_q} + V_{DVRq})^2} = V_{rated}$$

Squaring both the sides,

$$\Rightarrow (V_{i_d})^2 + (V_{i_q} + V_{DVRq})^2 = (V_{rated})^2$$

$$\Rightarrow (V_{i_d})^2 + (V_{i_q})^2 + (V_{DVRq})^2 + 2V_{i_q}V_{DVRq} = (V_{rated})^2$$

$$\Rightarrow (V_{DVRq})^2 + 2V_{i_q}V_{DVRq} + \left((V_{i_d})^2 + (V_{i_q})^2 \right) - (V_{rated})^2 = 0$$

$$\Rightarrow (V_{DVRq})^2 + 2V_{i_q}V_{DVRq} + |V_i|^2 - (V_{rated})^2 = 0$$

$$\Rightarrow V_{DVRq} = \frac{-2V_{i_q} \pm \sqrt{(2V_{i_q})^2 - 4(|V_i|^2 - (V_{rated})^2)}}{2}$$

$$\Rightarrow V_{DVRq} = -V_{i_q} \pm \sqrt{(V_{i_q})^2 - (|V_i|^2 - (V_{rated})^2)} \quad (6.5)$$

Computation of DVR voltage through injection/absorption with both real and reactive power:

When the compensation is done with both real and reactive power, the system assumes that 'x' percent of compensation/regulation is done with the reactive component, and

the remaining is done with the real power. Equation (6.3) is modified accordingly:

$$\left| (V_{i_d} + jV_{i_q}) + (x \cdot V_{DVR} + j\sqrt{100^2 - x^2} \cdot V_{DVR}) \right| = V_{rated}$$

Solving it to find the value of V_{DVR}

$$\Rightarrow \left| (V_{i_d} + x \cdot V_{DVR}) + j \left(V_{i_q} + \sqrt{100^2 - x^2} \cdot V_{DVR} \right) \right| = V_{rated}$$

$$\Rightarrow \sqrt{(V_{i_d} + x \cdot V_{DVR})^2 + \left(V_{i_q} + \sqrt{100^2 - x^2} \cdot V_{DVR} \right)^2} = V_{rated}$$

$$\Rightarrow (V_{i_d} + x \cdot V_{DVR})^2 + \left(V_{i_q} + \sqrt{100^2 - x^2} \cdot V_{DVR} \right)^2 = V_{rated}^2$$

$$\Rightarrow (V_{i_d})^2 + (x \cdot V_{DVR})^2 + 2xV_{i_d}V_{DVR} + (V_{i_q})^2 + \left(\sqrt{100^2 - x^2} \cdot V_{DVR} \right)^2$$

$$+ 2\sqrt{100^2 - x^2} \cdot V_{i_q}V_{DVR} = V_{rated}^2$$

$$\Rightarrow |V_i|^2 + 100^2(V_{DVR})^2 + 2 \left(xV_{i_d} + \sqrt{100^2 - x^2}V_{i_q} \right) V_{DVR} - V_{rated}^2 = 0$$

$$\Rightarrow 100^2(V_{DVR})^2 + 2 \left(xV_{i_d} + \sqrt{100^2 - x^2}V_{i_q} \right) V_{DVR} + |V_i|^2 - V_{rated}^2 = 0$$

$$\Rightarrow V_{DVR} = \frac{-2 \left(xV_{i_d} + \sqrt{100^2 - x^2}V_{i_q} \right) \pm \sqrt{\left(2 \left(xV_{i_d} + \sqrt{100^2 - x^2}V_{i_q} \right) \right)^2 - 4(100)^2(|V_i|^2 - V_{rated}^2)}}{2(100)^2}$$

$$\Rightarrow V_{DVR} = \frac{- \left(xV_{i_d} + \sqrt{100^2 - x^2}V_{i_q} \right) \pm \sqrt{\left(xV_{i_d} + \sqrt{100^2 - x^2}V_{i_q} \right)^2 - (100)^2(|V_i|^2 - V_{rated}^2)}}{(100)^2} \quad (6.6)$$

Once the voltage required to regulate the voltage in various conditions, such as normal operating condition, light loading and high RES injection, heavy loading and no RES injection, is known, the maximum value among them is selected. This maximum value can then be used to calculate the capacity of the DVR.

Similarly, the current flowing through the DVR must be calculated for all three

conditions using the ABCD based method discussed in Chapter 5. The maximum value should be selected, and the capacity of the DVR is given by Equation (6.6):

Capacity of DVR (in kVA) = $\sqrt{3}$ x Maximum voltage required to regulate the voltage at the terminal of DVR (in kV) x Maximum current flowing through the DVR (in A)

$$S_{DVR} = \sqrt{3}|V_{n_{DVR}}| \cdot I_{i-1,i} \quad (6.6)$$

Step 4: Evaluating the performance of the selected voltage regulator through simulation or testing to ensure that it meets the voltage regulation requirements of the microgrid. If necessary, the capacity of the voltage regulator is adjusted to better match the load requirements of the system. This may involve adding additional regulators or upgrading the capacity of existing regulators.

It's important to note that the capacity of a voltage regulator may need to be periodically re-evaluated as the load and operating conditions of the microgrid changes over time. Consistent monitoring and analysis are essential to maintain the long-term effectiveness and reliability of the system's voltage regulation.

6.4 11-Node Radial Microgrid: Case Study

The above developed algorithm is validated on an 11 node radial microgrid as considered in chapters with intermittent renewable energy sources (RES). Computation on the considered system and implementation of the obtained results through simulation are carried out to determine the voltage profile of the microgrid, ensuring the algorithm's suitability for deriving the number and location of voltage regulators, along with the capacity of OLTC-T and distributed DVRs in a radial microgrid. The system under consideration and the basic simulation diagram without any voltage regulator for the 11 node radial microgrid are the same as those presented in the previous chapter, and shown in Fig. 5.4 and Fig. 5.5, respectively both for

uniform feeder distribution and non-uniform feeder distribution.

Case 1: Uniform feeder distribution

Same system parameters, connected loads, RES injections are considered as has been done in the previous chapter for uniform feeder distribution conditions. The algorithm is applied to find out the numbers, locations and capacities of the DVRs. Importing the data from Table 5.1 -5.3 of chapter 5 for the nodal voltages, measuring the error at each nodal voltage from the rated voltage more than the desired range by 3% the algorithm is considered. Table 6.1 list the voltage magnitude, their difference from rated value and requirement of voltage regulator at that node. Studying all the three conditions in Table 6.1 it can be seen that the requirement of first voltage regulator emerges for two conditions at node 4, accordingly first DVR is identified to be placed between node 3 and node 4. The capacity of the voltage regulator can be calculated as:

$$V_{4max} = 9.3260 + 0.1240i \text{ kV}$$

$$V_{4min} = 8.3532 + 0.3179i \text{ kV}$$

Maximum current flowing through the DVR obtained from the ABCD based analysis

$$I_{max} = \max(9.77 - 62.89i, 167.29 - 111.92i, -128.28 - 22.9i)$$

$$I_{max} = 167.29 - 111.92i \text{ A}$$

$$|I_{max}| = 201.27 \text{ A}$$

$$V_{DVR} = j 2561.2 \text{ V (peak value)}$$

Capacity of voltage regulator computed as per equation (6.6) is given by:

$$V_{DVR} = 0.63 \text{ MVA}$$

Thus a DVR of this rating should be installed to get voltage regulation in all the cases.

In the current setup, the capacity calculation is on the higher side since it relies solely on reactive power for regulation. However, if we integrate a battery into the DC link of the DVR, we can enhance its performance by providing real power support. This

improvement can be achieved with a lower capacity requirement.

Table 6.1: Difference in nodal voltage from the reference voltage without voltage regulator in uniform distribution feeder

Nodal Voltage (in kV)	Rated Load and I _{RES} = 20 A			Light Load and I _{RES} = 40 A			Heavy Load and I _{RES} = 0 A		
	Mag.	Error	VR Req.	Mag.	Error	VR Req.	Mag.	Error	VR Req.
V0	8.982	0	0	8.982	0	0	8.982	0	0
V1	8.941	0.449	0	9.073	-1.024	0	8.784	2.198	0
V2	8.922	0.661	0	9.172	-2.127	0	8.628	3.929	1
V3	8.89	1.012	0	9.246	-2.946	0	8.474	5.652	1
V4	8.88	1.131	0	9.326	-3.845	1	8.359	6.928	1
V5	8.856	1.391	0	9.382	-4.457	1	8.245	8.199	1
V6	8.854	1.42	0	9.444	-5.152	1	8.169	9.039	1
V7	8.838	1.591	0	9.481	-5.562	1	8.094	9.876	1
V8	8.843	1.533	0	9.525	-6.052	1	8.057	10.293	1
V9	8.836	1.332	0	9.543	-6.829	1	8.019	10.709	1
V10	8.849	1.475	0	9.569	-6.542	1	8.019	10.709	1

Two condition calls for installation of DVR

When a DVR with adequate capacity is installed between nodes 3 and 4, and the entire process is repeated to identify the requirement of another voltage regulator and its location. Table 6.2 lists the data after the second iteration, and it is identified that another voltage regulator needs to be installed near node 6. The capacity of the voltage regulator in this case also be calculated in the similar manner as done before installing one voltage regulator.

Subsequently, two DVRs are installed respectively at, between node '3' and '4' and between node '5' and '6', the process is repeated again to gauge the further requirement of DVRs and their locations. The data obtained in the third iteration are listed in Table 6.3, demonstrating that the voltage at most nodes has been brought closer to the acceptable range. Thus the process comes to end after this iteration.

Table 6.2: Difference in nodal voltage from the rated voltage with one voltage regulator installed in uniform distribution feeder

Node Voltage (in kV)	Rated Load and $I_{RES} = 20 \text{ A}$			Light Load and $I_{RES} = 40 \text{ A}$			Heavy Load and $I_{RES} = 0 \text{ A}$		
	Mag.	Error	VR Req.	Mag.	Error	VR Req.	Mag.	Error	VR Req.
V0	8.982	0	0	8.982	0	0	8.982	0	0
V1	8.941	0.456	0	9.072	-1.003	0	8.773	2.32367	0
V2	8.921	0.677	0	9.169	-2.087	0	8.606	4.18304	1
V3	8.949	0.367	0	9.097	-1.285	0	8.82	1.80037	0
V4	8.937	0.491	0	9.179	-2.195	0	8.7	3.12977	1
V5	8.914	0.756	0	9.235	-2.817	0	8.582	4.45249	1
V6	8.911	0.788	0	9.298	-3.518	1	8.503	5.32762	1
V7	8.895	0.964	0	9.335	-3.933	1	8.425	6.19941	1
V8	8.9	0.907	0	9.379	-4.427	1	8.386	6.63364	1
V9	8.892	0.995	0	9.398	-4.633	1	8.347	7.06675	1
V10	8.905	0.852	0	9.424	-4.921	1	8.347	7.06675	1

Two condition calls for installation of DVR

Table 6.3: Difference in nodal voltage from the rated voltage with two voltage regulator installed in uniform distribution feeder

Node Voltage (in kV)	Rated Load and $I_{RES} = 20 \text{ A}$			Light Load and $I_{RES} = 40 \text{ A}$			Heavy Load and $I_{RES} = 0 \text{ A}$		
	Mag.	Error	VR Req.	Mag.	Error	VR Req.	Mag.	Error	VR Req.
V0	8.982	0	0	8.982	0	0	8.982	0	0
V1	8.94	0.461	0	9.072	-1.01	0	8.757	2.495	0
V2	8.92	0.686	0	9.17	-2.099	0	8.575	4.529	1
V3	8.947	0.383	0	9.056	-0.834	0	9.041	-0.664	0
V4	8.936	0.511	0	9.139	-1.749	0	8.911	0.786	0
V5	8.911	0.78	0	9.195	-2.376	0	8.781	2.232	0
V6	8.908	0.817	0	9.258	-3.083	1	8.692	3.22	1
V7	8.965	0.186	0	9.046	-0.718	0	9.118	-1.522	0
V8	8.97	0.131	0	9.091	-1.216	0	9.076	-1.053	0
V9	8.962	0.22	0	9.11	-1.425	0	9.03	-0.585	0
V10	8.975	0.077	0	9.135	-1.712	0	9.034	-0.585	0

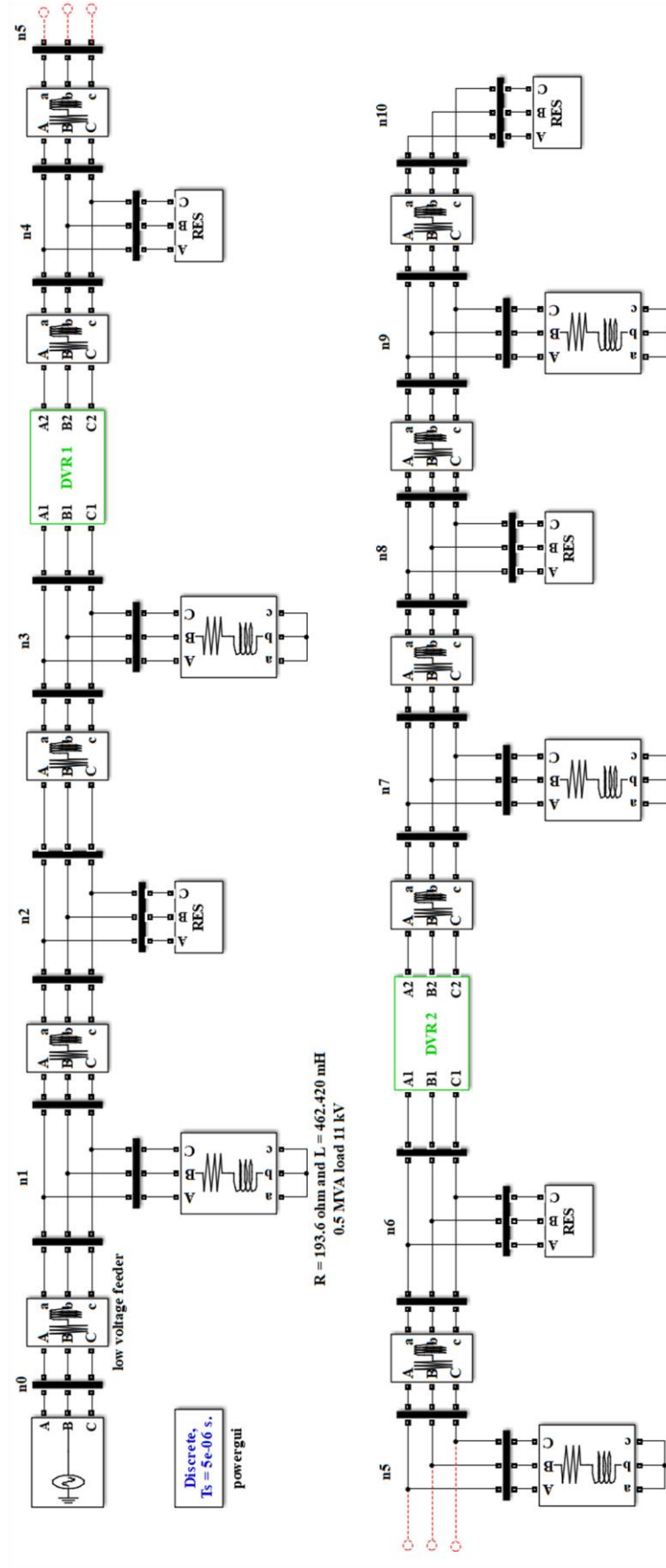


Fig. 6.2: Simulation diagram for 11 node radial microgrid with intermittent renewable energy sources with 2 DVR connected

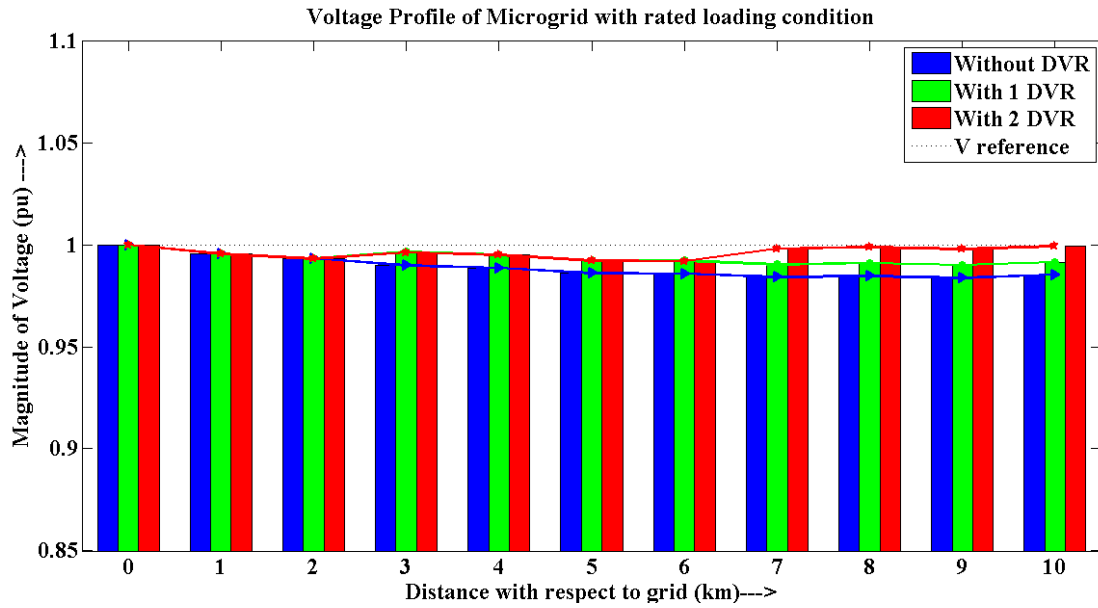


Fig. 6.3: Voltage profile of uniform feeder 11 node radial microgrid with RES connected under normal operating conditions

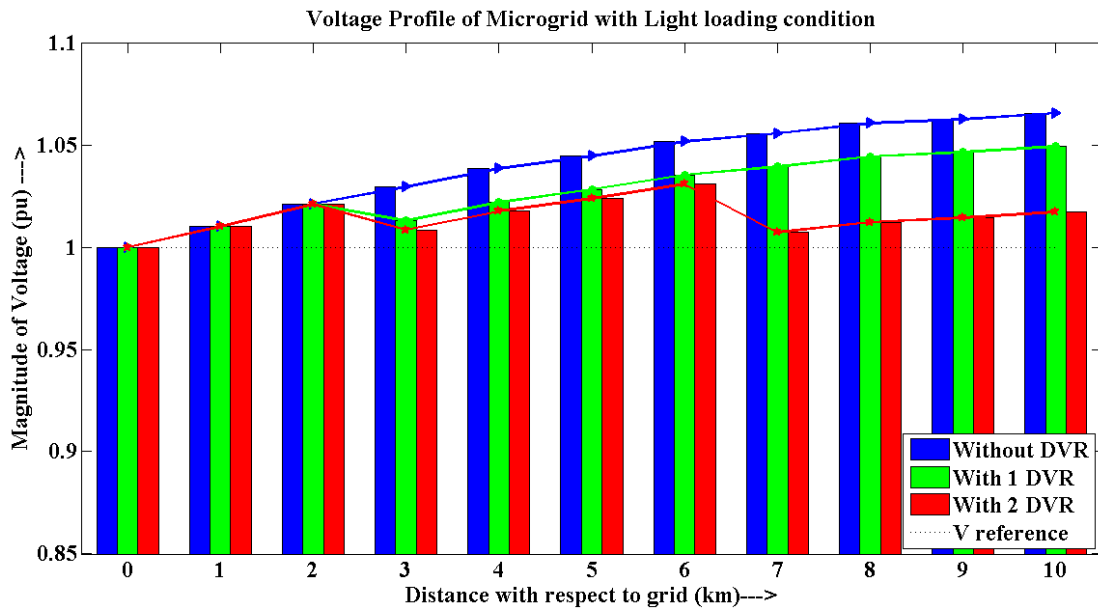


Fig. 6.4: Voltage profile of uniform feeder 11 node radial microgrid with RES connected under light load condition and high RES injection

After determining the optimal number and location of the voltage regulators through theoretical analysis, the system was simulated with the same parameters as before, but with the addition of two dynamic voltage restorers. The simulation diagram is presented in Fig. 6.2, while Fig. 6.3, Fig. 6.4, and Fig. 6.5 display the voltage profile

of the system under normal operating conditions, light loading and high RES current injection, and heavy loading and no RES current injection, respectively.

These voltage profiles clearly demonstrate that the installation of the dynamic voltage restorers in the feeder has significantly improved its voltage profile.

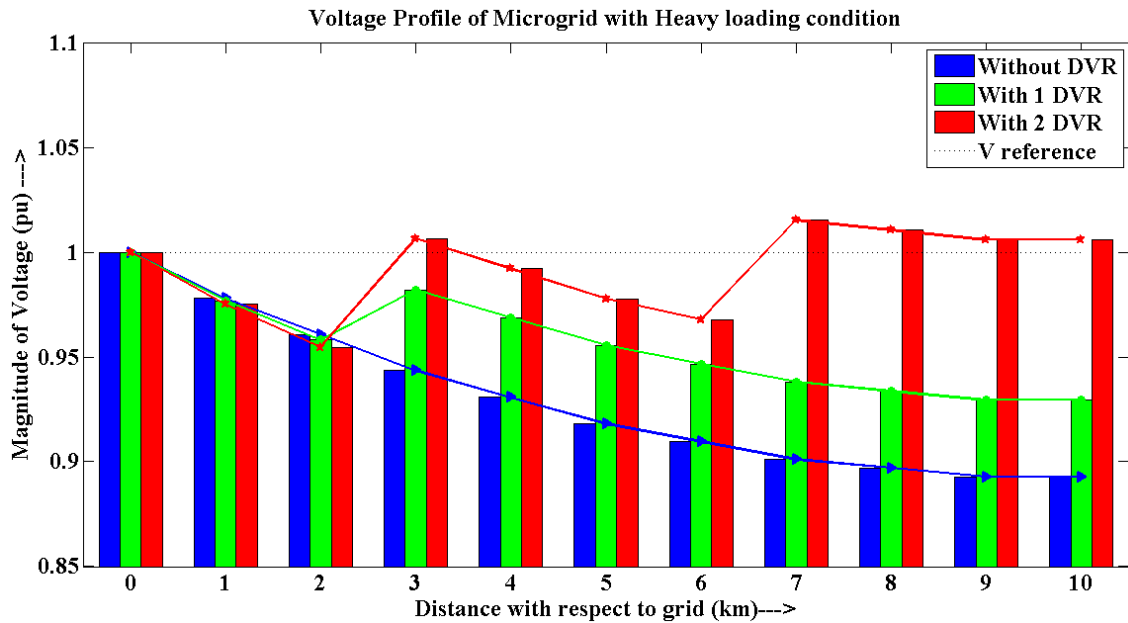


Fig. 6.5: Voltage profile of uniform feeder 11 node radial microgrid with RES connected under heavy loading and no RES injection

Case 2: Non uniform feeder distribution.

A similar approach was utilized to determine the locations and number of voltage regulators in a non-uniform distribution feeder. As noted in Table 5.4, Table 5.7, and Table 5.10, the system parameters were consistent with those used in the previous chapter for all operating conditions, while nodal voltages were obtained from Table 5.6, Table 5.9, and Table 5.12. These values are then employed to calculate deviations from the rated value for all conditions, enabling identification of the required voltage regulator as presented in Table 6.4.

Optimization of voltage regulator location led to placement of first DVR between

nodes 3 and 4. After installation of the voltage regulator, the process is repeated and results are reported in Table 6.5. These results indicate the need for the next voltage regulator after node 6. Subsequently, the ABCD-based algorithm is used again, and Table 6.6 shows that almost all nodes' voltage are within acceptable limits, thus concluding the process.

Once the voltage regulators are positioned on the identified locations, a MATLAB simulation is performed, with the same diagram as the previous case shown in Fig. 6.2. Simulation results are utilized to develop voltage profiles of the microgrid under different operating conditions, indicating a significant shift after voltage regulator installation at the estimated locations in the considered 11 node radial microgrid.

Table 6.4: Difference in nodal voltage from the rated voltage without voltage regulator installed in non-uniform distribution feeder

Node Voltage (in kV)	Rated Load and $I_{RES} = 20$ A			Light Load and $I_{RES} = 40$ A			Heavy Load and $I_{RES} = 0$ A		
	Mag.	Error	VR Req.	Mag.	Error	VR Req.	Mag.	Error	VR Req.
V0	8.982	0.000	0	8.982	0.000	0	8.982	0.000	0
V1	8.960	0.238	0	9.028	-0.519	0	8.904	0.868	0
V2	8.941	0.455	0	9.151	-1.885	0	8.764	2.427	0
V3	8.919	0.700	0	9.214	-2.590	0	8.671	3.462	1
V4	8.909	0.811	0	9.299	-3.539	1	8.580	4.472	1
V5	8.873	1.211	0	9.385	-4.491	1	8.445	5.979	1
V6	8.870	1.239	0	9.436	-5.064	1	8.396	6.518	1
V7	8.851	1.452	0	9.483	-5.580	1	8.324	7.326	1
V8	8.852	1.440	0	9.519	-5.979	1	8.295	7.647	1
V9	8.858	1.371	0	9.582	-6.681	1	8.251	8.129	1
V10	8.847	1.500	0	9.558	-6.423	1	8.251	8.129	1

Two condition calls for installation of DVR

Table 6.5: Difference in nodal voltage from the rated voltage with one voltage regulator installed in non-uniform distribution feeder

Node Voltage (in kV)	Rated Load and $I_{RES} = 20$ A			Light Load and $I_{RES} = 40$ A			Heavy Load and $I_{RES} = 0$ A		
	Mag.	Error	VR Req.	Mag.	Error	VR Req.	Mag.	Error	VR Req.
V0	8.982	0.000	0	8.982	0.000	0	8.982	0.000	0
V1	8.959	0.247	0	9.027	-0.501	0	8.901	0.897	0
V2	8.938	0.488	0	9.145	-1.823	0	8.755	2.525	0
V3	8.958	0.265	0	9.042	-0.678	0	8.886	1.068	0
V4	8.946	0.393	0	9.126	-1.610	0	8.793	2.102	0
V5	8.908	0.819	0	9.209	-2.534	0	8.654	3.649	1
V6	8.904	0.860	0	9.259	-3.091	1	8.604	4.202	1
V7	8.883	1.092	0	9.303	-3.581	1	8.530	5.029	1
V8	8.884	1.086	0	9.337	-3.960	1	8.501	5.349	1
V9	8.867	1.276	0	9.354	-4.151	1	8.457	5.842	1
V10	8.879	1.147	0	9.378	-4.410	1	8.457	5.842	1

Two condition calls for installation of DVR

Table 6.6: Difference in nodal voltage from the rated voltage with two voltage regulator installed in non-uniform distribution feeder

Node Voltage (in kV)	Rated Load and $I_{RES} = 20$ A			Light Load and $I_{RES} = 40$ A			Heavy Load and $I_{RES} = 0$ A		
	Mag.	Error	VR Req.	Mag.	Error	VR Req.	Mag.	Error	VR Req.
V0	8.982	0.000	0	8.982	0.000	0	8.982	0.000	0
V1	8.959	0.251	0	9.027	-0.503	0	8.899	0.924	0
V2	8.937	0.497	0	9.146	-1.832	0	8.747	2.616	0
V3	8.957	0.278	0	9.046	-0.723	0	8.881	1.115	0
V4	8.944	0.413	0	9.131	-1.661	0	8.784	2.202	0
V5	8.906	0.846	0	9.214	-2.593	0	8.638	3.828	1
V6	8.901	0.892	0	9.265	-3.153	1	8.584	4.425	1
V7	8.959	0.251	0	9.027	-0.503	0	8.899	0.917	0
V8	8.960	0.245	0	9.061	-0.886	0	8.869	1.249	0
V9	8.942	0.439	0	9.079	-1.080	0	8.823	1.765	0
V10	8.954	0.310	0	9.102	-1.339	0	8.823	1.765	0

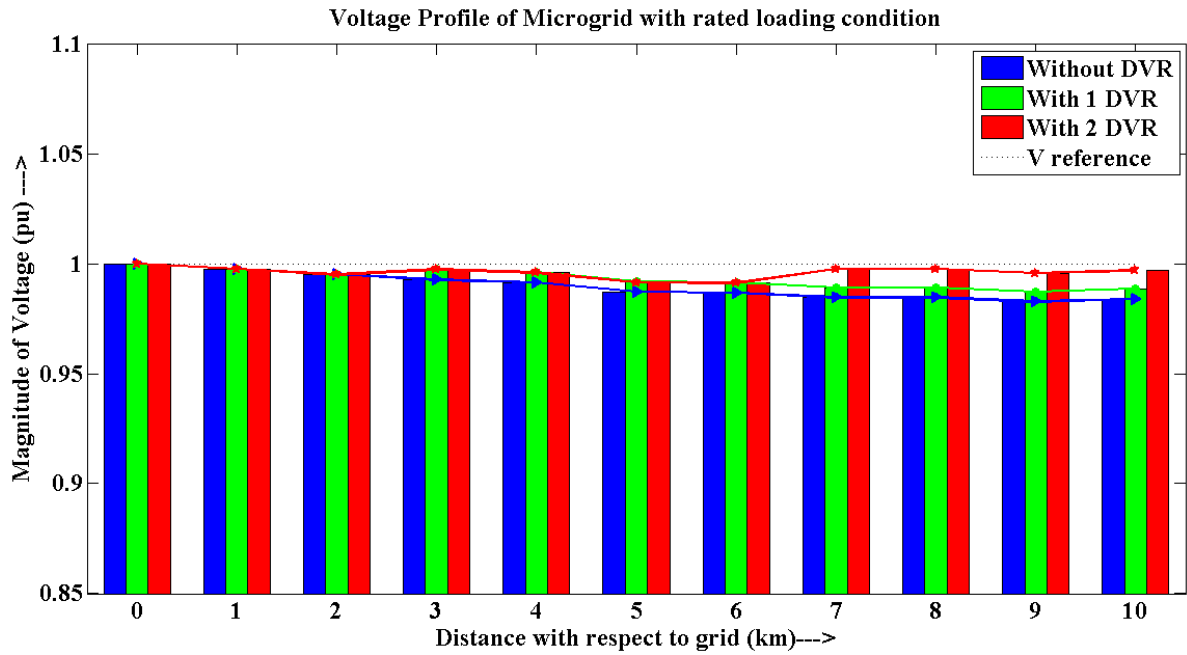


Fig. 6.6: Voltage profile of non-uniform feeder 11 node radial microgrid with RES connected under normal operating conditions

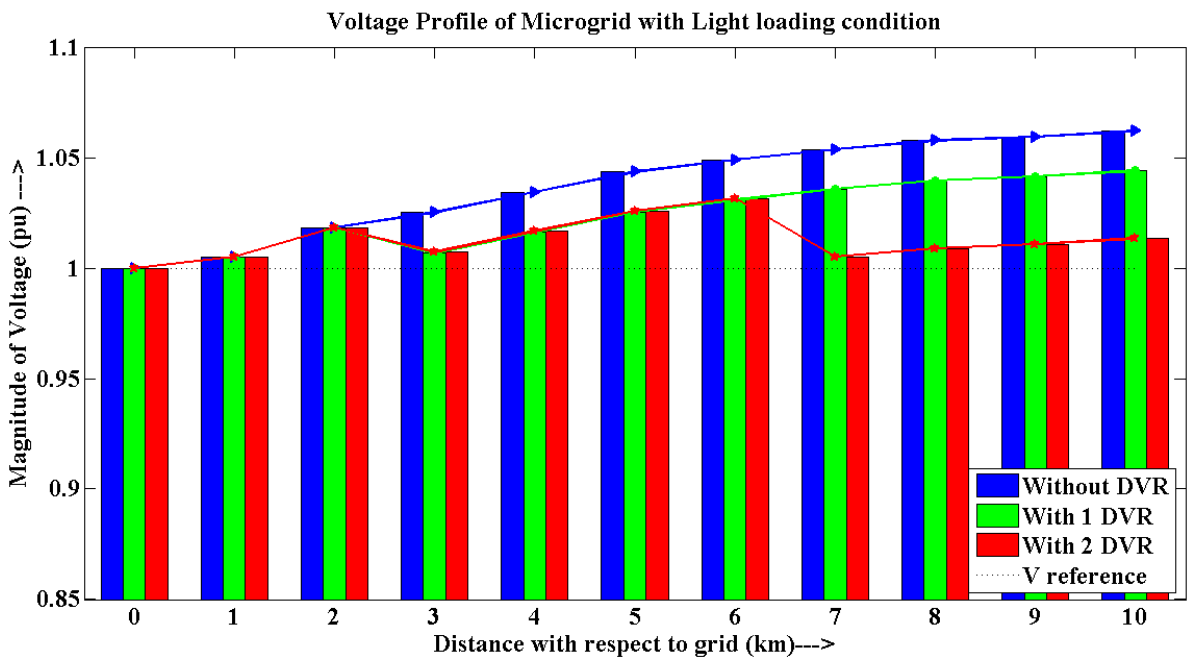


Fig. 6.7: Voltage profile of non-uniform feeder 11 node radial microgrid with RES connected under light loading and high RES condition

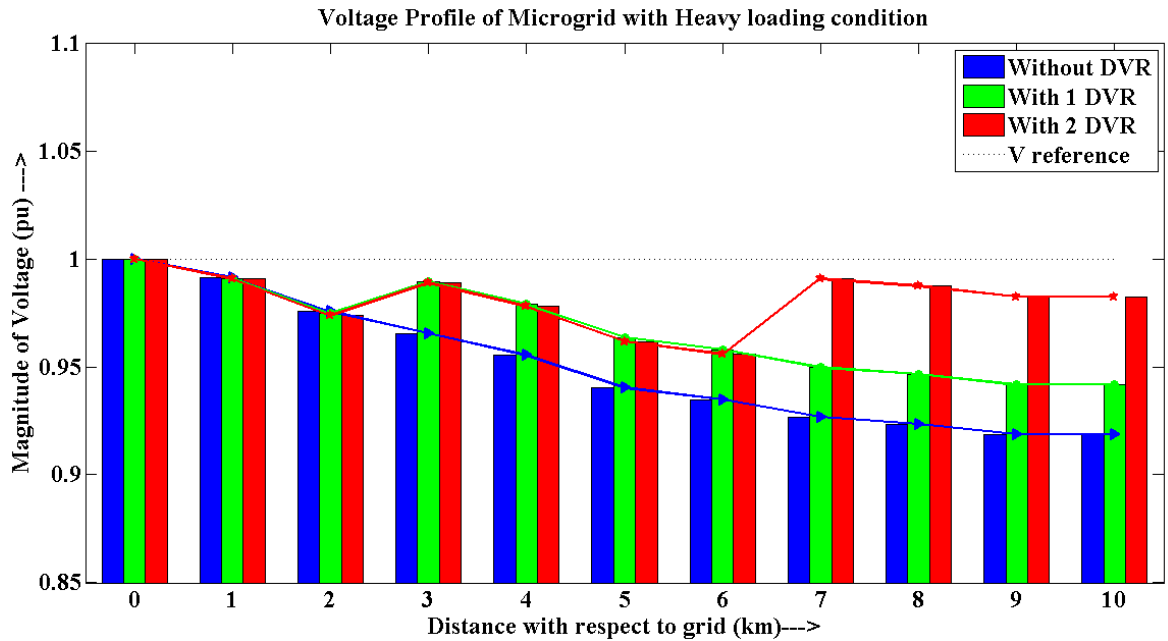


Fig. 6.8: Voltage profile of non-uniform feeder 11 node radial microgrid with RES connected under heavy loading and no RES injection

6.5 Conclusion

Application of developed ABCD based algorithm is successfully demonstrated and shown effective for determining the optimal number, location, and capacity of distributed voltage regulators for a given power of the distribution feeder with RES. The voltage profile drawn through obtained simulation results demonstrated that the chosen location, number and capacity of the voltage regulators were effective in improving the overall voltage profile of the radial microgrid. The potential practical implications of the findings are significant, as the ABCD-based method offers a valuable tool for power distribution system designers and operators to optimize number of voltage regulators and their effective location, typically in radial feeder highly populated with intermittent RES.

Chapter 7

MAIN CONCLUSION AND FUTURE SCOPE OF WORK

7.1 Main Conclusion

The main conclusions of the thesis and the research work conducted are:

- Based on the comprehensive investigation presented in this thesis, it can be concluded that integrating intermittent renewable energy sources (RES) into microgrids and distribution systems presents numerous benefits, but also poses several challenges that need to be addressed. One of the major challenges is the voltage issues that arise due to the intermittent nature and high penetration levels of RES. Therefore, the installation of voltage regulators in the distribution system/microgrid is important.
- There are different types of voltage regulators available which are generally installed in the distribution system, such as OLTC transformers, STATCOM, BESS, and DVR. After performing a detailed analysis and performance evaluation under different conditions like RES intermittency, load perturbation, and source voltage perturbation, it has been identified that the OLTC and DVR are suitable choices for voltage regulation in the radial microgrid or the distribution system with a high penetration of RES.
- Though individually they have certain drawbacks, their hybrid combination controlled through an autonomous yet coordinated control developed on the basis of I_d/I_q ratio has overcome them. The performance of the duo under

different conditions has been well demonstrated through the simulation results and the voltage profile drawn in chapter 4.

- The application of smart GCI inverters also adds to the beauty of the duo by providing an even more extensive range of regulation by operating in MPPT mode as well as the deloading mode. This is very well demonstrated from the simulation results shown for two extreme conditions of light loading along with the overvoltage at the source side and another condition being under voltage. Overall, their ability to work in unison improves the microgrid's performance and ensures efficient power distribution. The hybrid voltage regulators discussed offer a promising solution for voltage regulation in microgrids.
- As the system grows and the number of RES connected to the radial microgrid increases, the proposed ABCD-based method for the calculation of different node voltage under uniform and non-uniform feeder distribution has been proved to be a great tool as demonstrated through the comparison of computed and simulated data on an 11-node radial microgrid with a number of loads and RES connected to it. This has been done for various loading and RES injection conditions.
- Later, the extended ABCD parameter-based analysis is proposed to determine the number of connected voltage regulators and their location within the radial microgrid. The proposed algorithm is well-justified through the simulation as when the computed location and number of voltage regulators are placed in the considered 11-node radial microgrid, it provided a satisfactory voltage profile.

Overall, the thesis highlights the benefits and challenges of integrating intermittent renewable energy sources into microgrids and distribution systems. The proposed hybrid voltage regulator and ABCD-based method provide promising solutions for voltage regulation and calculation of different node voltage, respectively, in microgrids with high penetration of RES.

7.2 Future Scope of Work

The analysis and application of voltage regulators in radial microgrids presented in the thesis offer a lot of scope for the future such as:

- **Multi-objective optimization:** The extension of the developed ABCD parameter-based analysis with the multi objective optimization can yield even more accurate results for finding locations, numbers and capacities of the distributed VRs. Future research could focus on developing multi-objective optimization methods for number, type, locations and capacity of multimode compensators that can simultaneously optimize voltage regulation, power quality, and economic factors in microgrids with high RES penetration.
- **Advanced modelling and simulation:** Although the thesis present simulation results under various operating conditions, there is still room for developing more advanced models for profiling of radial microgrid populated with intermittent RES and distributed compensators with perturbing loads. Future research is needed to evaluate the effectiveness of the ABCD parameters - based method on parametric variations since the environmental conditions may alter parameters largely, besides variety of loads including non-linear loads.

- Field testing and validation: While simulation is a useful tool for evaluating the performance of voltage regulation on the developed models, there is a need for field testing and validation of the technique in real-world microgrid to assess their effectiveness and feasibility. Future research could focus on developing field testing protocols and evaluating the performance of voltage regulation techniques under real-world conditions.
- The analytical tool that has been developed is highly versatile and can serve multiple purposes. Distribution system operators can make use of it for the efficient management of feeders, while it can also be employed in smart grids for regulating the voltage across various nodes and achieving centralized control over renewable energy sources injection into the feeder.

References

- [1] Press Information Bureau Government of India <https://pib.gov.in/>
- [2] Ministry of New and Renewable Energy <https://www.mnre.gov.in>
- [3] J. Xie, I. Alvarez-Fernandez and W. Sun, "A Review of Machine Learning Applications in Power System Resilience," 2020 IEEE Power & Energy Society General Meeting (PESGM), Montreal, QC, Canada, 2020, pp. 1-5, doi: 10.1109/PESGM41954.2020.9282137. qq`
- [4] M. S. Alam, F. S. Al-Ismaïl, A. Salem and M. A. Abido, "High-Level Penetration of Renewable Energy Sources Into Grid Utility: Challenges and Solutions," in IEEE Access, vol. 8, pp. 190277-190299, 2020, doi: 10.1109/ACCESS.2020.3031481.
- [5] Kaushik, Ekata, Vivek Prakash, Om Prakash Mahela, Baseem Khan, Adel El-Shahat, and Almoataz Y. Abdelaziz. 2022. "Comprehensive Overview of Power System Flexibility during the Scenario of High Penetration of Renewable Energy in Utility Grid," *Energies*, vol. 15, no. 2: 516, 2022, doi: <https://doi.org/10.3390/en15020516>
- [6] Hossain, Md. Shouquat, Naseer Abboodi Madloul, Ali Wadi Al-Fatlawi, and Mamdouh El Haj Assad. 2023. "High Penetration of Solar Photovoltaic Structure on the Grid System Disruption: An Overview of Technology Advancement" *Sustainability*, vol. 15, no. 2: 1174, doi: <https://doi.org/10.3390/su15021174>
- [7] M. W. Altaf, M. T. Arif, S. N. Islam and M. E. Haque, "Microgrid Protection Challenges and Mitigation Approaches—A Comprehensive Review," in IEEE Access, vol. 10, pp. 38895-38922, 2022, doi: 10.1109/ACCESS.2022.3165011.
- [8] M. Jayachandran, K. Prasada Rao, Ranjith Kumar Gatla, C. Kalavani, C. Kalaiarasy, C. Logasabarirajan, "Operational concerns and solutions in smart electricity distribution systems," *Utilities Policy*, vol. 74, 2022, 101329, doi: <https://doi.org/10.1016/j.jup.2021.101329>.
- [9] D. Stanelytè and V. Radziukynas, "Analysis of Voltage and Reactive Power Algorithms in Low Voltage Networks," *Energies*, vol. 15, no. 5, p. 1843, Mar. 2022, doi: 10.3390/en15051843.
- [10] J. von Appen, M. Braun, T. Stetz, K. Diwold and D. Geibel, "Time in the Sun: The Challenge of High PV Penetration in the German Electric Grid," in IEEE Power and Energy Magazine, vol. 11, no. 2, pp. 55-64, March-April 2013, doi: 10.1109/MPE.2012.2234407.
- [11] Semich Impram, Secil Varbak Nese, and Bülent Oral, "Challenges of renewable energy penetration on power system flexibility: A survey," *Energy Strategy Reviews*, vol. 31, 2020, 100539, doi: <https://doi.org/10.1016/j.esr.2020.100539>.
- [12] Muhammad Shahzad Javed, Tao Ma, Jakub Jurasz, and Muhammad Yasir Amin, "Solar and wind power generation systems with pumped hydro storage: Review and future perspectives," *Renewable Energy*, vol. 148, 2020, pp. 176-192, doi: <https://doi.org/10.1016/j.renene.2019.11.157>.
- [13] Mlilo, N., Brown, J. and Ahfock, T, "Impact of intermittent renewable energy generation penetration on the power system networks – A review," *Technology and Economics of Smart Grids and Sustainable Energy*, vol. 6, no. 25 (2021), doi: <https://doi.org/10.1007/s40866-021-00123-w>.
- [14] Pavlos S. Georgilakis, "Technical challenges associated with the integration of wind

- power into power systems,” *Renewable and Sustainable Energy Reviews*, vol. 12, no. 3, 2008, pp. 852-863, doi: <https://doi.org/10.1016/j.rser.2006.10.007> .
- [15] Nasif Mahmud, and A. Zahedi, “Review of control strategies for voltage regulation of the smart distribution network with high penetration of renewable distributed generation,” *Renewable and Sustainable Energy Reviews*, vol. 64, 2016, pp. 582-595, doi: <https://doi.org/10.1016/j.rser.2016.06.030>
- [16] M. E. Baran and Ming-Yung Hsu, “Volt/VAr control at distribution substations,” *IEEE Transactions on Power Systems*, vol. 14, no. 1, pp. 312-318, Feb. 1999, doi: <https://doi.org/10.1109/59.744549>
- [17] Y. Zhang and A. Srivastava, “Voltage Control Strategy for Energy Storage System in Sustainable Distribution System Operation,” *Energies*, vol. 14, no. 4, 832, 2021, doi: [10.3390/en14040832](https://doi.org/10.3390/en14040832).
- [18] Hosseinzadeh, Nasser, Asma Aziz, Apel Mahmud, Ameen Gargoom, and Mahbub Rabbani, “Voltage Stability of Power Systems with Renewable-Energy Inverter-Based Generators: A Review,” *Electronics* 2021, vol. 10, no. 115. doi: <https://doi.org/10.3390/electronics10020115>
- [19] M. Soshinskaya, W.H.J. Crijns-Graus, J.M. Guerrero, and J.C. Vasquez, "Microgrids: Experiences, barriers and success factors," *Renewable and Sustainable Energy Reviews*, vol. 40, pp. 659-672, 2014. doi: <https://doi.org/10.1016/j.rser.2014.07.198>.
- [20] T. Tumiran, L.M. Putranto, S. Sarjiya, and E.Y. Pramono, "Maximum penetration determination of variable renewable energy generation: A case in Java–Bali power systems," *Renewable Energy*, vol. 163, pp. 561-570, 2021. doi: <https://doi.org/10.1016/j.renene.2020.08.048>.
- [21] Tanveer Ahmad, Rafal Madonski, Dongdong Zhang, Chao Huang, and Asad Mujeeb, “Data-driven probabilistic machine learning in sustainable smart energy/smart energy systems: Key developments, challenges, and future research opportunities in the context of smart grid paradigm,” *Renewable and Sustainable Energy Reviews*, vol. 160, 2022, 112128, doi: <https://doi.org/10.1016/j.rser.2022.112128>.
- [22] M. Lave, M. J. Reno and J. Peppanen, “Distribution System Parameter and Topology Estimation Applied to Resolve Low-Voltage Circuits on Three Real Distribution Feeders,” *IEEE Transactions on Sustainable Energy*, vol. 10, no. 3, pp. 1585-1592, July 2019, .1109/TSTE.2019.2917679. <https://doi.org/10.1109/TSTE.2019.2917679>
- [23] P. P. Barker and R. W. De Mello, "Determining the impact of distributed generation on power systems. I. Radial distribution systems," 2000 Power Engineering Society Summer Meeting (Cat. No.00CH37134), Seattle, WA, USA, 2000, pp. 1645-1656 vol. 3, doi: [10.1109/PESS.2000.868775](https://doi.org/10.1109/PESS.2000.868775).
- [24] Vanika Sharma, Syed Mahfuzul Aziz, Mohammed H. Haque, and Travis Kauschke, “Effects of high solar photovoltaic penetration on distribution feeders and the economic impact,” *Renewable and Sustainable Energy Reviews*, vol. 131, 2020, p. 110021, doi: <https://doi.org/10.1016/j.rser.2020.110021>.
- [25] A. Moghassemi and S. Padmanaban, “Dynamic Voltage Restorer (DVR): A Comprehensive Review of Topologies, Power Converters, Control Methods, and Modified Configurations,” *Energies*, vol. 13, no. 16, p. 4152, Aug. 2020, doi: [10.3390/en13164152](https://doi.org/10.3390/en13164152).
- [26] N. Abas, S. Dilshad, A. Khalid, M. S. Saleem and N. Khan, "Power Quality Improvement Using Dynamic Voltage Restorer," in *IEEE Access*, vol. 8, pp. 164325-164339, 2020, doi: [10.1109/ACCESS.2020.3022477](https://doi.org/10.1109/ACCESS.2020.3022477).

- [27] Shahid Ullah, Ahmed M.A. Haidar, Paul Hoole, Hushairi Zen, and Tony Ahfock, "The current state of Distributed Renewable Generation, challenges of interconnection and opportunities for energy conversion based DC microgrids," *Journal of Cleaner Production*, vol. 273, 2020, p. 122777, doi: <https://doi.org/10.1016/j.jclepro.2020.122777>
- [28] M. Farrokhhabadi et al., "Microgrid Stability Definitions, Analysis, and Examples," *IEEE Transactions on Power Systems*, vol. 35, no. 1, pp. 13-29, Jan. 2020, <https://doi.org/10.1109/TPWRS.2019.2925703>
- [29] K. Rafał, J. Biskupski, S. Bykuć, and P. Chaja, "Dynamic Voltage Regulation and Unbalance Compensation in a Low-Voltage Distribution Network Using Energy Storage System," *Applied Sciences*, vol. 12, no. 22, p. 11678, Nov. 2022, doi: 10.3390/app122211678.
- [30] A. S. A. Awad, D. Turcotte and T. H. M. El-Fouly, "Impact Assessment and Mitigation Techniques for High Penetration Levels of Renewable Energy Sources in Distribution Networks: Voltage-control Perspective," *Journal of Modern Power Systems and Clean Energy*, vol. 10, no. 2, pp. 450-458, March 2022, doi: <https://doi.org/10.35833/MPCE.2020.000177>
- [31] Seyed-Ehsan Razavi, Ehsan Rahimi, Mohammad Sadegh Javadi, Ali Esmaeel Nezhad, Mohamed Lotfi, Miadreza Shafie-khah, and João P.S. Catalão, "Impact of distributed generation on protection and voltage regulation of distribution systems: A review," *Renewable and Sustainable Energy Reviews*, vol. 105, 2019, pp. 157-167, doi: <https://doi.org/10.1016/j.rser.2019.01.050>
- [32] H. Sun et al., "Review of Challenges and Research Opportunities for Voltage Control in Smart Grids," *Transactions on Power Systems*, vol. 34, no. 4, pp. 2790-2801, July 2019, doi: <https://doi.org/10.1109/TPWRS.2019.2897948>
- [33] Ling Ai Wong, Vigna K. Ramachandaramurthy, Phil Taylor, J.B. Ekanayake, Sara L. Walker, and Sanjeevikumar Padmanaban, "Review on the optimal placement, sizing and control of an energy storage system in the distribution network," *Journal of Energy Storage*, vol. 21, 2019, pp. 489-504, doi: <https://doi.org/10.1016/j.est.2018.12.015>
- [34] Kola Sampangi Sambaiyah, and Thangavelu Jayabarathi, "Loss minimization techniques for optimal operation and planning of distribution systems: A review of different methodologies," *International Transactions on Electrical Energy Systems*, November 2019, doi: <https://doi.org/10.1002/2050-7038.12230>
- [35] Vivek Nikam, Vaiju Kalkhambkar, "A review on control strategies for microgrids with distributed energy resources, energy storage systems, and electric vehicles," *International Transactions on Electrical Energy Systems*, September 2020, doi: <https://doi.org/10.1002/2050-7038.12607>
- [36] M. Faisal, T. F. Karim, A. Ridwan Pavel, M. S. Hossen and M. S. Hossain Lipu, "Development of Smart Energy Meter for Energy Cost Analysis of Conventional Grid and Solar Energy," 2019 International Conference on Robotics, Electrical and Signal Processing Techniques (ICREST), Dhaka, Bangladesh, 2019, pp. 91-95, doi: <https://doi.org/10.1109/ICREST.2019.8644356>
- [37] Yongxi Zhang, Yan Xu, Hongming Yang, Zhao Yang Dong, "Voltage regulation-oriented co-planning of distributed generation and battery storage in active distribution networks," *International Journal of Electrical Power & Energy Systems*, vol. 105, 2019, pp. 79-88, <https://doi.org/10.1016/j.ijepes.2018.07.036>
- [38] Jianlin Li, Zhonghao Liang, Guanghui Li, Wei Zeng, Dufeng Cao, "Research on

- resonance mechanism and damping method of grid-connected inverter with LCL filter for battery energy storage system,” *Energy Reports*, vol. 8, no. 8, 2022, pp. 194-205, doi: <https://doi.org/10.1016/j.egy.2022.09.102>
- [39] Mamatha Sandhu & Tilak Thakur, “Modified Cascaded H-bridge Multilevel Inverter for Hybrid Renewable Energy Applications,” *IETE Journal of Research*, vol. 68, no. 6, pp. 3971-3983, 2020, doi: <https://doi.org/10.1080/03772063.2020.1784802>
- [40] A. M. Jasim, B. H. Jasim, B.-C. Neagu, and B. N. Alhasnawi, “Coordination Control of a Hybrid AC/DC Smart Microgrid with Online Fault Detection, Diagnostics, and Localization Using Artificial Neural Networks,” *Electronics*, vol. 12, no. 1, p. 187, Dec. 2022, doi: [10.3390/electronics12010187](https://doi.org/10.3390/electronics12010187).
- [41] Tripathi, K., Shrivastava, S., Banarjee, S., “Review in Recent Trends on Energy Delivery System and Its Issues in Smart Grid System,” *Algorithms for Intelligent Systems*. Springer, pp. 117-125, Singapore, doi: https://doi.org/10.1007/978-981-15-2369-4_11
- [42] Nirmala, M., and G. Karthikeyan. “Impact of GCIs performance on power quality of smart grid using fuzzy logic,” *International Journal of Multidisciplinary Educational Research*, vol. 2, no. 2, 2012, pp. 310-314.
- [43] Adekola, Olawale Ibrahim. “Design and development of a smart inverter system,” PhD dissertation. Cape Peninsula University of Technology, 2015.
- [44] O. I. Adekol, A. M. Almaktoof and A. K. Raji, "Design of a smart inverter system for Photovoltaic systems application," 2016 International Conference on the Industrial and Commercial Use of Energy (ICUE), Cape Town, South Africa, 2016, pp. 310-317.
- [45] I.A. Hiskens and E.M. Fleming, "Control of inverter-connected sources in autonomous microgrids", *Proceedings of the 2008 American Control Conference*, Seattle, WA, June 2008, pp. 586-590.
- [46] A. Safavizadeh, G. R. Yousefi and H. R. Karshenas, “Voltage Variation Mitigation Using Reactive Power Management of Distributed Energy Resources in a Smart Distribution System,” *IEEE Transactions on Smart Grid*, vol. 10, no. 2, pp. 1907-1915, March 2019, <https://doi.org/10.1109/TSG.2017.2781690>
- [47] M. Ebrahimi, S. A. Khajehoddin and M. Karimi-Ghartemani, “Fast and Robust Single-Phase DQ Current Controller for Smart Inverter Applications,” *IEEE Transactions on Power Electronics*, vol. 31, no. 5, pp. 3968-3976, May 2016, <https://doi.org/10.1109/TPEL.2015.2474696>
- [48] B. Kavya Santhoshi, K. Mohana Sundaram, S. Padmanaban, J. B. Holm-Nielsen, and P. K. K., “Critical Review of PV Grid-Tied Inverters,” *Energies*, vol. 12, no. 10, p. 1921, May 2019, doi: [10.3390/en12101921](https://doi.org/10.3390/en12101921).
- [49] Q. Liu, T. Caldognetto and S. Buso, “Review and Comparison of Grid-Tied Inverter Controllers in Microgrids,” *IEEE Transactions on Power Electronics*, vol. 35, no. 7, pp. 7624-7639, July 2020, doi: <https://doi.org/10.1109/TPEL.2019.2957975>
- [50] Ehsan Reihani, Saeed Sepasi, Leon R. Roose, Marc Matsuura, “Energy management at the distribution grid using a Battery Energy Storage System (BESS),” *International Journal of Electrical Power & Energy Systems*, vol. 77, 2016, pp. 337-344, doi: <https://doi.org/10.1016/j.ijepes.2015.11.035>.
- [51] M. Farrokhhabadi et al., “Energy Storage in Microgrids: Compensating for Generation and Demand Fluctuations While Providing Ancillary Services,” *IEEE Power and Energy Magazine*, vol. 15, no. 5, pp. 81-91, 2017, doi: <https://doi.org/10.1109/MPE.2017.2708863>

- [52] J. C. Beardsall, C. A. Gould and M. Al-Tai, "Energy storage systems: A review of the technology and its application in power systems," 2015 50th International Universities Power Engineering Conference (UPEC), Stoke on Trent, UK, 2015, pp. 1-6, doi: <https://doi.org/10.1109/UPEC.2015.7339794>
- [53] Jahedul Islam Chowdhury, Nazmiye Balta-Ozkan, Pietro Goglio, Yukun Hu, Liz Varga, Leah McCabe, "Techno-environmental analysis of battery storage for grid level energy services," *Renewable and Sustainable Energy Reviews*, vol. 131, 2020, p. 110018, doi: <https://doi.org/10.1016/j.rser.2020.110018>
- [54] Ramos, F.; Pinheiro, A.; Nascimento, R.; de Araujo Silva Junior, W.; Mohamed, M.A.; Annuk, A.; Marinho, M.H.N., "Development of Operation Strategy for Battery Energy Storage System into Hybrid AC Microgrids," *Sustainability* 2022, vol. 14, p. 13765, doi: <https://doi.org/10.3390/su142113765>
- [55] B. O. Alawode, U. T. Salman, and M. Khalid, "A Flexible Operation and Sizing of Battery Energy Storage System Based on Butterfly Optimization Algorithm," *Electronics*, vol. 11, no. 1, p. 109, Dec. 2021, doi: [10.3390/electronics11010109](https://doi.org/10.3390/electronics11010109).
- [56] S. F. Santos, M. Gough, D. Z. Fitiwi, A. F. P. Silva, M. Shafie-Khah and J. P. S. Catalão, "Influence of Battery Energy Storage Systems on Transmission Grid Operation With a Significant Share of Variable Renewable Energy Sources," *IEEE Systems Journal*, vol. 16, no. 1, pp. 1508-1519, March 2022, doi: <https://doi.org/10.1109/JSYST.2021.3055118>
- [57] Zeenat Hameed, Seyedmostafa Hashemi, Hans Henrik Ipsen, Chresten Træholt, "A business-oriented approach for battery energy storage placement in power systems," *Applied Energy*, vol. 298, 2021, p. 117186, doi: <https://doi.org/10.1016/j.apenergy.2021.117186>
- [58] Dhivya Sampath Kumar, Oktoviano Gandhi, Carlos D. Rodríguez-Gallegos, and Dipti Srinivasan "Review of power system impacts at high PV penetration Part II: Potential solutions and the way forward," *Solar Energy*, vol. 210, 2020, pp. 202-221, doi: <https://doi.org/10.1016/j.solener.2020.08.047>.
- [59] Dhivya Sampath Kumar, Oktoviano Gandhi, Carlos D. Rodríguez-Gallegos, Dipti Srinivasan, "Review of power system impacts at high PV penetration Part II: Potential solutions and the way forward," *Solar Energy*, vol. 210, 2020, pp. 202-221, doi: <https://doi.org/10.1016/j.solener.2020.08.047>
- [60] S. A. Rahman, A. Moharana, R. K. Varma and W. H. Litzemberger, "Bibliography of FACTS 2012: IEEE working group report," 2013 IEEE Power & Energy Society General Meeting, Vancouver, BC, Canada, 2013, pp. 1-21, doi: <https://doi.org/10.1109/PESMG.2013.6672936>
- [61] C. Gao and M. A. Redfern, "A review of voltage control techniques of networks with distributed generations using On-Load Tap Changer transformers," 45th International Universities Power Engineering Conference UPEC2010, Cardiff, UK, 2010, pp. 1-6.
- [62] Charles R. Sarimuthu, Vigna K. Ramachandaramurthy, K.R. Agileswari, and Hazlie Mokhlis "A review on voltage control methods using on-load tap changer transformers for networks with renewable energy sources," *Renewable and Sustainable Energy Reviews*, 2016, vol. 62, pp. 1154-1161, doi: <https://doi.org/10.1016/j.rser.2016.05.016>
- [63] Iria, José, Miguel Heleno, and Gonçalo Cardoso, "Optimal sizing and placement of energy storage systems and on-load tap changer transformers in distribution networks," *Applied Energy*, 2019, vol. 250, pp. 1147-1157, doi:

- <https://doi.org/10.1016/j.apenergy.2019.04.120>
- [64] Malkowski, Robert, Michał Izdebski, and Piotr Miller, "Adaptive algorithm of a tap-changer controller of the power transformer supplying the radial network reducing the risk of voltage collapse," *Energies*, vol. 13, no. 20, p. 5403, 2020, doi: <https://doi.org/10.3390/en13205403>
- [65] Kulkarni, Shrikrishna V., and Shrikrishna A. Khaparde, "Transformer engineering: design, technology, and diagnostics," CRC press, 2017.
- [66] T. Aziz and N. Ketjoy, "Enhancing PV Penetration in LV Networks Using Reactive Power Control and On Load Tap Changer With Existing Transformers," in *IEEE Access*, vol. 6, pp. 2683-2691, 2018, doi: 10.1109/ACCESS.2017.2784840.
- [67] Y. Liu, J. Bebic, B. Kroposki, J. de Bedout and W. Ren, "Distribution System Voltage Performance Analysis for High-Penetration PV," 2008 IEEE Energy 2030 Conference, Atlanta, GA, USA, 2008, pp. 1-8, doi: 10.1109/ENERGY.2008.4781069.
- [68] P. Singh, S. K. Bishnoi and N. K. Meena, "Moth Search Optimization for Optimal DERs Integration in Conjunction to OLTC Tap Operations in Distribution Systems," in *IEEE Systems Journal*, vol. 14, no. 1, pp. 880-888, March 2020, doi: 10.1109/JSYST.2019.2911534.
- [69] Sarimuthu, Charles R., et al., "A review on voltage control methods using on-load tap changer transformers for networks with renewable energy sources," *Renewable and Sustainable Energy Reviews*, 2016, vol. 62, pp. 1154-1161, doi: <https://doi.org/10.1016/j.rser.2016.05.016>
- [70] C. Gao and M. A. Redfern, "A review of voltage control techniques of networks with distributed generations using On-Load Tap Changer transformers," 45th International Universities Power Engineering Conference UPEC2010, Cardiff, UK, 2010, pp. 1-6.
- [71] Hoseinzadeh, Bakhtyar, and Frede Blaabjerg, "A novel control technique for on-load tap changer to enlarge the reactive power capability of wind power plants," *IET Generation, Transmission & Distribution*, 2022, vol. 16, no. 14, pp. 2928-2938., doi: <https://doi.org/10.1049/gtd2.12510>
- [72] E. O. Hasan, A. Y. Hatata, E. A. -E. Badran and F. H. Yossef, "Voltage Control of Distribution Systems Using Electronic OLTC," 2018 Twentieth International Middle East Power Systems Conference (MEPCON), Cairo, Egypt, 2018, pp. 845-849, doi: 10.1109/MEPCON.2018.8635151.
- [73] T. -T. Ku, C. -H. Lin, C. -S. Chen and C. -T. Hsu, "Coordination of Transformer On-Load Tap Changer and PV Smart Inverters for Voltage Control of Distribution Feeders," in *IEEE Transactions on Industry Applications*, vol. 55, no. 1, pp. 256-264, Jan.-Feb. 2019, doi: 10.1109/TIA.2018.2870578.
- [74] T. Tewari, A. Mohapatra and S. Anand, "Coordinated Control of OLTC and Energy Storage for Voltage Regulation in Distribution Network With High PV Penetration," in *IEEE Transactions on Sustainable Energy*, vol. 12, no. 1, pp. 262-272, Jan. 2021, doi: 10.1109/TSTE.2020.2991017.
- [75] Bustamante, Sergio, et al., "Determination of transformer oil contamination from the OLTC gases in the power transformers of a distribution system operator," *Applied Sciences*, vol. 10, no. 24, 2020, p. 8897 doi: <https://doi.org/10.3390/app10248897>.
- [76] CIGRE, "Ageing High Voltage Substation Equipment and Possible Mitigation Techniques," WG A3.29. Technical Brochure No. 725; CIGRE: Paris, France, 2018.
- [77] Bohatyrewicz, P.; Płowucha, J.; Subocz, J., "Condition Assessment of Power Transformers Based on Health Index Value," *Applied Science* 2019, vol. 9, p. 4877,

doi: <https://doi.org/10.3390/app9224877>

- [78] M. Zouiti, O. Bonnard, R. Desquiens, M. Cuevas and D. Bortolotti, "ONLINE MONITORING OF POWER TRANSFORMERS TO IMPROVE THEIR OPERATING AND MAINTENANCE MODEL," CIRED 2021 - The 26th International Conference and Exhibition on Electricity Distribution, Online Conference, 2021, pp. 496-499, doi: 10.1049/icp.2021.1503.
- [79] A. Nouri and A. Keane, "Planning of OLTC Transformers in LV Systems under Conservation Voltage Reduction Strategy," 2019 IEEE PES Innovative Smart Grid Technologies Europe (ISGT-Europe), Bucharest, Romania, 2019, pp. 1-5, doi: 10.1109/ISGTEurope.2019.8905765.
- [80] M. Liu, L. Ochoa and S. Low, "On the Implementation of OPF-Based Setpoints for Active Distribution Networks," 2022 IEEE Power & Energy Society General Meeting (PESGM), Denver, CO, USA, 2022, pp. 1-1, doi: 10.1109/PESGM48719.2022.9917064.
- [81] Khalil Gholami, Md. Rabiul Islam, Md. Moktadir Rahman, Ali Azizivahed, and Afef Fekih, "State-of-the-art technologies for volt-var control to support the penetration of renewable energy into the smart distribution grids," *Energy Reports*, vol. 8, 2022, pp. 8630-8651, doi: <https://doi.org/10.1016/j.egy.2022.06.080>
- [82] R. Yang, D. Zhang, Z. Li, K. Yang, S. Mo and L. Li, "Mechanical Fault Diagnostics of Power Transformer On-Load Tap Changers Using Dynamic Time Warping," in *IEEE Transactions on Instrumentation and Measurement*, vol. 68, no. 9, pp. 3119-3127, Sept. 2019, doi: 10.1109/TIM.2018.2872385.
- [83] Almeida, Dilini, Jagadeesh Pasupuleti, and Janaka Ekanayake, "Comparison of reactive power control techniques for solar PV inverters to mitigate voltage rise in low-voltage grids," *Electronics*, vol. 10, no. 13, 2021, p. 1569, doi: <https://doi.org/10.3390/electronics10131569>
- [84] Luo, Chen, et al., "Network partition-based hierarchical decentralised voltage control for distribution networks with distributed PV systems," *International Journal of Electrical Power & Energy Systems*, vol. 130, 2021, p. 106929, doi: <https://doi.org/10.1016/j.ijepes.2021.106929>
- [85] Wang, Licheng, Ruifeng Yan, and Tapan Kumar Saha, "Voltage regulation challenges with unbalanced PV integration in low voltage distribution systems and the corresponding solution," *Applied Energy*, vol. 256, 2019, p. 113927., doi: <https://doi.org/10.1016/j.apenergy.2019.113927>
- [86] Li, Changfu, et al., "Optimal OLTC voltage control scheme to enable high solar penetrations," *Electric Power Systems Research*, vol. 160, 2018, p. 318-326, doi: <https://doi.org/10.1016/j.epsr.2018.02.016>
- [87] Murty, Vallem Veera Venkata Satya Narayana, and Ashwani Kumar Sharma, "Optimal coordinate control of OLTC, DG, D-STATCOM, and reconfiguration in distribution system for voltage control and loss minimization," *International Transactions on Electrical Energy Systems*, vol. 29, no. 3, 2019, p. e2752, doi: <https://doi.org/10.1002/etep.2752>
- [88] A. Y. Hatata, E. O. Hasan, M. A. Alghassab and B. E. Sedhom, "Centralized Control Method for Voltage Coordination Challenges With OLTC and D-STATCOM in Smart Distribution Networks Based IoT Communication Protocol," in *IEEE Access*, vol. 11, pp. 11903-11922, 2023, doi: 10.1109/ACCESS.2023.3242236.
- [89] Stanelyte, Daiva, and Virginijus Radziukynas, "Review of voltage and reactive power

- control algorithms in electrical distribution networks,” *Energies*, vol. 13, no. 1, 2019, p. 58, doi: <https://doi.org/10.3390/en13010058>
- [90] S. W. Mohod and M. V. Aware, "A STATCOM-Control Scheme for Grid Connected Wind Energy System for Power Quality Improvement," in *IEEE Systems Journal*, vol. 4, no. 3, pp. 346-352, Sept. 2010, doi: 10.1109/JSYST.2010.2052943.
- [91] P. Garcia-Gonzalez and A. Garcia-Cerrada, "Control system for a PWM-based STATCOM," 1999 IEEE Power Engineering Society Summer Meeting. Conference Proceedings (Cat. No.99CH36364), Edmonton, AB, Canada, 1999, pp. 1140-1145 vol.2, doi: 10.1109/PSS.1999.787477.
- [92] Kun Yang, Xiaoxiao Cheng, Yue Wang, Lei Chen and Guozhu Chen, "PCC voltage stabilization by D-STATCOM with direct grid voltage control strategy," 2012 IEEE International Symposium on Industrial Electronics, Hangzhou, 2012, pp. 442-446, doi: 10.1109/ISIE.2012.6237127.
- [93] K. Ilango, A. Bhargav, A. Trivikram, P. S. Kavya, G. Mounika and M. G. Nair, "Power quality improvement using STATCOM with renewable energy sources," 2012 IEEE 5th India International Conference on Power Electronics (IICPE), Delhi, India, 2012, pp. 1-6, doi: 10.1109/IICPE.2012.6450462.
- [94] M. I. Mosaad, H. S. M. Ramadan, M. Aljohani, M. F. El-Naggar and S. S. M. Ghoneim, "Near-Optimal PI Controllers of STATCOM for Efficient Hybrid Renewable Power System," in *IEEE Access*, vol. 9, pp. 34119-34130, 2021, doi: 10.1109/ACCESS.2021.3058081.
- [95] B. Singh, R. Saha, A. Chandra and K. Al-Haddad, "Static synchronous compensators (STATCOM): a review," *IET Power Electronics*, vol. 2, no. 4, 2009, pp. 297-324, doi: <https://doi.org/10.1049/iet-pel.2008.0034>
- [96] P. Garcia-Gonzalez and A. Garcia-Cerrada, "Control system for a PWM-based STATCOM," 1999 IEEE Power Engineering Society Summer Meeting. Conference Proceedings (Cat. No.99CH36364), Edmonton, AB, Canada, 1999, pp. 1140-1145 vol.2, doi: 10.1109/PSS.1999.787477.
- [97] P. S. Sensarma, K. R. Padiyar and V. Ramanarayanan, "Analysis and performance evaluation of a distribution STATCOM for compensating voltage fluctuations," in *IEEE Transactions on Power Delivery*, vol. 16, no. 2, pp. 259-264, April 2001, doi: 10.1109/61.915492.
- [98] Sadiq, Rehan, et al., "A review of STATCOM control for stability enhancement of power systems with wind/PV penetration: Existing research and future scope," *International Transactions on Electrical Energy Systems*, vol. 31, no. 11, 2021, p. e13079, doi: <https://doi.org/10.1002/2050-7038.13079>
- [99] J. Qi, W. Zhao and X. Bian, "Comparative Study of SVC and STATCOM Reactive Power Compensation for Prosumer Microgrids With DFIG-Based Wind Farm Integration," in *IEEE Access*, vol. 8, pp. 209878-209885, 2020, doi: 10.1109/ACCESS.2020.3033058.
- [100] Smrithi, K., and B. Jayanand, "Sustainable power conversion topology based STATCOM for reactive power compensation," *Renewable Energy Focus*, vol. 43, 2022, pp. 277-290, doi: <https://doi.org/10.1016/j.ref.2022.10.007>
- [101] Monika Jain, Sushma Gupta, Deepika Masand and Gayatri Agnihotri, "Isolated Operation of Micro Grid Under Transient Conditions Using AI-Based VF Controller," *IETE Journal of Research* 68.2 (2022): 1277-1290. <https://doi.org/10.1080/03772063.2019.1644970>

- [102] C. M. Castiblanco-Pérez, D. E. Toro-Rodríguez, O. D. Montoya, and D. A. Giral-Ramírez, "Optimal Placement and Sizing of D-STATCOM in Radial and Meshed Distribution Networks Using a Discrete-Continuous Version of the Genetic Algorithm," *Electronics*, vol. 10, no. 12, p. 1452, Jun. 2021, doi: 10.3390/electronics10121452.
- [103] Ritika Gour, and Vishal Verma, "Comparative Performance of DVR and STATCOM for Voltage Regulation in Radial Microgrid with High Penetration of RES," *International journal of electrical and computer engineering systems*, vol. 13, no. 9, 2022, pp. 831-837, doi: <https://doi.org/10.32985/ijeces.13.9.12>
- [104] A. M. Shaheen, R. A. El-Sehiemy, A. Ginidi, A. M. Elsayed, and S. F. Al-Gahtani, "Optimal Allocation of PV-STATCOM Devices in Distribution Systems for Energy Losses Minimization and Voltage Profile Improvement via Hunter-Prey-Based Algorithm," *Energies*, vol. 16, no. 6, p. 2790, Mar. 2023, doi: 10.3390/en16062790.
- [105] A. Kaymanesh, A. Chandra and K. Al-Haddad, "Model Predictive Control of MPUC7-Based STATCOM Using Autotuned Weighting Factors," in *IEEE Transactions on Industrial Electronics*, vol. 69, no. 3, pp. 2447-2458, March 2022, doi: 10.1109/TIE.2021.3070502.
- [106] Arindam Chakraborty, Shravana K. Musunuri, Anurag K. Srivastava, and Anil K. Kondabathin, "Integrating STATCOM and battery energy storage system for power system transient stability: A review and application," *Advances in Power Electronics*, vol. 2012, 2012, p. 676010, doi: <https://doi.org/10.1155/2012/676010>
- [107] N. G. Hingorani, "FACTS Technology - State of the Art, Current Challenges and the Future Prospects," 2007 IEEE Power Engineering Society General Meeting, Tampa, FL, USA, 2007, pp. 1-4, doi: 10.1109/PES.2007.386032.
- [108] Md Alamgir Hossain, Hemanshu Roy Pota, Md Jahangir Hossain and Frede Blaabjerg, "Evolution of microgrids with converter-interfaced generations: Challenges and opportunities." *International Journal of Electrical Power & Energy Systems*, vol. 109, 2019, pp. 160-186, doi: <https://doi.org/10.1016/j.ijepes.2019.01.038>
- [109] Mezigebu Getinet Yenealem, Livingstone M. H. Ngoo, Dereje Shiferaw, and Peterson Hinga, "Management of voltage profile and power loss minimization in a grid-connected microgrid system using fuzzy-based STATCOM controller," *Journal of Electrical and Computer Engineering*, vol. 2020, 2020, pp. 1-13, doi: <https://doi.org/10.1155/2020/2040139>
- [110] S. D. Veeraganti and M. I. A, "OPTIMAL PLACEMENT AND SIZING OF DG and D-STATCOM IN A DISTRIBUTION SYSTEM: A REVIEW," 2022 International Virtual Conference on Power Engineering Computing and Control: Developments in Electric Vehicles and Energy Sector for Sustainable Future (PECCON), Chennai, India, 2022, pp. 1-13, doi: 10.1109/PECCON55017.2022.9851016.
- [111] Dey, Smiti, Nilakshi Deka, and Durlav Hazarika, "Power system planning for reduction in system losses using STATCOM and PSO technique," *Journal of The Institution of Engineers (India): Series B*, vol. 103, no. 4, 2022, pp. 1269-1281, doi: <https://doi.org/10.1007/s40031-022-00715-9>
- [112] Barrios-Martínez, Esther, and Cesar Ángeles-Camacho, "Technical comparison of FACTS controllers in parallel connection," *Journal of Applied Research and Technology*, vol. 15, no. 1, 2017, pp. 36-44, doi: <https://doi.org/10.1016/j.jart.2017.01.001>
- [113] D. Lijie, L. Yang and M. Yiqun, "Comparison of High Capacity SVC and STATCOM

- in Real Power Grid," 2010 International Conference on Intelligent Computation Technology and Automation, Changsha, China, 2010, pp. 993-997, doi: 10.1109/ICICTA.2010.586.
- [114] A. Raju, E. P. Cheriyan and R. Ramchand, "Nearly Constant Switching Frequency Hysteresis Current Controller for Multilevel Inverter based STATCOM," TENCON 2019 - 2019 IEEE Region 10 Conference (TENCON), Kochi, India, 2019, pp. 176-180, doi: 10.1109/TENCON.2019.8929458.
- [115] J. M. Guerrero, P. C. Loh, T. -L. Lee and M. Chandorkar, "Advanced Control Architectures for Intelligent Microgrids—Part II: Power Quality, Energy Storage, and AC/DC Microgrids," in IEEE Transactions on Industrial Electronics, vol. 60, no. 4, pp. 1263-1270, April 2013, doi: 10.1109/TIE.2012.2196889.
- [116] D. M. Vilathgamuwa, A. A. D. R. Perera and S. S. Choi, "Voltage Sag Compensation with Energy Optimized Dynamic Voltage Restorer," in IEEE Power Engineering Review, vol. 22, no. 10, pp. 63-63, Oct. 2002, doi: 10.1109/MPER.2002.4311764
- [117] Changjiang Zhan, A. Arularnalam, V. K. Ramchandaramurthy, C. Fitzer, A. Barnes and N. Jenkins, "Dynamic voltage restorer based on voltage-space-vector PWM control," in IEEE Transactions on Industry Applications, vol. 37, no. 6, pp. 1855-1863, Nov.-Dec. 2001, doi: 10.1109/28.968201.
- [118] J. G. Nielsen, M. Newman, H. Nielsen and F. Blaabjerg, "Control and testing of a dynamic voltage restorer (DVR) at medium voltage level," IEEE 34th Annual Conference on Power Electronics Specialist, 2003. PESC '03., Acapulco, Mexico, 2003, pp. 1248-1253 vol.3, doi: 10.1109/PESC.2003.1216626.
- [119] Abdul Hameed Soomro, Abdul Sattar Larik , Mukhtiar Ahmed Mahar, Anwer Ali Sahito, Amir Mahmood Soomro, and Ghulam Sarwar Kaloi., "Dynamic voltage restorer—A comprehensive review," Energy Reports, vol. 7, 2021, pp. 6786-6805, doi: <https://doi.org/10.1016/j.egyr.2021.09.004>
- [120] Rakeshwri Pal, and Sushma Gupta, "Topologies and control strategies implicated in dynamic voltage restorer (DVR) for power quality improvement," Iranian Journal of Science and Technology, Transactions of Electrical Engineering, vol. 44, 2020, pp. 581-603, doi: <https://doi.org/10.1007/s40998-019-00287-3>
- [121] Wael S. Hassanein, Marwa M. Ahmed, M. Osama abed el-Raouf, Mohamed G. Ashmawy and Mohamed I. Mosaad, "Performance improvement of off-grid hybrid renewable energy system using dynamic voltage restorer," Alexandria Engineering Journal, vol. 59, no. 3, 2020, pp. 1567-1581, doi: <https://doi.org/10.1016/j.aej.2020.03.037>
- [122] R. Nasrollahi, H. Feshki Farahani, M. Asadi, and M. Farhadi-Kangarlu, "Sliding mode control of a dynamic voltage restorer based on PWM AC chopper in three-phase three-wire systems," International Journal of Electrical Power & Energy Systems, vol. 134, 2022, pp. 107480, doi: <https://doi.org/10.1016/j.ijepes.2021.107480>
- [123] N. Abas, S. Dilshad, A. Khalid, M. S. Saleem and N. Khan, "Power Quality Improvement Using Dynamic Voltage Restorer," in IEEE Access, vol. 8, pp. 164325-164339, 2020, doi: 10.1109/ACCESS.2020.3022477.
- [124] R. Simanjorang, Y. Miura and T. Ise, "Controlling voltage profile in loop distribution system with Distributed Generation using series type BTB converter," 2007 7th International Conference on Power Electronics, Daegu, Korea (South), 2007, pp. 1167-1172, doi: 10.1109/ICPE.2007.4692562.
- [125] M. S. El Moursi, B. Bak-Jensen and M. H. Abdel-Rahman, "Coordinated Voltage

- Control Scheme for SEIG-Based Wind Park Utilizing Substation STATCOM and ULTC Transformer," in *IEEE Transactions on Sustainable Energy*, vol. 2, no. 3, pp. 246-255, July 2011, doi: 10.1109/TSTE.2011.2114375.
- [126] Arindam Ghosh, Gerard Ledwich, "Power quality enhancement using custom power devices," Springer science & business media, 2012.
- [127] A. Ghosh and G. Ledwich, "Compensation of distribution system voltage using DVR," in *IEEE Transactions on Power Delivery*, vol. 17, no. 4, pp. 1030-1036, Oct. 2002, doi: 10.1109/TPWRD.2002.803839.
- [128] S. S. Choi, J. D. Li and D. M. Vilathgamuwa, "A generalized voltage compensation strategy for mitigating the impacts of voltage sags/swells," in *IEEE Transactions on Power Delivery*, vol. 20, no. 3, pp. 2289-2297, July 2005, doi: 10.1109/TPWRD.2005.848442.
- [129] Linfang Yan, Xia Chen, Xin Zhou, Haishun Sun, and Lin Jiang, "Perturbation compensation-based non-linear adaptive control of ESS-DVR for the LVRT capability improvement of wind farms." *IET Renewable Power Generation*, vol. 12, no. 13, 2018, pp. 1500-1507, doi: <https://doi.org/10.1049/iet-rpg.2017.0839>
- [130] Singh, Bhim, et al., "Indirect control of capacitor supported DVR for power quality improvement in distribution system," 2008 IEEE Power and Energy Society General Meeting-Conversion and Delivery of Electrical Energy in the 21st Century. IEEE, 2008. <https://doi.org/10.1109/PES.2008.4596024>
- [131] P. Jayaprakash, B. Singh, D. P. Kothari, A. Chandra and K. Al-Haddad, "Control of Reduced-Rating Dynamic Voltage Restorer With a Battery Energy Storage System," in *IEEE Transactions on Industry Applications*, vol. 50, no. 2, pp. 1295-1303, March-April 2014, doi: 10.1109/TIA.2013.2272669.
- [132] P. Kanjiya, B. Singh, A. Chandra and K. Al-Haddad, "'SRF Theory Revisited" to Control Self-Supported Dynamic Voltage Restorer (DVR) for Unbalanced and Nonlinear Loads," in *IEEE Transactions on Industry Applications*, vol. 49, no. 5, pp. 2330-2340, Sept.-Oct. 2013, doi: 10.1109/TIA.2013.2261273.
- [133] Ramya, G., V. Ganapathy, and P. Suresh, "Power quality improvement using multi-level inverter based DVR and DSTATCOM using neuro-fuzzy controller," *International Journal of Power Electronics and Drive Systems*, vol. 8, no. 1, 2017, p. 316, doi: <http://doi.org/10.11591/ijpeds.v8.i1.pp316-324>
- [134] A. Ghosh, A. K. Jindal and A. Joshi, "Design of a capacitor-supported dynamic voltage restorer (DVR) for unbalanced and distorted loads," in *IEEE Transactions on Power Delivery*, vol. 19, no. 1, pp. 405-413, Jan. 2004, doi: 10.1109/TPWRD.2003.820198.
- [135] P. Kanjiya, V. Khadkikar, H. H. Zeineldin and B. Singh, "Reactive power estimation based control of self supported dynamic voltage restorer (DVR)," 2012 IEEE 15th International Conference on Harmonics and Quality of Power, Hong Kong, China, 2012, pp. 785-790, doi: 10.1109/ICHQP.2012.6381306.
- [136] R. Strzelecki and G. Benysek, "Control strategies and comparison of the Dynamic Voltage Restorer," 2008 Power Quality and Supply Reliability Conference, Parnu, Estonia, 2008, pp. 79-82, doi: 10.1109/PQ.2008.4653741.
- [137] M. Vilathgamuwa, A. A. D. Ranjith Perera and S. S. Choi, "Performance improvement of the dynamic voltage restorer with closed-loop load voltage and current-mode control," in *IEEE Transactions on Power Electronics*, vol. 17, no. 5, pp. 824-834, Sept. 2002, doi: 10.1109/TPEL.2002.802189.
- [138] Poh Chiang Loh, D. M. Vilathgamuwa, Seng Khai Tang and H. L. Long, "Multilevel

- dynamic voltage restorer," in *IEEE Power Electronics Letters*, vol. 2, no. 4, pp. 125-130, Dec. 2004, doi: 10.1109/LPEL.2004.840441.
- [139] C. Meyer, C. Romaus and R. W. De Doncker, "Optimized Control Strategy for a Medium-Voltage DVR," 2005 IEEE 36th Power Electronics Specialists Conference, Dresden, Germany, 2005, pp. 1887-1893, doi: 10.1109/PESC.2005.1581889.
- [140] C. Meyer, R. W. De Doncker, Y. W. Li and F. Blaabjerg, "Optimized Control Strategy for a Medium-Voltage DVR—Theoretical Investigations and Experimental Results," in *IEEE Transactions on Power Electronics*, vol. 23, no. 6, pp. 2746-2754, Nov. 2008, doi: 10.1109/TPEL.2008.2002299.
- [141] S. Jothibasu and M. K. Mishra, "A Control Scheme for Storageless DVR Based on Characterization of Voltage Sags," in *IEEE Transactions on Power Delivery*, vol. 29, no. 5, pp. 2261-2269, Oct. 2014, doi: 10.1109/TPWRD.2014.2316598.
- [142] A. Moghassemi and S. Padmanaban, "Dynamic Voltage Restorer (DVR): A Comprehensive Review of Topologies, Power Converters, Control Methods, and Modified Configurations," *Energies*, vol. 13, no. 16, p. 4152, Aug. 2020, doi: 10.3390/en13164152.
- [143] Rakeshwri Pal, and Sushma Gupta, "Topologies and control strategies implicated in dynamic voltage restorer (DVR) for power quality improvement," *Iranian Journal of Science and Technology, Transactions of Electrical Engineering*, vol. 44, 2020, pp. 581-603, doi: <https://doi.org/10.1007/s40998-019-00287-3>
- [144] Abdul Hameed Soomro, Abdul Sattar Larik , Mukhtiar Ahmed Mahar, Anwer Ali Sahito, Amir Mahmood Soomro, and Ghulam Sarwar Kaloi., "Dynamic voltage restorer—A comprehensive review," *Energy Reports*, vol. 7, 2021, pp. 6786-6805, doi: <https://doi.org/10.1016/j.egy.2021.09.004>
- [145] P. Mathew, S. Madichetty and S. Mishra, "A Multilevel Distributed Hybrid Control Scheme for Islanded DC Microgrids," in *IEEE Systems Journal*, vol. 13, no. 4, pp. 4200-4207, Dec. 2019, doi: 10.1109/JSYST.2019.2896927.
- [146] Yu Wang, Yan Xu, Yi Tang, Mazheruddin Hussain Syed, Efren Guillo-Sansano, and Graeme M. Burt, "Decentralised-distributed hybrid voltage regulation of power distribution networks based on power inverters," *IET Generation, Transmission & Distribution*, vol. 13, no. 3, 2019, pp. 444-451, doi: <https://doi.org/10.1049/iet-gtd.2018.5428>
- [147] A. R. Malekpour, A. M. Annaswamy and J. Shah, "Hierarchical Hybrid Architecture for Volt/Var Control of Power Distribution Grids," in *IEEE Transactions on Power Systems*, vol. 35, no. 2, pp. 854-863, March 2020, doi: 10.1109/TPWRS.2019.2941969.
- [148] Sahoo, Buddhadeva, Sangram Keshari Routray, and Pravat Kumar Rout, "AC, DC, and hybrid control strategies for smart microgrid application: A review," *International Transactions on Electrical Energy Systems*, vol. 31, no. 1, 2021, p. e12683, doi: <https://doi.org/10.1002/2050-7038.12683>
- [149] A. Y. Hatata, E. O. Hasan, M. A. Alghassab and B. E. Sedhom, "Centralized Control Method for Voltage Coordination Challenges With OLTC and D-STATCOM in Smart Distribution Networks Based IoT Communication Protocol," in *IEEE Access*, vol. 11, pp. 11903-11922, 2023, doi: 10.1109/ACCESS.2023.3242236.
- [150] Sarker, Krishna, Debashis Chatterjee, and S. K. Goswami, "A modified PV-wind-PEMFCS-based hybrid UPQC system with combined DVR/STATCOM operation by harmonic compensation," *International Journal of Modelling and Simulation*, vol. 41,

- no. 4, 2021, pp. 243-255, doi: <https://doi.org/10.1080/02286203.2020.1727134>
- [151] J. Qi, W. Zhao and X. Bian, "Comparative Study of SVC and STATCOM Reactive Power Compensation for Prosumer Microgrids With DFIG-Based Wind Farm Integration," in *IEEE Access*, vol. 8, pp. 209878-209885, 2020, doi: [10.1109/ACCESS.2020.3033058](https://doi.org/10.1109/ACCESS.2020.3033058).
- [152] Qiran Liu, Qunhai Huo, Jingyuan Yin, Jiaming Li, Longfei Sun, and Tongzhen Wei, "Research on coordinated control of flexible on-load voltage regulator and STATCOM," *Energy Reports*, vol. 8, 2022, pp. 994-1002, <https://doi.org/10.1016/j.egy.2022.08.091>
- [153] S. Song, C. Han, G. -S. Lee, R. A. McCann and G. Jang, "Voltage-Sensitivity-Approach-Based Adaptive Droop Control Strategy of Hybrid STATCOM," in *IEEE Transactions on Power Systems*, vol. 36, no. 1, pp. 389-401, Jan. 2021, doi: [10.1109/TPWRS.2020.3003582](https://doi.org/10.1109/TPWRS.2020.3003582).
- [154] Qiao, Feng, and Jin Ma, "Coordinated voltage/var control in a hybrid AC/DC distribution network," *IET Generation, Transmission & Distribution*, vol. 14, no. 11, 2020, pp. 2129-2137, doi: <https://doi.org/10.1049/iet-gtd.2019.0390>
- [155] Jayamaha, D. K. J. S., N. W. A. Lidula, and A. D. Rajapakse, "Protection and grounding methods in DC microgrids: Comprehensive review and analysis," *Renewable and Sustainable Energy Reviews*, vol. 120, 2020, p. 109631, doi: <https://doi.org/10.1016/j.rser.2019.109631>
- [156] Y. Wu, Y. Wu, J. M. Guerrero, J. C. Vasquez and J. Li, "AC Microgrid Small-Signal Modeling: Hierarchical Control Structure Challenges and Solutions," in *IEEE Electrification Magazine*, vol. 7, no. 4, pp. 81-88, Dec. 2019, doi: [10.1109/MELE.2019.2943980](https://doi.org/10.1109/MELE.2019.2943980).
- [157] J. Rocabert, A. Luna, F. Blaabjerg and P. Rodríguez, "Control of Power Converters in AC Microgrids," in *IEEE Transactions on Power Electronics*, vol. 27, no. 11, pp. 4734-4749, Nov. 2012, doi: [10.1109/TPEL.2012.2199334](https://doi.org/10.1109/TPEL.2012.2199334).
- [158] J. Lu, X. Liu, X. Hou and P. Wang, "A Distributed Control Strategy for State-of-Charge Balance of Energy Storage Without Continuous Communication in AC Microgrids," in *IEEE Transactions on Sustainable Energy*, vol. 14, no. 1, pp. 206-216, Jan. 2023, doi: [10.1109/TSTE.2022.3206327](https://doi.org/10.1109/TSTE.2022.3206327).
- [159] M. A. Ghalib and M. M. Samy, "Magnification of Performance Operation for Low Voltage DC Microgrids Based on Adaptive Droop Control Technique," 2021 22nd International Middle East Power Systems Conference (MEPCON), Assiut, Egypt, 2021, pp. 424-429, doi: [10.1109/MEPCON50283.2021.9686201](https://doi.org/10.1109/MEPCON50283.2021.9686201).
- [160] Aghaee, Mahdian Dehkordi, Bayati, and Hajizadeh, "Distributed Control Methods and Impact of Communication Failure in AC Microgrids: A Comparative Review," *Electronics*, vol. 8, no. 11, p. 1265, Nov. 2019, doi: [10.3390/electronics8111265](https://doi.org/10.3390/electronics8111265).
- [161] Bhaskar Patnaik, Manohar Mishra, Ramesh C. Bansal, and Ranjan Kumar Jena, "AC microgrid protection—A review: Current and future prospective," *Applied Energy*, vol. 271, 2020, p. 115210, doi: <https://doi.org/10.1016/j.apenergy.2020.115210>
- [162] Chandra, Ankan, Girish Kumar Singh, and Vinay Pant, "Protection of AC microgrid integrated with renewable energy sources—A research review and future trends," *Electric Power Systems Research*, vol. 193, 2021, p. 107036, doi: <https://doi.org/10.1016/j.epsr.2021.107036>
- [163] A. Mohammed, S. S. Refaat, S. Bayhan and H. Abu-Rub, "AC Microgrid Control and

- Management Strategies: Evaluation and Review," in *IEEE Power Electronics Magazine*, vol. 6, no. 2, pp. 18-31, June 2019, doi: 10.1109/MPEL.2019.2910292.
- [164] Muhammad Uzair, Li Li, Mohsen Eskandari, Jahangir Hossain, and Jian Guo Zhu, "Challenges, advances and future trends in AC microgrid protection: With a focus on intelligent learning methods," *Renewable and Sustainable Energy Reviews*, vol. 178, 2023, p. 113228, doi: <https://doi.org/10.1016/j.rser.2023.113228>
- [165] M. Ahmed, L. Meegahapola, A. Vahidnia and M. Datta, "Stability and Control Aspects of Microgrid Architectures—A Comprehensive Review," in *IEEE Access*, vol. 8, pp. 144730-144766, 2020, doi: 10.1109/ACCESS.2020.3014977.
- [166] M.A. Hannan, M. Faisal, Pin Jern Ker, R.A. Begum, Z.Y. Dong, and C. Zhang, "Review of optimal methods and algorithms for sizing energy storage systems to achieve decarbonization in microgrid applications," *Renewable and Sustainable Energy Reviews*, vol. 131, 2020, p. 110022, doi: <https://doi.org/10.1016/j.rser.2020.110022>
- [167] Li, Xueping, and Gerald Jones, "Optimal Sizing, Location, and Assignment of Photovoltaic Distributed Generators with an Energy Storage System for Islanded Microgrids," *Energies* 15.18 (2022): 6630. <https://doi.org/10.3390/en15186630>
- [168] Moradi, M. H., and M. Abedini, "A novel method for optimal DG units capacity and location in Microgrids," *International Journal of Electrical Power & Energy Systems*, vol. 75, 2016, pp. 236-244. <https://doi.org/10.1016/j.ijepes.2015.09.013>.
- [169] Dawoud, Samir M., Xiangning Lin, and Merfat I. Okba, "Optimal placement of different types of RDGs based on maximization of microgrid loadability." *Journal of Cleaner Production*, vol. 168, 2017, pp. 63-73, doi: <https://doi.org/10.1016/j.jclepro.2017.08.003>
- [170] Borghei, Moein, and Mona Ghassemi, "Optimal planning of microgrids for resilient distribution networks." *International Journal of Electrical Power & Energy Systems*, vol. 128, 2021, p. 106682, doi: <https://doi.org/10.1016/j.ijepes.2020.106682>
- [171] Y. Gupta, S. Doolla, K. Chatterjee and B. C. Pal, "Optimal DG Allocation and Volt-Var Dispatch for a Droop-Based Microgrid," in *IEEE Transactions on Smart Grid*, vol. 12, no. 1, pp. 169-181, Jan. 2021, doi: 10.1109/TSG.2020.3017952.
- [172] A. Engler and N. Souldanis, "Droop control in LV-grids," 2005 International Conference on Future Power Systems, Amsterdam, Netherlands, 2005, pp. 6 pp.-6, doi: 10.1109/FPS.2005.204224.
- [173] P. Bhatia, S. Mittal, S. Raizada and V. Verma, "Hybrid ANN based Incremental Conductance MPPT-Current Control Algorithm for Constant Power Generation of PV fed DC Microgrid," 2020 IEEE First International Conference on Smart Technologies for Power, Energy and Control (STPEC), Nagpur, India, 2020, pp. 1-7, doi: 10.1109/STPEC49749.2020.9297751.
- [174] A. Sangwongwanich, Y. Yang and F. Blaabjerg, "High-Performance Constant Power Generation in Grid-Connected PV Systems," in *IEEE Transactions on Power Electronics*, vol. 31, no. 3, pp. 1822-1825, March 2016, doi: 10.1109/TPEL.2015.2465151.

List of Publications

Journal

- [1] Ritika Gour, V. Verma, “Comparative Performance of DVR and STATCOM for Voltage Regulation in Radial Microgrid with High Penetration of RES,” *International Journal of Electrical and Computer Engineering Systems*, vol. 13, no. 9, pp. 831-837, 2022, <https://doi.org/10.32985/ijeces.13.9.12>, **SCOPUS Indexed Journal.**
- [2] R. Gour and V. Verma, “Voltage Regulation in a Radial Microgrid with High RES Penetration: Approach-Optimum DVR Control”, *Eng. Technol. Appl. Sci. Res.*, vol. 12, no. 4, pp. 8796–8802, Aug. 2022. <https://doi.org/10.48084/etasr.4965>, **ESCI Indexed Journal.**
- [3] Vishal Verma, Ramesh Singh, Ritika Gour, “ADSIG as Gen-Former providing three port network for soft coupling of distribution feeders in addition to wind energy harvesting”, in *International Journal of Electrical Power & Energy Systems*, Volume 117, 2020. <https://doi.org/10.1016/j.ijepes.2019.105573>, **SCIE Indexed Journal.**

Conferences

- [4] V. Verma and R. Gour, “OLTC-DVR hybrid for voltage regulation and averting reverse power flow in the micro-grid with intermittent renewable energy sources,” *2016 IEEE Industrial Electronics and Applications Conference (IEACon)*, Kota Kinabalu, 2016, pp. 81-87. <https://doi.org/10.1109/IEACON.2016.8067360>.
- [5] V. Verma and R. Gour, “Step-less voltage regulation on radial feeder with OLTC transformer-DVR hybrid,” *2015 6th International Conference on Power Electronics Systems and Applications (PESA)*, Hong Kong, 2015, pp. 1-6. <https://doi.org/10.1109/PESA.2015.7398912>.

Communicated Paper

- [6] Ritika Gour, Vishal Verma, "ABCD Parameter for Devising an Abating Voltage Profile amidst High Penetration of RES through Optimal VRs & Their Placement," Electric Power Systems Research, EPSR-S-23-05055.
- [7] Ritika Gour, Vishal Verma, "Voltage Regulation in a Radial Microgrid with High RES Penetration through Hybrid Approach: OLTC-T, DVR, De-loading Control of GCI," Sustainable Energy, Grids and Networks, SEGAN S-23-01706.

BIODATA

Name	Ritika Gour
Date of Birth	13.09.1991
Place of Birth	Lucknow, UP, India
Nationality	Indian
Fathers Name	Mr. M. L. Gour
Mothers Name	Ms. Neelam Gour
Husband	Dr. Ramesh Singh

Educational Qualifications

B.Tech. Electrical & Electronics	MAIT, Delhi, 2008-2012
M.Tech. Power Systems	DTU, Delhi, 2012-2014

Area of Interest

Micro-Grids, Renewable Energy Sources, Voltage Regulation, Power Quality.